



**Universiteit
Antwerpen**

Faculteit Farmaceutische, Biomedische en Diergeneeskundige Wetenschappen

Departement Farmaceutische Wetenschappen

An integrated strategy to characterize anti-inflammatory lead
compounds derived from *Filipendula ulmaria* (meadowsweet)

Een geïntegreerde strategie voor de karakterisatie van ontstekingsremmende
“lead” verbindingen aanwezig in *Filipendula ulmaria* (moerasspirea)

Proefschrift voorgelegd tot het behalen van de graad van
Doctor in de Farmaceutische Wetenschappen aan de Universiteit Antwerpen,
te verdedigen door

Anastasia VAN DER AUWERA

Promotoren

Prof. Dr. L. Pieters

Prof. Dr. N. Hermans

Antwerpen, 2023

TABLE OF CONTENTS

LIST OF ABBREVIATIONS	VII
<u>CHAPTER 1 : GENERAL INTRODUCTION AND OUTLINE OF THE THESIS</u>	<u>1</u>
PROLOGUE	3
1.1 CHRONIC INFLAMMATION IS A GLOBAL HEALTH CHALLENGE	3
1.2 NATURAL PRODUCTS AS SOURCES OF NEW DRUGS	4
1.3 BENEFICIAL EFFECTS OF POLYPHENOLS AND THEIR METABOLITES	6
1.4 DISSERTATION OUTLINE	9
REFERENCES	12
<u>CHAPTER 2 : COMPREHENSIVE EXTRACTION OF <i>FILIPENDULA ULMARIA</i></u>	<u>15</u>
INTRODUCTION	19
2.1 AIM	19
2.2 <i>FILIPENDULA ULMARIA</i>	19
2.2.1 General characteristics	19
2.2.2 Historical data and traditional use	22
2.2.3 Main constituents	24
2.2.4 Pharmacological activity studies	24
MATERIALS AND METHODS	32
2.3 A FIRST STEP IN THE QUEST FOR THE ACTIVE CONSTITUENTS IN <i>FILIPENDULA ULMARIA</i>	32
2.3.1 Chemicals	32
2.3.2 Preparations of standard solutions	33
2.3.3 Sample preparation and extraction	34

2.3.4	Instrumental analysis	35
2.4	BRIDGING THE GAP BETWEEN COMPREHENSIVE EXTRACTION PROTOCOLS IN PLANT METABOLOMICS STUDIES AND METHOD VALIDATION	38
2.4.1	Chemicals	38
2.4.2	Preparation of standard solutions	39
2.4.3	Sample preparation and extraction	39
2.4.4	Instrumental analysis	43
2.4.5	Method validation parameters	43
	RESULTS AND DISCUSSION	46
2.5	A FIRST STEP IN THE QUEST FOR THE ACTIVE CONSTITUENTS IN <i>FILIPENDULA ULMARIA</i>	46
2.6	BRIDGING THE GAP BETWEEN COMPREHENSIVE EXTRACTION PROTOCOLS IN PLANT METABOLOMICS STUDIES AND METHOD VALIDATION	66
2.6.1	Evaluation of comprehensive extraction protocols: polar phytochemicals	66
2.6.2	Evaluation of comprehensive extraction protocols: apolar phytochemicals	80
	CONCLUSION	85
	REFERENCES	87
 CHAPTER 3 : BIOTRANSFORMATION STUDIES OF <i>FILIPENDULA ULMARIA</i>		 97
	INTRODUCTION	101
3.1	AIM	101
3.2	THE GASTROINTESTINAL TRACT	101
3.2.1	The gut microbiota	101
3.3	GUT MICROBIAL BIOTRANSFORMATION OF POLYPHENOLS	106
3.3.1	General	106
3.3.2	Flavonols	109
3.3.3	Flavanones	110
3.3.4	Flavones	110

3.3.5	Flavan-3-ols	110
3.3.6	Anthocyanidins	111
3.3.7	Isoflavones	112
3.3.8	Hydrolyzable tannins	112
3.3.9	Stilbenes	113
3.3.10	Lignans	114
3.3.11	Chlorogenic acids	115
3.4	SIMULATING THE GASTROINTESTINAL TRACT	115
3.4.1	General	115
3.4.2	Static and dynamic digestion models	116
3.4.3	Fermentation models	119
3.5	METABOLOMICS	125
3.5.1	General	125
3.5.2	LC-MS pre-processing	126
3.5.3	Dynamic metabolomics	127
	MATERIALS AND METHODS	131
3.6	SAMPLE PREPARATION	131
3.7	GASTROINTESTINAL MODEL	131
3.7.1	Preparation of fecal slurry	132
3.7.2	Preparation of digestive juices	132
3.7.3	Simulation of the stomach, small intestine and colon	133
3.7.4	Viability and bacterial composition	134
3.7.5	Sampling time points and sample preparation	135
3.8	INSTRUMENTAL ANALYSIS	135
3.9	DATA ANALYSIS	136
	RESULTS AND DISCUSSION	138
3.10	BIOTRANSFORMATION OF THE POSITIVE CONTROL	138
3.11	BIOTRANSFORMATION OF A <i>FILIPENDULA ULMARIA</i> EXTRACT	140

3.11.1	Matrix components: biotransformation of bile acids	142
3.11.2	Biotransformation of glycosylated compounds	145
3.11.3	Biotransformation of ellagitannins	162
3.11.4	The effect of phytochemicals on microbial composition	164
	CONCLUSION	168
	REFERENCES	171

CHAPTER 4 : PHARMACOLOGICAL ACTIVITY STUDIES ON *FILIPENDULA ULMARIA* 185

	INTRODUCTION	189
4.1	AIM	189
4.2	WHAT IS INFLAMMATION?	189
4.2.1	Acute inflammation	190
4.2.2	Chronic inflammation	194
4.3	NF-κB SIGNALING IN INFLAMMATION	194
4.3.1	The NF-κB family	195
4.3.2	The NF-κB family signaling pathway	195
4.3.3	NF-κB in human pathologies	198
4.3.4	The NF-κB pathway as potential target for drug discovery	201
4.4	THE CYCLOOXYGENASE PATHWAY IN INFLAMMATION	204
4.4.1	The cyclooxygenase isoenzymes	204
4.4.2	Biochemistry and functions of prostanoids	206
4.4.3	Cyclooxygenase-2 in human pathologies	208
4.4.4	Cyclooxygenase inhibitors	210
	MATERIALS AND METHODS	215
4.5	NF-κB LUCIFERASE REPORTER GENE ASSAY	215
4.5.1	Reagents	215
4.5.2	L929 cell culture	215

4.5.3	Sample preparation	215
4.5.4	NF- κ B luciferase reporter gene assay	216
4.5.5	Cell viability assay	216
4.6	COX-1 AND COX-2 ENZYME INHIBITION	217
4.6.1	Reagents	217
4.6.2	Sample preparation	217
4.6.3	COX-1 and COX-2 enzyme inhibition assay	218
4.7	COX-2 GENE EXPRESSION	219
4.7.1	Reagents	219
4.7.2	THP-1 cell culture	219
4.7.3	Sample preparation	220
4.7.4	COX-2 gene expression assay	220
4.7.5	Cell viability assay	221
4.8	STATISTICAL ANALYSIS	221
	RESULTS AND DISCUSSION	222
4.9	NF- κ B LUCIFERASE REPORTER GENE ASSAY	223
4.10	COX-1 AND COX-2 ENZYME INHIBITION	227
4.11	COX-2 GENE EXPRESSION	239
4.12	CELL VIABILITY ASSAYS IN L929 AND THP-1 CELLS	242
	CONCLUSION	244
	REFERENCES	247
	GENERAL CONCLUSIONS AND FUTURE PERSPECTIVES	265
	SUMMARY	273
	SAMENVATTING	277
	ACKNOWLEDGEMENTS	281
	SCIENTIFIC CURRICULUM VITAE	287

LIST OF ABBREVIATIONS

AA	arachidonic acid
ACE	acetone
am	accurate mass
AP-2	activator protein-2
APCI	atmospheric pressure chemical ionization
ASE	accelerated solvent extraction
ATP	apolar to polar
AUC	area under the curve
BAFFR	B cell activating factor receptor
BC	before Christ
Bcl	B cell lymphoma
BCR	B cell receptor
BHT	butylated hydroxytoluene
BSH	bile salt hydrolase
C/EBP	CAAT enhancer binding protein
CBG	cytosolic β -glucosidase
CD	cluster of differentiation
cDNA	complementary DNA
CFU	colony forming unit

C.I.	confidence interval
ciAP	cellular inhibitors of apoptosis
CID	collision-induced dissociation
c-Myc	c-myelocytomatosis oncogene product
COMT	catechol- <i>O</i> -methyl transferase
COX	cyclooxygenase
CRE	cyclic AMP response element
DAD	diode array detector
DAMPs	damage-associated molecular patterns
DGM	dynamic gastric model
DMEM	Dulbecco's modified eagle medium
DMSO	dimethylsulfoxide
DNA	deoxyribonucleic acid
EDTA	ethylenediaminetetraacetic acid
EGFR	epidermal growth factor receptor
EIA	enzyme immunoassay
ELISA	enzyme-linked immunoassay
EMA	European Medicines Agency
ER	estrogen receptor
ESI	electrospray ionization
FA	formic acid
FBS	fetal bovine serum

FDA	U.S. Food and Drug Administration
FEX	<i>Filipendula ulmaria</i> extract
FWHM	full width at half maximum
GAPDH	Glyceraldehyde 3-phosphahate dehydrogenase
GC	gas chromatography
GDS	average gastric damage score
GIDM	gastrointestinal dialysis model
GIM	gastrointestinal model
GPCR	G-protein-coupled receptor
HCD	higher-energy collisional dissociation
HDCA	hyodeoxycholic acid
HEPES	4-(2-hydroxyethyl)-1-piperazineethanesulfonic acid
HESI	heated electrospray ionization
HHDP	hexahydroxydiphenic acid
HPLC	high-performance liquid chromatography
HR	high-resolution
IBC	Inflammatory breast cancer
IC ₅₀	half-maximal inhibitory concentration
IFN	interferon
IKK	inhibitory kappa B kinase
IL	interleukin

I κ B	inhibitory kappa B
LC	liquid chromatography
LD ₅₀	median lethal dose
LPH	lactase-phlorizin hydrolase
LPS	lipopolysaccharide
LT β R	lymphotoxin β receptor
MB	method blank
MIC	minimal inhibitory concentration
MMP	matrix metalloproteinase
MS	mass spectrometry
MTT	thiazolyl blue tetrazolium bromide
NC	negative control
NCD	noncommunicable disease
NCE	new chemical entity
NEMO	NF- κ B essential modulator
NF- κ B	nuclear factor κ B
NIK	NF- κ B-inducing kinase
NMR	nuclear magnetic resonance
NSAID	non-steroidal anti-inflammatory drug
ODN	oligodeoxynucleotide
PAMPs	pathogen-associated molecular patterns
PBS	phosphate buffered saline

PCR	polymerase chain reaction
PDA	photo diode array
P-ECSIM	proximal environmental control system for intestinal microbiota
PG	prostaglandin
PI3K	phosphoinositide 3-kinase
PMA	phorbol 12-myristate 13-acetate
PolyFermS	polyfermentor intestinal model
PPAR α	peroxisome proliferator-activated receptor
PPRE	peroxisome proliferator response element
PRR	pattern recognition receptor
PTA	polar to apolar
PTGS	prostaglandin endoperoxide synthase
QC	quality control
QTOF	quadrupole time-of-flight
RA	rheumatoid arthritis
RANK	receptor activator of NF- κ B
RNA	ribonucleic acid
ROC	receiver operator characteristic
RP	reversed phase
rpm	revolutions per minute
RPMI	Roswell Park Memorial Institute Medium

rt	retention time
SCFAs	short-chain fatty acids
SD	standard deviation
SHIME	simulator of the human intestinal microbial ecosystem
SIMGI	SIMulator gastrointestinal
SP1	specificity protein 1
SRE	sterol response element
SULT	sulfotransferase
TAD	transcription activation domain
Tc	cytotoxic T cell
TCR	T cell receptors
TF	tissue factor
Th	T helper cell
TIM	TNO gastrointestinal model
TLC	thin-layer chromatography
TLR	toll-like receptors
TNF	tumor necrosis factor
TNFR	tumor necrosis factor receptor
TOF	time-of-flight
TRAF	TNF receptor associated factor
TRIS	tris(hydroxymethyl)aminomethane

TXA	thromboxane
UGT	uridine-5'-diphosphate glucuronosyltransferase
UHPLC	ultra-high performance liquid chromatography
UV	ultraviolet
VEGF	vascular endothelial growth factor
WCA	Wilkins Chalgren agar
WHO	World Health Organization
XIC	extracted ion chromatogram



CHAPTER 1

GENERAL INTRODUCTION AND OUTLINE OF THE THESIS

1.1 CHRONIC INFLAMMATION IS A GLOBAL HEALTH CHALLENGE

Unresolved inflammation, often described as low-grade chronic inflammation, is increasingly being considered as a key factor contributing to many different disease states, such as cancer, neurological or metabolic disorders.^[1-3] The World Health Organization (WHO) defines such chronic conditions as Noncommunicable Diseases (NCDs), meaning that such disorders are not transmissible directly from one person to another, and are usually of long duration as well as slow in progression. NCDs are the leading global cause of death and are responsible for 70% of deaths worldwide, killing 41 million people each year. The WHO 2020 Progress Monitor data even indicates that 86% of all deaths in Belgium are because of NCDs. The four leading types of NCDs are cardiovascular diseases, followed by cancer, chronic respiratory diseases and diabetes. They continue to be a major public health challenge globally, which also burdens global expenses for public health care.^[3] Because of the involvement of inflammation in NCDs, anti-inflammatory drugs may have a preventive effect. Daily use of selective cyclooxygenase-2 inhibitors, for example, is associated with a reduction in cancer risk.^[4] Steroidal drugs have many systemic side effects, therefore non-steroidal anti-inflammatory drugs (NSAIDs) are often prescribed for long-term treatment of inflammation for all kinds of applications. NSAIDs are amongst the most commonly used medications in the world, either by prescription or over-the-counter, with more than 30 million people worldwide using these drugs daily because of their efficient anti-inflammatory, analgesic and antipyretic properties.^[5] They are also used as first-line therapeutics in the symptomatic treatment of osteoarthritis and rheumatoid arthritis.^[6] When looking at the statistics of Belgium in 2018, osteoarthritis and rheumatoid arthritis both appear in the top 10 of most reported chronic disorders in both men and

women above the age of 15. Osteoarthritis even climbs to the top 3 in people above the age of 65, being the number 1 reported chronic disorder in women at this age.^[7] NSAIDs are generally considered to be safe; however they can have serious adverse gastrointestinal effects. Thus, due to the high number of patients that depend on NSAIDs to alleviate inflammation and pain, the reduction or elimination of such side effects could have a huge impact on the patient's quality of life.

1.2 NATURAL PRODUCTS AS SOURCES OF NEW DRUGS

The burden of non-communicable diseases, as well as communicable diseases, and the challenges of finding new drug candidates that can treat these diseases with little or no side effects is a huge challenge. The academic world and the pharmaceutical industry are continuously looking for new drugs against various diseases. The “blockbuster model”, where a series of new blockbuster pharmaceuticals arrived regularly on the market, was the long-term forward for the industry. However, drug discovery and development did not guarantee a steady flow of new pharmaceuticals. Ultimately, drug development remains a lengthy process with a low rate of success and huge capital investment.^[8] Nature has been a vital source of active ingredients to treat diseases before the dawn of modern medicine. There has been a renewed interest in natural products due to the problems associated with the common drug discovery methods to deliver new lead compounds in key therapeutic areas.^[9] From an evolutionary perspective, plants have developed a rich diversity of compounds to ward off attacks from animals and environmental insults, offering an interesting pool for novel leads or templates for the development of new drugs.^[10] Examples of medicines that were derived from plants are aspirin from the bark of *Salix*, digoxin from *Digitalis lanata* and morphine from the opium of *Papaver somniferum*.^[11] More recently, in 2015, a Nobel Prize has been awarded to Youyou Tu for her work on isolating artemisinin from the traditional Chinese herb *Artemisia annua*. Artemisinin revealed a profound activity against malaria, and its derivatives artesunate and artemether are part of the

established malaria combination treatment protocols worldwide.^[12] The continuing role of natural products in drug discovery is also highlighted by the data presented in the review from Newman and Cragg, who covered 39 years (1981-09/2019) of data in their paper. A major difference was obvious in 2004, when only 24 NCEs (new chemical entities) were approved, though interestingly 7 (or 29%) of that year's approvals were assigned to the natural product derivative (ND) category (i.e. a compound derived from a natural product, usually a semisynthetic modification). There was a rebound to 52 in 2005, with 25% being unaltered natural products (N) or ND, but 37% being biologicals (B) or vaccines (V). The next four years from 2006 to 2009 averaged 40, with 35-45% being vaccines or biologicals. However, in these 4 years, 4 botanicals (NB category, i.e. defined mixtures) were approved. In 2010 and 2011, the figures dropped again to 33 and 34, respectively. However, in 2012 to 2018, figures rebounded to 61, 47, 68, 69, 52, 70, and 75, respectively, with 48 in 2019 as of September 30. Figure 1.1 shows an overview of these findings.^[13]

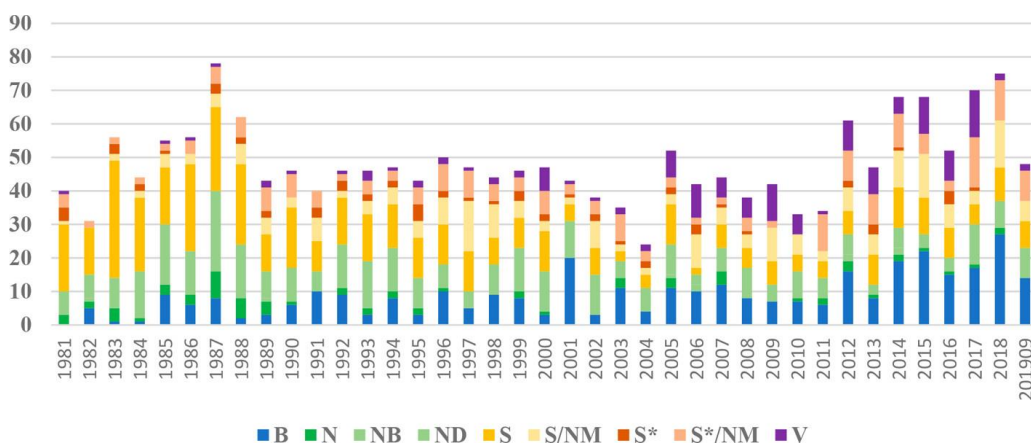


FIGURE 1.1: ALL NEW APPROVED DRUGS BY SOURCE/YEAR (N = 1881), WHERE NEARLY 4 DECADES (1981–09/2019) WERE COVERED. ABBREVIATIONS: BIOLOGICAL (B), UNALTERED NATURAL PRODUCTS (N), BOTANICALS (NB), NATURAL PRODUCT DERIVATIVE (ND), SYNTHETIC DRUGS (S), SYNTHETIC DRUGS WITH A NATURAL PRODUCT PHARMACOPHORE (S*), VACCINES (V) AND NM IS A MIMIC OF NATURAL PRODUCTS. FIGURE FROM THE REVIEW OF NEWMAN AND CRAGG.^[13]

In addition, untargeted metabolomics approaches are transcending the classical workflow of lead compound discovery from diverse natural sources. The classical

approach typically starts with biological screening of crude extracts, followed by (bioassay-guided) fractionation and isolation, plus identification of bioactive compounds. Although proven to be successful, this approach is often inefficient, labor-intensive and time-consuming. To overcome this bottleneck, the “omics” approach, which combines analytical, computational and statistical tools, can be an indispensable and powerful tool for the analysis of thousands of metabolites present in natural extracts. Analytical methods such as mass spectrometry (MS) and nuclear magnetic resonance (NMR) spectroscopy are employed in metabolomics to comprehensively elucidate the plant constituents for screening and drug discovery. The metabolomics workflow provides a potential strategy to streamline the classic and very laborious process of isolating these natural products, which often involves the re-isolation and identification of known compounds.^[14,15]

1.3 BENEFICIAL EFFECTS OF POLYPHENOLS AND THEIR METABOLITES

The WHO recommends increasing the consumption of fruit, vegetables and fiber as a key lifestyle change that could help to reduce the risk of NCDs.^[16] Fruit and vegetables contain many essential vitamins and minerals, but also a class of phytochemicals called polyphenols. These polyphenols, which are omnipresent in plants, are known to promote health benefits and show promising results in clinical trials against certain NCDs.^[17-21] Polyphenols consist of a large class of molecules including subclasses such as flavonoids, phenolic acids, stilbenes and lignans. Flavonoids constitute the main subclass and share a structural C6-C3-C6 backbone, formed by 2 aromatic rings (A and B), linked by a bridge of 3 carbon atoms. This C3 bridge forms a third heterocycle containing an oxygen atom (ring C) for most flavonoids. Flavonoids can thus be further divided into flavan-3-ols, flavonols, flavones, isoflavones, flavanones and anthocyanins, based on the presence or absence of a double bond between C2 and C3, a carbonyl group at C4 and a hydroxyl group at C3 (see Figure 1.2). A rich structural diversity is seen in hydroxylation and/or methoxylation patterns on these backbones. Naturally

occurring flavonoids mostly exist as glycosides (C- and O-glycosylation) and non-glycosylated conjugates, which can highly influence their bioavailability.^[22,23]

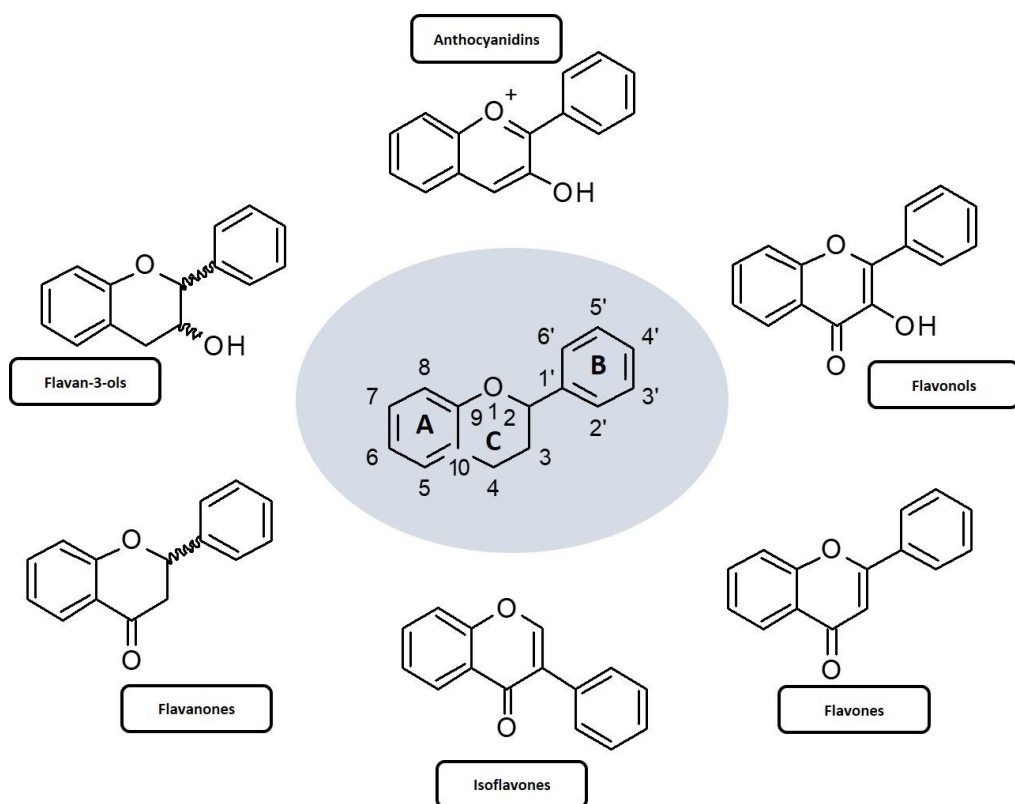


FIGURE 1.2: BASIC STRUCTURE OF FLAVONOID SUBCLASSES.

Epidemiological studies are backed by *in vitro* and *in vivo* animal studies; however, these studies often overlook the poor absorption and extensive metabolism of polyphenols, although it is a key factor for their bioactivity. As discussed in more detail in chapter 3, a significant amount of polyphenols enter the colon where the colonic microbiota transforms these compounds to more absorbable molecules with potential bioactivity. It is thus crucial to have a good understanding of these biotransformations in order to draw correct conclusions and unravel their mechanisms of action.^[24] Equol, for example, is a soy isoflavone-derived metabolite formed from daidzin (the glycoconjugate) via daidzein (the aglycon) by bacteria in the distal region of the small

intestine and colon (see Figure 1.3). Equol is more stable and is more easily absorbed than its precursor daidzin. Moreover, equol shows strong estrogenic activity and epidemiological data suggest that regular intake of isoflavones from soy reduces the incidence of menopausal symptoms in women, osteoporosis, cardiovascular diseases and cancer.^[25] The global or primary mechanism of action of polyphenols was originally thought to be explained by their antioxidant effect. However, the reality is much more complex and these antioxidant effects are no longer considered to be very relevant *in vivo*, as these compounds do not reach sufficiently high concentrations in most tissues to have a significant antioxidant effect in terms of scavenging free radicals. Biological effects involve other biochemical and molecular mechanisms, regulating intra- and intercellular signaling pathways such as nuclear transcription factors and modulating the synthesis of inflammatory mediators, including cytokines, tumor necrosis factor α and pro-inflammatory interleukins.^[26]

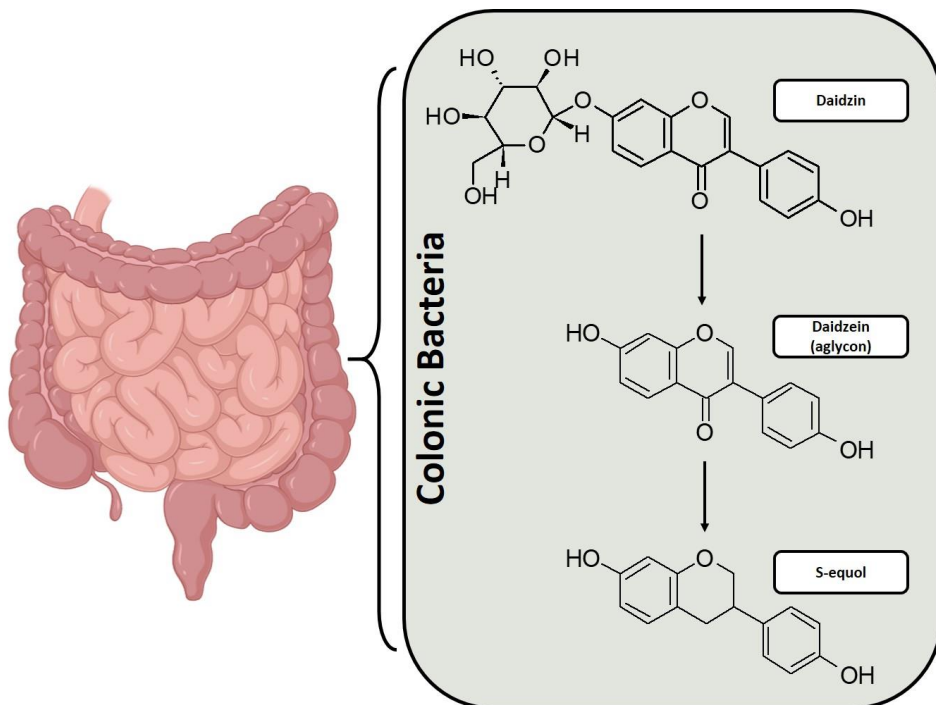


FIGURE 1.3: BIOCONVERSION OF ISOFLAVONE DAIDZIN BY COLONIC MICROBIOTA INTO ITS AGLYCON DAIDZEIN, RESULTING IN ITS BIOACTIVE METABOLITE EQUOL.

1.4 DISSERTATION OUTLINE

Since many NSAIDs show severe gastrointestinal side effects, there is a high need for new and safer anti-inflammatory drugs. An integrated strategy was developed to characterize new anti-inflammatory lead compounds derived from *Filipendula ulmaria*. Medicinal plants such as willow bark (*Salix* spp. including *Salix alba* and others) and meadowsweet (*Filipendula ulmaria*) extracts are widely used since ancient times because of their anti-inflammatory properties. Preparations from the herb and/or flowers of *Filipendula ulmaria* have been used traditionally since the late 16th and 17th century for the treatment of inflammatory diseases, as a diuretic and antirheumatic. In some countries of the European Union, tinctures or tincture-based products containing alcoholic extracts of Filipendulae Herba are on the market as food supplements used for complaints such as rheumatic and arthritic pain. Salicylic acid, the *in vivo* metabolite of salicylic alcohol derivatives present in *Salix* or *Filipendula* species, is thought to be responsible for part of their pharmacological activity, but there is increasing evidence that other constituents (genuine or formed after *in vivo* metabolism, such as catechol for *Salix* extracts) contribute as well.^[27] Similar to *Salix* species, meadowsweet also contains salicylates and its precursors (methyl salicylate, salicylaldehyde, salicylalcohol and their glycosides), as well as other phenolic constituents. It has been shown to contain flavonoid aglycons (e.g. quercetin and kaempferol), glycosylated flavonoids (such as rutin, hyperoside, quercitrin, avicularin and astragalgin) and hydrolysable tannins (tellimagrandin I and II, rugosin A, B, D, and E), which all may undergo biotransformations in the colon. However, its active constituents are not known, although obviously it can be expected that the salicylates will play a role. Anti-inflammatory activity has been documented by *in vitro* and animal studies. This supports the use of meadowsweet preparations against inflammatory diseases.^[28] Therefore, *Filipendula ulmaria* was selected for this PhD project.

Chapter 2 further describes the fascinating historical use of *Filipendula ulmaria*, its general characteristics and its reported activity in literature. The **optimization of a generic and comprehensive extraction protocol and the phytochemical composition** of this plant species, analyzed by UPLC-DAD-HRMS, will be discussed in this chapter. In view of the phenolic nature of the main constituents, extensive biotransformation after oral intake before absorption can be expected. Natural products are often pro-drugs, which must undergo *in vivo* metabolic conversion. This urges the need for identification and activity profiling of the intestinal metabolites.

Chapter 3 gives an in depth explanation of the gastrointestinal tract, the importance of the relationship between polyphenols and the gut microbiota and a general breakdown of the biotransformation of the different polyphenol classes. In this chapter, it is described how a *Filipendula ulmaria* extract was processed in an *in vitro* **Gastrointestinal Biotransformation Model**. This model, previously developed at the lab of NatuRA, was used to mimic human biotransformation processes in the stomach, small intestine and colon including fermentation by pooled human feces. Samples before, during and after biotransformation were analyzed by UPLC-DAD-HRMS. In order to process the complex and dynamic data of the biotransformation experiment, a novel, in-house **automated data analysis workflow was implemented** to render as much information as possible from the longitudinal LC-MS data and to select the most interesting time profiles.

Chapter 4 completes the project by discussing the **anti-inflammatory activity of *Filipendula ulmaria* and its possible metabolites**. NSAIDs block the biosynthesis of prostaglandins, which mediate the typical signs of inflammation, through inhibition of cyclooxygenase (COX) enzymes. Therefore, cell-based COX-2 gene expression, as well as COX-1 and -2 enzyme inhibition were used to evaluate anti-inflammatory activity. Activation of nuclear factor κ B (NF- κ B) is one of the main key regulatory mechanisms of inflammation, modulating DNA transcription of inflammatory proteins such as

chemokines, cytokines, interleukins, interferons and COX-2. For this reason, a NF- κ B gene reporter assay was also applied as described in chapter 4, to give additional information on the anti-inflammatory activity of *Filipendula ulmaria* and its constituents. An overview is illustrated in Figure 1.4.

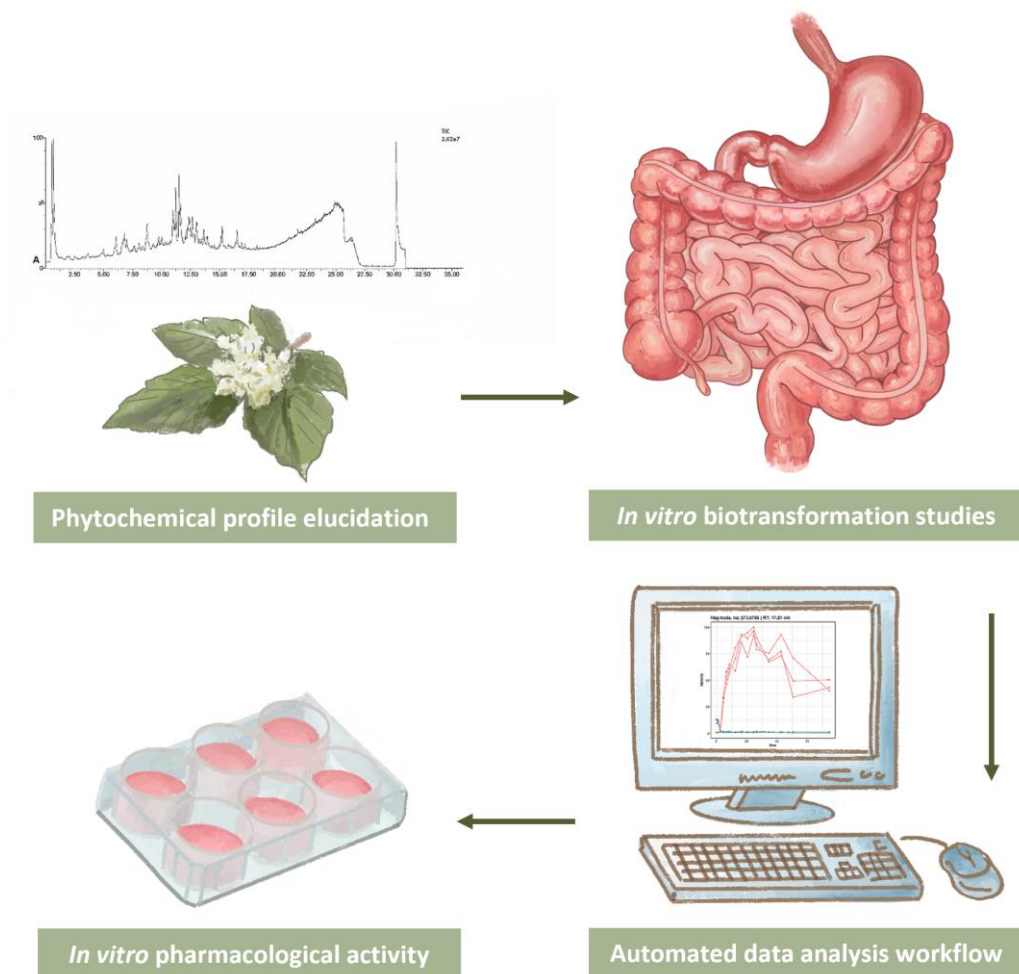


FIGURE 1.4: OUTLINE OF THE THESIS. CHAPTER 2 WILL DISCUSS THE OPTIMIZATION OF A GENERIC AND COMPREHENSIVE EXTRACTION PROTOCOL AND THE PHYTOCHEMICAL COMPOSITION OF *FILIPENDULA ULMARIA*. CHAPTER 3 WILL DESCRIBE THE *IN VITRO* GASTROINTESTINAL BIOTRANSFORMATION OF A *FILIPENDULA ULMARIA* EXTRACT. AN IN-HOUSE AUTOMATED DATA ANALYSIS WORKFLOW WILL BE IMPLEMENTED IN ORDER TO PROCESS THE COMPLEX AND DYNAMIC DATA OF THE BIOTRANSFORMATION EXPERIMENT AND TO SELECT THE MOST INTERESTING TIME PROFILES. CHAPTER 4 WILL DISCUSS THE ANTI-INFLAMMATORY ACTIVITY OF *FILIPENDULA ULMARIA* AND ITS POSSIBLE METABOLITES.

REFERENCES

- [1] Chen L, Deng H, Cui H, Fang J, Zuo Z, Deng J, et al. Inflammatory responses and inflammation-associated diseases in organs. *Oncotarget*. 2018;9(6):7204-18.
- [2] Fleit HB. Chronic Inflammation. McManus LM, Mitchell RN, editors. *Pathobiology of Human Disease*. San Diego, USA: Academic Press; 2014. p. 300-14.
- [3] WHO. Noncommunicable diseases progress monitor 2020 Geneva, Switzerland: WHO; 2020; Available from: <https://www.who.int/publications/i/item/ncd-progress-monitor-2020>.
- [4] Harris RE, Beebe-Donk J, Alshafie GA. Cancer chemoprevention by cyclooxygenase 2 (COX-2) blockade: results of case control studies. *Subcell Biochem*. 2007;42:193-212.
- [5] Conaghan PG. A turbulent decade for NSAIDs: update on current concepts of classification, epidemiology, comparative efficacy, and toxicity. *Rheumatol Int*. 2012;32(6):1491-502.
- [6] Crofford LJ. Use of NSAIDs in treating patients with arthritis. *Arthritis Res Ther*. 2013;15 Suppl 3:S2.
- [7] Sciensano. Chronische ziekten en aandoeningen: gezondheidsenquête 2018 Brussels: Sciensano; 2019; Available from: <https://www.sciensano.be/nl/biblio/gezondheidsenquête-2018-chronische-ziekten-en-aandoeningen-0>.
- [8] Taylor D. The pharmaceutical industry and the future of drug development. Hester RE, Harisson RM, editors. *Pharmaceuticals in the Environment*. Royal society of chemistry; 2016. p. 1-33.
- [9] Lahlou M. The success of natural products in drug discovery. *Pharm. Pharmacol*. 2013;4(3):17-31.
- [10] Thomford NE, Senthebane DA, Rowe A, Munro D, Seele P, Maroyi A, et al. Natural products for drug discovery in the 21st Century: Innovations for novel drug discovery. *Int J Mol Sci*. 2018;19(6).
- [11] Butler MS. The role of natural product chemistry in drug discovery. *J Nat Prod*. 2004;67(12):2141-53.
- [12] Efferth TZ, S.; Georgiev, M. I.; Liu, L.; Wagner, H.; Panossian, A. Nobel Prize for artemisinin brings phytotherapy into the spotlight. *Phytomedicine*. 2015;22:A1-3.
- [13] Newman DJ, Cragg GM. Natural products as sources of new drugs over the nearly four decades from 01/1981 to 09/2019. *J Nat Prod*. 2020;83(3):770-803.

- [14] Salem MA, Perez de Souza L, Serag A, Fernie AR, Farag MA, Ezzat SM, et al. Metabolomics in the context of plant natural products research: from sample preparation to metabolite analysis. *Metabolites*. 2020;10(1).
- [15] Demarque DP, Dusi RG, de Sousa FDM, Grossi SM, Silverio MRS, Lopes NP, et al. Mass spectrometry-based metabolomics approach in the isolation of bioactive natural products. *Sci Rep*. 2020;10(1):1051.
- [16] WHO. Diet, Nutrition and the prevention of chronic diseases Geneva, Switzerland: WHO; 2003; Available from: <https://www.who.int/dietphysicalactivity/publications/trs916/en/>.
- [17] Hollman PC, Geelen A, Kromhout D. Dietary flavonol intake may lower stroke risk in men and women. *J Nutr*. 2010;140(3):600-4.
- [18] Hooper L, Kroon PA, Rimm EB, Cohn JS, Harvey I, Le Cornu KA, et al. Flavonoids, flavonoid-rich foods, and cardiovascular risk: a meta-analysis of randomized controlled trials. *Am J Clin Nutr*. 2008;88(1):38-50.
- [19] Guo XF, Yang B, Tang J, Jiang JJ, Li D. Apple and pear consumption and type 2 diabetes mellitus risk: a meta-analysis of prospective cohort studies. *Food Funct*. 2017;8(3):927-34.
- [20] Benetou V, Orfanos P, Laggiou P, Trichopoulos D, Boffetta P, Trichopoulou A. Vegetables and fruits in relation to cancer risk: evidence from the Greek EPIC cohort study. *Cancer Epidemiol Biomarkers Prev*. 2008;17(2):387-92.
- [21] Inoue M, Tajima K, Mizutani M, Iwata H, Iwase T, Miura S, et al. Regular consumption of green tea and the risk of breast cancer recurrence: follow-up study from the Hospital-based Epidemiologic Research Program at Aichi Cancer Center (HERPACC), Japan. *Cancer Lett*. 2001;167(2):175-82.
- [22] Fraga CG, Croft KD, Kennedy DO, Tomás-Barberán FA. The effects of polyphenols and other bioactives on human health. *Food Funct*. 2019;10(2):514-28.
- [23] Moga MA, Dimienescu OG, Arvatescu CA, Mironescu A, Dracea L, Ples L. The role of natural polyphenols in the prevention and treatment of cervical cancer-an overview. *Molecules*. 2016;21(8).
- [24] Teng H, Chen L. Polyphenols and bioavailability: an update. *Crit Rev Food Sci Nutr*. 2019;59(13):2040-51.
- [25] Mayo B, Vazquez L, Florez AB. Equol: A bacterial metabolite from the daidzein isoflavone and its presumed beneficial health effects. *Nutrients*. 2019;11(9).
- [26] Williamson G. The role of polyphenols in modern nutrition. *Nutr Bull*. 2017;42(3):226-35.
- [27] Freischmidt A, Jürgenliemk G, Kraus B, Okpanyi SN, Müller J, Kelber O, et al. Contribution of flavonoids and catechol to the reduction of ICAM-1 expression in endothelial cells by a standardised Willow bark extract. *Phytomedicine*. 2012;19(3):245-52.
- [28] EMA. Assessment report on *Filipendula ulmaria* (L.) Maxim., herba and *Filipendula ulmaria* (L.) Maxim., flos. European Medicines Agency; 2011.



CHAPTER 2

COMPREHENSIVE EXTRACTION OF FILIPENDULA ULMARIA

*Section 2.3 of this chapter is part of an article published in *Planta medica*: Bijttebier S, **Van der Auwera A**, Voorspoels S, Noten B, Hermans N, Pieters L, et al. A first step in the quest for the active constituents in *Filipendula ulmaria* (meadowsweet): comprehensive phytochemical identification by liquid chromatography coupled to quadrupole-orbitrap mass spectrometry. *Planta Med.* 2016;82(6):559-72.^[1] Contribution of Bijttebier S was experimental work and manuscript writing. Contribution of Van der Auwera A was experimental work and manuscript revision.*

*Section 2.4 of this chapter is part of an article published in *Analytica Chimica Acta*: Bijttebier S, **Van der Auwera A**, Foubert K, Voorspoels S, Pieters L, Apers S. Bridging the gap between comprehensive extraction protocols in plant metabolomics studies and method validation. *Anal Chim Acta.* 2016;935:136-50.^[2] Contribution of Bijttebier S was experimental work and manuscript writing. Contribution of Van der Auwera A was experimental work and manuscript revision.*

2.1 AIM

The aim of this chapter is the optimization of a generic and comprehensive profiling protocol, including extraction and analysis. The complete phytochemical profile of a plant species cannot be extracted with one solvent, nor analyzed by one analytical method. Therefore, the phytochemical composition of *Filipendula ulmaria* was investigated with two complementary generic UHPLC-PDA-amMS methods, combined for the first time into a platform for comprehensive phytochemical characterization. One method is optimized for moderately polar compounds, such as phenolic constituents and another for apolar phytochemicals, such as phytosterols. The design of extraction methods developed for plant metabolomics is important, as this will greatly affect the overall quality of the metabolomics study. *Filipendula ulmaria* was extracted with comprehensive extraction protocols adapted from literature (including extraction with accelerated solvent extraction and flash chromatography) and analyzed with a generic LC-PDA-amMS platform.

2.2 *FILIPENDULA ULMARIA*

2.2.1 GENERAL CHARACTERISTICS

Filipendula ulmaria (L.) Maxim. belongs to the family of the Rosaceae, which is the 19th largest family of plants.^[3] The Rosaceae family is composed of circa 3000 species divided in more than 90 genera with a worldwide distribution and occurs in a wide variety of habitats. They are particular diverse in the temperate Northern Hemisphere. Rosaceae include many well-known species of economic importance as edible fruits (apples, pears, peaches, cherries, almonds,...), also highly valued ornamental plants like

roses, timber crops such as black cherry wood and traditional medicines.^[4,5] Classification within Rosaceae into subfamilies has shifted throughout the years. The most widely adopted classification used to be based on fruit types, which generated 4 subfamilies: Maloideae, Spiraeoideae, Amygdaloideae and Rosoideae. This was changed in 2007 by Potter et al. to 3 subfamilies: Spiraeoideae, Rosoideae and Dryadoideae.^[6] Eventually, the subfamily Spiraeoideae was corrected to Amygdaloideae in 2014.^[7] An overview of this classification is given in Figure 2.1. Because of its diversity, many plants of the Rosaceae family have a long history of being traditionally used as medicinal plants all over the world, including the Balkan countries^[8-11], Italy^[12], Turkey^[13], Lebanon^[14,15] and Pakistan^[16] to name a few.

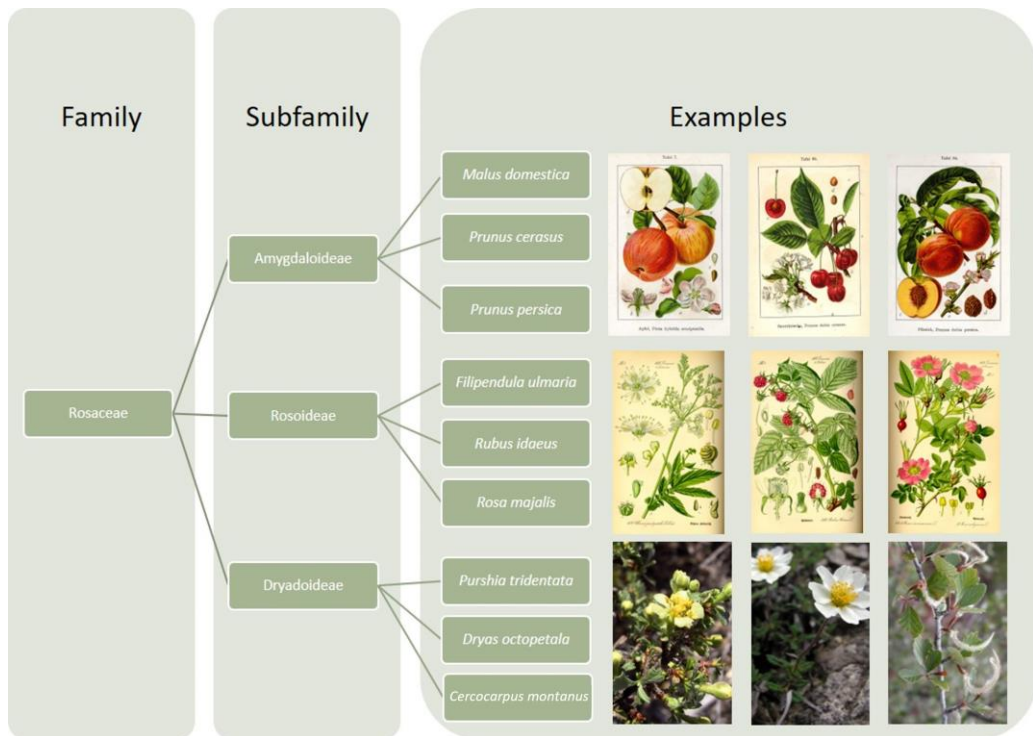


FIGURE 2.1: OVERVIEW OF THE SUBFAMILIES BELONGING TO THE ROSACEAE FAMILY. [17-19]

Filipendula ulmaria is also known under common English names as ‘meadowsweet’, ‘queen of the meadows’, ‘lady of the meadows’ and ‘bridewort’. In Dutch it is more commonly known as ‘moerasspirea’, ‘olmkruid’ or ‘koningin der velden’. Meadowsweet prefers to grow in damp conditions and is indigenous to Europe and western Asia. It has also been introduced to other places including North America. The perennial herb can grow up to two meters tall, has several reddish, erect and rhizomatous stems. The inflorescence contains numerous small white to cream-colored hermaphrodite flowers which are densely clustered. These flowers consist of five rounded petals and five sepals with a great number of stamens. They blossom from June to August, are very fragrant, get pollinated by bees and also attract other wildlife. The leaves of *Filipendula ulmaria* are dark green and are made up of five to nine toothed leaflets. The undersides are silvery and tomentose. The terminal leaflet is bigger and tri-divided, with typically underdeveloped and tiny leaves at the rachis. The plant also bears fruit in the form of achene, which ripen from August to September, measures 2 mm and is twisted into a spiral.^[20,21] Figure 2.2 illustrates the botanical characteristics of *Filipendula ulmaria*.



FIGURE 2.2: ILLUSTRATION AND PHOTOS OF THE PLANT PARTS OF *FILIPENDULA ULMARIA*.^[17,22]

2.2.2 HISTORICAL DATA AND TRADITIONAL USE

Findings show that meadowsweet clearly was a flower of importance to our ancestors. The application of pollen analysis to samples from different archaeological Bronze Age and Iron Age sites shows the importance of meadowsweet, especially in Northern Europe. The exact relationship of the flower and the people back then is still under debate, but most of the evidence suggests the use of meadowsweet for mead production (i.e. 'honey-wine', an ancient alcoholic beverage made by fermenting honey and sometimes fruits, spices, grains and hops). The pollen of this plant are not uncommon in honey residues, but the amount of pollen found in most of these sites is beyond what is expected for just honey. This is probably indicative for the use of *Filipendula ulmaria* as a sort of flavoring agent, which also indicates a mead or other alcoholic beverages. The pollen analysis of human coprolites from Birka, Sweden (a Viking Age site, 8th-10th century AD) and Dürrnberg, Austria (an important Iron Age salt-mining area, 6th-4th century BC) suggested the consumption of honey. Significantly high values of *Filipendula ulmaria* pollen suggests that it was most likely added to mead and that it was part of the former diet.^[23] In Aberdeenshire, Scotland, the remains of a young man were found in a short burial cist together with a beaker dating back to the Bronze Age. Analysis of the pot showed a high percentage of *Filipendula ulmaria* pollen in the fill residue, which suggest that the pot was probably filled with a liquid containing these flowers. This could have been a concentrated *Filipendula ulmaria* floral extract, a general tonic or even mead.^[24] A similar Bronze Age grave has been found in Ashgrove, Scotland, where pollen analysis of a bucket also revealed high amounts of *Filipendula ulmaria*.^[25] Many examples of other pollen analysis of Bronze Age burial beakers, vessels and stains in Scotland and also in Denmark, where high values of immature meadowsweet pollen were detected, exist. The immature pollen indicate the intentional addition of the flowers to alcoholic drinks for flavoring and preservation.^[23,26] Interestingly, the oldest record of mead so far known, was discovered in 2007. In southern Georgia, at the Kodiani burial mound, a huge amount

of meadowsweet pollen were found in a pot. This is many years before the Scottish or Danish samples, during Georgia's Bronze Age around 27th-25th century BC.^[27] Meadowsweet was one of the three most sacred herbs for the Druids, together with vervain and water-mint. In medieval period, meadowsweet was commonly used as a known remedy for headaches. In 'The Knight's Tale', from Geoffrey Chaucer's 14th century *The Canterbury Tales*, a drink called 'Save' is mentioned. This drink contains meadwort, i.e. an older name of *Filipendula ulmaria*, as one of the 50 ingredients. The root was also frequently added to white wine to aid with fevers. A hot water infusion using the leaves was used against headaches and rheumatic pain. In the same manner the flowers were infused to help combat colds, influenza, as well as helping with edema and arthritis.^[28] Moreover, *Filipendula ulmaria* is known for its sweet and almond-like smell, which was apparently very popular with Queen Elizabeth I (16th century AD) who loved it as a fragrant strewing herb in her chambers.^[29] Other than combating fever and pain, *Filipendula ulmaria* was also traditionally used to treat conditions of the gastrointestinal tract, such as dyspepsia, heartburn, gastritis, gastroenteritis and children's diarrhea. Additionally, it was used in the treatment of rheumatism, kidney problems, urinary stones and as a diuretic.^[30,31] Nowadays, it is still used as a digestive remedy or diuretic, as supportive therapy for colds or influenza, for analgesia (headaches and toothaches), and for minor painful articular conditions. Currently, sachets containing comminuted herbal substance for tea, hard capsules of the powdered herbal substance, hard capsules with dry aqueous or ethanolic extract and tinctures have been reported to be on the market in the European Union. In accordance to regulatory guidelines in Belgium, the indication must be stated as: "Traditionally used for painful articular conditions although its activity has not been proved in accordance with current evaluation criteria for medicines".^[32]

2.2.3 MAIN CONSTITUENTS

It has been shown that meadowsweet contains phenolic constituents such as flavonoid aglycons (e.g. quercetin, kaempferol), glycosylated flavonoids (e.g. rutin, hyperoside, quercitrin, avicularin and astragalin) and hydrolysable tannins (tellimagrandin I and II, rugosin A, B, D, and E), as well as salicylates (salicylic acid, methyl salicylate, salicylaldehyde, salicylalcohol and their glycosides).^[33-39] Only a limited number of non-phenolic constituents such as phytosterols, carotenoids, triterpenes and chlorophyll derivatives have been reported.^[37,40] Nevertheless, the chemistry of meadowsweet has not been studied in a comprehensive manner and its active constituents remain to be revealed.

2.2.4 PHARMACOLOGICAL ACTIVITY STUDIES

2.2.4.1 POSOLOGY

As seen above, *Filipendula ulmaria* has been traditionally known for its use against various medical conditions such as colds and respiratory problems, acid indigestion, peptic ulcers, diarrhea, arthritis and rheumatism. According to the assessment report of the EMA (European Medicines Agency), the recommended daily adult doses are as follows: (comminuted) herbal substance (for tea preparation) of 2 - 18 g (single dose of 1.5 - 6 g), powdered herbal substance dosage of 250 - 1500 mg (single dose of 250 - 500 mg) and tincture dosage of 2 - 12 mL (single dose of 2 - 4 mL). The flowers can be taken as a herbal tea as well, with a daily adult dose of 2.5 - 6 g (single dose of 2.5 - 3 g).^[32] A posology overview can be found in Table 2.1.

TABLE 2.1: RECOMMENDED POSOLOGY OF *FILIPENDULA ULMARIA*.^[32]

Type of Preparation	Single Dose	Daily Dose
Herb: (comminuted) herbal substance (for tea preparation)	1.5 - 6 g	2 - 18 g
Herb: powdered herbal substance	250 - 500 mg	250 - 1500 mg
Herb: tincture	2 - 4 mL	2- 12 mL
Flowers: herbal substance (for tea preparation)	2.5 - 3 g	2.5 - 6 g

2.2.4.2 SIDE EFFECTS AND TOXICITY

Clinical safety data on *Filipendula ulmaria* are very limited. On the other hand, no safety problems concerning the traditional use of *Filipendula ulmaria* or its preparations have been reported. *Filipendula ulmaria* should not be used in cases of hypersensitivity to salicylates; however, side effects, interactions and contra-indications commonly associated with aspirin are considered unlikely. In general, preparations of *Filipendula ulmaria* are considered not harmful when used in the recommended dosages for the specified indications.^[32] The acute toxicity of orally administered lyophilized flower infusions of meadowsweet in Swiss Webster mice showed good safety profiles, with the median lethal dose (LD₅₀) of the tested extracts being greater than 2000 mg/kg bodyweight.^[41] *Filipendula ulmaria* root extract demonstrated the absence of genotoxic activity in *Drosophila melanogaster* using a comet assay.^[42]

2.2.4.3 ANTI-INFLAMMATORY ACTIVITY

As discussed in the previous paragraph about the history of the plant, the anti-inflammatory properties of *Filipendula ulmaria* have been frequently claimed in ethnomedicine. Its effects on different inflammatory markers found in literature are touched briefly in the following part, the importance of the different inflammatory cells and markers can be found in chapter 4 in more detail. Halkes et al. found strong inhibitory activities on the classical pathway of the complement system of root, flower and herb extracts of meadowsweet.^[43] Activation of the complement system is known to contribute to the pathology in a number of autoimmune and inflammatory diseases, including rheumatoid arthritis.^[44] TNF- α (tumor necrosis factor) and IL- β (interleukin) are pro-inflammatory cytokines secreted by activated macrophages in chronic inflammation and are detectable in synovial fluid of patients with rheumatoid arthritis. Drummond et al. have assessed the response of activated THP-1 macrophages (human monocytotic leukemic cell line, differentiated with phorbol-12-myristate-13-acetate) on an aqueous *Filipendula ulmaria* extract by measuring cytokine production via ELISA. The extract, containing 3 μ M quercetin, significantly reduced TNF- α and IL-1 β .^[45] In an *ex vivo* experiment in human platelets, the effect of *Filipendula ulmaria* and *Filipendula vulgaris* (aqueous extract of the flowers) on eicosanoid biosynthesis was evaluated. These extracts, at a concentration range of 0,25 - 10 mg/mL, decreased the production of these proinflammatory eicosanoids. Several isolated flavonoids, present in both plants, were also found to suppress their biosynthesis indicating the contribution of active constituent different from salicylic acid contributing to the anti-inflammatory effect.^[46] Trouillas et al. examined the anti-inflammatory properties of plants found in the Limousin countryside in France. *Filipendula ulmaria* belonged to the group of plants with the highest inhibitory activity against 15-lipoxygenase, which is an important enzyme in the leukotriene biosynthesis pathway. Leukotrienes are potent pro-inflammatory mediators which play a role in a variety of inflammatory diseases.^[47] Another research team examined the anti-inflammatory efficacy of herbal drugs

reported in Austrian folk medicine, including *Filipendula ulmaria*. The flower extract, with a test concentration of 10 µg/mL, showed an activation of nuclear factors PPARα (peroxisome proliferator-activated receptor) and PPARγ. These nuclear factors are important molecular players inhibiting NF-κB (Nuclear factor κB) responses, a master switch for pro-inflammatory gene transcription. An inhibition of NF-κB by the herbal extract was detected as well. Both *in vitro* experiments were transactivation assays with a luciferase transporter gene in HEK293 cells.^[48] Methanolic meadowsweet extracts of both the aerial part and the roots was assessed in a COX-1 and -2 (cyclooxygenase) enzyme inhibition assay (50 µg/mL), and a COX-2 gene expression assay (25 µg/mL). Both extracts inhibited the enzyme activity of COX-1 and -2, whereby the aerial extract was twice as effective as the roots. The extracts showed no significant effect on COX-2 gene expression in THP-1 cells.^[49] Cholet et al. also studied the anti-inflammatory effects of *Filipendula ulmaria* (methanolic extract of the aerial parts, 50 µg/mL) on COX-2 and its enzymatic product PGE₂ (prostaglandin E₂). This study suggested that the extract does indeed have an anti-inflammatory effect on COX-2 and PGE₂; however, it also appeared to have an impact on immune response. *Filipendula ulmaria* likely works as an immunostimulant, improving neutrophil and monocyte recruitment, as well as activating monocytes, macrophages, Th1 and presumably Th17.^[50] Finally, two publications exist with *in vivo* anti-inflammatory results on *Filipendula ulmaria*. As mentioned before, it is important to confirm *in vitro* activity of extracts with *in vivo* assays, since the constituents of the extracts can be metabolized after oral ingestion. In the first publication by Katanić et al. the hot-plate test (i.e. antinociceptive activity, expressed as latency to respond) and the carrageenan-induced paw edema model (i.e. local acute inflammatory response) in male Wistar rats were employed, testing 100 and 200 mg/kg bodyweight of aerial or root extract orally. Both doses and type of extract significantly increased latency time versus the control group in the hot-plate test. Also, the maximum swelling in the paw edema assay decreased with treatment.^[49] Samardzic et al. looked at the antihyperalgesic and antiedematous

activities of a meadowsweet flower extract in Wistar rats with carrageen-induced paw edema. The extract caused a significant dose-dependent (100 - 300 mg/kg bodyweight) pain lowering effect. However, contrary to Katanić et al., they did not find a significant effect on reducing paw edema.^[41]

2.2.4.4 ANTI-ULCEROGENIC ACTIVITY

In a 1980 Russian study by Barnaulov et al., a decoction of *Filipendula ulmaria* flowers lowered the formation of lesions of the glandular part of the stomach after injections of reserpine to rats and mice, as well as phenylbutazone to rats. It was also able to prevent acid-induced stomach lesions by acetylsalicylic acid in rats. The extract promoted healing of chronic ulcers in rats after injection of 70% ethanol into the luminal wall of the glandular part.^[51] A more recent study was conducted by Serbian scientists in 2018. *Filipendula ulmaria* was administered (dose: 100 mg/kg, 200 mg/kg and 300 mg/kg) one hour before induction of gastric lesions in male Wistar rats, which was done by oral gavage of absolute ethanol. All doses of meadowsweet demonstrated a gastroprotective effect when looking at the average gastric damage scores (GDSs) compared to controls which received the vehicle (water). Interestingly, the researchers also found a decrease in GDSs when administering isolated compounds spiraeoside (50 mg/kg) and tellimagrandin II (40 mg/kg).^[46]

2.2.4.5 ANTIBACTERIAL AND ANTIFUNGAL ACTIVITY

Rauha et al. screened several Finnish plants, including a *Filipendula ulmaria* extract, for their antimicrobial effects. Meadowsweet appeared to be one of the most active plant extracts in this study with a bactericidal effect on the growth of *Staphylococcus aureus* and *Escherichia coli*. Interestingly, pure flavonoid aglycons (present in the plant), such as quercetin and naringenin, also showed inhibition while the glycosidic forms, rutin and naringin, respectively, showed no clear effect.^[52] Denev et al. showed that aerial parts of meadowsweet had an antimicrobial effect against a broad spectrum of human pathogens. The extract demonstrated antimicrobial activity in the diffusion assay

against *Staphylococcus aureus* strains, *Proteus vulgaris*, *Klebsiella pneumoniae* and *Candida albicans*, even in low test concentrations. Low MIC₅₀ values were also observed against *Staphylococcus aureus*, *Proteus vulgaris* and *Klebsiella pneumoniae*. Lastly, meadowsweet also showed high activity against genetically modified *Escherichia coli*.^[53] Another study found that an hydroethanolic extract of the *Filipendula ulmaria* herb inhibited the growth of *Helicobacter pylori* in a microdilution assay. *Helicobacter pylori* is the major cause of acute and chronic gastritis, as well as being the predisposing factor for peptic ulcer disease and gastric carcinoma. It has even been classified by the WHO as a class 1 carcinogen. Even though *Filipendula ulmaria* was one of the most active tested extracts, it has to be noted that the IC₅₀ values found by Cwikla et al. showed a much lower efficacy than the marketed antibiotics, which emphasizes the use of the herbal extract as an adjunct treatment.^[54] Lastly, medicinal flowers from Portugal, including *Filipendula ulmaria*, were evaluated for antifungal properties. In this study promising antifungal activity was revealed against *Candida albicans*, *Candida glabrata*, *Candida parapsilosis* and *Candida tropicalis*.^[38]

2.2.4.6 ANTICANCER ACTIVITY

The first experimental study concerning the anticancer activities of *Filipendula ulmaria* extract was investigated in mice with cervical dysplasia, which was induced by 7,12-dimethyl-benz(a)anthracene. In this Russian publication from 1993, a 39% drop in the frequency of squamous cell carcinoma of the cervix and vagina was observed after administering a local decoction of the flower. In the same paper, a clinical study in 48 patients with cervical dysplasia was also described. After local application of an ointment containing a meadowsweet flower decoction, an improvement was seen in 32 patients and 25 cases even achieved complete remission. No recurrence was observed in 10 of the cured patients over a 12 month period.^[55] In a second article, the authors looked at the cytotoxic effect on cultured human lymphoblastoid Raji cells. A crude ethanol extract of meadowsweet appeared to be cytotoxic at a concentration of

10 and 50 µg/mL by disrupting processes of cytokinesis in addition to growth suppression, displaying a comparable activity to that of fluorouracil.^[56] Based on these results, Lima et al. carried out a study with meadowsweet on 3 different human cell lines, representing 3 types of cancer: non-small cell lung cancer (NCI-H460), melanoma (A375-C5) and breast adenocarcinoma (MCF-7). Different flower extracts of *Filipendula ulmaria* (infusion, decoction, methanol and methanol:water) inhibited the growth of these human tumor cell lines, which is in agreement with the cytotoxic effects found in the previous study. Moreover, the effect of the decoction on the NCI-H460 cells was further investigated. The extract reduced cellular proliferation and increased cellular p21 levels, which might partly explain its mechanism of action as cyclin-dependent kinase inhibitor p21 is one of these factors that promote cell cycle arrest.^[57] In the last years, literature about the *in vivo* anticancer effect of *Filipendula ulmaria* started growing rapidly because of the research of Bespalov et al. They published several articles about the effect of daily administration of a *Filipendula ulmaria* decoction on multiple types of cancer in rats. In all experiments, the average daily intake of meadowsweet was about 1 g/kg bodyweight, which was given until the end of each experiment. In a 2017 publication, they demonstrated the ability of meadowsweet to inhibit neurocarcinogenesis induced transplacentally (by ethylnitrosourea) in rat offspring.^[58] An inhibitory effect on radiation-induced carcinogenesis in rats was also observed. Multiplicity of all tumors and incidence of malignant tumors, especially for breast tumors, were reduced in γ -irradiated rats receiving meadowsweet in their drinking water over 16 months.^[59,60] Since *Filipendula ulmaria* possesses anti-inflammatory properties, and chronic inflammation is linked to development of colorectal cancer, another animal experiment was conducted in rats. This time colorectal carcinogenesis was induced by methylnitrosourea locally and, again, the animals were given meadowsweet decoction daily. Carcinogenesis was significantly inhibited, especially in the colon, i.e. decrease in incidence and multiplicity of all tumors and malignant neoplasms.^[61] In yet another

paper, Bespalov et al. described the inhibitory effect (significant decrease in both incidence and multiplicity) of the meadowsweet extract on mammary carcinogenesis after injecting female rats with methylnitrosourea directly into mammary gland tissue.^[62] Research from Amosova et al. evaluated the effect of an ethanolic extract from the aerial part of meadowsweet on the development of Lewis lung carcinoma in mice and the effectiveness of cytostatic therapy. They found a dose-dependent (50 and 100 mg/kg bodyweight) antimetastatic action in C57BL/6 mice with Lewis lung carcinoma. Combined treatment with cyclophosphamide increased the antitumor effect of the cytostatic drug, indicating the possibility of adjuvant therapy with meadowsweet.^[63]

MATERIALS AND METHODS

2.3 A FIRST STEP IN THE QUEST FOR THE ACTIVE CONSTITUENTS IN

FILIPENDULA ULMARIA

A wide diversity of phytochemical structures is produced in nature. Consequently, the complete metabolite profile cannot be extracted with one solvent nor be analyzed with one analytical method. Comprehensive phytochemical characterization should, therefore, be performed with several analytical methods to cover the whole range of plant metabolites present in plants. The goal of this experiment was to explore the phytochemical composition of *Filipendulae Ulmariae Herba* in a comprehensive manner. A generic characterization platform consisting of two UHPLC-PDA-amMS methods, complementary in terms of polarity, was used to analyze the broad spectrum of phytochemicals present in *Filipendulae Ulmariae Herba* as a first step in the search for the active constituents of *Filipendula ulmaria*.

2.3.1 CHEMICALS

UHPLC-grade methanol, acetonitrile, and ethyl acetate were purchased from Biosolve (Valkenswaard, The Netherlands). Ultrapure water with a resistivity of $18.2 \times M\Omega \times cm$ at 25 °C was generated with a Millipore system. Dichloromethane for gas chromatography, *n*-hexane for gas chromatography, acetone for gas chromatography and sodium hydrogen carbonate were purchased from Merck (Darmstadt, Germany). Formic acid, acetic acid, ammonium formate, ammonium acetate, (D-Ala²)-leucine enkephalin, butylated hydroxytoluene (BHT), and sand (quartz) were supplied by Sigma-Aldrich. Commercially available mixtures to calibrate the mass spectrometer, i.e. MSCAL5-1EA (caffeine, tetrapeptide “Met-Arg-Phe-Ala”, Ultramark) for the positive ion mode and MSCAL6-1EA (sodium dodecylsulfate, taurocholic acid sodium salt,

Ultramark) for the negative ion mode, were purchased from Supelco. The following analytical standards were purchased from Phytolab: apigenin, luteolin, isorhamnetin, kaempferol, kaempferol-3-*O*-glucoside (astragalín), quercetin, quercetin-3-*O*-glucoside (isoquercitrin), quercetin-3-*O*-galactoside (hyperin), quercetin-3-*O*-rutinoside (rutin), quercetin-3-*O*-arabínoside (avicularin), quercetin-3-*O*-rhamnoside (quercitrin), galangin, phloretin, naringenin, (+)-catechin, (-)-epicatechin, (+)-dihydrokaempferol [(+)-aromadendrin], cyanidin-3-*O*-glucoside chloride (kuromanin chloride), cyanidin-3-*O*-rutinoside chloride (keracyanin chloride), procyanidin B2, ellagic acid and eriodictyol. Analytical standards of salicylic acid, protocatechuic acid, gallic acid, *p*-coumaric acid, caffeic acid, chlorogenic acid, β -carotene, stigmasterol, β -sitosterol, miquelianin (quercetin 3-*O*-glucuronide), tannic acid, γ -tocopherol, α -tocopherol and quinic acid were obtained from Sigma-Aldrich. Lutein and violaxanthin were purchased from Carotenature. *Filipendulae Ulmariae Herba* (batch number 19969) was bought from Tilman SA (Baillonville, Belgium). A certificate of analysis describing the identification of *Filipendulae Ulmariae Herba* was in accordance with the specifications of organoleptic, microscopic, macroscopic, chromatographic and steam distillation tests described in the European Pharmacopoeia and was provided by Tilman SA.

2.3.2 PREPARATIONS OF STANDARD SOLUTIONS

Standard stock solutions for the phenolic analytes were prepared at a concentration of 1 mg/mL in UHPLC-grade methanol for each analyte separately and stored in the dark at 4 °C. Dilutions of these solutions were prepared in 60:40 (*v/v*) methanol:40 mM ammonium formate buffer (aqueous). Standard stock solutions and working solutions for the non-phenolic analytes were prepared for each analyte separately at a concentration of approximately 200 μ g/mL. The stock solutions of phytosterols and lipid-soluble vitamins were prepared in methanol + 0.1% BHT. Stock solutions of carotenoids were prepared in dichloromethane + 0.1% BHT. Standard stock and working solutions were stored at -25 °C in the dark under an inert atmosphere

(nitrogen). Dilutions of these solutions were prepared in dichloromethane + 0.1% BHT for analysis.

2.3.3 SAMPLE PREPARATION AND EXTRACTION

The sample material was ground prior to extraction with an MF 10 basic Microfine grinder drive (IKA-Werke GmbH & Co. KG, Staufen, Germany) using a sieve mesh size of 0.5 mm. Two generic sample preparation protocols were developed previously with the aim to be complementary in terms of polarity of extracted compounds.^[64,65] During this study, these two complementary extraction protocols were combined and used in parallel for the first time. The combination of the two extraction methods enables the full range of phytochemical constituents to be extracted. All sample extractions were performed in triplicate.

2.3.3.1 EXTRACTION OF MODERATELY POLAR PHYTOCHEMICALS

An extraction protocol previously developed by De Paepe et al. was applied for the extraction of moderately polar phytochemicals.^[64] Briefly, 1 g of *Filipendulae Ulmariae* Herba was extracted with methanol:40 mM ammonium formate buffer (aqueous) (20:80; v/v) in a first step and 40 mM ammonium formate in methanol in a second step. Each extraction was performed by ultrasound-assisted solid-liquid extraction with 10 mL of the appropriate solvent by using a 2200 R-4 Ultrasonic sonicator (40 kHz, 100 W) (Branson Ultrasonic Corporation) for 60 min at room temperature. After 30 min of extraction, the solutions were vortex mixed (IKA MS2 Minishaker, IKA Werke GmbH & Co. KG). During sonication, the temperature was kept below 40 °C. The samples were subsequently centrifuged at 3000 rpm (approximately 1450 g) using an Allegra™ Centrifuge (Beckman Coulter Inc.). Following the two consecutive extraction cycles, the supernatants were combined, diluted 5 times, and stored at 4 °C until analysis.

2.3.3.2 EXTRACTION OF APOLAR PHYTOCHEMICALS

A method previously developed by Bijttebier et al. was used for the extraction of a wide array of apolar phytochemicals.^[65] Approximately 1 g of *Filipendulae Ulmariae Herba* was spiked with *trans*- β -Apo-8'-carotenal (internal standard). The sample was subsequently mixed with approximately 1 g of sodium hydrogen carbonate and sand. Ultrapure water was added until the sample was hydrated (approximately 3 mL) and was let to rest in the dark under N₂ for 30 min to allow swelling of the matrix for better analyte extraction. Afterwards, the mixture was homogenized with sand and loaded into a 33 mL Accelerated Solvent Extraction (ASE) cell (Thermo Fisher Scientific). The mixture was extracted 3 times with 70:30 acetone:methanol + 0.1% BHT (v/v) with an ASE 200 (Thermo Fisher Scientific). The ASE settings were as follows: oven temperature 40 °C, pressure 1050 psi, preheating 0 min, heating 5 min, static 2 min, flush percentage 65%, purge 100 s. The three extracts were combined in a separating funnel and 100 mL of 10% NaCl (aqueous) and 15 mL of *n*-hexane was added. The *n*-hexane phase was transferred into a recipient after vigorous shaking and the polar phase was extracted twice more with 15 mL hexane. The combined *n*-hexane fractions were evaporated to dryness, dissolved in 10 mL dichloromethane + 0.1% BHT and stored in the dark under nitrogen at -25 °C until analysis.

2.3.4 INSTRUMENTAL ANALYSIS

Analogous to the complementary extraction methods, two generic LC-PDA-amMS methods were developed previously on an orbitrap MS (Exactive; Thermo Fisher Scientific) with the aim to be complementary in the polarity range of analyzed compounds.^[64,65] These methods were used for the first time in parallel during the current study to enable the characterization of the full range of phytochemical constituents. Moreover, the analytical methods were further improved by using a hybrid quadrupole-orbital trap MS analyzer (Q Exactive; Thermo Fisher Scientific), thereby enabling selective ion fragmentation to obtain clean compound spectra.

Because of the limitations in acquisition speed of the orbitrap detector, the sample extracts had to be analyzed 3 times to gather the desired spectral information. A first analysis was performed by switching polarities (positive and negative) during ionization to comprehensively detect compounds in both polarities in a single run. A second and third analysis was performed to selectively fragment the generated ions with HCD (Higher-energy Collisional Dissociation) in the HCD cell before detection with the orbitrap mass analyzer. The precursor ions generated by ionization were selected for fragmentation based on their abundances during ddMS² (data-dependent fragmentation). These consecutive ddMS² experiments were performed in positive and negative ionization modes, respectively. In cases where ddMS² did not allow for the full characterization of the compound substructures because of insufficient product ions, in-source CID (Collision-Induced Dissociation) fragmentation was used in combination with HCD fragmentation to obtain pseudo MS³ spectra.

2.3.4.1 ANALYSIS OF MODERATELY POLAR PHYTOCHEMICALS

The extracts containing moderately polar compounds were analyzed with methodology adapted from De Paepe et al.^[64] For analysis, 5 µL of extract were injected with a CTC PAL autosampler (CTC Analytics) on a Waters Acquity UPLC BEH SHIELD RP18 column (3.0 mm × 150 mm, 1.7 µm; Waters) and thermostatically (40 °C) eluted with an Accela quaternary solvent manager and a Hot Pocket column oven (Thermo Fisher Scientific). The mobile phase solvents consisted of water + 0.1% formic acid (A) and acetonitrile + 0.1% formic acid (B), and the gradient was set as follows (min/A%): 0.0/100, 9.91/74, 18.51/35, 18.76/0, 20.76/0, 20.88/100, 23.00/100. For detection, an amMS (Q Exactive™; Thermo Fisher Scientific) was used with HESI (Heated Electrospray Ionization). During the first analysis, full scan data were acquired using polarity switching with a *m/z* range of 120-1800 and resolving power set at 70 000 at FWHM (full width at half maximum). The spray voltage was set at ± 2.5 kV, sheath gas and auxiliary gas at 47 and 15 (adimensional), respectively, and capillary temperature at

350 °C. Data were also recorded using ddMS² in the positive and negative ionization modes (one analysis per mode) to obtain additional structural information (resolving power set at 17 500 FWHM, stepped collision energy 10, 30, 50 V, isolation window: 4 *m/z*, top 10 of most abundant ions selected for fragmentation). The PDA detector was set to scan from 190 to 800 nm during all analyses.

2.3.4.2 ANALYSIS OF APOLAR PHYTOCHEMICALS

The extracts containing apolar compounds were analyzed with methodology adapted from Bijttebier et al.^[65] For analysis, 1.25 µL of extract was injected on a Waters Acquity UPLC HSS C18 SB column (2.1 mm × 100 mm, 1.8 µm; Waters) and thermostatically (35 °C) eluted. The mobile phase solvents consisted of 50:22.5:22.5:5 (v/v/v/v) water + 5 mM ammonium acetate:methanol:acetonitrile:ethyl acetate (A) and 50:50 (v/v) acetonitrile:ethyl acetate (B), and the gradient was set as follows (min/A%): 0.0/90, 0.1/90, 0.8/70, 20.0/9, 20.1/0, 20.4/0, 20.5/90, 23.0/90. Atmospheric pressure chemical ionization (APCI) was used as an MS ionization technique. During the first analysis, full scan data were acquired using polarity switching with a *m/z* range of 90-1400 and resolving power set at 70 000 at FWHM. The corona discharge current was set at ± 5 µA, the vaporizer and capillary temperatures were set at 450 °C for both the positive and negative APCI. Lock mass correction with (D-Ala²)-leucin enkephalin was applied. Data were also recorded using ddMS² in the positive and negative ionization modes (one analysis per mode) to obtain additional structural information (resolving power set at 17 500 FWHM, stepped collision energy 10, 30, 50 V, isolation window: 4 *m/z*, top 10 of most abundant ions selected for fragmentation). The PDA detector was set to scan from 190 to 800 nm during all analyses.

2.4 BRIDGING THE GAP BETWEEN COMPREHENSIVE EXTRACTION PROTOCOLS IN PLANT METABOLOMICS STUDIES AND METHOD VALIDATION

It is vital to pay much attention to the design of extraction methods developed for plant metabolomics, as any non-extracted or converted metabolites will greatly affect the overall quality of the metabolomics study. Method validation is however often omitted in plant metabolome studies, as the well-established methodologies for classical targeted analyses such as recovery optimization cannot be strictly applied. The aim of the present study is to thoroughly evaluate state-of-the-art comprehensive extraction protocols for plant metabolomics with LC-PDA-amMS by bridging the gap with method validation. Validation of an extraction protocol in untargeted plant metabolomics should ideally be accomplished by validating the protocol for all possible outcomes, i.e. for all secondary metabolites potentially present in the plant. In an effort to approach this ideal validation scenario, two plant matrices were selected based on their wide versatility of phytochemicals: *Filipendula ulmaria* for its polyphenols content, and spicy paprika powder (from the genus *Capsicum*) for its apolar phytochemicals content (carotenoids, phytosterols, capsaicinoids). These matrices were extracted with comprehensive extraction protocols adapted from literature and analyzed with a generic LC-PDA-amMS characterization platform that was previously validated for broad range phytochemical analysis. The performance of the comprehensive sample preparation protocols was assessed based on extraction efficiency, repeatability and intermediate precision and on ionization suppression/enhancement evaluation.

2.4.1 CHEMICALS

Paragraph 2.3.1 described all used solvents, commercially available mixtures to calibrate the mass spectrometer, analytical standards and the

Filipendulae Ulmariae Herba batch. Furthermore, chloroform for HPLC was bought from Acros (Geel, Belgium). Spicy paprika powder (99% paprika, chili pepper) from Versteegen Spices & Sauces N.V. was bought in a local store.

2.4.2 PREPARATION OF STANDARD SOLUTIONS

Standard stock solutions for the phenolic analytes, phytosterols, lipid-soluble vitamins and carotenoids were prepared according to the protocol mentioned in 2.3.2 of the materials and methods section.

2.4.3 SAMPLE PREPARATION AND EXTRACTION

Filipendula ulmaria was ground prior to extraction with an MF 10 basic Microfine grinder drive (IKA-Werke GmbH & Co. KG, Staufen, Germany) using a sieve mesh size of 0.5 mm. The spicy paprika powder was extracted without grinding. Sample extractions were performed in triplicate unless indicated otherwise.

2.4.3.1 REFERENCE EXTRACTION PROTOCOLS

The polar reference extraction method was the extraction protocol previously developed by De Paepe et al., see description 2.3.3.1 in materials and methods section.^[64] For the apolar reference extraction method, the method previously developed by Bijttebier et al. was used for the extraction of a wide array of apolar phytochemicals.^[65] The full explanation can be found under 2.3.3.2 in the materials and methods section.

2.4.3.2 COMPREHENSIVE EXTRACTION PROTOCOLS

2.4.3.2.1 ETHYL ACETATE EXTRACTION

Ethyl acetate extraction was adapted from Halabalaki et al.: 12.5 mL ethyl acetate was added to 1 g of sample. The mixture was shaken for 2 h followed by 1 h of ultrasound-assisted extraction. The mixture was subsequently centrifuged for 5 min at

approximately 1450 g. For analysis of polar metabolites, the extract was diluted 20 times with 60:40 (v/v) methanol:water + 40 mM ammonium formate and stored at 4 °C until analysis. For analysis of apolar metabolites, the extract was evaporated and dissolved in a 10 mL solution of *trans*- β -apo-8'-carotenal in dichloromethane + 0.1% BHT and stored in the dark under nitrogen at -25 °C until analysis.^[66]

2.4.3.2.2 WATER:ETHYL ACETATE EXTRACTION

The extraction procedure is similar to ethyl acetate extraction as described above; however, in addition 3 mL of water was added to the sample before extraction.

2.4.3.2.3 CHLOROFORM:METHANOL:WATER EXTRACTION

Chloroform:methanol:water extraction was based on Theodoridis et al.^[67] and Pimenta et al.^[68]: 2 mL of water, 4 mL of methanol and 4 mL of chloroform were added to 1 g of sample. The mixture was subsequently vortex mixed for 1 min followed by 5 min of ultrasound-assisted extraction, 15 min of shaking and 5 min of centrifugation at approximately 1450 g. For analysis of polar metabolites, an aliquot of the upper phase was diluted 40 times with 60:40 (v/v) methanol:water + 40 mM ammonium formate and stored at 4 °C before analysis. For analysis of apolar metabolites, the upper phase was removed and the lower apolar phase was collected. Additionally, 4 mL of chloroform was added to the remaining wet biomass and vigorously shaken for several seconds. The mixture was centrifuged for 5 min at approximately 1450 g and the lower phase was combined with the previously collected apolar fraction. The combined chloroform extracts were evaporated, dissolved in a 10 mL solution of *trans*- β -apo-8'-carotenal in dichloromethane + 0.1% BHT and stored in the dark under nitrogen at -25 °C until analysis.

2.4.3.2.4 CONTINUOUS EXTRACTION

Continuous extraction was adapted from Yuliana et al.: a frit was inserted into an empty solid phase extraction column. Approximately 1 g of sample was mixed (not grinded)

with 4 g of sea sand and loaded into the extraction column, followed by insertion of a frit on top of the sample mixture. The sample extraction column was subsequently mounted into a Reveleris iES flash instrument (Grace Davison, Columbia, USA) and extracted with a continuous flow of solvents at 8 mL/min. Fractions of 1 min (approximately 8 mL) were collected during the entire extraction cycle rendering 39 fractions (due to dead volume, no solvent is collected in fraction 1). The extraction solvents consisted of *n*-hexane (A), acetone (B), methanol (C) and water (D). The gradient for the continuous extraction from apolar to polar solvents (hereafter called ATP continuous extraction) was set as follows (min/A%/B%/C%): 0.0/100/0/0, 5.0/100/0/0, 15.0/0/100/0, 25.0/0/0/100, 35.0/0/0/0, 40.0/0/0/0. The gradient for the continuous extraction from polar to apolar solvents (hereafter called PTA continuous extraction) is the inverse of the above described gradient. For quantitative analysis of polar metabolites, the 25 most polar fractions were combined and diluted with methanol to 200 mL. For analysis of apolar metabolites, the 25 most apolar fractions were combined, evaporated, dissolved in a 10 mL solution of *trans*- β -apo-8'-carotenal in dichloromethane + 0.1% BHT and stored in the dark under nitrogen at -25 °C until analysis.^[69]

2.4.3.2.5 POLAR TO APOLAR ACCELERATED SOLVENT EXTRACTION (PTA ASE)

Approximately 1 g of sample was homogenized (mixed, not grinded) with sand and loaded into a 33 mL ASE cell (Thermo Fisher Scientific). The sample was extracted in 4 extraction cycles with 1) 50:50 (v/v) methanol:water + 40 mM ammonium formate, 2) methanol, 3) 50:50 (v/v) methanol:acetone, 4) acetone. The ASE settings were as follows: oven temperature 40 °C, pressure 1500 psi, preheat 0 min, heat 5 min, static 2 min, flush percentage 65%, purge 100 sec. Each extraction cycle rendered 45 mL of extract. For analysis of polar metabolites, the extracts were diluted 5 times with 60:40 (v/v) methanol:water + 40 mM ammonium formate and stored at 4 °C until analysis. For analysis of apolar metabolites, all extracts were evaporated until only water

remained or until dryness (depending on the solvent composition), and were subsequently extracted with or dissolved in a 10 mL solution of *trans*- β -apo-8'-carotenal in dichloromethane + 0.1% BHT and stored in the dark under nitrogen at 25 °C until analysis. The 4 different solvent fractions obtained for each sample were analyzed separately. The areas obtained for the different fractions were summed for comparison with the other extraction protocols.

2.4.3.3 EVALUATION OF ARTEFACTS FORMATION

Water extraction: hot water extraction was carried out by adding 10 mL of water at 90 °C to 1 g of sample, which was then placed in a hot water bath at 90 °C for 5 min. The sample was vortex mixed for 1 min and placed back into the hot water bath for 9 min. The sample was cooled in a water bath to room temperature and subsequently centrifuged for 5 min at approximately 1450 g. After removal of the water extract, 10 mL of water at 90 °C was added to the sample followed by ultrasound-assisted extraction at 80 °C for 15 min. The sample was cooled in a water bath to room temperature, the water extracts were combined and centrifuged for 5 min at approximately 1450 g. The extract was diluted 5 times with 60:40 (v/v) methanol:water + 40 mM ammonium formate and stored at 4 °C until analysis. Water extraction at room temperature was carried out using the same extraction procedure at room temperature.

The methylation reaction was adapted from Makkar^[70]: 2 mL of methanol and 200 μ L of sulfuric acid ($\geq 95\%$) were added to separate vials containing 5 mg of gallic acid and ferulic acid, respectively. The vials were capped and stored for 20 h at 85 °C. After the solutions were cooled to room temperature, a solution of 0.1 g/mL NaOH in water was added until a pH between 5 and 6 was reached. These solutions were diluted with 60:40 (v/v) methanol:water, centrifuged for 5 min at approximately 1450 g and analyzed.

2.4.4 INSTRUMENTAL ANALYSIS

During this study, the instrumental analysis follows the same LC-PDA-amMS protocols for polar and apolar phytochemicals as mentioned in 2.3.4 of the materials and methods section. The extracted ion chromatograms (XICs) of the most abundant precursor ions of the phytochemicals were used for quantitative LC-amMS analysis. Detection of phytochemicals with the polar LC-PDA-amMS method was in general more sensitive in negative ion mode, while during analysis with the apolar LC-PDA-amMS method phytochemical detection was more sensitive in positive ion mode. Quantitation with the polar LC-PDA-amMS method was therefore performed in negative ion mode. Quantitation with the apolar LC-PDA-amMS method was performed in positive ion mode. Quality control (QC) during data acquisition with the generic LC-PDA-amMS method for polar phytochemicals was conducted by injecting a standard solution of a mixture of polyphenols before, between and after the sample extracts. The standard solution used for QC consisted of a mixture of phenolic and hydroxycinnamic acids, flavonoid aglycons and glycosides and tannins. The compounds in this standard solution are native to *Filipendula ulmaria* and are therefore representative for the polar phytochemical composition of *Filipendula ulmaria*. During data acquisition with the generic LC-PDA-amMS method for apolar phytochemicals, the internal standard was used to correct for instrumental fluctuations.

2.4.5 METHOD VALIDATION PARAMETERS

2.4.5.1 PROCESS EFFICIENCY

The process efficiency, as described by Krueve et al., is represented by the relative abundances of the phytochemicals per extraction method.^[71] The relative abundances of the phytochemicals were calculated from the average areas of three replicates per extraction protocol, with the extraction protocol yielding the highest average area value set as 100%.

2.4.5.2 MATRIX EFFECTS ON IONIZATION EFFICIENCY

Changes in ionization efficiency caused by co-extracted matrix compounds were assessed by infusing a (D-Ala²)-leucine enkephalin solution. Sample extracts and solvent blanks were analyzed with the LC-PDA-amMS methods while a 0.5 mg/mL solution of (D-Ala²)-leucine enkephalin in methanol was infused post-column via a T-piece at a flow rate of 100 µL/min. During the infusion experiments changes in ionization efficiency were investigated in both positive and negative mode.

2.4.5.3 REPEATABILITY

The intra-day repeatability of the different extraction methods is represented by the standard deviations of three replicates per extraction method, prepared and analyzed on the same day. A more in depth evaluation of the repeatability was carried out for the ATP continuous extraction protocol. Aliquots of *Filipendula ulmaria* and spicy paprika powder were extracted five times per day on three different days with the ATP continuous extraction protocol. The repeatability and intermediate precision were determined simultaneously according to the Eurachem guidelines.^[72] The within-group mean squares (MS_b), representing the within-group variances, and the between-group mean squares (MS_w) were obtained with one-way ANOVA. Absolute values for the repeatability (within-group standard deviation or s_r), the between-group standard deviation ($s_{between}$) and the intermediate precision (s_I) were calculated as follows:

$$s_r = \sqrt{MS_w} \quad (1)$$

$$s_{between} = \sqrt{\frac{MS_b - MS_w}{5}} \quad (2)$$

$$s_I = \sqrt{s_r^2 + s_{between}^2} \quad (3)$$

Relative values (relative standard deviations or RSDs) of the repeatability and intermediate precision were obtained by:

$$RSD = \frac{s \times 100}{\text{average of 15 measurements}} \quad (4)$$

RESULTS AND DISCUSSION

2.5 A FIRST STEP IN THE QUEST FOR THE ACTIVE CONSTITUENTS IN

FILIPENDULA ULMARIA

Two generic LC-PDA-amMS methods were previously designed to be complementary in terms of polarity: one method for moderately polar compounds such as phenolic constituents and another for apolar phytochemicals such as among others carotenoids and phytosterols.^[64,65] This is the first time that both methods were combined into a platform for comprehensive phytochemical characterization. A hybrid quadrupole-orbital trap MS analyzer was used, which enables selective ion fragmentation, a functionality that contributes significantly to compound identification by generating clean product ion spectra. Selective ion fragmentation is particularly useful for associating product ions with precursor ions during coelution of multiple compounds, as is often the case in complex plant extracts. Although ddMS² provides vast amounts of structural information, in some cases, the generated product ions may not suffice for full characterization of the substructures (e.g. aglycon moieties of flavonoid glycosides). In these cases, in-source CID fragmentation was used to generate substructure product ions in a first step. These in-source product ions were subsequently selected with the quadrupole for HCD fragmentation to obtain pseudo MS³ spectra for their tentative identification.

Structures were assigned to unknown peaks only when both the m/z ratios and molecular formulae of the precursor and product ions were in agreement. PDA spectra and retention times often provided additional confirmation of the proposed structures. The information obtained by this kind of analysis is, however, not always sufficient for peak identification at an acceptable confidence level. Additional information for

successful dereplication was often acquired from in-house and commercial compound databases and peer reviewed publications. Table 2.2 and Table 2.4 show the diagnostic amMS and PDA data used for chromatographic peak identification, as well as the literature consulted for confirmation of compound identity.

Application of a generic LC-PDA-amMS method for the identification of moderately polar phytochemicals enabled the identification of a multitude of phenolic constituents, many of which have never been reported before in *Filipendula ulmaria* (indicated in italics in Table 2.2 and Table 2.4). Figure 2.3 provides an overview of the retention times and m/z values in the heated electrospray ionization (HESI) negative mode of the compounds identified with this method. The data labels match the compound numbers in Table 2.2.

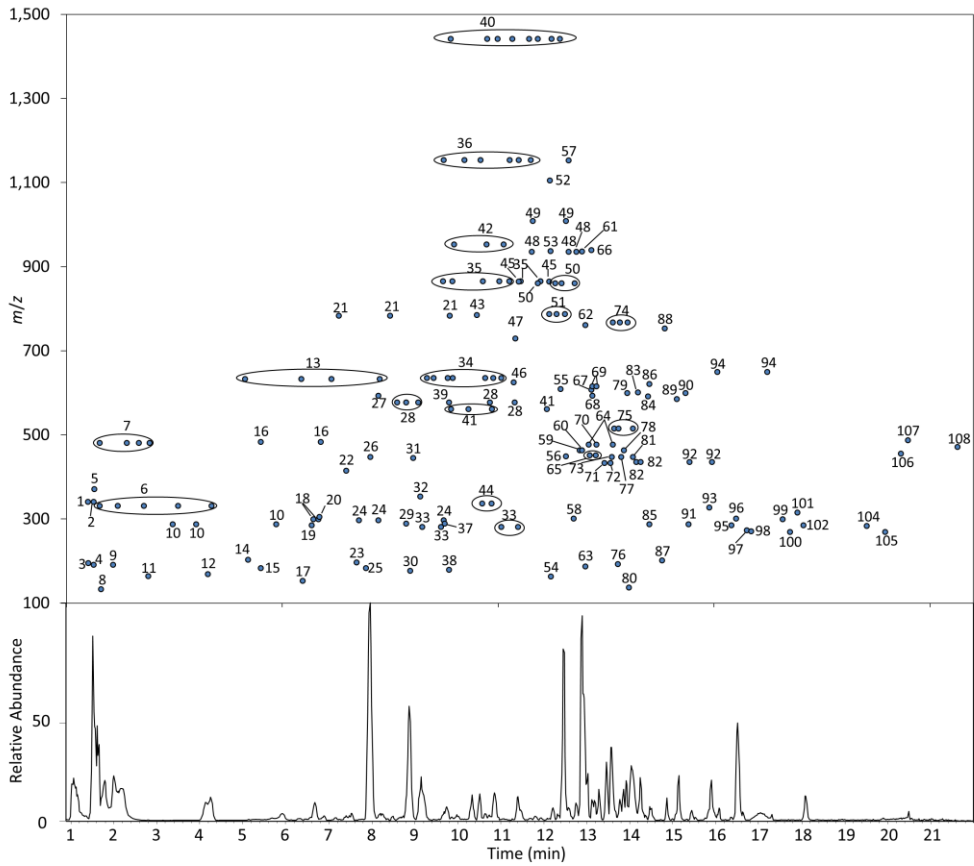


FIGURE 2.3: PLOT OF THE RETENTION TIMES VERSUS m/z VALUES OF THE COMPOUNDS IDENTIFIED IN *FILIPENDULA ULMARIA* DETECTED WITH A GENERIC LC-PDA-amMS METHOD FOR MODERATELY POLAR PHYTOCHEMICALS. THE DATA LABELS MATCH THE COMPOUND NUMBERS IN TABLE 2.2.

TABLE 2.2: CHROMATOGRAPHIC AND SPECTRAL DATA OF THE (TENTATIVELY) IDENTIFIED COMPOUNDS IN *FILIPENDULA ULMARIA* DETECTED WITH A GENERIC LC-PDA-amMS METHOD FOR MODERATELY POLAR PHYTOCHEMICALS. THE COMPOUND NUMBERS MATCH THE DATA LABELS IN FIGURE 2.3.

Compound number	Compound	Molecular formula	HESI neg full MS ^c	HESI neg ddMS ²	HESI pos full MS ^d	HESI pos ddMS ²	Retention time (min)	Maximum absorbance (nm)	Previously reported in literature	Plant part examined in literature
1	sucrose ^a	C ₁₂ H ₂₂ O ₁₁	341.10893	179.1; 161.0; 143.0; 119.0	343.12349	-	1.5; 1.6	-	[40]	in
2	trehalose ^a	C ₁₂ H ₂₂ O ₁₁	341.10893	179.1; 161.0; 143.035; 119.0	343.12349	-	1.5; 1.6	-	[40]	in
3	gluconic acid	C ₆ H ₁₂ O ₇	195.05103	177.0; 159.0; 151.1; 141.0; 129.0	-	-	1.5	-	-	-
4	quinic acid ^b	C ₇ H ₁₂ O ₆	191.05611	173.0; 127.0	-	-	1.6	-	-	-
5	quinic acid desoxyhexoside ^a	C ₁₃ H ₂₄ O ₁₂	371.11950	327.1; 191.1; 163.1	-	-	1.6	-	-	-
6	monogalloylhexoside ^a	C ₁₃ H ₁₆ O ₁₀	331.06707	211.0; 169.0	333.08162	315.1; 153.0	1.8; 2.2; 2.8; 3.6; 4.4	-	-	-
7	HHDP-hexoside isomers ^a	C ₂₀ H ₁₈ O ₁₄	481.06238	301.0; 275.0; 257.0; 249.0; 229.0	483.07693	-	1.8; 2.4; 2.7; 2.9	-	-	-
8	malic acid ^b	C ₄ H ₆ O ₅	133.01425	115.0; 89.0; 71.0	-	-	1.8	-	-	-
9	citric acid ^a	C ₆ H ₈ O ₇	191.01973	173.0; 129.0; 111.0; 87.0; 85.0	-	-	2.1 ^e	-	-	-
10	galloyl-threonic acid ^a	C ₁₁ H ₁₂ O ₉	287.04086	169.0; 135.0	289.05541	-	3.5; 4.0; 5.9	-	-	-
11	phenylalanine ^a	C ₉ H ₁₁ NO ₂	164.07170	147.0; 121.0	166.08626	149.1; 131.0; 120.1; 103.0	2.9	-	-	-
12	gallic acid ^b	C ₇ H ₆ O ₅	169.01425	125.0	-	-	4.3	268	[36-39]	in
13	HHDP-monogalloyl-hexoside ^a	C ₂₇ H ₂₂ O ₁₈	633.07334	301.0; 275.0; 257.0; 249.0; 169.0	635.08789	277.0; 259.0; 231.0; 153.0	5.1; 6.4; 7.1; 8.3	-	-	-
14	tryptophan ^a	C ₁₁ H ₁₂ N ₂ O ₂	203.08260	-	205.09715	188.1; 170.1; 159.1; 146.1; 132.1; 118.1	5.2	-	-	-
15	2-pyrone-4,6-dicarboxylic acid ^a	C ₇ H ₄ O ₆	182.99351	139.0	185.00806	-	5.5 ^e	-	[73]	-
16	digalloylhexoside ^a	C ₂₀ H ₂₀ O ₁₄	483.07803	331.1; 313.1; 211.0; 169.0	485.09258; 507.07453 [M+Na] ⁺	467.1; 153.0	5.5; 6.9	-	-	-

Compound number	Compound	Molecular formula	HESI neg full MS ⁻	HESI neg ddMS ²	HESI pos full MS ⁺	HESI pos ddMS ²	Retention time (min)	Maximum absorbance (nm)	Previously reported in literature	Plant part examined in literature
17	protocatechuic acid ^b	C ₇ H ₆ O ₄	153.01933	109.0	-	-	6.5	259; 294	[36]	in
18	salicylic acid hexoside ^a	C ₁₃ H ₁₆ O ₈	299.07724	137.0; 93.0	323.07374 [M+Na] ⁺ ; 318.11834 [M+NH ₄] ⁺	-	6.7; 6.8	-	[74]	in; he
19	isosalicin ^a	C ₁₃ H ₁₈ O ₇	285.09798	179.1; 161.0; 143.0	309.09447 [M+Na] ⁺ ; 304.13908 [M+NH ₄] ⁺	107.0	6.7	-	[75]	-
20	epigallocatechin ^a	C ₁₅ H ₁₄ O ₇	305.06668	179.0; 137.0; 125.0	307.08123	163.0; 139.0	6.9	-	[39]	ae
21	pedunculagin ^a	C ₃₄ H ₂₄ O ₂₂	783.06865	301.0; 275.0	785.08320	303.0; 277.0; 259.0; 231.0; 153.0	7.3, 8.5, 9.9	-	[33]	le
22	spiraecin ^a		461.13006 [M-H+FA] ⁻ ; 415.12458	415.1; 293.1; 121.030; 93.0	439.12108 [M+Na] ⁺ ; 434.16569 [M+NH ₄] ⁺ ; 417.13914	295.1; 123.0	7.5	311	[38,76]	in
23	syringic acid ^a	C ₉ H ₁₀ O ₅	197.04555	181.0; 167.1; 153.0; 125.0	-	-	7.7	-	[39]	ae
24	caffeoyl-threonic acid ^a	C ₁₃ H ₁₄ O ₈	297.06159	179.0; 135.0	299.07614	163.0; 145.0; 135.0	7.8, 8.2, 9.7	-	-	-
25	methyl gallate ^a	C ₈ H ₈ O ₅	183.02990; 367.06707 [2M-H] ⁻	168.0; 124.0	185.04445	153.0	7.9	272	-	-
26	kuromanin ^b	C ₂₁ H ₂₁ ClO ₁₁	447.09328	465.1; 284.0; 285.0; 255.0	449.10784	287.1	8	279; 517	-	-
27	keracyanin ^b	[C ₂₇ H ₃₁ O ₁₅] ⁺	593.15119	-	595.16575	287.1	8.2	280; 517	-	-
28	procyanidin dimer ^a	C ₃₀ H ₂₆ O ₁₂	577.13515	425.1; 407.1; 289.1; 245.1	579.14970	427.1; 409.1; 291.1; 289.1; 287.1	8.7, 8.9, 9.2, 9.9, 10.8, 11.4	-	-	-
29	catechin ^b	C ₁₅ H ₁₄ O ₆	289.07176	245.1; 205.0; 137.0	291.08741	139.0; 123.0	8.9	279	[39]	ae
30	aesculetin ^a	C ₉ H ₆ O ₄	177.01933	133.0; 105.0; 89.0	179.03389	149.0	9	-	[37]	ae

Compound number	Compound	Molecular formula	HESI neg full MS ⁻	HESI neg ddMS ²	HESI pos full MS ⁺	HESI pos ddMS ²	Retention time (min)	Maximum absorbance (nm)	Previously reported in literature	Plant part examined in literature
31	monotropin ^a	C ₁₉ H ₂₆ O ₁₂	491.14063 [M-H+FA] ⁻ ; 445.13515	445.1; 293.1; 151.0; 137.0	469.13165 [M+Na] ⁺ ; 464.17625 [M+NH ₄] ⁺	295.1; 153.1	9	-	[35,75,76]	-
32	chlorogenic acid ^b	C ₁₆ H ₁₈ O ₉	353.08781	351.1; 191.1	355.10236	163.0	9.2	326	[37]	ae
33	<i>coumaroylthreonic acid</i> ^a	C ₁₃ H ₁₄ O ₇	281.06668	193.0; 163.0; 135.0; 119.0	283.08123	147.0; 119.0	9.2, 9.7, 11.1, 11.5	-	-	-
34	<i>trigalloylhexoside</i> ^a	C ₂₇ H ₂₄ O ₁₈	635.08899	483.1; 465.1; 423.1; 313.1; 271.1; 211.0; 193.0; 169.0; 125.0	637.10354	619.1; 153.0	9.4; 9.5; 9.8; 10.0; 10.7; 10.9; 11.1	-	-	-
35	<i>procyanidin trimer</i> ^a	C ₄₅ H ₃₈ O ₁₈	865.19854	575.1; 407.1; 289.1; 287.1; 245.0; 243.0	867.21309	577.1; 409.1; 247.1; 245.0	9.7, 9.9, 10.6, 11.0, 11.3, 11.5, 12.0	-	-	-
36	<i>procyanidin tetramer</i> ^a	C ₆₀ H ₅₀ O ₂₄	1153.26193; 576.12732 [M-2H] ²⁻	863.2; 575.1; 407.1; 289.1; 287.1; 245.0; 243.0	1,155.27648	867.2; 577.1; 409.1; 247.1; 245.0	9.7, 10.2, 10.6, 11.3, 11.5, 11.8	-	-	-
37	epicatechin ^b	C ₁₅ H ₁₄ O ₆	289.07176	245.1; 205.1; 137.0	-	-	9.8	280	[39]	ae
38	3,4-dihydroxycinnamic acid ^b	C ₉ H ₈ O ₄	179.03498	135.0	181.04954	163.0	9.9	-	[37,39]	ae
39	procyanidin B2 ^b	C ₃₀ H ₂₆ O ₁₂	577.13515	425.1; 407.1; 289.1; 245.1	579.14970	427.1; 409.1; 291.1; 289.1; 287.1	9.9	-	[39]	ae
40	<i>procyanidin pentamer</i> ^a	C ₇₅ H ₆₂ O ₃₀	1441.32531; 720.15902 [M-2H] ²⁻	1151.2; 863.2; 575.1; 407.1; 289.1; 287.1; 245.0; 243.0	1443.33987; 722.17357 [M+2H] ²⁺	-	9.9; 10.8; 11.0; 11.3; 11.7; 11.9; 12.2; 12.4	-	-	-
41	<i>(epi)catechin coupled to C₁₅H₁₄O₅</i> ^a	C ₃₀ H ₂₆ O ₁₁	561.14023	435.1; 425.1; 407.1; 289.1; 273.1; 271.1; 245.1	563.15479	409.1; 299.1; 291.1; 289.1; 287.1; 275.1; 257.0; 231.1; 179.0; 147.0	9.9, 10.3, 10.9, 12.1	-	-	-
42	rugosin B ^a	C ₄₁ H ₃₀ O ₂₇	953.09017	909.1; 785.1; 766.1; 597.0; 301.0; 275.0; 249.0; 169.0	955.10472	785.1; 467.1; 453.0; 427.0; 261.0; 153.0	10.0, 10.7, 11.1	-	[33,36,39]	in
43	tellimagrandin I ^a	C ₃₄ H ₂₆ O ₂₂	785.08430	301.0; 275.0; 249.0; 169.0	787.09885	277.0; 259.0; 231.0; 153.0	10.5	-	[33,36,38,39]	in

Compound number	Compound	Molecular formula	HESI neg full MS ⁻	HESI neg ddMS ²	HESI pos full MS ⁺	HESI pos ddMS ²	Retention time (min)	Maximum absorbance (nm)	Previously reported in literature	Plant part examined in literature
44	<i>coumaroylquinic acid</i> ^a	C ₁₆ H ₁₈ O ₈	337.09289	191.1	339.10744; 361.08939 [M+Na] ⁺	165.1; 147.0	10.6; 10.8	-	-	-
45	<i>procyanidin hexamer</i> ^a	C ₉₀ H ₇₄ O ₃₆	864.19071 [M-2H] ²⁻	-	-	-	11.5; 12.2	-	-	-
46	<i>quercetin-O-dihexoside</i> ^a	C ₂₇ H ₃₀ O ₁₇	625.14102	463.1; 301.0; 271.0; 255.0; 179.0; 151.0	627.15558	465.1; 303.0; 153.0	11.4	-	[39]	ae
47	<i>procyanidin dimer gallate</i> ^a	C ₃₇ H ₃₀ O ₁₆	729.14611	577.1; 407.1; 289.1; 245.0; 243.0; 169.0	731.16066	411.1; 287.1; 271.1; 259.1; 247.1; 153.0	11.4	-	-	-
48	<i>casuarinin/casuarictin</i> ^a	C ₄₁ H ₂₈ O ₂₆	935.07960	785.1; 633.1; 483.1; 451.0; 425.0; 301.0; 275.0; 169.0	937.09416	767.1; 467.1; 453.0; 427.0; 153.0	11.8, 12.6, 12.8	-	[33]	le
49	<i>procyanidin heptamer</i> ^a	C ₁₀₅ H ₈₆ O ₄₂	1008.22241 [M-2H] ²⁻	-	-	-	11.8; 12.6	-	-	-
50	<i>rugosin E</i> ^a	C ₇₅ H ₅₄ O ₄₈	860.08195 [M-2H] ²⁻	937.1; 785.1; 597.0; 301.0; 275.0; 249.0; 169.0	-	-	11.9, 12.3, 12.5, 12.8	-	[33,36,39]	in
51	<i>tetragalloylglucose</i> ^b	C ₃₄ H ₂₈ O ₂₂	787.09995	635.1; 617.1; 465.1; 447.1; 313.1; 295.0; 169.0	811.09644	-	12.2; 12.4; 12.6	-	-	-
52	<i>rugosin A</i> ^a	C ₄₈ H ₃₄ O ₃₁	1105.10113; 552.04693 [M-2H] ²⁻	530.0; 891.1; 301.0; 169.0	-	-	12.2	-	[33,34,39]	in
53	<i>tellimagrandin II</i> ^a	C ₄₁ H ₃₀ O ₂₆	937.09525	301.0; 275.0; 249.0; 169.0	-	-	12.2	-	[33,36,38, 39]	in
54	<i>p-coumaric acid</i> ^b	C ₉ H ₈ O ₃	163.04007	119.0	165.05462	-	12.2	-	[39]	ae
55	<i>rutin</i> ^b	C ₂₇ H ₃₀ O ₁₆	609.14611	300.0; 271.0; 255.0; 243.0	611.16066	465.1; 303.0	12.4	256; 355	[36,37,39]	in
56	<i>galloyl-caffeoyl-threonic acid</i> ^a	C ₂₀ H ₁₈ O ₁₂	449.07255	297.1; 287.0; 179.0; 169.0; 135.0	451.08710	287.1; 163.0; 153.0; 145.0; 135.0	12.6	-	-	-
57	<i>procyanidin octamer</i> ^a	C ₁₂₀ H ₉₈ O ₄₈	1152.25410 [M-2H] ²⁻	-	-	-	12.6	-	-	-
58	<i>ellagic acid</i> ^b	C ₁₄ H ₆ O ₈	300.99899	284.0; 257.0; 229.0; 201.0; 185.0	-	-	12.8	367	[39]	ae
59	<i>hyperoside</i> ^b	C ₂₁ H ₂₀ O ₁₂	463.08820	300.0; 271.0; 255.0; 243.0; 151.0	465.10275	303.0	12.9	256; 352	[36,39]	in
60	<i>isoquercitrin</i> ^b	C ₂₁ H ₂₀ O ₁₂	463.08820	300.0; 271.0; 255.0; 243.0; 151.0	465.10275	303.0	12.9	256; 352	[34,36,37, 39]	in; ae

Compound number	Compound	Molecular formula	HESI neg full MS ^c	HESI neg ddMS ²	HESI pos full MS ^c	HESI pos ddMS ²	Retention time (min)	Maximum absorbance (nm)	Previously reported in literature	Plant part examined in literature
61	rugosin D ^a	C ₈₂ H ₅₈ O ₅₂	936.08743 [M-2H] ²⁻	1061.1; 917.1; 851.1; 767.1; 749.1; 465.1; 301.0; 275.0; 249.0; 169.0	-	-	12.9	-	[33,36,39]	in
62	quercetin-O-galloyldihexoside ^a	C ₃₄ H ₃₄ O ₂₀	761.15707	301.0; 271.0; 255.0; 243.0; 227.0; 179.0; 151.0; 121.0; 107.0	763.17162	617.1; 461.1; 315.1; 303.0; 285.0; 257.0; 229.0; 201.1; 165.0; 163.0; 153.0; 149.0; 137.0	13	258; 351	-	-
63	azelaic acid ^a	C ₉ H ₁₆ O ₄	187.09758	169.1; 143.1; 125.1	-	-	13	-	-	-
64	isorhamnetin-O-hexoside ^a	C ₂₂ H ₂₂ O ₁₂	477.10385	314.0; 299.0; 285.0; 271.0; 243.0; 169.0	479.11840	317.1; 302.0	13.1; 13.7	-	[38]	in
65	cinchonain Ib and/or Ia ^a	C ₂₄ H ₂₀ O ₉	451.10346	341.1; 299.1; 231.0; 217.0; 189.0; 177.0	453.11801	411.1; 343.1; 317.1; 313.1; 301.1; 271.1; 259.1	13.1; 13.3	-	-	-
66	pentagalloylglucose ^b	C ₄₁ H ₃₂ O ₂₆	939.11090	769.1; 617.1; 465.1; 447.1; 295.0; 169.0	963.10740	-	13.2	-	-	-
67	methoxyflavonoid-O-hexoside-deoxyhexoside ^a	C ₂₈ H ₃₂ O ₁₅	607.16684	298.0; 283.0	609.18140	463.1; 301.1; 286.0	13.2	-	-	-
68	kaempferol-O-hexoside-deoxyhexoside ^a	C ₂₇ H ₃₀ O ₁₅	593.15119	285.0; 255.0; 169.0	595.16575	449.1; 287.1	13.2	-	[36,39]	in
69	quercetin-O-galloylhexoside ^a	C ₂₈ H ₂₄ O ₁₆	615.09916	313.1; 301.0; 271.0; 255.0; 243.0; 227.0; 179.0; 151.0; 121.0; 107.0	617.14071	315.1; 303.0; 257.0; 229.0; 201.1; 165.0; 163.0; 153.0; 149.0; 137.0	13.2; 13.3	-	-	-
70	miquelianin ^b	C ₂₁ H ₁₈ O ₁₃	477.06746	301.0; 271.0; 255.0; 179.0; 151.0	479.08202	303.0; 257.0	13.3	257; 357	[39]	ae
71	quercetin-O-pentoside ^a	C ₂₀ H ₁₈ O ₁₁	433.07763	301.0; 300.0; 271.0; 255.0; 243.0; 179.0; 151.0	435.09219	303.0; 285.0; 257.0; 229.0; 201.1; 165.0; 163.0; 153.0; 149.0; 137.0	13.5	-	-	-
72	avicularin/avicularoside ^b	C ₂₀ H ₁₈ O ₁₁	433.07763	301.0; 300.0; 271.0; 255.0; 243.0; 179.0; 151.0	435.09219	303.0	13.6	256; 355	[34,37,39]	ae
73	astragalin ^b	C ₂₁ H ₂₀ O ₁₁	447.09328	284.0; 255.0; 227.0	449.10784	287.1	13.6	265; 348	[36,39]	in; ae
74	quercetin-O-digalloylhexoside ^a	C ₃₅ H ₂₈ O ₂₀	767.11012	615.1; 465.1; 313.1; 301.0; 169.0; 125.0; 271.0; 255.0; 243.0; 227.0; 179.0; 151.0; 121.0; 107.0	769.12467	467.1; 303.0; 285.0; 257.0; 229.0; 201.1; 165.0; 163.0; 153.0; 149.0; 137.0	13.7; 13.8; 14.0	-	-	-
75	di-O-caFFEYLQUINIC acid ^a	C ₂₅ H ₂₄ O ₁₂	515.11950	447.1; 353.1; 191.1; 179.0; 135.0	517.13405	-	13.7, 13.8 and 14.1	-	[39]	ae

Compound number	Compound	Molecular formula	HESI neg full MS ⁻	HESI neg ddMS ²	HESI pos full MS ⁺	HESI pos ddMS ²	Retention time (min)	Maximum absorbance (nm)	Previously reported in literature	Plant part examined in literature
76	<i>methyl caffeate</i> ^a	C ₁₀ H ₁₀ O ₄	193.05063	178.0; 161.0; 134.0	195.06519	163.0; 145.0; 135.0	13.8	-	-	-
77	quercitrin ^b	C ₂₁ H ₂₀ O ₁₁	447.09328	300.0; 285.0; 271.0; 255.0; 243.0	449.10784	303.0; 287.1	13.8	265; 346	[36,39]	in
78	quercetin-O-hexoside ^a	C ₂₁ H ₂₀ O ₁₂	463.08820	301.0; 179.0; 151.0	465.10275	377.0; 359.0; 303.0; 287.1; 177.1; 153.0	13.9	-	[36-39]	in
79	<i>flavonoid-O-galloylhexoside</i> ^a	C ₂₈ H ₂₄ O ₁₅	599.10424	463.1; 313.1; 301.0; 285.0	601.11880	315.1; 287.1; 153.0	14	-	-	-
80	salicylic acid ^b	C ₇ H ₆ O ₃	137.02442	93.0	-	-	14	236; 302	[35-37,39]	in
81	kaempferol-O-hexoside ^a	C ₂₁ H ₂₀ O ₁₁	447.09328	284.0; 227.0; 151.0	449.10784	-	14.1	-	[36,39]	in
82	<i>deoxy-cinchonain Ia and/or Ib</i> ^a	C ₂₄ H ₂₀ O ₈	435.10854	341.1; 231.0; 217.0; 189.0; 177.0	437.12309	395.1; 343.1; 317.1; 285.1; 243.1; 191.0	14.2; 14.3	-	-	-
83	<i>digalloyl-caffeoyl-threonic acid</i> ^a	C ₂₇ H ₂₂ O ₁₆	601.08351	449.1; 297.1; 287.0; 179.0; 169.0; 135.0	603.09806	423.1 253.0; 163.0; 153.0; 145.0; 135.0	14.2	-	-	-
84	<i>methoxyflavonoid-O-hexoside-deoxyhexoside</i> ^a	C ₂₈ H ₃₂ O ₁₄	637.17741 [M-H+FA] ⁻ ; 591.17193	591.2; 283.1; 268.0	593.18648	447.1; 285.1; 270.0	14.5	270; 332	-	-
85	<i>aromadendrin</i> ^b	C ₁₅ H ₁₂ O ₆	287.05611	259.1; 243.1; 215.1; 201.1; 177.1; 151.0; 125.0	289.07066	-	14.5	-	-	-
86	<i>dimethoxyflavonoid-O-hexoside-deoxyhexoside</i> ^a	C ₂₉ H ₃₄ O ₁₅	667.18797 [M-H+FA] ⁻ ; 621.18249	621.2; 313.1; 298.0; 283.0	623.19705	477.1; 315.1; 300.1	14.5	270; 332	-	-
87	<i>sebacic acid</i> ^a	C ₁₀ H ₁₈ O ₄	201.11323	183.1; 139.1	-	-	14.8	-	-	-
88	<i>trigalloyl-caffeoyl-threonic acid</i> ^a	C ₃₄ H ₂₆ O ₂₀	753.09447	601.1; 449.1; 297.1; 287.0; 179.0; 169.0; 135.0	755.10902	-	14.9	-	-	-
89	<i>digalloyl-coumaroyl-threonic acid</i> ^a	C ₂₇ H ₂₂ O ₁₅	585.08859	433.1; 281.1; 169.0; 163.0; 135.0	587.10424	423.1; 153.0; 147.0	15.1	-	-	-
90	<i>quercetin-O-galloyldeoxyhexoside</i> ^a	C ₂₈ H ₂₄ O ₁₅	599.10424	301.0; 271.0; 255.0; 243.0; 227.0; 179.0; 169.0; 151.0; 121.0; 107.0	601.11880	303.0; 257.0; 229.0; 153.018	15.3	-	-	-
91	<i>eriodictyol</i> ^b	C ₁₅ H ₁₂ O ₆	287.05611	151.0; 135.0; 125.0	289.07066	163.0; 153.0; 145.0; 135.0; 123.0	15.4	-	-	-
92	<i>protocatechuic acid-salicyl-hexoside</i> ^a	C ₂₀ H ₂₀ O ₁₁	435.09328	315.1; 297.1; 153.0; 137.0; 109.0	-	-	15.4; 16.0	-	-	-

Compound number	Compound	Molecular formula	HESI neg full MS ^c	HESI neg ddMS ²	HESI pos full MS ^c	HESI pos ddMS ²	Retention time (min)	Maximum absorbance (nm)	Previously reported in literature	Plant part examined in literature
93	<i>trihydroxyoctadecadienoic acid</i>	C ₁₈ H ₃₂ O ₅	327.21770	291.2; 239.1; 229.1; 193.1; 171.1	-	-	15.9	-	-	-
94	tormentoside ^a	C ₃₆ H ₅₈ O ₁₀	649.39572; 487.34290 [M-H-sugar] ⁻	-	489.35745 [M+H-sugar] ⁺	471.3; 453.3; 435.3; 425.3; 407.3; 201.2; 207.2; 205.2; 189.2; 187.2	16.1; 17.2	-	[43]	-
95	<i>luteolin</i> ^b	C ₁₅ H ₁₀ O ₆	285.04046	199.0; 151.0; 133.0	287.05501	153.0 135.0	16.4	-	-	-
96	quercetin ^b	C ₁₅ H ₁₀ O ₇	301.03538	271.0; 245.0; 193.0; 179.0; 151.0; 121.0; 107.0	303.04993	285.0; 257.0; 229.0; 201.1; 165.0; 163.0; 153.0; 149.0; 137.0	16.5	255; 372	[36,37,39]	in
97	<i>phloretin</i> ^b	C ₁₅ H ₁₄ O ₅	273.07685	167.0; 151.0; 123.0; 119.0	275.09140	-	16.8	-	-	-
98	<i>naringenin</i> ^b	C ₁₅ H ₁₂ O ₅	271.06120	253.0; 227.1; 177.0; 151.0; 119.0	273.07575	153.0; 147.0; 119.0; 107.0	16.9	-	-	-
99	<i>methoxyflavonoid</i> ^a	C ₁₆ H ₁₂ O ₆	299.05611	284.0; 271.0; 151.0; 179.1	301.07066	286.0; 258.0	17.6	-	-	-
100	apigenin ^b	C ₁₅ H ₁₀ O ₅	269.04555	225.1; 151.0	271.06010	-	17.8	-	[39]	ae
101	<i>isorhamnetin</i> ^b	C ₁₆ H ₁₂ O ₇	315.05103	300.0; 151.0	317.06558	302.0; 285.0; 153.0	17.9	-	-	-
102	kaempferol ^b	C ₁₅ H ₁₀ O ₆	285.04046	-	287.05501	258.0; 241.0; 231.1; 165.0; 153.0; 137.0; 121.0	18.1	265; 364	[36,37,39]	in
103	<i>dimethoxyflavonoid</i> ^a	C ₁₇ H ₁₄ O ₆	-	-	315.08631	300.1; 168.0	19.4	-	-	-
104	<i>methoxyflavonoid</i> ^a	C ₁₆ H ₁₂ O ₅	283.06120	268.0	285.07575	270.0; 242.1	19.5	-	-	-
105	<i>galangin</i> ^b	C ₁₅ H ₁₀ O ₅	269.04555	-	271.06010	-	20	-	-	-
106	ursolic acid ^a	C ₃₀ H ₄₈ O ₃	455.35307	-	457.36762	439.4; 411.4; 393.4; 203.2; 191.2; 189.2; 187.2	20.3	-	[43]	ro
107	<i>tormentic acid</i> ^a	C ₃₀ H ₄₈ O ₅	487.34290	-	489.35745	471.4; 453.3; 435.3; 425.3; 407.3; 201.2; 205.2; 189.2; 187.2	20.5	-	-	-
108	pomolic acid ^a	C ₃₀ H ₄₈ O ₄	471.34798	-	473.36254	455.4; 437.3; 201.2; 191.2	21.6	-	[43]	ro

^aTentative identification based on accurate mass. ^bIdentification with an analytical standard. ^cDe protonated molecules unless stated otherwise. ^dProtonated molecules unless stated otherwise. ^ebroad peak. *Italics*: not reported in *Filipendula ulmaria* before. in: inflorescence. in: herba. ae: aerial part. le: leaves. ro: roots

TABLE 2.3: CONCENTRATIONS OF PHENOLIC CONSTITUENTS IN FILIPENDULAE ULMARIAE HERBA IN $\mu\text{g/g}$, CALCULATED WITH REFERENCE STANDARDS USING LC-amMS. THE MEASUREMENT UNCERTAINTIES ARE EXPRESSED AS THE STANDARD DEVIATION OF THREE REPLICATES.

Compound	Concentration ($\mu\text{g/g}$)
kaempferol	64 \pm 3
quercetin	1040 \pm 40
quercitrin	215 \pm 5
salicylic acid	630 \pm 20
astragalin	99 \pm 1
isoquercitrin	530 \pm 40
hyperin	4400 \pm 200
ellagic acid	1540 \pm 60
rutin	3100 \pm 200
p-coumaric acid	31 \pm 1
procyanidin b2	144 \pm 6
caffeic acid	47 \pm 2
epicatechin	83 \pm 4
chlorogenic acid	640 \pm 10
catechin	1900 \pm 100
kuromarin	122 \pm 5
protocatechuic acid	74 \pm 3
gallic acid	1340 \pm 70
quinic acid	1800 \pm 100

TABLE 2.4: CHROMATOGRAPHIC AND SPECTRAL DATA OF THE (TENTATIVELY) IDENTIFIED COMPOUNDS IN *FILIPENDULA ULMARIA* DETECTED WITH A GENERIC LC-PDA-amMS METHOD FOR APOLAR PHYTOCHEMICALS.

Compound number	Compound	Molecular formula	HESI neg full MS ^c	HESI neg ddMS ²	HESI pos full MS ^d	HESI pos ddMS ²	Retention time (min)	Maximum absorbance (nm)	Previously reported in literature	Plant part examined in literature
109	cis- and trans-violaxanthin ^b	C ₄₀ H ₅₆ O ₄	-	-	60.142.514	-	6.9; 7.1	418; 442; 472	-	-
110	Lutein ^b	C ₄₀ H ₅₆ O ₂	-	-	569.43531; 551.42474 [M-H-H ₂ O] ⁺ ; 533.41418 [M-H-2H ₂ O] ⁺	-	10.1	430; 455; 482	-	-
111	<i>dihydroxychlorophyll a and a^{na}</i>	C ₅₅ H ₇₀ O ₇ N ₄ Mg	981.52334 [M-H+FA]; 921.50222	642.2; 584.2; 569.2	945.49871 [M+Na] ⁺ ; 923.51677	-	11.4; 11.5	460; 649	-	-
112	<i>chlorophyll b and b^{na}</i>	C ₅₅ H ₇₀ O ₆ N ₄ Mg	965.52843 [M-H+FA]; 905.50730	626.2; 555.2; 540.2	90751783	879.5; 629.2; 597.2; 569.2; 541.2	12.0; 12.6	461; 645	[40]	in
113	<i>hydroxychlorophyll a or a^{na}</i>	C ₅₅ H ₇₂ O ₆ N ₄ Mg	967.54408 [M-H+FA]; 907.52295	849.5; 628.2; 570.2; 555.2	931.51945 [M+Na] ⁺	-	12.9	427; 662	-	-
114	<i>chlorophyll a and a^{na}</i>	C ₅₅ H ₇₂ O ₅ N ₄ Mg	951.54917 [M-H+FA]; 891.52804	612.2; 541.2; 526.2	915.52453 [M+Na] ⁺ ; 893.54259	833.5; 614.2; 583.2; 555.2	13.4; 13.8	431; 617; 663	[40]	in
115	<i>campesterol^b</i>	C ₂₈ H ₄₈ O	-	-	383.36723 [M+H-H ₂ O] ⁺	-	15.3	-	-	-
116	<i>phaeophytin b and b^{na}</i>	C ₅₅ H ₇₂ N ₄ O ₆	88.353.791	533.2; 518.2	88555246	607.3; 579.3; 547.2	15.5	436; 653	-	-
117	<i>β-sitosterol^b</i>	C ₂₉ H ₅₀ O	-	-	397.38288 [M+H-H ₂ O] ⁺	-	15.8	-	-	-
118	<i>phaeophytin a and a^{na}</i>	C ₅₅ H ₇₄ N ₄ O ₅	86.955.864	519.2; 504.2	893.55514 [M+Na] ⁺ ; 871.57320	593.3; 533.3	16.5; 16.9	408; 664	-	-
119	<i>cis- and trans-isomers of β-carotene^b</i>	C ₄₀ H ₅₆	-	-	537.44548; 536.43765; 445.38288	-	16.6; 16.7; 17.1	430; 455; 482	[40]	in

^aTentative identification based on accurate mass. ^bIdentification with an analytical standard. ^cDe protonated molecules unless stated otherwise. ^dProtonated molecules unless stated otherwise. *Italics*: not reported in *Filipendula ulmaria* before. in: inflorescence.

Predominantly deprotonated molecules ($[M-H]^-$) were formed in the negative ionization mode. Formic acid adducts ($[M-H+FA]^-$), deprotonated dimers ($[2M-H]^-$), doubly deprotonated molecules ($[M-2H]^{2-}$) and product ions caused by in-source fragmentation were also observed (Table 2.2). In the positive ionization mode, predominantly protonated molecules ($[M+H]^+$) were generated and, to a lesser extent, also sodium adducts, ammonium adducts, doubly protonated molecules ($[M+Na]^+$, $[M+NH_4]^+$ and $[M+2H]^{2+}$, respectively) and product ions caused by in-source fragmentation (Table 2.2).

Flavonoids chiefly occurred as glycoconjugates (with hexose, pentose, deoxyhexose, dihexose and hexose-deoxyhexose moieties (Table 2.2). Several of the glycosides were identified with analytical standards. Other flavonoid glycoconjugates were identified with ddMS²: HCD fragmentation resulted in the distinct presence of product ions caused by the loss of sugar moieties, indicating glycosidic *O*-linkages. Various glycosyl flavonoids acylated with (di)galloyl moieties were also detected. In-source CID fragmentation and subsequent HCD fragmentation of the aglycon moiety (pseudo MS³) often allowed for the tentative identification of the flavonoid moieties. Fragmentation of flavonoid aglycons has been reviewed in detail previously, among others by Cuyckens and Claeys.^[77] The main flavonoid moieties of the detected glycosides consisted of quercetin and kaempferol, in line with previous studies.^[36,39] Multiple flavonoid aglycons were found, such as among others quercetin, kaempferol, catechin, epicatechin, epigallocatechin, apigenin, isorhamnetin and luteolin. Several flavonoids that were previously reported (e.g., ulmarioside, epigallocatechingallate and isorhamnetin acetylhexoside) were not detected, which is probably due to natural phytochemical variations in between plants and plant parts examined or due to a difference in method and/or instrument sensitivity.^[38,39] Nevertheless, various flavonoid aglycons and glycoconjugates, of which several have never been described in

Filipendula ulmaria before (indicated in italics in Table 2.2), have been identified during the current study.

Some phenolic acids such as gallic acid, protocatechuic acid, syringic acid and salicylic acid and hydroxycinnamic acids such as caffeic acid and *p*-coumaric acid were detected in the free form (Table 2.2), in agreement with previous studies.^[35,39] All free phenolic and hydroxycinnamic acids, except syringic acid, were identified with analytical standards. The product ions of syringic acid generated by ddMS² matched with those described by Sun et al.^[78] Glycosylated salicyl derivatives (salicylic acid hexoside, isosalicin, monotropitin and spiraein) were also present, while methyl salicylate, salicyl alcohol and salicyl aldehyde, previously reported in this plant species, were not found.^[35,75,76] Next to salicylates, a rich diversity of phenolic and hydroxycinnamic acid oligomers was detected, most of which have never been reported before in *Filipendula ulmaria*. Tentative identification of these oligomers was based on the consecutive loss of phenolic monomer units during ddMS² (Table 2.2).^[79] The phenolic oligomers consisted predominantly of structures containing galloyl, caffeoyl, quinoyl and coumaroyl moieties. Several phenolic acid and hydroxycinnamic acid oligomers were also detected as glycoconjugates. Often multiple chromatographic peaks were found for the same precursor ion, indicating the presence of structural isomers due to different linkage sites and/or different sugar moieties.

Several of the tentatively identified oligomeric phenolic acid structures described in the previous section may be classified as gallotannins (hydrolysable tannins).^[80] Some of these gallotannins are metabolic precursors of ellagitannins in plants (e.g. pentagalloylglucose is a precursors of tellimagrandin II).^[79,81] Meadowsweet has been described as a rich source of various monomeric ellagitannins such as casuarinin, casuarictin, pedunculagin, tellimagrandins I and II, rugosins A and B, and dimeric ellagitannins rugosins D and E.^[33,36,38,39] Such hydrolysable tannins consist of one or more hexahydroxydiphenic acid (HHDP) moieties and several galloyl and glucose

moieties.^[33,36] During the current study, ionization of dimeric rugosins resulted in significant amounts of $[M-2H]^{2-}$ ions (Table 2.2). The fragmentation patterns of the ellagitannins were characterized by consecutive losses of monomeric units (Table 2.2). Next to previously reported hydrolysable tannins, other ellagitannins were also tentatively identified during this study (indicated in italics, Table 2.2): several HHDP-monogalloyl-hexoside and HHDP-hexoside isomers, similar to the structures of tellimagrandins, were detected. Ellagic acid, which may be formed by hydrolysis of ellagitannins and occurs in multiple plants, fruits and nuts, was also identified during this study using an analytical standard.^[82]

Olennikov and Kruglova detected procyanidins B1 and B2 in meadowsweet.^[39] A multitude of procyanidins ranging from dimeric to octameric isomers was tentatively identified. Procyanidin dimer gallate was also tentatively identified. The fragmentation pattern of the detected procyanidins obtained with ddMS² corresponded to that of an analytical standard solution of procyanidin B2 and is in accordance with their fragmentation described by Rigueiro et al.^[79] Increasing amounts of $[M-2H]^{2-}$ ions were observed with increasing procyanidin mass, starting from tetramers. For hexamers, heptamers and octamers, only the $[M-2H]^{2-}$ ion was observed. Because of the low abundant $[M-2H]^{2-}$ signals of the procyanidin hexamers, heptamers and octamers, selective fragmentation could not be used to confirm their identity. Nonetheless, the use of a hybrid orbitrap mass analyzer enabled the tentative identification of a large amount of tannins that have never been reported before in *Filipendula ulmaria* (indicated in italics, Table 2.2).

Based on the most abundant signals observed with PDA detection, the main phenolic constituents were identified: gallic acid (12), procyanidin dimer (28 ; not B2), rugosin A (52) or tellimagrandin II (53), rutin (55), hyperoside (59), isoquercitrin (60), quercetin-*O*-galloyldihexoside (62), kaempferol-*O*-hexoside-deoxyhexoside (68), quercetin-*O*-galloylhexoside (69), quercetin-*O*-pentoside (71), avicularoside (72),

astragalin (73), quercetin-*O*-hexoside (78), digalloyl-caffeoyl-threonic acid (83), methoxyflavonoid-*O*-hexoside-deoxyhexoside (84), dimethoxyflavonoid-*O*-hexoside-deoxyhexoside (86), digalloyl-coumaroyl-threonic acid (89) and quercetin (96). These results show that the main constituents predominantly consist of flavonoid glycosides and tannins. Compounds for which a reference standard was available were quantified with LC-amMS (Table 2.3). The concentrations detected during this study are in accordance with those found by Fecka, who investigated the concentration of selected polyphenols in dried flowers of meadowsweet.^[36]

Consistent with previous literature, only few and frequently low abundant non-phenolic phytochemicals were detected. Some triterpenes were tentatively identified with the generic LC-PDA-amMS method for moderately polar phytochemicals, while chlorophyll derivatives, phytosterols and carotenoids were detected with the complementary LC-PDA-amMS method for apolar phytochemicals. Ionization in the negative and positive modes during analysis with the LC-PDA-amMS method for apolar phytochemicals predominantly rendered $[M-H]^-$ and $[M-H+FA]^-$ ions and $[M+H]^+$ and $[M+Na]^+$ ions, respectively. Product ions due to in-source fragmentation (e.g. loss of water and sugar moieties) were also observed (Table 2.4).

Ursolic acid, pomolic acid and tormentoside (a glycoside of tormentic acid) have been described to be present in the roots of *Filipendula ulmaria*.^[43] During this study, these compounds were also tentatively identified based on product ions formed by selective HCD fragmentation in positive ionization mode (Table 2.2). Formation of product ions by retro Diels-Alder fragmentation according to the fragmentation proposed by Li et al. was observed for all triterpenes.^[83] Consecutive losses of water and CO₂ moieties (and a sugar moiety for tormentoside) were also detected. Two chromatographic peaks were detected for tormentoside, indicating the presence of two isomers. Next to the previously reported triterpenes, tormentic acid was tentatively identified for the first

time in the plant, with a fragmentation pattern similar to the other triterpene aglycons (Table 2.2).

Barros et al. reported the presence of chlorophylls a and b in meadowsweet.^[40] These compounds were also tentatively identified based on their MS fragmentation spectra and UV absorbance maxima. Two chromatographic peaks were observed for the respective chlorophylls, corresponding to chlorophyll epimers a and a' and b and b'.^[84] Moreover, other chlorophyll derivatives that have not been reported before in *Filipendula ulmaria*, such as phaeophytins, hydroxychlorophylls and dihydroxychlorophylls were also detected (Table 2.4).

Although only present in low amounts, two phytosterols (campesterol and β -sitosterol) that have not been described previously in the plant were identified with analytical standards (Table 2.4). Both phytosterols were characterized by abundant $[M+H-H_2O]^+$ ions due to in-source fragmentation. These main $[M+H-H_2O]^+$ ions of both phytosterols appeared at several retention times throughout the chromatogram (data not shown). Application of the same LC-PDA-amMS method in a former study has shown that the main in-source produced ion of a free sterol is also the main detected ion of its derivatives, i.e. acylated sterols, steryl glycosides and acylated steryl glycosides, generated by the loss of the attached sugar/fatty acid moieties due to in-source fragmentation.^[65] The deprotonated molecules of the derivatives usually are detected in the negative ionization mode, thereby revealing the identity of the attached sugar and/or fatty acid. Due to their low abundances, they could, however, not be detected during the present experiment.

Carotenoids have only been scarcely investigated in meadowsweet. Barros et al. has reported the presence of lycopene and β -carotene in inflorescences.^[40] Lycopene was not detected during the current study. Small amounts of β -carotene, lutein and violaxanthin were, however, identified with analytical standards (Table 2.4).

Barros et al. identified tocopherols in inflorescences of *Filipendula ulmaria*, but they were not detected during this study.^[40] Other compounds such as organic acids, amino acids, free sugars and lipids were tentatively identified with the LC-PDAamMS platform (data not shown). Although these findings are interesting from an analytical perspective, the biological functions of these compounds are known and no direct contribution to the specific pharmacological activity of *Filipendula ulmaria* is expected.

Salicylic acid, the *in vivo* metabolite of salicylic alcohol derivatives, could be responsible for part of the pharmacological activity of *Filipendula ulmaria*.^[35,85] During the current study, several metabolic precursors of salicylic acid were detected. However, a large diversity of other phytochemicals were identified that are likely to contribute as well to the activity. A versatile range of phytochemicals that were tentatively identified during this study are reported to be beneficial for human health. *Filipendula ulmaria* or extracts thereof may therefore be considered as a promising source for future functional ingredients, as flavonoid intake is known to be negatively correlated with the incidence of several chronic diseases including cardiovascular diseases, type II diabetes, neurodegenerative diseases and cancer.^[86,87] In view of the phenolic nature of the main constituents, extensive biotransformation after oral intake before absorption can be expected. It has been estimated that more than 90% of ingested polyphenols are not absorbed in the small intestine and, thus, remain in the colon at a high concentration where they are extensively fermented by gut microbiota to produce smaller molecules.^[88]

Generally, biochemical transformations by the gut microbiota include three major catabolic processes: hydrolysis (deglycosylations and ester hydrolysis), cleavage (C-ring cleavage, delactonization, demethylation) and reductions (dehydroxylation and double bond reduction).^[89] The intestinal microbiota is equipped with a rich diversity of different enzymes such as, α -rhamnosidase, β -glucuronidase, β -glucosidase, sulfatase and esterases, generating various metabolites. The gut microbiota thus influences the

bioavailability of polyphenols by modifying the structure of aglycons, glycosides and conjugates.^[90] Although the exact structure of the phenolic constituents identified during this study (e.g. the nature of the sugars and the interglycosidic linkages of glycosides) often cannot be established with LC-amMS without reference standards, these linkages are thus frequently broken during biotransformation. Comprehensive and fast LC-amMS profiling should be combined with pharmacological evaluation of plant extracts before and after metabolization to enable the identification of potential pro-drugs that otherwise may be overlooked. The findings on the extensive transformation of phenolic constituents thus urge the need for a shift of (poly)phenol research towards intestinal, colonic and hepatic metabolites as the principal bioactives. In chapter 3 these biotransformation reactions on the different classes of polyphenols by colonic bacteria are discussed in depth. Dietary ellagitannins for example, are hydrolyzed to release ellagic acid which can further be metabolized by the colon microbiota to produce dibenzopyranones. These are known as urolithin derivatives, which are less potent antioxidants as they have lost their free-radical scavenging activity, but have estrogenic and/or antiestrogenic activities, as well as anti-inflammatory and prebiotic effects. Ellagitannins absorption is very low and the extensive catabolism to urolithins in the gut suggest that these urolithins are the actual bioactive compounds rather than ellagitannins or ellagic acid.^[91,92] Procyanidins have been shown to mediate several anti-inflammatory mechanisms involved in the development of cardiovascular disease.^[93] A possible degradation into flavan-3-ols and low molecular weight products such as phenolic acids and valerolactones can be an explanation for the health effect of procyanidins.^[94,95] Likewise, hydroxycinnamic acids, naturally occurring anti-inflammatory bioactive compounds, are also extensively biotransformed after oral intake.^[96]

Next to phenolic compounds, only few and often low abundant non-phenolic phytochemicals were detected in *Filipendulae Ulmariae Herba*. Several triterpenes

were tentatively identified. Ursolic and pomolic acid were previously identified by Halkes as being the major compounds in the roots of *Filipendula ulmaria* inhibiting T lymphocyte proliferation.^[43] Ursolic acid belongs to the pentacyclic triterpenes class of compounds, which is widely distributed in the plant kingdom and is primarily responsible for the anti-inflammatory activity of a variety of medicinal plants.^[97] The chlorophyll derivatives, phytosterols and carotenoids detected in low abundance during this study are ubiquitously present in nature and no relevant contribution to the specific pharmacological activity of *Filipendula ulmaria* is expected.

In conclusion, the versatile phytochemical composition of Filipendulae Ulmariae Herba was comprehensively characterized for the first time with two complementary generic UHPLC-PDAamMS methods. Selective ion fragmentation with a hybrid quadrupole-orbital trap MS analyzer proved to be a valuable tool for identification of unknown compounds in a complex matrix such as *Filipendula ulmaria*. A total of 119 compounds (not including isomers) were tentatively identified, of which 69 compounds have never been reported in *Filipendula ulmaria* before. Several metabolic precursors of salicylic acid, an *in vivo* metabolite which might be responsible for part of the pharmacological activity of *Filipendula ulmaria*, were detected. However, next to salicylates, a rich diversity of phenolic constituents (including various oligomeric phenols) was tentatively identified. Only few and often low abundant non-phenolic phytochemicals were detected. Various detected phytochemicals are reported to be beneficial for human health; however, in view of the phenolic nature of the main constituents, extensive biotransformation after oral intake before absorption can be expected. This urges the need for research towards the identification and activity of the intestinal, colonic and hepatic metabolites of meadowsweet.

2.6 BRIDGING THE GAP BETWEEN COMPREHENSIVE EXTRACTION PROTOCOLS IN PLANT METABOLOMICS STUDIES AND METHOD VALIDATION

2.6.1 EVALUATION OF COMPREHENSIVE EXTRACTION PROTOCOLS: POLAR PHYTOCHEMICALS

The results from the comparison of the extraction methods with the polar LC-PDA-amMS method are depicted in Table 2.5. As described by Krueve et al., it is useful to make a distinction between recovery and process efficiency. Recovery refers to the losses and gains (caused by decomposition of other metabolites) of analyte during sample preparation, while process efficiency refers to loss or gain of analyte signal including the effects from sample preparation (recovery) and analyte ionization/detection.^[71] Both process efficiency and the influence of matrix components on analyte ionization were investigated in this experiment. The relative abundances presented in Table 2.5 describe the process efficiency. Next to various phenolic derivatives and some triterpenes, other compounds such as amino acids, sugars and organic acids were also detected. As amino acids, sugars and organic acids are out of the scope of this thesis, they are not included in Table 2.5.

The intensity drift during analysis calculated for the quality control samples was $\leq 15\%$ for approximately 94% of the quality control injections, thereby confirming instrumental stability. A first view on the results in Table 2.5 shows that even for the limited polarity range that is investigated here, none of the tested extraction methods is able to exhaustively extract the metabolites. Nevertheless, an overall good repeatability was observed for all extraction methods, even when low relative abundances were encountered (an RSD $\leq 15\%$ (n=3) is obtained for approximately 96% of the compounds with a process efficiency $\geq 5\%$). The lowest process efficiencies were

obtained when the plant matrix was extracted with ethyl acetate. Only a small fraction of the compounds was extracted in comparison with the other extraction methods, except for several apolar triterpene derivatives which mark the apolar boundary of the polar LC-PDA-amMS method. These results are in contrast with the results of Halabalaki et al. who reported that ethyl acetate was the most suitable solvent for extraction: during the current study dry *Filipendulae Ulmariae* Herba was extracted, while during the study of Halabalaki et al., *Vitis* wood samples were used for extraction solvent selection.^[66] Possibly the apolar character of ethyl acetate prohibits good permeation of the dry herbal *Filipendula* matrix. Michel et al. compared different extraction solvents and also observed that hydrophilic compounds were more abundant in the methanol extracts of *Olea europaea* than in the ethyl acetate extract, although not to the same extent as was observed during the current study.^[98] Liquid-liquid extraction of wine with ethyl acetate has been used previously for the extraction of phenolic constituents.^[99,100] Therefore, an extraction with ethyl acetate in combination with water was tried during the current experiment. The results in Table 2.5 show that the addition of water leads to a large increase in the extractability of a select group of phenolic constituents: process efficiency increases for flavonoids in the order of diglycosides < monoglycosides < aglycons with regard to the other extraction methods.

TABLE 2.5: RELATIVE ABUNDANCES (%) OF PHYTOCHEMICALS FROM *FILIPENDULA ULMARIA* OBTAINED WITH THE SELECTED EXTRACTION PROTOCOLS AND ANALYZED WITH THE POLAR LC-PDA-AMMS METHOD. THE RESULTS ARE EXPRESSED AS AVERAGE RELATIVE ABUNDANCE ± STANDARD DEVIATION OF 3 EXTRACTIONS. *ATP = APOLAR TO POLAR; **PTA = POLAR TO APOLAR

	polar reference	ethyl acetate	water:ethyl acetate	chloroform:methanol: water polar fraction	ATP* continuous (25 most polar fractions)	PTA** continuous (25 most polar fractions)	PTA** ASE (summation of 4 fractions)
gallic acid	72 ± 2	< 1	100 ± 3	21.3 ± 1	22 ± 1	44 ± 5	26 ± 3
methyl gallate	100 ± 7	< 1	< 1	2.3 ± 0.2	4.6 ± 0.3	12 ± 1	5.7 ± 0.4
protocatechuic acid	100 ± 1	6.1 ± 0.4	84 ± 3	72 ± 3	79 ± 10	83 ± 3	91 ± 3
salicylic acid	88 ± 1	6.7 ± 0.4	79 ± 3	73 ± 2	80 ± 10	96 ± 4	100 ± 2
syringic acid	93 ± 3	< 1	3.7 ± 0.7	90 ± 2	100 ± 3	79 ± 4	80 ± 2
methyl caffeate	100 ± 5	< 1	< 1	< 1	< 1	2.1 ± 0.3	2.17 ± 0.09
caffeic acid	25.3 ± 0.7	< 1	100 ± 5	5.8 ± 0.3	7 ± 0.4	7.6 ± 0.7	6.3 ± 0.1
p-coumaric acid	25.1 ± 0.9	1.56 ± 0.07	100 ± 3	7.4 ± 0.2	10 ± 1	13.7 ± 0.7	12.9 ± 0.5
kurumanin	89 ± 1	1.7 ± 0.4	1.3 ± 0.1	81 ± 4	75 ± 4	84 ± 6	100 ± 2
catechin	83 ± 2	6.3 ± 0.6	66 ± 2	74 ± 3	75 ± 4	88 ± 5	100 ± 3
epicatechin	80.3 ± 0.8	6 ± 0.8	63 ± 3	69 ± 1	77 ± 2	84 ± 4	100 ± 4
epigallocatechin	100 ± 3	< 1	46.4 ± 0.6	87 ± 2	85 ± 2	88 ± 5	100 ± 3
quercetin	39 ± 3	1.3 ± 0.6	100 ± 2	3.8 ± 0.1	5 ± 0.3	15 ± 1	8.2 ± 0.1
naringenin	100 ± 8	8.5 ± 0.5	79 ± 3	16.3 ± 0.1	32 ± 2	57 ± 3	38 ± 1
aromadendrin	88 ± 5	5 ± 0.8	100 ± 4	23.8 ± 0.7	30.9 ± 0.6	50 ± 4	44 ± 2
eriodictyol	91 ± 9	3.7 ± 0.5	100 ± 5	19.4 ± 0.3	30 ± 3	50.6 ± 0.7	45 ± 2
luteolin	65 ± 5	5.1 ± 0.9	100 ± 7	18 ± 1	21 ± 2	34 ± 2	26.2 ± 0.7
methoxyflavonoid	57 ± 6	35 ± 3	100 ± 5	5.6 ± 0.6	25 ± 2	47 ± 3	41 ± 3
methoxyflavonoid	61 ± 2	11 ± 1	100 ± 5	15.5 ± 1	35 ± 3	50 ± 0.3	43 ± 3
kaempferol	38 ± 3	1.8 ± 0.2	100 ± 5	3 ± 0.2	4 ± 0.4	13 ± 1	6.2 ± 0.2
isorhamnetin	38 ± 2	3.7 ± 0.3	100 ± 8	9 ± 1	10 ± 1	22 ± 1	19 ± 1
ursolic acid	25 ± 2	59.1 ± 0.4	49 ± 1	5.3 ± 0.5	18 ± 3	80 ± 6	100 ± 7
tormentic acid	44.6 ± 0.5	72 ± 1	60 ± 2	8.3 ± 0.1	15 ± 2	58 ± 2	100 ± 3
pomolic acid	41 ± 2	72 ± 4	60 ± 7	13.8 ± 0.4	31 ± 2	61 ± 3	100 ± 2
2-pyrone-4,6-dicarboxylic acid	96 ± 2	2.6 ± 0.5	1.5 ± 0.02	78 ± 2	100 ± 2	74 ± 4	76 ± 2
ellagic acid	100 ± 3	8 ± 3	77 ± 4	46 ± 4	93 ± 3	73 ± 3	66 ± 8
HHDP-hexoside isomers	100 ± 4	1.5 ± 0.4	1.2 ± 0.1	34 ± 1	41 ± 1	47 ± 2	43 ± 3
HHDP-monoalloyl-hexoside isomers	100 ± 7	< 1	9.2 ± 0.4	15.1 ± 0.9	18.2 ± 0.7	28 ± 5	15 ± 2
galloyl-threonic acid isomers	100 ± 3	< 1	< 1	43 ± 3	64 ± 7	52 ± 1	50 ± 10
monogalloylhexoside isomers	100 ± 3	2.2 ± 0.4	2.4 ± 0.1	76 ± 3	84 ± 3	72 ± 3	83 ± 5
digalloylhexoside isomers	100 ± 3	2.2 ± 0.5	11.5 ± 0.5	65 ± 3	69 ± 2	64 ± 4	67 ± 5
trigalloylhexoside isomers	94 ± 2	5 ± 1	27.8 ± 0.8	94 ± 4	96 ± 4	85 ± 5	100 ± 7
caffeoyl-threonic acid	100 ± 2	2.4 ± 0.6	2.5 ± 0.1	76 ± 3	90 ± 7	78 ± 1	80 ± 10
galloyl-caffeoyl-threonic acid	100 ± 0.7	1.8 ± 0.4	18.9 ± 0.7	60 ± 4	74 ± 6	61 ± 1	55 ± 9
digalloyl-caffeoyl-threonic acid	100 ± 0.4	2.9 ± 0.6	23 ± 1	82 ± 5	89 ± 5	82 ± 1	80 ± 10
trigalloyl-caffeoyl-threonic acid	74 ± 3	< 1	9 ± 1	88 ± 6	89 ± 6	91 ± 3	100 ± 10
coumaroylthreonic acid isomers	87 ± 2	3.2 ± 0.7	8.9 ± 0.4	78 ± 3	86 ± 6	85 ± 4	100 ± 4
digalloyl-coumaroyl-threonic acid	93 ± 2	3.9 ± 0.9	40 ± 2	88 ± 5	91 ± 5	86 ± 2	100 ± 10
di-O-caffeoylquinic acid isomers	100 ± 9	2.2 ± 0.3	55 ± 2	74 ± 6	83 ± 9	77 ± 8	90 ± 2
chlorogenic acid	94 ± 2	3.2 ± 0.6	4 ± 0.2	79 ± 3	96 ± 6	91 ± 2	100 ± 10
coumaroylquinic acid isomers	81 ± 2	3.5 ± 0.6	7.6 ± 0.4	80 ± 3	87 ± 4	84 ± 4	100 ± 2
pedunculagin isomer	64 ± 2	6 ± 1	3.8 ± 0.1	60 ± 5	96 ± 7	81 ± 2	71 ± 9
rugosin A	45 ± 2	2.9 ± 0.6	< 1	79 ± 7	100 ± 5	65 ± 1	70 ± 10
rugosin B	100 ± 5	2.6 ± 0.7	1 ± 0.1	64 ± 4	84 ± 3	88 ± 5	70 ± 10
rugosin D	60 ± 3	5.7 ± 1	7.1 ± 0.4	97 ± 2	100 ± 4	99 ± 5	87 ± 7
rugosin E	75 ± 3	4.9 ± 0.8	5.4 ± 0.3	83 ± 6	89 ± 2	100 ± 0.9	88 ± 10

*ATP: apolar to polar

**PTA: polar to apolar

TABLE 2.5: RELATIVE ABUNDANCES (%) OF PHYTOCHEMICALS FROM *FILIPENDULA ULMARIA* OBTAINED WITH THE SELECTED EXTRACTION PROTOCOLS AND ANALYZED WITH THE POLAR LC-PDA-AMMS METHOD. THE RESULTS ARE EXPRESSED AS AVERAGE RELATIVE ABUNDANCE ± STANDARD DEVIATION OF 3 EXTRACTIONS (CONTINUED).

	polar reference	ethyl acetate	water:ethyl acetate	chloroform:methanol: water polar fraction	ATP* continuous (25 most polar fractions)	PTA** continuous (25 most polar fractions)	PTA** ASE (summation of 4 fractions)
tellimagrandin I	79 ± 3	6 ± 1	22 ± 1	76 ± 4	100 ± 5	65 ± 1	76 ± 7
tellimagrandin II	43 ± 0.9	5.1 ± 0.9	14 ± 2	88 ± 8	100 ± 2	49 ± 1	86 ± 7
casuarinin/casuarictin	58 ± 1	5 ± 1	18 ± 2	59 ± 4	100 ± 3	42 ± 2	66 ± 4
(epi)catechin coupled to C ₁₅ H ₁₄ O ₅	92 ± 3	5.5 ± 0.8	58.7 ± 1	84 ± 2	77 ± 3	81 ± 4	100 ± 3
procyanidin dimer isomers	90 ± 2	5.8 ± 0.8	39 ± 1	84 ± 3	81 ± 3	85 ± 3	100 ± 3
procyanidin trimer isomers	99 ± 3	6.1 ± 0.9	28.1 ± 0.8	88 ± 3	81 ± 4	83 ± 5	100 ± 4
procyanidin tetramer isomers	100 ± 3	3.9 ± 0.6	12.9 ± 0.6	89 ± 5	81 ± 4	81 ± 4	92 ± 3
procyanidin pentamer isomers	89 ± 3	4.6 ± 0.8	7.2 ± 0.5	81 ± 2	73 ± 3	86 ± 4	100 ± 2
procyanidin hexamer isomers	93 ± 3	3 ± 0.8	10.7 ± 0.2	83 ± 1	75 ± 2	85 ± 4	100 ± 3
procyanidin heptamer isomers	100 ± 6	< 1	< 1	80 ± 3	81 ± 3	92 ± 4	97 ± 5
procyanidin dimer gallate	100 ± 2	4.6 ± 0.9	58 ± 1	89 ± 5	80 ± 4	81 ± 3	95 ± 4
isosalicin	76 ± 1	2.9 ± 0.3	5.2 ± 0.3	80 ± 4	88 ± 6	83 ± 4	100 ± 3
spiraein	2.5 ± 0.1	5.2 ± 0.6	< 1	43 ± 3	85 ± 3	21 ± 6	100 ± 2
monotropitin	2.3 ± 0.09	5.2 ± 0.7	< 1	26 ± 2	57 ± 2	7 ± 3	100 ± 3
salicylic acid hexoside	94 ± 2	4.7 ± 0.6	< 1	92 ± 4	97 ± 3	84 ± 4	100 ± 2
rutin	69.5 ± 0.5	3.1 ± 0.5	2.5 ± 0.3	75 ± 2	70 ± 4	84 ± 4	100 ± 1
quercitrin	72 ± 2	5.2 ± 0.5	63 ± 2	65 ± 3	61 ± 3	68 ± 4	100 ± 3
hyperoside + isoquercitrin	64 ± 3	3.8 ± 0.5	30 ± 1	61 ± 1	59 ± 2	87 ± 4	100 ± 2
astragalin	79.9 ± 0.4	5.8 ± 0.7	50 ± 2	73 ± 2	77 ± 3	100 ± 5	99 ± 2
miquelianin	100 ± 2	3.1 ± 0.6	3.3 ± 0.1	75 ± 3	90 ± 8	83 ± 5	86 ± 7
quercetin- <i>O</i> -galloyldihexoside	83 ± 1	3 ± 0.6	14.8 ± 0.5	75 ± 2	64 ± 1	91 ± 6	100 ± 2
isorhamnetin- <i>O</i> -hexoside isomer	100 ± 3	5 ± 1	46 ± 3	90 ± 10	95 ± 5	98 ± 7	57 ± 3
methoxyflavonoid- <i>O</i> -hexoside-deoxyhexoside	72.8 ± 0.7	11 ± 1	4.3 ± 0.2	60.8 ± 0.4	63 ± 3	70 ± 3	100 ± 2
quercetin- <i>O</i> -galloylhexoside isomers	100 ± 1	4.5 ± 0.9	64 ± 1	87 ± 3	77 ± 3	85 ± 5	99 ± 3
kaempferol- <i>O</i> -hexoside-deoxyhexoside	62 ± 3	3.9 ± 0.6	4.2 ± 0.6	68.4 ± 0.9	67 ± 3	73 ± 4	100 ± 2
quercetin- <i>O</i> -pentoside	82.9 ± 0.2	5.1 ± 0.7	61 ± 2	70 ± 1	71 ± 3	82 ± 5	100 ± 6
isorhamnetin- <i>O</i> -hexoside isomer	78 ± 2	3.1 ± 0.1	52 ± 4	60 ± 2	55 ± 1	71 ± 4	100 ± 2
flavonoid- <i>O</i> -galloylhexoside	97 ± 2	4.2 ± 0.8	80 ± 3	83 ± 3	73 ± 2	84 ± 2	100 ± 3
quercetin- <i>O</i> -digalloylhexoside isomers	92 ± 1	3.4 ± 0.9	80 ± 1	86 ± 3	70 ± 3	80 ± 3	100 ± 4
kaempferol- <i>O</i> -hexoside	50 ± 2	5 ± 0.7	39 ± 2	55 ± 1	65 ± 2	73 ± 2	100 ± 3
methoxyflavonoid- <i>O</i> -hexoside-deoxyhexoside	81 ± 5	10 ± 1	14.5 ± 0.1	54 ± 5	58 ± 2	90 ± 6	100 ± 2
dimethoxyflavonoid- <i>O</i> -hexoside-deoxyhexoside	93 ± 3	9.3 ± 0.8	14.6 ± 0.1	60 ± 5	64 ± 4	96 ± 10	100 ± 4
quercetin- <i>O</i> -galloyldeoxyhexoside	96 ± 2	4.4 ± 0.6	91 ± 1	83 ± 4	65 ± 4	83 ± 3	100 ± 3
avicularin/avicularoside	84 ± 2	5.3 ± 0.8	63 ± 2	67 ± 2	68 ± 3	83 ± 5	100 ± 5
aesculetin	68 ± 4	2.9 ± 0.5	74 ± 3	28 ± 2	43 ± 4	57 ± 2	100 ± 10

*ATP: apolar to polar

**PTA: polar to apolar

Most phenolic and hydroxycinnamic acids are also extracted in high amounts, whereas the majority of the tannins is not well extracted. As described by Naczki et al., solubility of phenolic compounds is governed by several factors such as solvent used, as well as interaction of phenolics with other constituents, and there is no uniform procedure that is suitable for extracting all phenolics in plant materials.^[101] During this study it was observed that some of the phenolic constituents are even much better extracted with the water:ethyl acetate mixture than with the polar reference method. For instance, for kaempferol a relative abundance of only 38% is obtained with the reference protocol, which is in contrast with the high recovery for kaempferol obtained with spiking experiments on dry apple matrix during method validation (92%).^[64] This discrepancy in results might be caused by the difference in matrix composition or the fact that spiked compounds are not encapsulated in the matrix.

Analysis of the polar fraction of the chloroform:methanol:water extraction revealed that a much broader range of polar metabolites is extracted with this protocol than with ethyl acetate extraction (Table 2.5). Tannins and glycosylated flavonoids are well extracted. On the other hand, some of the phenolic acids, most of the flavonoid aglycons, the hydroxycinnamic acids and the triterpenes are only recovered in minor amounts. To check whether polar compounds did partition into the apolar chloroform fraction, the chloroform extracts were back-extracted with 2:1 (v/v) methanol:water. Analysis revealed that for approximately 60% of the compounds in Table 2.5 less than 5% of the total extracted amount was partitioned to the apolar phase. For approximately 21% of the compounds more than 15% of the total amount (ranging between 15% and 61%) was partitioned to the apolar phase. This group consisted mostly of flavonoid aglycons, hydroxycinnamic acids and triterpene derivatives, compounds of which only minor amounts are extracted with the chloroform:methanol:water extraction protocol. Partitioning of compounds into the

apolar chloroform phase therefore only has minor influence on the relative abundances in Table 2.5.

The notion that the extraction method giving the highest signal intensity is optimum may not always be true, because high recovery of one metabolite may be caused by decomposition of other metabolites.^[102] For instance, the physicochemical properties of methyl gallate and methyl caffeate are not that different from other phenolic compounds detected in *Filipendula ulmaria*. Nonetheless, their relative abundance profile is very different from that of the other phenolic constituents. Relative to the polar reference extraction method, only low amounts of methyl gallate and methyl caffeate are obtained with the other extraction methods (Table 2.5). This suggests potential artefact formation during extraction with the reference method. It has been described that in case of methanol as extraction solvent it is difficult to know whether a methoxy group is naturally occurring or is an artefact from the solvent.^[103,104] Thus, methyl gallate and methyl caffeate may potentially be formed by methylation of gallic acid and caffeic acid, both present in high abundance in *Filipendula ulmaria*.^[1] To investigate the source of these methylated acids, reference standards of gallic acid and caffeic acid were diluted in 80:20 (v/v) water:methanol + 40 mM ammonium formate and methanol + 40 mM ammonium formate. Aliquots of the dilutions were subsequently sonicated for 2 h. Analysis with LC-PDA-MS revealed no differences in composition before and after sonication, thereby excluding non-enzymatic methylation reactions. As an additional test, aliquots of *Filipendula ulmaria* were extracted with the polar reference method, however, with the order of solvents in reverse (i.e. first with 100% methanol + 40 mM ammonium formate to cause enzyme denaturation and secondly with 80:20 (v/v) water:methanol + 40 mM ammonium formate). Results showed that extraction with the same solvents in reverse order decreased the level of extracted methyl gallate and methyl caffeate to approximately 5% and 2%, respectively. This large decrease suggests that these compounds are formed by

enzymes. To confirm these findings, ferulic acid, a compound which is not natively present in meadowsweet but has a structure very similar to gallic acid and caffeic acid, was added before extraction to induce enzymatic methyl ferulate formation. Extraction of *Filipendula ulmaria* according to the polar reference method in the presence of 5 mg ferulic acid did however only lead to the formation of minor amounts methyl ferulate. In contrast to the ratios of the areas of methyl caffeate/caffeic acid (4.0) and methyl ferulate/ferulic acid (4.7), the methyl ferulate/ferulic acid ratio remained very low (0.0004). Possibly, methyl gallate and methyl caffeate are formed enzymatically from the various galloyl and caffeoyl containing phenolic oligomers present in *Filipendula ulmaria*, and not from gallic acid and caffeic acid.

During the above described experiments, gallic acid and caffeic acid were identified with reference standards. However, no standards of methyl gallate, methyl caffeate and methyl ferulate were available, so their identification during LC-PDA-amMS analysis remained tentative. To confirm their presence, gallic acid and ferulic acid were methylated with a method adapted from Makkar.^[70] LC-PDA-amMS analysis of the reaction products confirmed the identities of methyl gallate and methyl ferulate, thereby supporting the above hypothesis.

Inactivation of enzymes prior to extraction to avoid unpredictable artefact formation could be performed by using denaturing agents, heating or by using acids.^[105] Care should on the other hand be taken to assure that the enzymatic inactivation procedure itself does not lead to artefact formation. For example, labile compounds such as carotenoids can degrade or isomerize under the influence of light, oxygen, enzymes, heat, oxidants and acid or alkaline conditions. Carotenoids containing 5,6-epoxide moieties for instance easily undergo rearrangements to 5,8-epoxides, a reaction which is catalyzed by acids.^[65] Similarly, freeze-drying of tissue to remove water may lead to the irreversible adsorption of metabolites on cell walls and membranes.^[105]

The comprehensive extraction protocol developed by Yuliana et al. consists of a continuous extraction with solvents ranging from apolar to polar. During the current study, extractions similar to that of Yuliana et al. were carried out with solvents ranging from apolar to polar and vice versa, hereafter referred to as apolar to polar (ATP) and polar to apolar (PTA) continuous extraction, respectively (Table 2.5).^[69] Because of the large solvent volumes used during this continuous extraction process (approximately 300 mL), the constituents are heavily diluted. Nevertheless, the sensitivity of LC-PDA-amMS analysis allows to omit a concentration step. To investigate the process efficiency of moderately polar constituents with the ATP and PTA continuous extraction protocols, the 25 most polar fractions were combined, discarding the remaining apolar fractions. All compounds in Table 2.5, with the exception of the apolar triterpenes, were predominantly recovered in the 25 most polar fractions of both the ATP and PTA continuous extraction. The relative abundances of the compounds extracted with the ATP and PTA continuous extraction were generally slightly elevated in comparison to those obtained in the polar fraction of the chloroform:methanol:water extraction. The relative abundances obtained with PTA continuous extraction are similar to those obtained for ATP continuous extraction. However, in contrast with ATP continuous extraction, very low recoveries were found for salicylic primveroside derivatives monotropitin and spiraein (Table 2.5). Such low recoveries for primveroside derivatives were also observed for the polar reference extraction method, of which the first extraction solvent consists of 80:20 (v/v) water methanol + 40 mM ammonium formate (Table 2.5). It has been reported that monotropitin, present in the leaves of *Gaultheria procumbens*, is hydrolyzed in the presence of water by the enzyme gaultherase to produce methyl salicylate and a sugar, primverose.^[106] To test whether the low recoveries for the primveroside derivatives encountered during the current study were due to interaction with enzymes, aliquots of *Filipendula ulmaria* were extracted with the polar reference method, however, with the order of solvents in reverse. This resulted in high process efficiencies for the primveroside derivatives, suggesting

enzymatic degradation during the extraction methods starting with water or water:methanol mixtures. For confirmation, aliquots of *Filipendula ulmaria* were extracted with water at room temperature and with water heated to 90 °C, causing denaturation of enzymes. The extraction with water at 90 °C resulted in high process efficiencies for the salicylic primveroside derivatives, comparable to those obtained during ATP continuous extraction. The extraction with water at room temperature resulted in very low process efficiencies (0-2%). Flavonoid glycosides on the other hand were extracted well with both water at 90 °C and at room temperature, indicating that the difference in salicylic primveroside derivatives extraction is not temperature related but caused by enzymatic interactions. The reactivation of enzymes during extraction of fresh or dried plant material may lead to biased results: in the case of *Filipendula ulmaria*, part of the pharmacological effect can be explained by its salicylic acid component, which is released via oxidation from various aglycones (e.g. salicylaldehyde and methyl salicylate) developed from glycosides through hydrolysis in the digestive system.^[35] Low extraction yields of salicylic primveroside derivatives might therefore lead to lower activity or false negative results.

Several method parameters were changed in an effort to optimize the process efficiency of the continuous extraction protocols, such as extraction with a lower flow rate (4 mL/min instead of 8 mL/min) or change in the steepness of the solvent gradient. None of the changes led to significant improvements. Continuous extraction with heated solvents could potentially lead to higher extraction efficiencies of phytochemicals. However, initial experiments with heated solvents revealed rapid and uncontrollable decreases in solvent temperature. Instrument tubings should therefore be isolated during future experiments to prevent these losses.

Extraction of *Filipendula ulmaria* with ASE was carried out sequentially with different solvents ranging from polar to apolar (PTA ASE). The relative abundances that were obtained for PTA ASE (Table 2.5) are in general slightly better than those of all other

tested comprehensive extraction protocols. Moreover, no degradation of salicylic primveroside derivatives was observed. It was found previously during optimization of the apolar reference method that swelling of the matrix with water prior to ASE with an apolar extraction solvent caused a significant decrease in concentration of the C17-polyacetylenes falcarinol and falcarindiol. Experimental data indicated that this decrease during sample swelling was most probably caused by enzymatic interactions.^[107] On the contrary, the wetting step caused a significant increase in extracted carotenoids. So a trade-off may exist between unpredictable enzymatic breakdown and lower extraction yields. In a metabolomics experiment unpredictable changes to the metabolite composition are undesirable and therefore wetting of the sample should be avoided. To find out whether these effects caused by wetting of the sample prior to extraction also occurred with PTA ASE, *Filipendula ulmaria* was let to swell before PTA ASE: ultrapure water was added to the sample until it was hydrated (approximately 3 mL). Thereafter the sample was let to rest in the dark under N₂ for 30 min to allow swelling of the matrix. Analysis of the extracts revealed that for most compounds process efficiencies were comparable to those obtained with PTA ASE without sample wetting (data not shown). For hydroxycinnamic and phenolic acids and some flavonoid aglycons, however, higher extraction yields were obtained in comparison to PTA ASE without sample wetting. On the other hand, as with the polar reference method, very low recoveries were obtained for the salicylic primveroside derivatives, caused by enzymatic degradation during sample wetting. Because of the higher pressures and temperatures applied during ASE, apolar to polar ASE without wetting of the sample prior to extraction could potentially result in process efficiencies that are better than those obtained for ATP and PTA continuous extraction, combined with lower solvent consumption.

In LC-MS analysis, ionization efficiency of the analytes may be strongly altered by co-eluting compounds which may cause a reduction or an increase of the analyte

signal.^[108] To find out whether (part of) the differences in relative abundances that were observed in Table 2.5 were caused by changes in ionization efficiency, a post-column infusion experiment was carried out with (D-Ala²)-leucine enkephalin. Comparison of the (D-Ala²)-leucine enkephalin intensity profile during analysis of the *Filipendula ulmaria* extracts with that of a solvent blank revealed similar effects for the different sample preparation protocols: major ionization suppression and enhancement effects were detected in the beginning of the chromatogram (1-3 min). These effects, observed in both positive and negative ionization mode, are caused by early eluting polar bulk compounds such as sugars and organic acids. Only one of the secondary metabolites listed in Table 2.5, namely HHDP-hexoside, elutes in the 1-3 min region. Figure 2.4 shows a comparison of the (D-Ala²)-leucine enkephalin intensity profile during analysis of a *Filipendula ulmaria* extract from the polar reference method with that of a solvent blank (expressed as percent deviation). Due to instrumental fluctuations, variation in the (D-Ala²)-leucine enkephalin could not be excluded. This prohibited investigation of minor changes in ionization efficiency caused by matrix effects. Nonetheless, as no other major ion suppression/enhancement effects were observed, the differences in relative abundances in Table 2.5 are thus predominantly caused by differences in extraction efficiency.

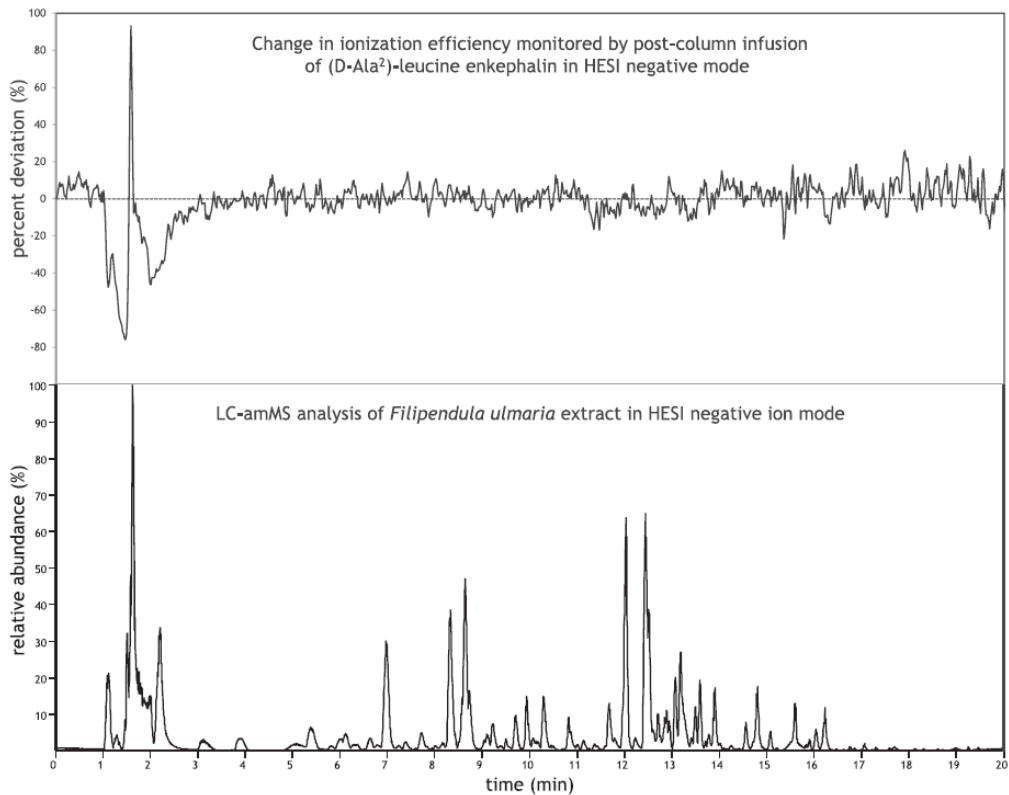


FIGURE 2.4: A COMPARISON OF THE (D-ALA²)-LEUCINE ENKEPHALIN INTENSITY PROFILE DURING ANALYSIS OF A *FILIPENDULA ULMARIA* EXTRACT FROM THE POLAR REFERENCE METHOD WITH THAT OF A SOLVENT BLANK (EXPRESSED AS PERCENT DEVIATION). MAJOR CHANGES IN IONIZATION EFFICIENCY CAUSED BY MATRIX COMPOUNDS ARE RESTRICTED THE FIRST 3 MIN OF THE ANALYSIS.

The data in Table 2.5 show that the extraction efficiency changes depending on the solvents and techniques used: a non-compound-specific extraction protocol cannot be achieved. Oldiges et al. therefore suggested that the basic requirement in a metabolomics experiment is the reproducibility of the protocol to allow direct comparison between samples, although the protocol potentially discriminates between chemical properties of the compounds.^[109] During the current study it was investigated whether an extraction method that allows only partial extraction of phytochemicals is quantitatively repeatable over several days. The repeatability and intermediate precision were calculated for the ATP continuous extraction protocol as described in section 2.4.5.3. The intermediate precision data in Figure 2.5 show that the 15% boundary recommended by the U.S. Food and Drug Administration (FDA) regarding the analytical variability for targeted analysis, is only crossed for 5% of the compounds.^[110] Although metabolomics is of a whole different fundamental analytical nature, the FDA guidance is used as a benchmark towards the repeatability evaluation of metabolomics approaches.^[111] The repeatability data in Figure 2.5 demonstrate that even in the case of low extraction efficiencies for polar phytochemicals, extracts with highly similar composition are produced over different days with the ATP continuous extraction protocol. A thorough investigation of the stability of the phytochemicals in the (dried) extracts should be carried out in future experiments to determine a time frame in which the extracts may be used for metabolomics experiments.

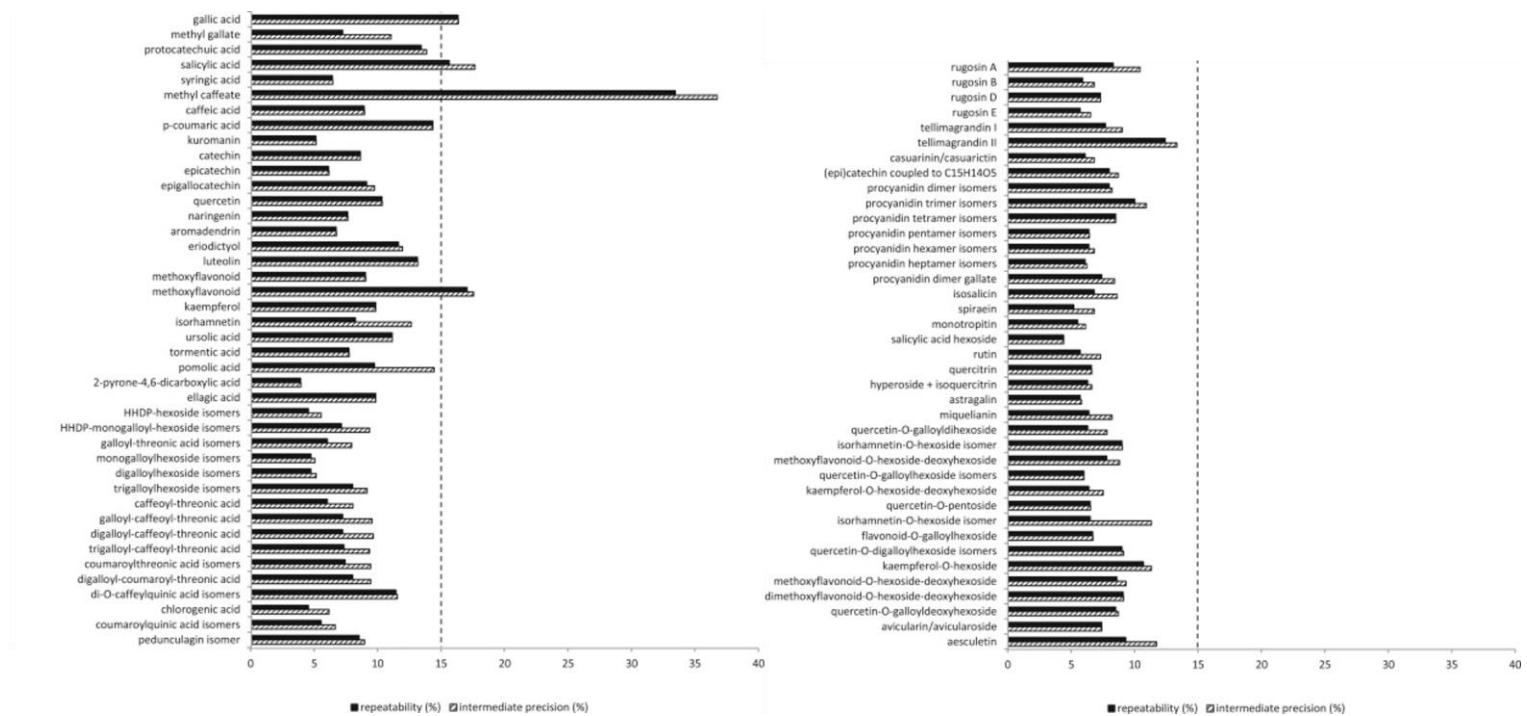


FIGURE 2.5: REPEATABILITY AND INTERMEDIATE PRECISION OF PHYTOCHEMICALS FROM *FILIPENDULA ULMARIA* OBTAINED WITH THE ATP CONTINUOUS EXTRACTION, CALCULATED ACCORDING TO THE EURACHEM.^[72]

2.6.2 EVALUATION OF COMPREHENSIVE EXTRACTION PROTOCOLS: APOLAR PHYTOCHEMICALS

Filipendula ulmaria only contains minor amounts of apolar phytochemicals.^[1] As the genus *Capsicum* is a rich source of apolar phytochemicals, it was decided to use spicy paprika powder consisting of a mixture of paprika (*Capsicum annuum*) and chili pepper (*Capsicum frutescens*) for in depth evaluation of the performance of the comprehensive extraction protocols. The process efficiencies of selected comprehensive extraction procedures were compared with an apolar reference extraction method, previously developed for the generic extraction of apolar plant metabolites.^[65] The results obtained from the comparison of the extraction methods with the apolar LC-PDA-amMS method are depicted in Table 2.6. A large variety of compounds such as carotenes, free and esterified xanthophylls, phytosterol aglycons and glycosides, capsaicinoids and a lipid soluble vitamin, was investigated. The relative abundances describe the process efficiencies.

The results in Table 2.6 show that also for apolar metabolites large differences in relative abundances are observed between extraction methods. Nonetheless, a good repeatability was obtained for the greater part of compounds (RSD $\leq 15\%$ (n=3) for approximately 80% of the compounds). High relative abundances were obtained for a broad spectrum of apolar metabolites during ethyl acetate and water:ethyl acetate extraction, which is in contrast with the low extraction efficiencies observed during polar phytochemical extraction (Table 2.5). Similar results were obtained during chloroform:methanol:water extraction. To check whether apolar compounds partitioned into the polar fraction during chloroform:methanol:water extraction, the polar fractions were back-extracted with a solution of *trans*- β -apo-8'-carotenal in dichloromethane + 0.1% BHT. Analysis revealed that the most polar compounds among the investigated apolar compounds, namely the capsaicinoids and glycosylated sterols, were partitioned only in small amounts to the polar phase (9%-13% of the total

extracted amount). The other apolar compounds were only partitioned for 2% or less into the polar phase.

TABLE 2.6: RELATIVE ABUNDANCES (%) OF PHYTOCHEMICALS FROM SPICY PAPRIKA POWDER OBTAINED WITH THE SELECTED EXTRACTION PROTOCOLS AND ANALYZED WITH THE APOLAR LC-PDA-amMS METHOD. THE RESULTS ARE EXPRESSED AS AVERAGE RELATIVE ABUNDANCE ± STANDARD DEVIATION OF 3 EXTRACTIONS. *ATP = APOLAR TO POLAR; **PTA = POLAR TO APOLAR

	apolar reference	ethylacetate	water:ethyl acetate	chloroform:methanol: water apolar fraction	ATP* continuous extraction (25 most apolar fractions)	PTA** continuous extraction (summation of polar and apolar fraction)	PTA** ASE (summation of 4 fractions)
nordihydrocapsaicin	5.3 ± 0.7	55 ± 2	75 ± 5	64 ± 6	74 ± 2	44 ± 4	100 ± 7
capsaicin	5.2 ± 0.6	54 ± 4	77 ± 4	60 ± 7	67 ± 1	41 ± 4	100 ± 4
dihydrocapsaicin	9.6 ± 0.7	58 ± 2	77 ± 5	70 ± 4	75 ± 3	35 ± 5	100 ± 8
homodihydrocapsaicin	15 ± 2	61 ± 4	75 ± 5	64 ± 6	78 ± 3	27 ± 9	100 ± 8
cycloviolaxanthin	90 ± 4	89 ± 1	92 ± 4	84 ± 9	89 ± 4	45 ± 5	100 ± 6
campesteryl-glycoside	22.5 ± 0.8	45 ± 3	60 ± 3	47 ± 4	52 ± 2	40 ± 10	100 ± 5
cis-capsanthin	47.8 ± 1	61 ± 3	68 ± 5	50 ± 4	43 ± 2	47 ± 8	100 ± 6
capsanthin	92 ± 3	84 ± 4	90 ± 10	90 ± 7	97 ± 6	70 ± 4	100 ± 8
β-sitosteryl-glycoside	28.7 ± 0.8	46 ± 2	57 ± 3	49 ± 4	48 ± 2	40 ± 10	100 ± 9
antheraxanthin	98 ± 8	96 ± 3	99 ± 9	90 ± 10	100 ± 2	63 ± 6	70 ± 20
γ-tocopherol	89 ± 6	76 ± 2	78 ± 8	80 ± 10	79 ± 4	90 ± 10	100 ± 5
campesterol	74 ± 3	61 ± 4	62 ± 5	73 ± 5	71 ± 1	70 ± 10	100 ± 9
capsorubin-myristate	97 ± 5	89 ± 7	91 ± 9	100 ± 10	95 ± 5	70 ± 10	60 ± 20
capsanthin-laurate isomer	100 ± 8	85 ± 7	81 ± 7	100 ± 10	95 ± 7	90 ± 10	60 ± 10
β-sitosterol	74 ± 7	61 ± 2	65 ± 1	73 ± 7	71 ± 4	63 ± 10	100 ± 10
capsanthin-laurate isomer	100 ± 6	81 ± 3	85 ± 6	90 ± 10	90 ± 10	85 ± 6	79 ± 9
antheraxanthin-laurate	89 ± 3	99 ± 7	100 ± 10	80 ± 10	94 ± 3	50 ± 40	20 ± 20
capsanthin-myristate isomer	97 ± 9	95 ± 6	100 ± 8	87.8 ± 0.2	100 ± 20	90 ± 20	70 ± 20
β-carotene	98 ± 4	100 ± 5	100 ± 6	84 ± 9	94 ± 2	70 ± 30	40 ± 10
phytofluene	96 ± 3	86 ± 5	85 ± 5	91 ± 6	91 ± 5	90 ± 10	100 ± 6
capsanthin-myristate isomer	100 ± 20	93.8 ± 0.9	100 ± 9	86 ± 8	92 ± 10	80 ± 20	70 ± 20
antheraxanthin-myristate	95 ± 4	100 ± 5	100 ± 20	90 ± 20	100 ± 8	40 ± 40	20 ± 20
phytoene	79 ± 2	66 ± 3	64 ± 5	71 ± 9	76 ± 3	80 ± 10	100 ± 5
capsanthin-di-laurate	88 ± 7	83 ± 1	81 ± 4	90 ± 10	100 ± 6	90 ± 20	70 ± 7
capsanthin-laurate-myristate	100 ± 10	87 ± 5	90 ± 10	96 ± 8	100 ± 10	90 ± 20	70 ± 8

The highest relative abundances for capsaicinoids and phytosterol glycosides were obtained for PTA ASE. In contrast, the lowest relative abundances for these compounds were encountered during extraction with the apolar reference method. This apolar reference method consists of three ASE cycles with 70:30 (v/v) acetone:methanol + 0.1% BHT followed by the addition of an aqueous NaCl-solution and back-extraction with *n*-hexane, thereby favoring the extraction of apolar compounds.

To investigate the process efficiency of apolar phytochemicals with the ATP and PTA continuous extraction protocols, the 25 most apolar fractions were combined for analysis. It was noticed that in contrast with ATP continuous extraction, during PTA continuous extraction the greater part of capsaicinoids was recovered in the remaining

polar fractions (78-88%). Other compounds were predominantly found in the 25 most apolar fractions during both ATP and PTA continuous extraction ($\geq 96\%$). It was therefore decided to combine the results of the polar and apolar fractions of the PTA continuous extraction in the calculation of the relative abundances tabulated in Table 2.6. Still, higher relative abundances were found for capsaicinoids during ATP continuous extraction: these results may however be influenced by incomplete recovery of capsaicinoids during back-extraction of the remaining polar fractions with dichloromethane. Although the extraction solvents used during continuous extraction are also applied during PTA ASE (except hexane), lower relative abundances were obtained for capsaicinoids and phytosterol glycosides during continuous extraction. This is probably due to the differences in temperature and pressure applied during extraction. Lower relative abundances were observed for the compounds tentatively identified as antheraxanthin-laurate and antheraxanthin-myristate, and β -carotene (identified with analytical standard) during PTA ASE and PTA continuous extraction (with a large variability between replicates). The cause of these lower relative abundances should be investigated during future experiments. Nonetheless, the data in Table 2.6 show that none of the tested extraction methods is able to exhaustively extract the metabolites.

It is known that when using APCI high abundant matrix compounds such as lipids can cause major ionization suppression effects.^[112] The ionization efficiency during analysis of the spicy paprika powder extracts was examined by post-column infusion of (D-Ala²)-leucine enkephalin as described in section 2.4.5.2. No major ion suppression/enhancement effects were observed, indicating that the differences in relative abundances in Table 2.6 are predominantly caused by differences in extraction efficiency. Nonetheless, as different ionization effects may be observed even for very similar matrices, ionization efficiency should ideally be evaluated for every new matrix.^[113]

It was investigated whether the extraction of apolar phytochemicals with the ATP continuous extraction protocol is quantitatively repeatable over several days. The experiments were conducted as described in section 2.4.5.3. The results in Figure 2.6 show that the 15% boundary proposed by the FDA is only crossed for 3 compounds.^[110] These data demonstrate that extracts with highly similar composition are produced over different days with the ATP continuous extraction protocol.

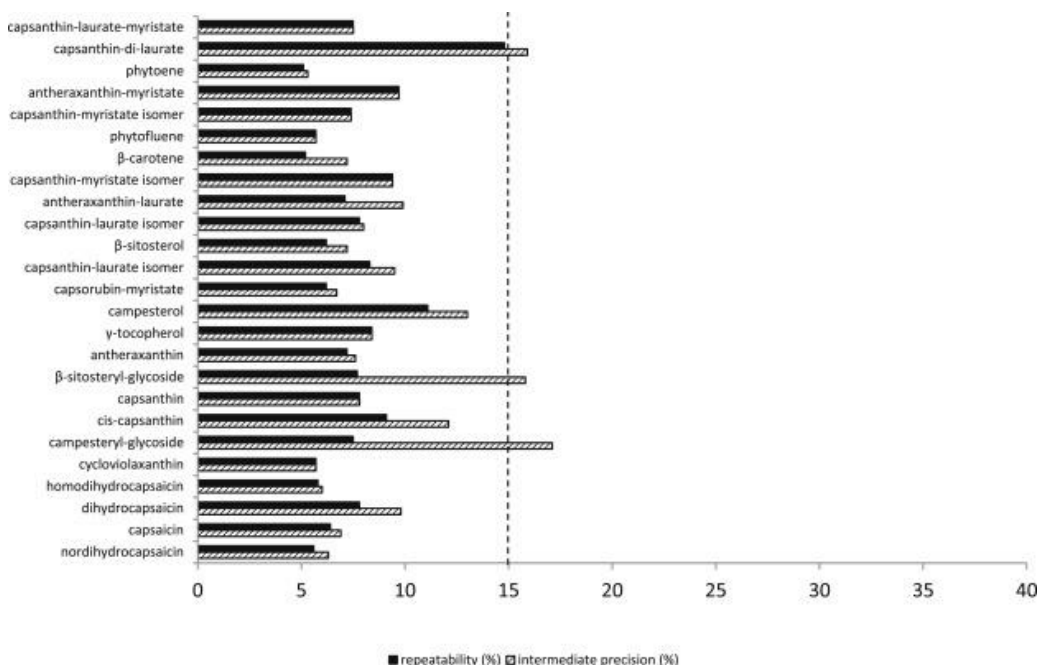


FIGURE 2.6: REPEATABILITY AND INTERMEDIATE PRECISION OF PHYTOCHEMICALS FROM SPICY PAPRIKA POWDER OBTAINED WITH THE ATP CONTINUOUS EXTRACTION, CALCULATED ACCORDING TO THE EURACHEM.^[72]

When combining the extraction efficiency data from Table 2.5 and Table 2.6, it can be concluded that the extraction efficiency is dependent on the solvents and techniques used: none of the comprehensive extraction methods is non-compound specific. The most remarkable differences were observed for moderately polar phytochemicals. In contrast with other studies, ethyl acetate and water:ethyl acetate extraction resulted in very low extraction efficiencies for most polar compounds. With regard to the other tested extraction methods, the extraction efficiency of most compounds increases in

the order of chloroform:methanol:water extraction < continuous extraction < PTA ASE. Nonetheless, in plants metabolomics studies other criteria besides extraction efficiency, such as ease of use, fractionation and dilution factor should also be considered. Chloroform:methanol:water is for instance easily scalable and only requires low amounts of solvent, while ASE and continuous extraction are less flexible in scalability and demand the availability of dedicated instrumentation. Furthermore, high amounts of organic solvents are consumed during continuous extraction, thereby resulting in heavily diluted fractions. During selection of the most appropriate extraction method, a compromise has to be made.

As described by Halabalaki et al., either generic extraction procedures are used, or protocols are adapted to a given set of samples. A generic approach has the advantage of enabling comparisons between very different samples. A protocol adapted to a given sample type on the other hand has the advantage that detailed comparisons among a given set of samples can be obtained, as is required for the comparison of different cultivars. The disadvantage of such a carefully adapted protocol is that the data generated are valid only for very specific samples and cannot be compared with other studies.^[66] In the search for bioactive constituents of plants, it is important that the phytochemical composition of the extract is representative for the natural phytochemical composition of the plant material. Large differences in extraction efficiency between plant constituents could for example skew the results of pharmacological tests, leading towards wrong conclusions. In order to obtain an extract that represents the natural phytochemical composition of the plant material, extracts of different methods could be combined. The polar phytochemical composition of water:ethyl acetate and chloroform:methanol:water extraction is for example very complementary (Table 2.5). Combination of these extracts should result in an extract with a well-balanced phytochemical profile, i.e. an extract that is truly representative for the phytochemical composition native to the plant material under study.

CONCLUSION

During the first experiment, the phytochemical composition of *Filipendula ulmaria* was comprehensively characterized for the first time with two complementary generic ultrahigh-performance liquid chromatography-photodiode array-accurate mass spectrometry methods. Selective ion fragmentation experiments with a hybrid quadrupole-orbital trap mass spectrometer significantly contributed to compound identification: a total of 119 compounds were tentatively identified, of which 69 new to *Filipendula ulmaria*. A rich diversity of phenolic constituents was detected and only a few non-phenolic phytochemicals were observed. Biotransformation and pharmacological studies should be conducted to investigate which of these constituents or metabolites there of contribute to the activity of *Filipendula ulmaria* after oral intake.

The second experimental part fills an existing gap in the understanding of the role of sample preparation protocols in the outcome of plant metabolomics studies. Evaluation of the performance of extraction methods is often omitted in plant metabolomics. This can greatly affect the overall quality of the study. This study is the first to thoroughly evaluate and compare state-of-the-art comprehensive extraction protocols for untargeted plant metabolomics. Meadowsweet and spicy paprika powder were selected as matrices for extraction method comparison based on their versatile and complementary phytochemical composition (e.g. polyphenols, terpenes, capsaicinoids, phytosterols and carotenoids). Generic LC-PDA-amMS methodology developed for wide range phytochemical analysis allowed evaluating the comprehensive extraction methods on compound level: it was shown that none of the tested comprehensive extraction methods is able to exhaustively extract the phytochemicals. Furthermore, discrepancies in results with other studies, such as in the case of ethyl acetate extraction, show that phytochemical extraction is highly

dependent on the plant matrix under study. It was also found that depending on the extraction conditions enzymatic activation can occur, thereby potentially leading to lower activity or false negative results. Nevertheless, an overall good repeatability was observed for all extraction methods, even when low relative abundances were encountered: this is essential to allow direct comparison between samples. Multiple criteria are important when selecting the most suitable extraction method such as extraction efficiency, repeatability, fractionation power, ease of use, speed, dilution factor and scalability. Based on these criteria, the extraction method that best fits the goals and constraints of the metabolomics experiment as a whole should be selected. As shown during this study, no single procedure performs best in terms of all these criteria and a compromise will have to be made. The polar phytochemical composition of water:ethyl acetate and chloroform:methanol:water extraction is very complementary and a combination of these extracts should result in an extract with a well-balanced phytochemical profile.

REFERENCES

- [1] Bijttebier S, **Van der Auwera A**, Voorspoels S, Noten B, Hermans N, Pieters L, et al. A first step in the quest for the active constituents in *Filipendula ulmaria* (meadowsweet): comprehensive phytochemical identification by liquid chromatography coupled to quadrupole-orbitrap mass spectrometry. *Planta Med.* 2016;82(6):559-72.
- [2] Bijttebier S, **Van der Auwera A**, Foubert K, Voorspoels S, Pieters L, Apers S. Bridging the gap between comprehensive extraction protocols in plant metabolomics studies and method validation. *Anal Chim Acta.* 2016;935:136-50.
- [3] Hummer KE, Janick J. Rosaceae: taxonomy, economic importance, genomics. Foltá KM, Gardiner SE, editors. *Genetics and Genomics of Rosaceae*. New York, USA: Springer New York; 2009. p. 1-17.
- [4] Zhang SD, Jin JJ, Chen SY, Chase MW, Soltis DE, Li HT, et al. Diversification of Rosaceae since the Late Cretaceous based on plastid phylogenomics. *New Phytol.* 2017;214(3):1355-67.
- [5] Lee J. Rosaceae products: Anthocyanin quality and comparisons between dietary supplements and foods. *NFS Journal.* 2016;4:1-8.
- [6] Potter D, Eriksson T, Evans RC, Oh S, Smedmark JEE, Morgan DR, et al. Phylogeny and classification of Rosaceae. *Plant Syst Evol.* 2007;266(1-2):5-43.
- [7] Chin SW, Shaw J, Haberle R, Wen J, Potter D. Diversification of almonds, peaches, plums and cherries - Molecular systematics and biogeographic history of *Prunus* (Rosaceae). *Mol Phylogenet Evol.* 2014;76:34-48.
- [8] Saric-Kundalic B, Dobes C, Klatté-Asselmeyer V, Saukel J. Ethnobotanical study on medicinal use of wild and cultivated plants in middle, south and west Bosnia and Herzegovina. *J Ethnopharmacol.* 2010;131(1):33-55.
- [9] Gilca M, Tiplica GS, Satavastru CM. Traditional and ethnobotanical dermatology practices in Romania and other Eastern European countries. *Clin Dermatol.* 2018;36(3):338-52.
- [10] Menkovic N, Savikin K, Tasic S, Zdunic G, Stesevic D, Milosavljevic S, et al. Ethnobotanical study on traditional uses of wild medicinal plants in Prokletije Mountains (Montenegro). *J Ethnopharmacol.* 2011;133(1):97-107.
- [11] Savikin K, Zdunic G, Menkovic N, Zivkovic J, Cujic N, Terescenko M, et al. Ethnobotanical study on traditional use of medicinal plants in South-Western Serbia, Zlatibor district. *J Ethnopharmacol.* 2013;146(3):803-10.
- [12] Cappelletti EM, Trevisan R, Caniato R. External anti-rheumatic and anti-neuralgic herbal remedies in the Traditional Medicine of Northeastern Italy. *J Ethnopharmacol.* 1982;6(2):161-90.

- [13] Korkmaz M, Karakus S, Selvi S, Cakilcioglu U. Traditional knowledge on wild plants in Uzumlu (Erzincan-Turkey). *Indian J Tradit Know*. 2016;15(4):538-45.
- [14] Marc EB, Nelly A, Annick DD, Frederic D. Plants used as remedies antirheumatic and antineuralgic in the traditional medicine of Lebanon. *J Ethnopharmacol*. 2008;120(3):315-34.
- [15] Baydoun S, Lamis C, Helena D, Nelly A. Ethnopharmacological survey of medicinal plants used in traditional medicine by the communities of Mount Hermon, Lebanon. *J Ethnopharmacol*. 2015;173:139-56.
- [16] Khan MQ, Shinwari ZK. The Ethnomedicinal Profile of family Rosaceae; a study on Pakistani plants. *Pak J Bot*. 2016;48(2):613-20.
- [17] Sturm J. Deutschlands Flora in Abbildungen. 1796; Available from: <http://www.biolib.de/sturm/flora/sturm.pdf>.
- [18] Thomé O. Flora von Deutschland, Österreich und der Schweiz. 1885; Available from: http://www.biolib.de/thome/thome_flora_von_deutschland_tafeln.pdf.
- [19] USDA. Plant of the week gallery. Available from: <https://www.fs.usda.gov/>.
- [20] Busia K. Fundamentals of herbal medicine: major plant families, analytical methods, *Materia Medica*. UK: Xlibris UK; 2016.
- [21] Botanical online. Characteristics of meadowsweet. 2019; Available from: <https://www.botanical-online.com/en/botany/meadowsweet-characteristics>.
- [22] Wilde planten in Nederland en België. Moerasspirea. Available from: <https://wilde-planten.nl/moerasspirea.htm>.
- [23] Moe D, Oeggel K. Palynological evidence of mead: a prehistoric drink dating back to the 3rd millennium BC. *Veg Hist Archaeobot*. 2014;23(5):515-26.
- [24] Murray H, Shepard I, Lamb C, Kerr N, Davies A, Jay M, Tipping R, Mukherjee A, Evershed R, Richards M. Excavation of a beaker cist burial with meadowsweet at Home Farm, Udney Green, Aberdeenshire. *PSASS*. 2008;137:35-58.
- [25] Dickson JH. Bronze-Age Mead. *Antiquity*. 1978;52(205):108-13.
- [26] Guerra-Doce E. The Origins of Inebriation: Archaeological evidence of the consumption of fermented beverages and drugs in Prehistoric Eurasia. *J Archaeol Method Th*. 2015;22(3):751-82.
- [27] Kvavadze E, Gambashidze I, Mindaashvili G, Gogochuri G. The first find in southern Georgia of fossil honey from the Bronze Age, based on palynological data. *Veg Hist Archaeobot*. 2007;16(5):399-404.
- [28] Mount T. *Dragon's blood & willow bark: the mysteries of medieval medicine*. Gloucestershire, UK: Amberley Publishing Limited; 2015.
- [29] Jones FA. Herbs: useful plants. *J Roy Soc Med*. 1996;89(12):717-9.
- [30] Grieve M. *A modern herbal: the medicinal, culinary, cosmetic and economic properties, cultivation and folk-lore of herbs, grasses, fungi, shrubs & trees with their modern scientific uses*. Massachusetts, USA: Dover Publications; 1971.
- [31] Bartram T. *Bartram's encyclopedia of herbal medicine*. London, UK: Grace Publishers; 1995.

- [32] EMA. Assessment report on *Filipendula ulmaria* (L.) Maxim., herba and *Filipendula ulmaria* (L.)Maxim., flos. European Medicines Agency; 2011.
- [33] Okuda T, Yoshida T, Hatano T, Iwasaki M, Kubo M, Orime T, et al. Hydrolysable tannins as chemotaxonomic markers in the rosaceae. *Phytochemistry*. 1992;31(9):3091-6.
- [34] Pemp E, Reznicek G, Krenn L. Fast quantification of flavonoids in *Filipendulae ulmariae flos* by HPLC/ESI-MS using a nonporous stationary phase. *J Anal Chem*. 2007;62(7):669-73.
- [35] Papp I, Simandi B, Blazics B, Alberti Á, Héthelyi É, Szőke É, Kéry Á. Monitoring volatile and non-volatile salicylates in *Filipendula ulmaria* by different chromatographic techniques. *Chromatographia*. 2008;68(1):125-9.
- [36] Fecka I. Qualitative and quantitative determination of hydrolysable tannins and other polyphenols in herbal products from meadowsweet and dog rose. *Phytochem Anal*. 2009;20(3):177-90.
- [37] Shilova IV, Semenov AA, Suslov NI, Korotkova EI, Vtorushina AN, Belyakova VV. Chemical composition and biological activity of a fraction of meadowsweet extract. *Pharm Chem J*. 2009;43(4):185-90.
- [38] Barros L, Alves CT, Dueñas M, Silva S, Oliveira R, Carvalho AM, et al. Characterization of phenolic compounds in wild medicinal flowers from Portugal by HPLC–DAD–ESI/MS and evaluation of antifungal properties. *Ind Crops and Prod*. 2013;44:104-10.
- [39] Olennikov DN, Kruglova MY. A new quercetin glycoside and other phenolic compounds from the genus *Filipendula*. *Chemistry of Natural Compounds*. 2013;49(4):610-6.
- [40] Barros L, Cabrita L, Vilasboas M, Carvalho A, Ferreira I. Chemical, biochemical and electrochemical assays to evaluate phytochemicals and antioxidant activity of wild plants. *Food Chemistry*. 2011;127.
- [41] Samardzic S, Tomic M, Pecikoza U, Stepanovic-Petrovic R, Maksimovic Z. Antihyperalgesic activity of *Filipendula ulmaria* (L.) Maxim. and *Filipendula vulgaris* Moench in a rat model of inflammation. *J Ethnopharmacol*. 2016;193:652-6.
- [42] Matic S, Katanić J, Stanic S, Mladenovic M, Stankovic N, Mihailovic V, et al. *In vitro* and *in vivo* assessment of the genotoxicity and antigenotoxicity of the *Filipendula hexapetala* and *Filipendula ulmaria* methanol extracts. *J Ethnopharmacol*. 2015;174:287-92.
- [43] Halkes SBA, Beukelman CJ, Kroes BH, van den Berg AJJ, Labadie RP, van Dijk H. *In vitro* immunomodulatory activity of *Filipendula ulmaria*. *Phyther Res*. 1997;11(7):518-20.
- [44] Okroj M, Heinegard D, Holmdahl R, Blom AM. Rheumatoid arthritis and the complement system. *Ann Med*. 2007;39(7):517-30.
- [45] Drummond EM, Harbourne N, Marete E, Martyn D, Jacquier J, O'Riordan D, et al. Inhibition of proinflammatory biomarkers in THP1 macrophages by

- polyphenols derived from chamomile, meadowsweet and willow bark. *Phytother Res.* 2013;27(4):588-94.
- [46] Samardzic S, Arsenijevic J, Bozic D, Milenkovic M, Tesevic V, Maksimovic Z. Antioxidant, anti-inflammatory and gastroprotective activity of *Filipendula ulmaria* (L.) Maxim. and *Filipendula vulgaris* Moench. *J Ethnopharmacol.* 2018;213:132-7.
- [47] Trouillas P, Calliste CA, Allais DP, Simon A, Marfak A, Delage C, Duroux JL. Antioxidant, anti-inflammatory and antiproliferative properties of sixteen water plant extracts used in the Limousin countryside as herbal teas. *Food Chem.* 2003;80(3):399-407.
- [48] Vogl S, Picker P, Mihaly-Bison J, Fakhrudin N, Atanasov AG, Heiss EH, et al. Ethnopharmacological *in vitro* studies on Austria's folk medicine-an unexplored lore *in vitro* anti-inflammatory activities of 71 Austrian traditional herbal drugs. *J Ethnopharmacol.* 2013;149(3):750-71.
- [49] Katanić J, Boroja T, Mihailovic V, Nikles S, Pan SP, Rosic G, et al. *In vitro* and *in vivo* assessment of meadowsweet (*Filipendula ulmaria*) as anti-inflammatory agent. *J Ethnopharmacol.* 2016;193:627-36.
- [50] Cholet J, Decombat C, Vareille-Delarbre M, Gainche M, Berry A, Ogeron C, et al. Comparison of the anti-inflammatory and immunomodulatory mechanisms of two medicinal herbs: meadowsweet (*Filipendula ulmaria*) and harpagophytum (*Harpagophytum procumbens*). *IJPAES.* 2019;9:145-63.
- [51] Barnaulov OD, Denisenko PP. Anti-ulcer action of a decoction of the flowers of the dropwort, *Filipendula ulmaria* (L.) Maxim. *Farmakol Toksikol.* 1980;43(6):700-5.
- [52] Rauha JP, Remes S, Heinonen M, Hopia A, Kahkonen M, Kujala T, et al. Antimicrobial effects of Finnish plant extracts containing flavonoids and other phenolic compounds. *Int J Food Microbiol.* 2000;56(1):3-12.
- [53] Denev P, Kratchanova M, Ciz M, Lojek A, Vasicek O, Blazheva D, et al. Antioxidant, antimicrobial and neutrophil-modulating activities of herb extracts. *Acta Biochim Pol.* 2014;61(2):359-67.
- [54] Cwikla C, Schmidt K, Matthias A, Bone KM, Lehmann R, Tiralongo E. Investigations into the antibacterial activities of phytotherapeutics against *Helicobacter pylori* and *Campylobacter jejuni*. *Phytother Res.* 2010;24(5):649-56.
- [55] Peresun'ko AP, Bepalov VG, Limarenko AI., Aleksandrov VA. Clinico-experimental study of using plant preparations from the flowers of *Filipendula ulmaria* (L.) Maxim for the treatment of precancerous changes and prevention of uterine cervical cancer. *Vopr Onkol.* 1993;39(7-12):291-5.
- [56] Spiridonov NA, Konovalov DA, Arkhipov VV. Cytotoxicity of some Russian ethnomedicinal plants and plant compounds. *Phytother Res.* 2005;19(5):428-32.

- [57] Lima MJ, Sousa D, Lima RT, Carvalho AM, Ferreira I, Vasconcelos MH. Flower extracts of *Filipendula ulmaria* (L.) Maxim inhibit the proliferation of the NCI-H460 tumour cell line. *Ind Crops Prod.* 2014;59:149-53.
- [58] Bespalov VG, Alexandrov VA, Vysochina GI, Kostikova Vcapital AC, Baranenko DA. The inhibiting activity of meadowsweet extract on neurocarcinogenesis induced transplacentally in rats by ethylnitrosourea. *J Neurooncol.* 2017;131(3):459-67.
- [59] Bespalov VG, Alexandrov VA, Semenov AL, Kovan'ko EG, Ivanov SD, Vysochina GI, et al. The inhibitory effect of meadowsweet (*Filipendula ulmaria*) on radiation-induced carcinogenesis in rats. *Int J Radiat Biol.* 2017;93(4):394-401.
- [60] Bespalov VG, Baranenk DA, Aleksandrov VA, Semenov AL, Kovan'ko EG, Ivanov SD. Chemoprevention of radiation-induced carcinogenesis using decoction of meadowsweet (*Filipendula ulmaria*) flowers. *Pharm Chem J.* 2019;52(10):44-6.
- [61] Bespalov VG, Alexandrov VA, Semenov AL, Vysochina GI, Kostikova VA, Baranenko DA. The inhibitory effect of *Filipendula ulmaria* (L.) Maxim. on colorectal carcinogenesis induced in rats by methylnitrosourea. *J Ethnopharmacol.* 2018;227:1-7.
- [62] Bespalov VG, Alexandrov VA, Vysochina GI, Kostikova VA, Semenov AL, Baranenko DA. Inhibitory effect of *Filipendula ulmaria* on mammary carcinogenesis induced by local administration of methylnitrosourea to target organ in rats. *Anticancer Agents Med Chem.* 2018;18(8):177-83.
- [63] Amosova EN, Shilova IV, Zueva EP, Rybalkina OY. Influence of *Filipendula ulmaria* (L.) Maxim. extract on Lewis lung carcinoma development and cytostatic therapy effectiveness in mice. *Pharm Chem J.* 2019;53(5):458-61.
- [64] De Paepe D, Servaes K, Noten B, Diels L, De Loose M, Van Droogenbroeck B, et al. An improved mass spectrometric method for identification and quantification of phenolic compounds in apple fruits. *Food Chem.* 2013;136(2):368-75.
- [65] Bijttebier S, Zhani K, D'Hondt E, Noten B, Hermans N, Apers S, et al. Generic characterization of apolar metabolites in red chili peppers (*Capsicum frutescens* L.) by orbitrap mass spectrometry. *J Agric Food Chem.* 2014;62(20):4812-31.
- [66] Halabalaki M, Bertrand S, Stefanou A, Gindro K, Kostidis S, Mikros E, et al. Sample preparation issues in NMR-based plant metabolomics: optimisation for Vitis wood samples. *Phytochem Anal.* 2014;25(4):350-6.
- [67] Theodoridis G, Gika H, Franceschi P, Caputi L, Arapitsas P, Scholz M, et al. LC-MS based global metabolite profiling of grapes: solvent extraction protocol optimisation. *Metabolomics.* 2012;8(2):175-85.
- [68] Pimenta LPS, Kim HK, Verpoorte R, Choi YH. NMR-based metabolomics: a probe to utilize biodiversity. Roessner U, Dias DA, editors. *Metabolomics Tools for*

Natural Product Discovery: Methods and Protocols. New Jersey, USA: Humana Press; 2013. p. 117-27.

- [69] Yuliana ND, Khatib A, Verpoorte R, Choi YH. Comprehensive extraction method integrated with NMR metabolomics: a new bioactivity screening method for plants, adenosine A1 receptor binding compounds in *Orthosiphon stamineus* Benth. *Anal Chem*. 2011;83(17):6902-6.
- [70] Makkar H. Quantification of tannins in tree and shrub foliage: a laboratory manual: Springer Science & Business Media; 2003.
- [71] Krueve A, Rebane R, Kipper K, Oldekop ML, Evard H, Herodes K, et al. Tutorial review on validation of liquid chromatography-mass spectrometry methods: part II. *Anal Chim Acta*. 2015;870:8-28.
- [72] Magnusson B, Ornemark U. Eurachem Guide: the fitness for purpose of analytical methods - a laboratory guide to method validation and related topics 2014, 2; Available from: www.eurachem.org.
- [73] Wilkes S, Glasl H. Isolation, characterization, and systematic significance of 2-pyrone-4,6-dicarboxylic acid in Rosaceae. *Phytochemistry*. 2001;58(3):441-9.
- [74] Blazics B. Analysis of medicinal plant phenoloids by coupled tandem mass spectrometry (dissertation). Budapest, Hungary: Semmelweis University; 2010.
- [75] Krasnov EA, Raldugin VA, Shilova IV, Avdeeva EY. Phenolic compounds from *Filipendula ulmaria*. *Chem Nat Compd*. 2006;42(2):148-51.
- [76] Mills S, Bone K. Principles and practice of phytotherapy: modern herbal medicine. 2 ed. Edinburgh, Scotland: Churchill Livingstone; 2013.
- [77] Cuyckens F, Claeys M. Mass spectrometry in the structural analysis of flavonoids. *J Mass Spectrom*. 2004;39(1):1-15.
- [78] Sun J, Liang F, Bin Y, Li P, Duan CQ. Screening non-colored phenolics in red wines using Liquid Chromatography/Ultraviolet and Mass Spectrometry/Mass Spectrometry libraries. *Molecules*. 2007;12:679-93.
- [79] Regueiro J, Sanchez-Gonzalez C, Vallverdu-Queralt A, Simal-Gandara J, Lamuela-Raventos R, Izquierdo-Pulido M. Comprehensive identification of walnut polyphenols by liquid chromatography coupled to linear ion trap-Orbitrap mass spectrometry. *Food Chem*. 2014;152:340-8.
- [80] Li M, Kai Y, Qiang H, Dongying J. Biodegradation of gallotannins and ellagitannins. *J Basic Microbiol*. 2006;46(1):68-84.
- [81] Niemetz R, Gross G, Schilling G. Ellagitannin biosynthesis: Oxidation of pentagalloylglucose to tellimagrandin II by an enzyme from *Tellima grandiflora* leaves. *Chemical Communications*. 2001;2001:35-6.
- [82] Iranzo JM. Ellagitannins, ellagic acid and their derived metabolites: A review about source, metabolism, functions and health. *Food Res Int*. 2011;44:1150-60.
- [83] Li YJ, Wei HL, Qi LW, Chen J, Ren MT, Li P. Characterization and identification of saponins in *Achyranthes bidentata* by rapid-resolution liquid chromatography

- with electrospray ionization quadrupole time-of-flight tandem mass spectrometry. *Rapid Commun Mass Spectrom*. 2010;24(20):2975-85.
- [84] Bale NJ, Airs RL, Llewellyn CA. Type I and Type II chlorophyll-a transformation products associated with algal senescence. *Org Geochem*. 2011;42(5):451-64.
- [85] Butterweck V, Nahrstedt A. What is the best strategy for preclinical testing of botanicals? A critical perspective. *Planta Med*. 2012;78:747-54.
- [86] Del Rio D, Rodriguez-Mateos A, Spencer JP, Tognolini M, Borges G, Crozier A. Dietary (poly)phenolics in human health: structures, bioavailability, and evidence of protective effects against chronic diseases. *Antioxid Redox Signal*. 2013;18(14):1818-92.
- [87] Lu MF, Xiao ZT, Zhang HY. Where do health benefits of flavonoids come from? Insights from flavonoid targets and their evolutionary history. *Biochem Biophys Res Commun*. 2013;434(4):701-4.
- [88] Cardona F, Andres-Lacueva C, Tulipani S, Tinahones FJ, Queipo-Ortuno MI. Benefits of polyphenols on gut microbiota and implications in human health. *J Nutr Biochem*. 2013;24(8):1415-22.
- [89] Espin JC, Gonzalez-Sarrias A, Tomás-Barberán FA. The gut microbiota: A key factor in the therapeutic effects of (poly)phenols. *Biochem Pharmacol*. 2017;139:82-93.
- [90] Duda-Chodak A, Tarko T, Satora P, Sroka P. Interaction of dietary compounds, especially polyphenols, with the intestinal microbiota: a review. *Eur J Nutr*. 2015;54(3):325-41.
- [91] Espín JC, Larrosa M, García-Conesa MT, Tomás-Barberán F. Biological significance of urolithins, the gut microbial ellagic acid-derived metabolites: the evidence so far. *eCAM*. 2013;2013:270418.
- [92] Larrosa M, González-Sarrias A, García-Conesa M, Tomás-Barberán F, Espín JC. Urolithins, ellagic acid-derived metabolites produced by human colonic microflora, exhibit estrogenic and antiestrogenic activities. *J Agric Food Chem*. 2006;54:1611-20.
- [93] Rasmussen SE, Frederiksen H, Struntze Krogholm K, Poulsen L. Dietary proanthocyanidins: occurrence, dietary intake, bioavailability, and protection against cardiovascular disease. *Mol Nutr Food Res*. 2005;49(2):159-74.
- [94] Choy YY, Waterhouse A. Proanthocyanidin metabolism, a mini review. *Nutrition and Aging*. 2014;2:111-6.
- [95] Rzeppa S, Bittner K, Doll S, Danicke S, Humpf HU. Urinary excretion and metabolism of procyanidins in pigs. *Mol Nutr Food Res*. 2012;56(4):653-65.
- [96] Farrell T, Poquet L, Dionisi F, Barron D, Williamson G. Characterization of hydroxycinnamic acid glucuronide and sulfate conjugates by HPLC–DAD–MS2: Enhancing chromatographic quantification and application in Caco-2 cell metabolism. *J Pharm Biomed Anal*. 2011;55(5):1245-54.

- [97] Alvarado HL, Abrego G, Garduno-Ramirez ML, Clares B, Calpena AC, Garcia ML. Design and optimization of oleanolic/ursolic acid-loaded nanoplateforms for ocular anti-inflammatory applications. *Nanomedicine*. 2015;11(3):521-30.
- [98] Michel T, Khelif I, Kanakis P, Termentzi A, Allouche N, Halabalaki M, et al. UHPLC-DAD-FLD and UHPLC-HRMS/MS based metabolic profiling and characterization of different *Olea europaea* organs of Koroneiki and Chetoui varieties. *Phytochem Lett*. 2015;11:424-39.
- [99] Ma Y, Tanaka N, Vaniya A, Kind T, Fiehn O. Ultrafast polyphenol metabolomics of red wines using MicroLC-MS/MS. *J Agric Food Chem*. 2016;64(2):505-12.
- [100] Porgali E, Büyüktuncel E. Determination of phenolic composition and antioxidant capacity of native red wines by high performance liquid chromatography and spectrophotometric methods. *Food Res Int*. 2012;45(1):145-54.
- [101] Naczki M, Shahidi F. Extraction and analysis of phenolics in food. *J Chromatogr A*. 2004;1054(1-2):95-111.
- [102] Vuckovic D. Current trends and challenges in sample preparation for global metabolomics using liquid chromatography-mass spectrometry. *Anal Bioanal Chem*. 2012;403(6):1523-48.
- [103] Verpoorte R, Choi Y, Mustafa N, Kim H. Metabolomics: back to basics. *Phytochem Rev*. 2008;7(3):525-37.
- [104] Abou-Zaid MM, Lombardo DA, Nozzolillo C. Methyl gallate is a natural constituent of maple (Genus *Acer*) leaves. *Nat Prod Res*. 2009;23(15):1373-7.
- [105] Wolfender J-L, Rudaz S, Hae Choi Y, Kyong Kim H. Plant metabolomics: from holistic data to relevant biomarkers. *Curr Med Chem*. 2013;20(8):1056-90.
- [106] Daniel M. Medicinal plants: chemistry and properties. New York, USA CRC Press; 2006.
- [107] Bijttebier S, D'Hondt E, Noten B, Hermans N, Apers S, Exarchou V, et al. Automated analytical standard production with supercritical fluid chromatography for the quantification of bioactive C17-polyacetylenes: A case study on food processing waste. *Food Chem*. 2014;165:371-8.
- [108] Krueve A, Rebane R, Kipper K, Oldekop ML, Evard H, Herodes K, et al. Tutorial review on validation of liquid chromatography-mass spectrometry methods: Part I. *Anal Chim Acta*. 2015;870:29-44.
- [109] Oldiges M, Lütz S, Pflug S, Schroer K, Stein N, Wiendahl C. Metabolomics: current state and evolving methodologies and tools. *Appl Microbiol Biotechnol*. 2007;76(3):495-511.
- [110] FDA. Guidance for industry: bioanalytical method validation 2001; Available from: <http://www.fda.gov/cder/Guidance/4252fnl.pdf>.
- [111] t'Kindt R, Morreel K, Deforce D, Boerjan W, Van Bocxlaer J. Joint GC-MS and LC-MS platforms for comprehensive plant metabolomics: Repeatability and sample pre-treatment. *J Chromatogr B*. 2009;877(29):3572-80.

- [112] Bijttebier S, D'Hondt E, Noten B, Hermans N, Apers S, Voorspoels S. Improving method reliability in carotenoid analysis through selective removal of glycerolipid interferences by lipase treatment. *J Agric Food Chem* 2014;62(14):3114-24.
- [113] Faccin H, Viana C, do Nascimento PC, Bohrer D, de Carvalho LM. Study of ion suppression for phenolic compounds in medicinal plant extracts using liquid chromatography-electrospray tandem mass spectrometry. *J Chromatogr A*. 2016;1427:111-24.



CHAPTER 3

BIOTRANSFORMATION STUDIES OF FILIPENDULA ULMARIA

*This chapter is part of an article published in Pharmaceutics: **Van der Auwera A, Peeters L, Foubert K, Piazza S, Vanden Berghe W, Hermans N, Pieters L. In vitro biotransformation and anti-inflammatory activity of constituents and metabolites of Filipendula ulmaria. Pharmaceutics. 2023;15(4):1291.***^[1]

3.1 AIM

This chapter focusses on the biotransformation of the constituents of a *Filipendula ulmaria* extract after interaction with the gut microbiota. Alterations of phytochemicals by the gut microbiota could result in more bioavailable and/or bioactive metabolites, since many natural products are considered to be prodrugs. When using the classical approaches, this aspect is usually completely overlooked in the search for new therapeutic compounds. A multiclass experiment was thus performed over multiple timepoints in an *in vitro* gastrointestinal biotransformation model simulating the ingestion of a *Filipendula ulmaria* extract. Study samples were compared to a blank and negative control sample in the stomach phase, small intestinal phase and colon phase with a total of 72 h of fermentation. However, revealing such metabolic pathways after *in vitro* biotransformation experiments is complex and generates a massive amount of data. Therefore, a metabolomics workflow was developed to elucidate the compounds undergoing biotransformation as well as their formed metabolites.

3.2 THE GASTROINTESTINAL TRACT

3.2.1 THE GUT MICROBIOTA

3.2.1.1 COMPOSITION AND DEVELOPMENT OF THE HUMAN GUT MICROBIOTA

The adult human gastrointestinal tract houses an incredible amount of microorganisms, including an abundance of bacteria, archaea and eukaryotes that mainly reside in the ileum and colon.^[2] To illustrate: the human gastrointestinal tract is colonized by 10^{13} to 10^{15} microorganisms, which is about 10 times more bacterial cells compared to the total number of human cells, and their genomic content surpasses the

Homo sapiens genome by a 100 fold. This also showcases our beneficial symbiotic relationship: this co-evolution provided us with functional features which we did not have to evolve ourselves.^[2-4] The development of this gut microbiota composition starts from birth, since the womb is considered to be sterile environment. Nevertheless, some recent studies suggest that colonization already may have started *in utero* since the presence of bacteria in the placenta, amniotic cavity, umbilical cord and meconium has been reported.^[5-7] However, generally it is assumed that colonization of the gastrointestinal tract of neonates occurs rapidly straight after birth, which also appears to be greatly affected by the mode of delivery. The microbiota of vaginally born infants resembles that of the mother's vaginal and fecal flora, while the microbiota of babies delivered by caesarean section is closer to that of the maternal skin.^[8,9] Then, in the first following months, the gut microbiota is still quite low in diversity. However, the composition of the infant's gut microbiota after one year of life becomes more unique, increases in diversity and converges to an adult-like profile. Between two and five years of age, the composition, diversity and functionality of the microbiota is essentially the same as that of an adult. Enormous dietary changes, environmental exposures, as well as maturation of the immune system strongly shape the gut microbiota in those first years.^[8,10] In adulthood, our enterotype stays quite stable, with the main intestinal microbiota belonging to the phylum Firmicutes (including *Ruminococcus*, *Clostridium* and *Lactobacillus*) and Bacteroidetes (e.g. *Bacteroides*, *Prevotella* and *Xylanibacter*). The other three abundant phyla are Actinobacteria (such as *Bifidobacterium* and *Collinsella*), Proteobacteria (including *Escherichia*) and Verrucomicrobia (like *Akkermansia*).^[11,12] The microbiota of elderly people show a different gut microbiota compared to healthy adults. This could be related to a decline in general health and well-being, such as changed lifestyle (lesser mobility and altered diet), weakened immune system, recurrent infections and hospitalizations, medication,...^[13,14] Figure 3.1 gives a clear overview of all the changes in the core microbiome and its diversity across the age groups, as well as the many possible driving factors. As mentioned above, the

microbiota have an important impact on the host and the microbial pattern is influenced by age^[13], diet (vegetarian and vegan diets or ethnical and geographical differences in diet)^[15,16], hygiene^[17], medication (non-antibiotics and antibiotics)^[18,19], infection and diseases^[14,20], genetics^[21] and many other variables.

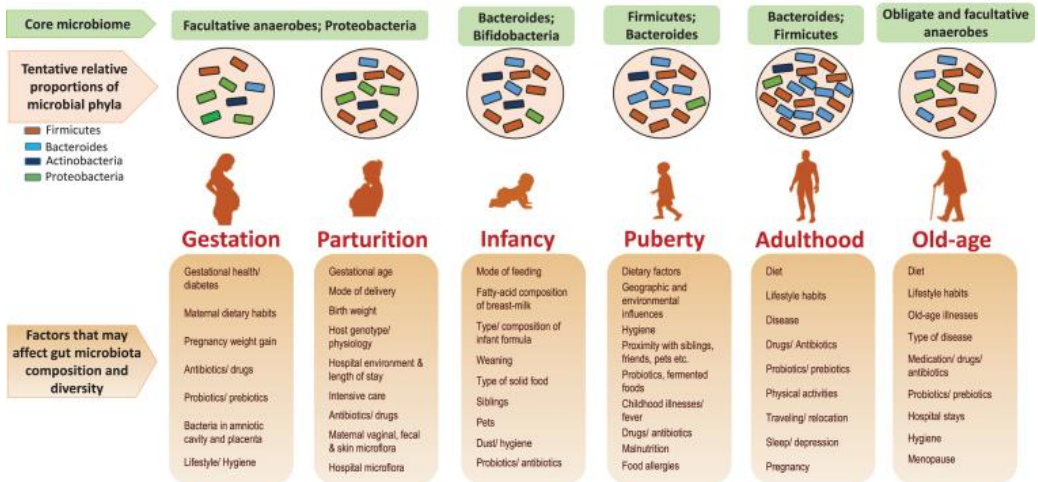


FIGURE 3.1: CHANGES IN THE HUMAN GUT MICROBIOTA DURING THE DIFFERENT LIFE STAGES AND POTENTIAL FACTORS AFFECTING THE COMPOSITION. FIGURE ADAPTED FROM NAGPAL ET AL.^[13]

3.2.1.2 BIOGEOGRAPHY OF THE HUMAN GUT MICROBIOTA IN THE GASTROINTESTINAL TRACT

The gastrointestinal tract forms a continuous passageway for digestion and includes the stomach, small intestine (subdivided in duodenum, jejunum and ileum) and large intestine (cecum, ascending, transverse, descending and sigmoid colon) as the main organs, plus the accessory organs of digestion such as the tongue, salivary glands, pancreas, liver and gallbladder. The stomach is the first important step in digestion by contracting periodically to enhance digestion, creating an acid environment and releasing pepsin (initiating protein degradation). Absorption in the stomach is limited because of its small epithelial surface and rate of gastric emptying, but some compounds do however appear to undergo limited absorption at this location.^[22,23] The small intestine is the longest part of the gastrointestinal tract and has a total length of about five meters. Here, digestion is further completed and most nutrients are

absorbed. The small intestine is slightly alkaline. Bile (aids in efficient fat and cholesterol absorption) as well as pancreatic enzymes (trypsinogen, amylases, lipases, cholesterol esterases,...) are secreted in the duodenum. The small intestine has an enormously increased surface area because of its submucosal folds, villi and microvilli. Nutrients or other compounds can be absorbed by passive transcellular diffusion, active or passive carrier-mediated transport, passive paracellular diffusion through tight junctions or transcytosis. The small intestine is also highly vascularized as nearly one-third of the cardiac output flows through. The blood then passes to the liver via the hepatic portal vein. The colon is the final major part, measuring around 1.5 meters. The surface area is less than in the small intestine, but crypts, folded mucosae and microvilli are still present. Its main functions are: absorption of sodium and chloride ions and water while exchanging it for bicarbonate and potassium ions and feces storage and compaction.^[24] Moving along the gastrointestinal tract, there is a progressive increase in both the amount and diversity of bacteria. The number of bacterial cells shifts from about 10^1 bacteria per gram of contents in the stomach, to 10^7 bacteria per gram of contents in the ileum, to 10^{12} cells per gram in the colon. Compared to the stomach and the small intestine, the colon is colonized by a much larger population of bacteria, comprised by mainly obligate anaerobe bacteria since it is a strictly anaerobic environment.^[25,26] Figure 3.2 summarizes the heterogeneity and the number of the microbiota across the gastrointestinal tract. There is also a latitudinal variation (see Figure 3.2): there is a difference in microbiota composition in the intestinal lumen, in the mucus layer and in proximity of the epithelial crypts.^[25] The mucus layer consists of two parts: the striated inner layer that keeps a safe barrier between the bacteria and the epithelial cells, and the looser outer layer that also provides structural scaffolding and nutrients for the microbiota. The thick and physiochemically complex mucus layers, as well as the crypts, create different microenvironments because of mucus rigidity, lower fluid shear, low oxygen concentrations coming from the epithelial cells (which are beneficial for oxygen-

tolerant bacteria), having the capacity to thrive on mucin glycans as a food source, presence of antimicrobial host secretions,...^[27-29]

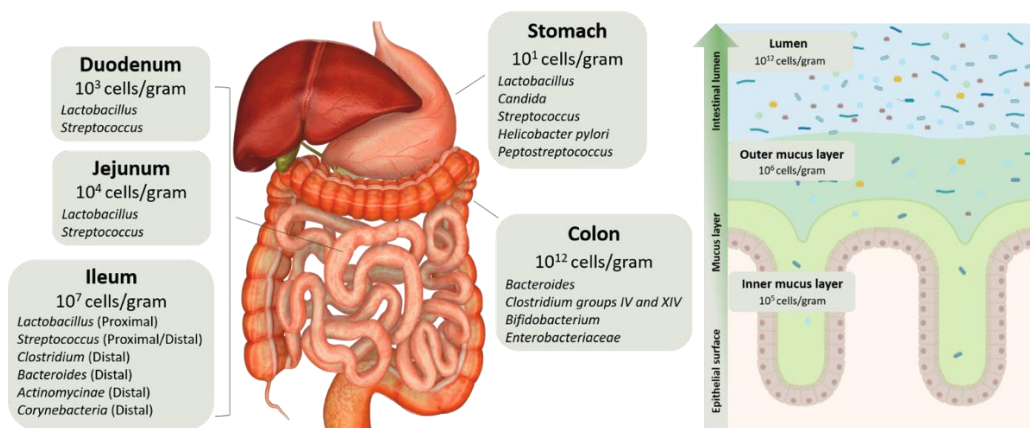


FIGURE 3.2: LUMINAL CONCENTRATIONS OF THE DOMINANT MICROBIAL SPECIES ACROSS THE GASTROINTESTINAL TRACT (LEFT). LONGITUDINAL VARIATIONS FROM THE COLON EPITHELIUM TO THE LUMEN (RIGHT). FIGURES BASED ON SEKIROV ET AL., SARTOR ET AL. AND DE WEIRD ET AL.^[25,26,28]

3.2.1.3 ROLE OF THE HUMAN GUT MICROBIOTA IN HEALTH

The gut microbiota contributes to normal digestive function, but also aids human metabolism by fermenting unabsorbed nutrients, e.g. breakdown of polysaccharides, dietary polyphenols, bile acids or even drugs. The complex carbohydrates that escape digestion in the small intestine require breakdown by microbiota via fermentation (generating energy for the microbiota) which leads to short-chain fatty acids (SCFAs) as end products such as butyrate, acetate and propionate. These SCFAs, in their turn, are an important energy source for the colonic epithelium and the host. They are also involved in the regulation of many cellular processes e.g. gene expression, proliferation and apoptosis. Moreover, the gut flora plays an important role in *de novo* synthesis of B vitamins, such as vitamin B12, thiamin (B1), biotin (B8), folate (B9) and riboflavin (B2), but also vitamin K. In addition, it is demonstrated that the colon epithelium can absorb a wide range of these vitamins and metabolites.^[30,31] Therefore, our gut microbiota can be viewed as an organ in an organ that is capable of more biochemical conversions than the liver, or at least having equally the extensive activity of the liver enzymes.^[30,32]

Because of the gut microbiota's large genomic content, as well as its metabolic activity, the members of the human gut flora are considered to be key-players in the host's health. They have an impact on epithelial homeostasis and integrity and development of the immune system, and changes in microbial populations or dysbiosis has been (tentatively) linked to diseases such as inflammatory bowel disease^[33], diabetes^[34], asthma^[35] or even depression.^[36]

3.3 GUT MICROBIAL BIOTRANSFORMATION OF POLYPHENOLS

3.3.1 GENERAL

Polyphenols exhibit structural diversity, which can vary immensely and impact their bioavailability, metabolism, and bioactivity. The main groups comprise phenolic acids (hydroxybenzoic acids, hydroxycinnamic acids), flavonoids (flavonols, flavones, isoflavones, flavanones, anthocyanidins and flavan-3-ols), stilbenes and lignans. Polymers and oligomers of flavonoids are known as tannins and are classified into two groups: condensed tannins and hydrolysable tannins.^[37] An overview of their basic structure is summarized in chapter 1, Figure 1.2. Most polyphenols, especially flavonoids, are present in plants as glycosides. They are thus conjugated to various sugars, most commonly glucose, galactose, rhamnose, xylose, rutinose, arabinopyranose and arabinofuranose. Polyphenols also occur as non-conjugated oligomers as in the case of condensed tannins. In general, this causes most polyphenols to have a low bioavailability.^[38] The stomach is the minor location of absorption of polyphenols. Despite the low pH, low molecular weight polyphenols are stable and glucose-bound polyphenols are only partially hydrolyzed in the stomach.^[39] Most aglycons of polyphenols can be absorbed from the small intestine, but the polyphenols in the form of esters, glycosides or polymers are absorbed very poorly or not at all. Generally, about 90 - 95% of the polyphenol intake reaches the colon unaltered.^[37,40] Thus, interaction with the microbiota present in the gut leads to biotransformation of

the parent polyphenols resulting in more bioavailable metabolites.^[39] Bacterial metabolites are different from those generated by human enzymes, and their impact on both host health and intestinal microbiota thus differs. The potential of the intestinal microbiome for biochemical conversions is much higher than, or at least equal to that of the liver and includes other types of reactions not found in the liver.^[32] The major differences between hepatic and microbial metabolism is that the liver is primarily responsible for oxidation and conjugation reactions producing hydrophilic high molecular weight metabolites. The gut microbiome, on the other hand, occurs in an anaerobic environment and is involved in mainly reduction and hydrolysis reactions generating non-polar low molecular weight metabolites.^[41] Generally, biochemical transformations by the gut microbiota include three major catabolic processes: hydrolysis (deglycosylations and ester hydrolysis), cleavage (C-ring cleavage, delactonization, demethylation) and reductions (dehydroxylation and double bond reduction).^[42] These processes are illustrated with some examples in Figure 3.3. The intestinal microbiota is equipped with a rich diversity of different enzymes such as α -rhamnosidase, β -glucuronidase, β -glucosidase, sulfatase and esterases, generating various metabolites. The gut microbiota thus influences the bioavailability of polyphenols by modifying the structure of aglycons, glycosides and conjugates.^[43] In the stomach, only part of the *O*-glycosides are converted to their aglycon because of the acidic conditions. Flavonoid monoglucosides are also deglycosylated to their aglycon through the brush-border enzyme lactase-phlorizin hydrolase (LPH) or cytosolic β -glucosidase (CBG) of the intestinal cells.^[37,39] To illustrate, LPH effectively hydrolyzes daidzin to daidzein, and this can also be realized via hydrolysis by the colon microflora.^[44,45] Other glycosides bound to sugars other than glucose, such as rhamnosides and rutinosides, are not substrates for these intestinal enzymes. Rutin and hesperidin, for example, are thus barely metabolized in the small intestine and need to be hydrolyzed by gut microbial enzymes to their aglycon, quercetin and hesperetin respectively, upon reaching the colon.^[37,39,42] After intestinal absorption and passage in

the liver, these compounds undergo phase I (oxidation, reduction and hydroxylation) and phase II (mainly involving sulfation by sulfotransferases (SULT), glucuronidation by uridine-5'-diphosphate glucuronosyltransferases (UGT) and methylation by catechol-O-methyl transferase (COMT)) metabolism. Intestinal cells also contain phase II enzymes and convert absorbed aglycons into O-glucuronide / O-sulfate conjugated metabolites. These conjugated polyphenols enter into systemic circulation or they undergo enterohepatic circulation, meaning that they are excreted in the bile and thus re-enter the intestinal tract.^[39,45,46]

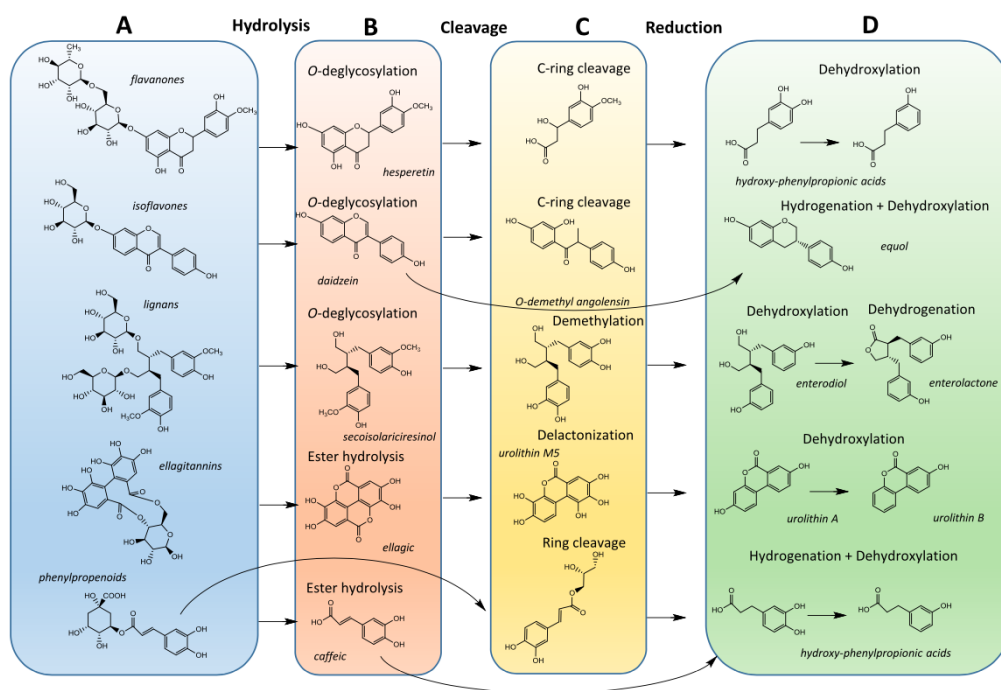


FIGURE 3.3: GUT MICROBIOTA BIOTRANSFORMATION OF POLYPHENOLS. (A) NATIVE POLYPHENOLS AS FOUND IN FOOD AND PLANTS. FLAVANONES (HESPERIDIN), ISOFLAVONES (DAIDZIN), LIGNANS (SECOISOLARICRESINOL DIGLUCOSIDE), ELLAGITANNINS (HEXAHYDROXYDIPHENIC GLUCOSIDE) AND CHLOROGENIC ACIDS (CHLOROGENIC ACID). (B) GUT MICROBIOTA MEDIATED HYDROLYSIS PRODUCTS. (C) RING-CLEAVAGE AND DE-METHYLATION PRODUCTS. RING CLEAVAGE CAN OCCUR IN THE NATIVE COMPOUND AS IN CHLOROGENIC ACID LEADING TO CAFFEYOYL-GLYCERIN AFTER BREAKING THE QUINIC ACID RESIDUE. DAIDZEIN CAN LEAD TO O-DESMETHYLANGOLENSIN BY A RING-CLEAVAGE REACTION. (D) REDUCTION REACTIONS (DEHYDROXYLATION AND HYDROGENATION). THESE REACTIONS LEAD TO THE FINAL ACTIVE METABOLITES PRODUCED IN THE GUT. THE CONVERSION OF ENTERODIOL INTO ENTEROLACTONE IS INCLUDED HERE ALTHOUGH IT IS A DEHYDROGENATION REACTION WHICH IS NOT A REDUCTION. FIGURE ADAPTED FROM ESPÍN ET AL.^[42]

In the colon, bacterial β -glucuronidase activity, e.g. seen in Firmicutes and Bacteroidetes, allows for the re-absorption of phenolics and their gut microbiota metabolites which extends the residence time of some polyphenols.^[30,47] Studies on the biochemical transformation of polyphenols by the intestinal microbiota are therefore crucial for understanding the role of these compounds and their effects on our health. These catabolites might thus be responsible for the health promoting effects that are attributed to the parent compound.

3.3.2 FLAVONOLS

For flavonols like quercetin and kaempferol, which are mainly found in plants as glycosides, the type of glycosylation pattern effects their degradation rates in the colon. Di- and tri-saccharides are degraded much slower than flavonol monosaccharides. The type of bond, C- or O-glycosides also influences this degradation rate, with C-glycosidic bonds being cleaved much slower.^[38] Gut microbiota that have been involved with flavonol hydrolysis (e.g. releasing the aglycon from quercetin glycosides such as rutin) are *Bacteroides distasonis*, *Bacteroides uniformis*, *Bacteroides ovatus*, *Enterococcus casseliflavus* and *Eubacterium ramulus*.^[37,38,43] The position of the hydroxyl groups also appears to play a role in the degradation rate, with flavonoids without hydroxyl groups at the C-5, C-7, and C-4' positions being degraded slower.^[38] Cleavage reactions appear to be a characteristic catabolic reaction of the gut microbiota.^[48] Flavonols that have been hydrolyzed to their aglycons undergo extensive degradation via A- and B-ring metabolism, which generates simpler and smaller phenolic compounds after breaking down the flavonoid C-ring. Some examples of gut microbiota involved in this C-ring breakdown are *Eubacterium oxidoreducens*, *E. ramulus*, *E. casseliflavus*, *Clostridium orbiscidens* and bacteria belonging to *Butyrivibrio* genus. This C-ring cleavage gives rise to multiple phenolic acids, since this cleaving takes place at different positions, such as the bond between C-1 and C-2, C-3 and C-4 or between C-4 and C-10. After C-ring fission, dehydroxylation reactions occur at the two remaining phenolic rings. For

example, when looking at the breakdown of quercetin, 2-(3,4-dihydroxyphenyl)-acetic acid is a metabolite originating from the A-ring and protocatechuic acid from the B-ring.^[38]

3.3.3 FLAVANONES

Hesperidin and naringin, examples of flavanones, have their disaccharides consisting of glucose and rhamnose attached at position C-7. They share a similar degradation pathway to flavonols, with as a first step glycosylation resulting in the formation of their aglycones hesperetin and naringenin. In the colon, hesperidin and naringin are exposed to α -rhamnosidases that remove the rhamnose moiety, followed by β -glucosidases that remove glucose. The aglycons are absorbed via passive diffusion and proton-coupled active transport or they are further broken down by the gut microbiota. C-ring cleavage is observed between C-1 and C-2 or between C-4 and C-10. These transformations can be carried out by *Clostridium* species and *E. ramulus*.^[38] Some examples of their metabolites include phloroglucinol, 4-hydroxyphenylacetic acid, protocatechuic acid and 3-(4-hydroxyphenyl)propionic acid (see also Figure 3.3).^[49]

3.3.4 FLAVONES

Flavones, such as luteolin and apigenin, are also present in plants as their corresponding glycosides and are hydrolyzed at the intestinal level as well. Unabsorbed aglycons are broken down by the colon microbiota, e.g. by *Clostridium orbiscindens* and *Enterococcus avium*, breaking down their C-ring towards phloretin chalcone, 3-(3,4-dihydroxyphenyl)-propionic acid, 3-(4-hydroxyphenyl)-propionic acid, 3-(3-hydroxyphenyl)-propionic acid and 4-hydroxycinnamic acid.^[38]

3.3.5 FLAVAN-3-OLS

Flavan-3-ols comprise monomeric forms (catechin, epicatechin gallo catechin, epigallocatechin and gallate esters) and their polymeric forms (i.e. proanthocyanidins

or condensed tannins), which can reach up to 50 units or even more. The polymerization degree and galloylation effects their bioavailability, as oligomers with a degree of polymerization >3 are not absorbed in the small intestine.^[48] Generally, monomeric flavan-3-ols are readily absorbed in the small intestine and consequently subjected to glucuronidation, sulfation and/or *O*-methylation.^[39] The absorption of dimeric proanthocyanidins has been a subject of speculation: it was first thought that procyanidins could be depolymerized to bioavailable monomers under the acidic conditions of the stomach, however, later *in vivo* studies failed to demonstrate this.^[50] Structures with higher polymerization degrees are metabolized by the intestinal microbiota in the colon in order to release free monomeric forms. These free monomers are available for transformation and are converted into diphenylpropan-2-ols by opening of the C-ring, followed by transformation to phenyl- γ -valerolactones. These latter intermediate metabolites are exclusive to flavan-3-ols. Phenyl- γ -valerolactones can be further broken down by breaking the valerolactone ring and by dihydroxylation, forming various phenylvaleric acids. The microbiota produce different hydroxylated forms of phenyl and benzoic acids from phenyl- γ -valerolactones and phenylvaleric acids. The 3,4-dihydroxylated phenolic acids are dehydroxylated at C-3 and C-4, producing 4- and 3-monohydroxylated phenolic acids respectively.^[48,51] Bacteria responsible for these metabolic reactions belong to the genera *Bifidobacterium* (*Bifidobacterium infantis*) and *Clostridium* (*Clostridium coccooides*).^[38] Vanillic acid, homovanillic acid, hippuric acid or *p*-coumaric acid are also metabolites of flavan-3-ols, although not specific as they can also be metabolites from other flavonoids.^[51]

3.3.6 ANTHOCYANIDINS

Anthocyanins, the glycosylated form of anthocyanidin aglycons, are barely absorbed in the small intestine. Large amounts of anthocyanins enter the colon, where the gut microbiota cleave the 3-*O*-glycosidic linkages by bacterial β -glucosidase. This causes

instability of the anthocyanidin at neutral pH and rapid breakdown of the heterocyclic ring. The major resulting metabolites are corresponding phenolic acids (derived from the B-ring) and phloroglucinol derivatives (derived from the A-ring). Some of these metabolites include protocatechuic acid, gallic acid, syringic acid, *p*-coumaric and vanillic acid.^[43,48,52] Examples of species responsible for this degradation are *Lactobacillus plantarum*, *Lactobacillus casei*, *Lactobacillus acidophilus* and *Bifidobacterium lactis*.^[38]

3.3.7 ISOFLAVONES

Isoflavones are found mainly as glycosides and require the conversion to their aglycons via β -glucosidase to promote absorption. A well-known example is daidzin which is hydrolyzed to daidzein (see Figure 3.3).^[53] Enzymatic reduction of the double bond between C-2 and C-3 results in the formation of dihydrodaidzein. Further reductive transformations result in the formation of tetrahydrodaidzein and eventually in the active metabolite equol. An alternative metabolic route converts dihydrodaidzein into *O*-desmethylangolensin via C-ring cleavage.^[48] Interestingly, daidzein is transformed into *O*-desmethylangolensin or equol if the adequate microbiota is present. The prevalence of equol producers and *O*-desmethylangolensin producers in humans is approximately 30 - 50 and 80 - 90%, respectively. This indicates that some people are unable to produce equol due to differences in gut microflora composition.^[43] *Eubacterium ramulus* and *Clostridium* spp. have been described to catalyze the biotransformation to *O*-desmethylangolensin. Equol producing bacteria, on the other hand, are bacteria of the *Eggerthella* species, but also *Adlercreutzia equolifaciens*, *Slackia equolifaciens*, *Slackia isoflavoniconvertens*.^[30,48]

3.3.8 HYDROLYZABLE TANNINS

Hydrolyzable tannins include gallotannins and ellagitannins. Upon gut microbial hydrolysis gallotannins yield gallic acid and glucose. Ellagitannins are esters of

hexahydroxydiphenic acid (HHDP) and glucose, and the hydrolysis of this ester bonds releases HHDP which then undergoes spontaneous cyclization to produce ellagic acid. Ellagitannins and ellagic acid absorption is very low and ellagic acid is thus further converted by the colon microbiota into urolithin M5 through opening of the lactone ring and decarboxylation, which is catalyzed by *Gordonibacter* strains.^[42,53] Urolithins are dibenzopyran-6-one derivatives with different hydroxyl substitutions. Hydroxyl groups are sequentially removed from different positions, which first results in tetrahydroxy-urolithin isomers (urolithin D and M6). Trihydroxy-urolithins (urolithin C and M7) are then produced after a second hydroxyl removal. This is preceded by a third hydroxyl removal in order to obtain the end metabolites urolithin A, isourolithin A and the monohydroxylated analog urolithin B (see Figure 3.3).^[54] These steps are conducted by different bacterial species, such as those belonging to the genus *Gordonibacter* (*G. pamelaiae* and *G. urolithinifaciens*) and *Ellagibacter isourolithinifaciens*. Individuals can be divided into three urolithin metabotypes: metabotype A, metabotype B and metabotype O. Metabotype A is characterized by the production of urolithin A, whereas metabotype B produces urolithin A, isourolithin A and urolithin B. However, metabotype O does not produce any of these final urolithins.^[55,56]

3.3.9 STILBENES

Resveratrol, 3,5,4'-trihydroxy-*trans*-stilbene, belongs to the stilbene family and is found in its *trans* isomer form in e.g. red wine. Resveratrol also naturally occurs in its glycosylated form, which is known as piceid and polydatin.^[57,58] A role for both LPH and CBG in the cleavage of piceid was supported before.^[59] Moreover, *Bifidobacteria infantis* and *Lactobacillus acidophilus* are also known to be responsible for the hydrolysis of the glucoside moieties from piceid and polydatin. In turn, resveratrol is transformed by the gut microbiota to different metabolites. Dihydroresveratrol was the first and main microbial derivative identified, which is

produced by *Slackia equolifaciens* and *Adlercreutzia equolifaciens* through a reduction of the double bond between the two phenol rings. Two other bacterial metabolites include 3,4'-dihydroxy-trans-stilbene and 3,4'-dihydroxybibenzyl (known as lunularin). Lunularin may be formed via dehydroxylation of the intermediate dihydroresveratrol or through reduction of the intermediate 3,4'-dihydroxy-trans-stilbene.^[57,58] Similar to the previous examples of daidzin and ellagitannins, a large inter-individual variation in metabolite production is observed. In the case of resveratrol, some subjects appear to be lunularin producers, dihydroresveratrol producers or mixed producers. Lunularin producers were associated with a higher abundance of Bacteroidetes, Actinobacteria, Verrucomicrobia and Cyanobacteria and a lower abundance of Firmicutes than either the dihydroresveratrol or mixed producers.^[60]

3.3.10 LIGNANS

Biological activity of lignans (i.e. phytoestrogens) is related to the activation of these compounds by the colon microbiota to produce enterolactone and enterodiol. Secoisolariciresinol di-*O*-glucoside, one of the most abundant lignans which is found in flaxseed, is first hydrolyzed by *Bacteroides* (*B. distasonis*, *B. fragilis* and *B. ovatus*) and *Clostridium* species (*C. cocleatum* and *C. saccharogumia*) releasing secoisolariciresinol. Demethylation of secoisolariciresinol involves strains of *Butyribacterium methylotrophicum*, *Eubacterium callanderi*, *Eubacterium limosum*, *Blautia producta* and *Peptostreptococcus productus*. Dehydroxylation is typically catalyzed by *Clostridium scindens* and *Eggerthella lenta*. Dehydrogenation of enterodiol to enterolactone and closure of the lactone ring is catalyzed by subdominant populations of *Clostridiales*, in particular *Lactonifactor longoviformis*.^[30,38] These reactions are also summarized in Figure 3.3.

3.3.11 CHLOROGENIC ACIDS

Chlorogenic acids are a family of esters formed between quinic acid and certain hydroxycinnamic acids, most commonly caffeic, p-coumaric, and ferulic acid. These compounds have been investigated in multiple studies and are extensively biotransformed by the colon microbiota. An example is chlorogenic acid (see also Figure 3.3), an ester of caffeic acid and quinic acid. First, the ester bond is cleaved by *Escherichia coli*, *Bifidobacterium lactis*, *Lactobacillus gasseri* or *Lactobacillus acidophilus*, releasing caffeic acid. The next step includes the reduction of the double bond of caffeic acid and dehydroxylation to produce one of the main caffeic acid metabolites, namely 3-hydroxyphenyl propionic acid. Sequentially, β -oxidation of the side chain further converts the metabolite to benzoic acid.^[38,61] Alternatively, the quinic acid ring opening occurs before hydrolysis, leaving a glycerol residue esterified with caffeic acid (i.e. caffeoyl-glycerol).^[42]

3.4 SIMULATING THE GASTROINTESTINAL TRACT

3.4.1 GENERAL

As discussed earlier on in this chapter, the digestive tract is highly complex and involves specialized compartments in order to efficiently extract the optimum amount of nutrients while protecting us from dangerous pathogens. The initial input starts in the mouth (mastication and mixing of food with saliva, including starch hydrolysis by amylase), continuous to the acidic gastric compartment (where food is partially digested and sterilized), followed by passage through the small intestine (primary site of digestion and absorption) and finally the colon (where fermentation by the gut flora breaks down dietary fiber and where ingested compounds are subjected to biotransformation). Human *in vivo* digestion experiments can be performed in healthy volunteers, diseased patients, patients with ileostomy or sudden death victims and are

needless to say the most biologically significant. However, these studies are difficult to perform since the procedures to access the colon are invasive, expensive, time-consuming and raise ethical concerns.^[62] Animal models, such as rats^[63], mice^[64], pigs^[65] and zebrafish^[66] are also used to investigate the gut microbiota. The advantage of using these models is that researchers can conduct more controlled experiments or they can test interventions which are not yet approved for human trials. Having direct access to intestinal contents, tissues and organs at autopsy is also of great value. However, animal models are quite expensive as well and there is also a need to reduce and replace these type of studies because of ethical constraints. Moreover, inter-species variability between man and animals could affect the translation of data.^[62] *In vitro* models are valuable tools to overcome some of these limitation in order to investigate digestive changes in the gastrointestinal tract and biotransformation processes inside of the colon. A variety of *in vitro* gut fermentation models can be found in literature, each of which varies in its design and complexity needed for the experiment. Since the colon is the main site for bacterial fermentation, human fecal samples have been frequently used to investigate these fermentation processes. It is suggested that the microbial composition in feces is representative of that of the distal large intestine.^[67] It should be kept in mind that the fecal communities should be considered a mixture of microbes from the entire gastrointestinal tract and that certain microorganisms may not be well-represented since they might be part of the colonic mucosal microflora. However, fecal samples still represent the colonic microbiota well, and are easy and fast to collect from donors.^[68,69]

3.4.2 STATIC AND DYNAMIC DIGESTION MODELS

Static models are the simplest to simulate the physiological conditions of the gastrointestinal digestion. The tested products remain largely immobile while mimicking the chemical and enzymatic environment of each compartment (gastric, intestinal and sometimes also oral) in a single static bioreactor; more complex digestive

processes such as shearing, peristalsis, gastric emptying, hydration or changes in conditions over time are not covered.^[70] Most methods only include a gastric and intestinal setup in two consecutive steps, since significant compound dissolution is not expected in the oral phase. This is because of the neutral salivary pH value and the short transit time (few seconds to minutes) in the mouth. Most protocols describe a simplified homogenization step and possible addition of salivary amylase.^[71-73] Moreover, following the international consensus within the COST Infogest network, liquid (food) samples can also directly be exposed to the gastric phase.^[74] The gastric phase is usually performed for 1 to 3 h (or even 30 min to 1 h for liquid meals) at an acidic pH adjusted with just HCl or in combination with pepsin while working under a fixed pH and constant temperature of 37 °C. Pepsin is most active between a pH value of 2 - 4. The intestinal phase usually starts by neutralizing the sample with NaOH or NaHCO₃, followed by addition of isolated pancreatic enzymes (lipase, amylase, trypsin, protease) or porcine pancreatin (which contains all important enzymes), with or without emulsifying bile salts. The working pH is set at 6.5 - 7.5, since the jejunum and ileum are the main places of digestion. This step can take one to 5 h depending on the experimental setup and a temperature of 37 °C is used. This intestinal step can be done in the same bioreactor after the gastric phase.^[75] The gastric and intestinal step are mostly performed by shaking in a warm water bath. Human enzymes can be used, but porcine enzymes are also often added instead because of the similarities between pigs and humans. Of course, the human digestive tract is much more complex and is strictly regulated by several feedback systems in order to optimize digestion and nutrient uptake. Our stomach is designed to gradually deliver the ingested meal to the duodenum. The food bolus is first stored in the upper part of the stomach and will then gradually move to the lower part where it is mixed with chyme and ground in smaller particles until it can pass through the pylorus into the small intestine. This means that the gastric content is actually not so homogenous as mimicked by static models. Moreover, the pH of the stomach is not typically fixed: ingested food increases the pH

which is slowly lowered again by the secretion of hydrochloric acid. Plus, the inside of the food bolus can also have a prolonged higher pH compared to the other fractions of the ingested meal. Although static models are less representative for the *in vivo* situation, they do have the advantage that representative samples can be taken, since the whole tested sample is constantly exposed to the same constant pH as well as the added enzymes.^[74] To address the simplistic approach of the static models, several dynamic digestion models have been developed. These models also take into account the geometry, physical forces and changes in biochemistry. The shape, size and orientation of the compartments has an impact on the physical forces on the chyme, e.g. shape of the gastric compartment. Physical forces such as shearing, grinding and simulating peristaltic movements are also part of the dynamic design. The biochemistry is similar to that of the static models, with the main difference that conditions change over time, such as different digestive secretions over time or addition of hydrochloric acid because of real-time monitoring of the pH. An example of a successful dynamic model is TIM-1 (TNO gastrointestinal model), which has been used to study the bio-accessibility of nutrients, minerals, vitamins and bioactive compounds. TIM-1 consists of 4 compartments, namely the stomach, duodenum, jejunum and ileum. These compartments are connected and transfer a controlled amount of chyme through peristaltic valve pumps. TIM-1 differs from static models because of the gradual secretion of digestive fluids, the variable pH, different transit times, mixing via alternating pressure on flexible walls and absorption of water and nutrients through dialysis membranes. The protocol is computer simulated and can be adjusted to different *in vivo* settings (species, age, pathology,...).^[76-78] Another example is the DGM, Dynamic Gastric Model, which combines the mechanical and biochemical aspects of the digestion in the stomach. The model simulates the 2 distinct gastric zones: the upper part (fundus/main body) and the lower part (antrum). The upper part is mimicked by gentle rhythmic squeezing of the food bolus, while the antrum processes the bolus via high shear and peristaltic mixing (using a system of barrel and piston

movements). The addition of acid and enzymes are controlled dynamically (a pH electrode is present in the fundus) and are secreted through a perforated hoop around the wall of the fundus. The model can be continued with an intestinal phase mimicking the duodenum by adjusting the pH, adding enzymes and bile salts.^[79,80]

3.4.3 FERMENTATION MODELS

The available methods range from simple batch incubation to complex dynamic continuous models that are even capable of simulating different parts of the colon. Batch style simulators represent closed bottles containing (single or mixed) bacterial strains or even controlled reactors containing fecal suspensions. These kind of assays are usually operated under anaerobic conditions and are ideal for short-term fermentation experiments to study the production of microbial metabolites and to elucidate biotransformation pathways. Batch fermentation models also give the opportunity to study interindividual variability, e.g. response to a compound, and to test a relative large number of substrates or doses of compounds. These experiments are inexpensive and easy to operate. However, the disadvantage is substrate depletion and accumulation of microbial end products, which affects the *in vivo* relevance in longer simulations. Continuous fermentation models on the other hand, allow long-term experiments thanks to establishing a relatively stable microbial ecosystem under physiologically relevant colon conditions by controlling the composition and rate of the nutrients provided. Moreover, these kinds of models are operated under controlled environmental parameters such as anaerobic conditions, physiological pH and temperature. Therefore, these models are more representative when looking at the composition of the gut microbiota, as well as facilitating the functional link of their role in health and disease. Continuous fermentation models can thus also be used to evaluate the spatial and temporal adaptation of the colonic microbiota to dietary compounds.^[81-83] Some examples of these more complex models include: infant colonic models^[84], TIM-2^[85], P-ECSIM (the Proximal Environmental Control System For

Intestinal Microbiota)^[86], PolyFermS (Polyfermentor Intestinal Model)^[87], EnteroMix^[88], SHIME (Simulator of the Human Intestinal Microbial Ecosystem)^[89], Twin-SHIME^[90], M-SHIME^[89], SIMGI (SIMulator gastrointestinal)^[91] and GIDM (Gastrointestinal Dialysis Model)^[92]. TIM, SHIME, SIMGI and GIDM will be discussed in more detail since these models simulate both the upper gastrointestinal digestion as well as colon fermentation.

3.4.3.1 THE TIM MODELS

The TIM modules operate separately (see schematic diagram in Figure 3.4). The dynamic model TIM-1, which simulates digestion in the upper gastrointestinal tract, was already discussed in detail in paragraph 3.4.2. TIM-2 is a separate completely computer-controlled module simulating fermentation. The model operates at 37 °C, works with a flexible membrane to simulate peristaltic movements, is kept anaerobic through flushing N₂ gas and uses a dialysis system. Dialysis is implemented in order to maintain a highly active microbiota, even up to 3 weeks, since further fermentation can be inhibited because of metabolite production. Plus, it also simulates the *in vivo* uptake of these metabolites via colonocytes. TIM-2 is incubated with fecal donations, which can be obtained from healthy volunteers, volunteers with a disease, different age-classes,... In some experiments, e.g. for lactulose, fecal donations from individuals are introduced separately into the different units in order to compare the activity of the microbiota of different volunteers on the same substrate. However, multiple substrates can also be compared with the same microbiota when using a mix of fecal donations of several donors. This creates a pool of fecal donations which consequently can be used for multiple experiments. The TIM-2 model uses a pH of 5.8, the pH occurring in the proximal colon. An adaptation period of 16 h in specialized nutritional medium and a starvation period of 2-4 h is applied for the microbiota, after which the experimental period starts. Samples for chemical and microbial analysis can be taken from the lumen and the dialysate.^[85]

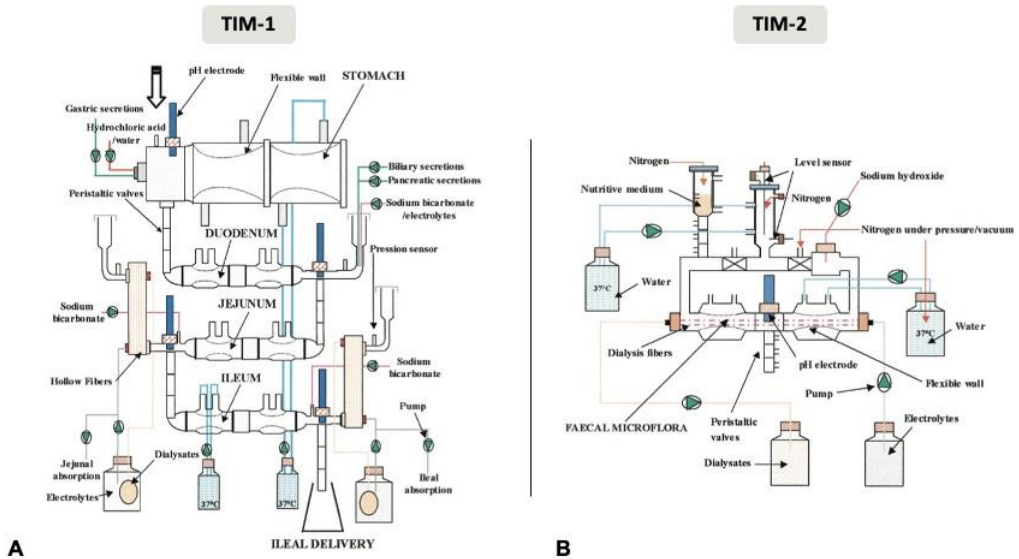


FIGURE 3.4: SCHEMATIC DIAGRAM OF THE TNO NUTRITION AND FOOD RESEARCH INSTITUTE (ZEIST, THE NETHERLANDS) (A) TIM-1 SIMULATING THE GASTRIC-SMALL INTESTINAL SYSTEM (B) TIM-2 SIMULATING THE COLON.^[93]

3.4.3.2 THE SHIME MODEL

The SHIME model (Ghent University - Prodigest, Belgium) integrates the stomach (pH 2), small intestine (slightly acidic to neutral pH) and colon into one system, all kept at 37 °C. A schematic overview is given in Figure 3.5. The colon compartment is also divided into the ascending (pH 5.6 - 5.9), transverse (pH 6.1 - 6.4) and descending colon (pH 6.6 - 6.9). The gastric and small intestinal compartment work according to a fill-and-draw principle. Peristaltic pumps add a defined amount of nutritional medium to the gastric compartment and pancreatic and bile liquid to the small intestine. The digested slurry is then pumped into the ascending colon and transferred sequentially to the other vessels, simulating a 72 h transit time. The three colon compartments are continuously stirred with magnetic stir bars and kept anaerobic by flushing the headspace with N₂ gas or a 90/10% mix of N₂/CO₂ gas. The colon compartments are inoculated with the fecal microbiome from one individual. A typical experiment consists of a 2 week stabilization period (adaptation of the fecal microbial community and creating colon region-specific microbiota), a 2 week basal period (reactor operated

under nominal conditions), a 2 - 4 week treatment period and a 2 week washout period (evaluating the reversibility of a treatment). By combining all these compartments, the SHIME model can be used to study the activity and stability of pre- and probiotics, the metabolism of pharmaceuticals and the microbial conversion of bioactive food components. As mentioned before, the mucosal microbiome is part of the gut microbial ecosystem. The M-SHIME, or mucosal SHIME, is an optimized version of the SHIME where the mucosal microbial colonization is mimicked by integration of mucin-covered microcosms. The Twin-SHIME model, on the other hand, consists of two identical SHIME units which allows to study e.g. the shift in gut microbiota upon different dietary patterns or antibiotic treatment by running two reactors in parallel. In contrast to the shorter timeframe of experiments in the TIM-2 model, SHIME often has an experimental period of more than one week to several weeks. This is interesting when researching e.g. the adaptation of the microbiota to changing conditions. Another big difference between TIM-2 and SHIME is that the SHIME setup lacks dialysis and peristalsis. However, dialysis modules can be incorporated after the small intestine and colon.

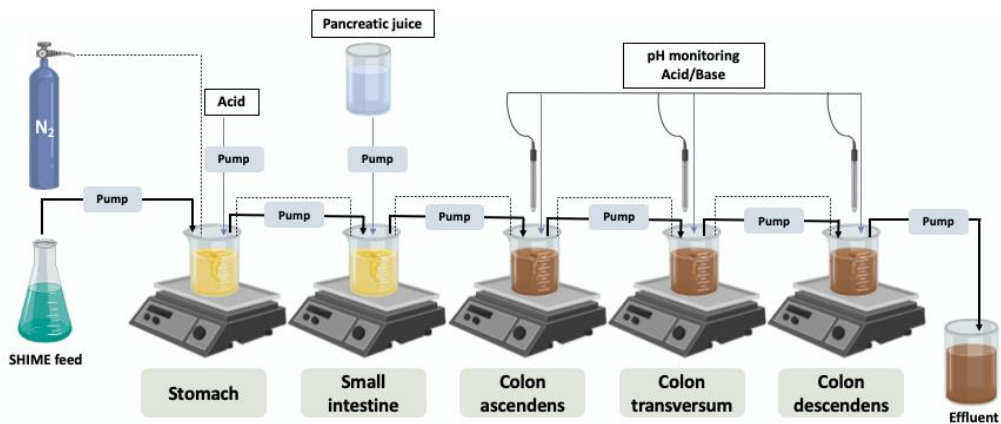


FIGURE 3.5: SCHEMATIC REPRESENTATION OF THE SHIME MODEL. ILLUSTRATION ADAPTED FROM VAN DE WIELE ET AL.^[89]

3.4.3.3 THE SIMGI MODEL

The SIMGI model (see Figure 3.6) is recently developed at the Institute of Food Science Research CIAL in Madrid, Spain. The model is computer-controlled and dynamically simulates digestion in the stomach and small intestine, as well as colonic fermentation. The gastric compartment operates via peristaltic movements and has ports for input to add samples, gastric juice and HCl. This is where SIMGI differs from SHIME, which has no peristalsis. The digestion in the small intestine takes 2 h and is a continuously stirred reactor vessel kept at a pH of 6.8, mixed with pancreatic juice and bile. The colon is simulated in three reactors: ascending (pH 5.6), transverse (pH 6.3) and descending (pH 6.8) colon. All compartments operate at 37 °C and the small intestine and the three colon reactors are continuously flushed with N₂ gas. The colon vessels are inoculated with fresh fecal slurry, followed by a stabilization period of 2 weeks to reach a steady-state microbial environment.^[91]

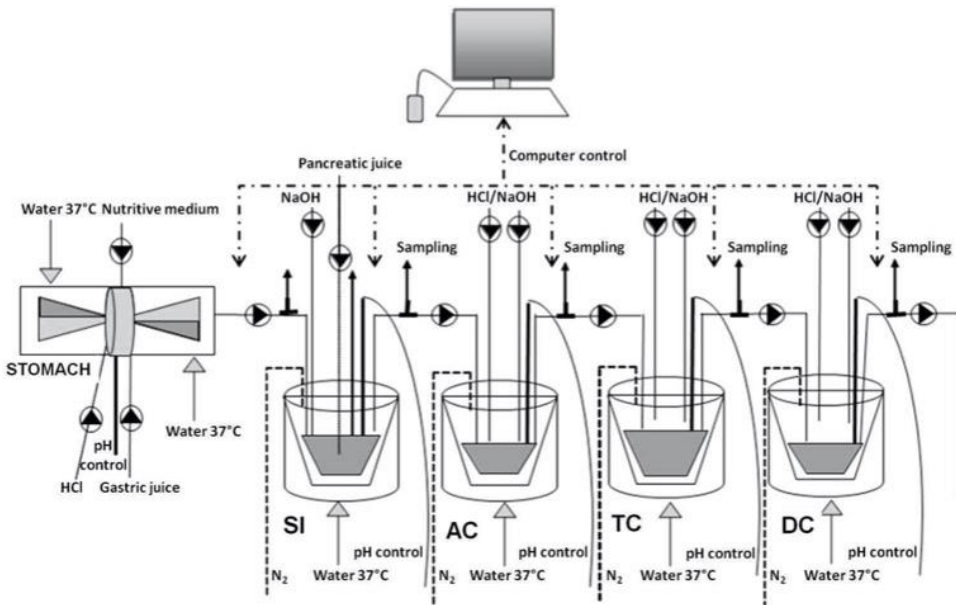


FIGURE 3.6: SCHEMATIC REPRESENTATION OF THE SIMGI MODEL. ILLUSTRATION ADAPTED FROM BARROSO ET AL.^[91]

3.4.3.4 THE GIDM

The GIDM was developed in-house at NatuRA (University of Antwerp, Belgium). The gastrointestinal model operates at 37 °C and is equipped with a continuous dialysis system to simulate passive diffusion from lumen to mucosa. Briefly, the gastric phase is performed at a pH of 2 in shaking flasks (120 strokes/min) and is simulated by the addition of pepsin solution. The gastric digest is then transferred to Amicon stirred cells equipped with a dialysis membrane. The small intestinal phase is performed by gradually increasing the pH to 7.5 and adding pancreatin-bile mixture. The small intestine and colon phase are both performed in an anaerobic glove box, which is set at 37 °C and continuously flushed with gas containing 5% CO₂, 5% H₂ and 90% N₂. Similar to TIM-2, the colon phase simulates the proximal colon where the pH is set at 5.8 and cultivated fecal suspension is added to the sample. The GIDM uses a pooled fecal fraction from 3 donors, which can be used for multiple experiments. The fecal suspension has an adaptation period of 18h in Wilkins-Chalgren anaerobe broth before the experimental period. The anaerobic glove box and dialysis cell is pictured in Figure 3.7.

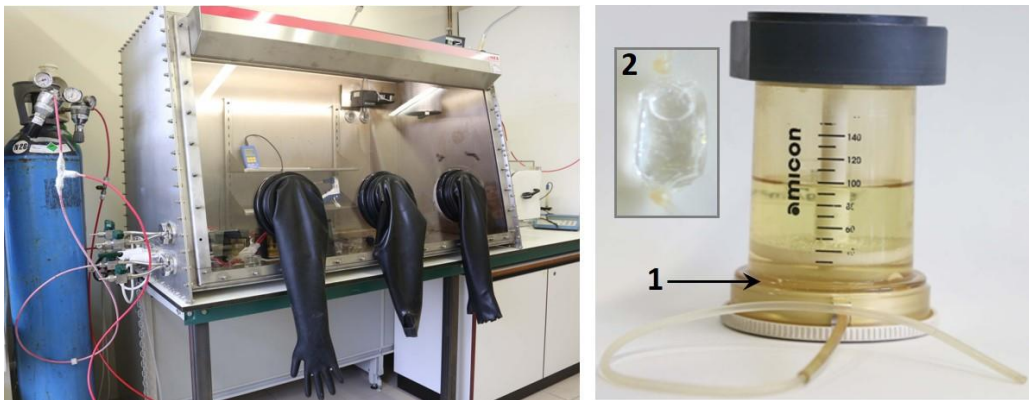


FIGURE 3.7: THE ANAEROBIC ENVIRONMENT IN THE GLOVE BOX, PICTURED ON THE LEFT, IS CREATED BY FLUSHING WITH A MIXTURE OF 5% H₂, 5% CO₂ AND 90% N₂ GAS. ON THE RIGHT, A DIALYSIS CELL IS SHOWN INCLUDING THE DIALYSIS MEMBRANE (1) AND THE DIALYSIS TUBING CONTAINING 1M NAHCO₃ (2).

Samples for analysis can be taken from the lumen (retentate) as well as the dialysate. The GIDM permits a fast (few days to one week), easy and non-expensive way to investigate the metabolites of polyphenols as well as their absorption after digestion in the gut. Moreover, different replicas of the substrate as well as a negative control and blank sample can be performed in one experiment.^[92,94]

3.5 METABOLOMICS

3.5.1 GENERAL

This chapter focusses on the biotransformations of polyphenols after interaction with the gut microbiota. As mentioned before, these biotransformations result in more bioavailable metabolites and/or bioactive metabolites, since many natural products are considered to be prodrugs. Phytochemicals in plants often occur in their glycosylated form. And thus, after oral administration of a herbal extract such as *Filipendula ulmaria*, gastrointestinal enzymes and the colon microbiota might lead to the biotransformation of these compounds into their final active form.^[95] Nevertheless, even though it is well known that biotransformation in the human body is crucial for the activation of prodrugs, this aspect is usually overlooked in natural product research. However, revealing such metabolic pathways after *in vitro* biotransformation experiments is complex: concentrations of phytochemicals and their metabolites can increase, decrease or show any combination of these patterns during biotransformation. Moreover, these experiments also generate a massive amount of data. Data processing and analysis is therefore an important part of these biotransformation experiments in order to reveal the dynamics of the metabolites. Metabolomics is an increasingly emerging 'omics' science. The field of metabolomics studies the end products of cellular processes, known as metabolites. Metabolomics is progressively being used to understand disease mechanisms, diagnose disease, identify new drug targets, monitor therapeutic outcomes or even to provide a functional readout of microbial activity.^[96,97]

The most commonly used techniques to study such broad coverage of metabolites are nuclear magnetic resonance (NMR) spectroscopy, gas chromatography - mass spectrometry (GC-MS) and mass spectrometry coupled to liquid chromatography (LC-MS).^[96] However, these techniques (especially LC-MS) often result in enormous amounts of data. Moreover, many standardized workflows are available for many standard type of experiments (e.g. case versus control), but the number of methods available to analyze dynamic data (i.e. longitudinal or time-resolved data) is limited and most of them are not specifically designed for metabolomics.^[98] In this thesis, a multiclass experiment was performed over multiple timepoints in an *in vitro* gastrointestinal biotransformation model simulating the ingestion of a *Filipendula ulmaria* extract. Study samples were thus compared to a blank and negative control sample in the stomach phase, small intestinal phase and colon phase with a total of 72 h of fermentation. Since there is no common default strategy to analyze such large-scale, dynamic data with a large variety of time profiles in an untargeted fashion, a new approach was necessary to compare the data of these three groups over time in order to elucidate the compounds undergoing biotransformation as well as their formed metabolites. The metabolomics workflow consists of multiple steps: the experimental, data processing (including file conversions and pre-processing steps) and data analysis part.

3.5.2 LC-MS PRE-PROCESSING

The first step after the experimental part in the metabolomics workflow, is pre-processing, which is used to convert the raw LC-MS data from the instrument into a smaller and useable data matrix ready for statistical analysis and machine learning. In this case, the rows of the data matrix represent samples, the columns represent features (i.e. a group of peaks at a certain m/z and retention time location) and the individual matrix elements represent intensities (i.e. the peak height for that sample and feature combination). In order to facilitate manipulation of data, which is difficult

and limited with vendor data formats, open-source software (such as ProteoWizard) have been developed to transform the LC-MS data files to an open data format, like mzML (includes mzData and mzXML).^[99,100] XCMS is the most commonly used open-source software for metabolomics data processing. Data are thus first converted to the open source .mzXML format to allow further XCMS processing. The next step in pre-processing with XCMS software is peak-picking, where peaks in the files containing spectra are detected. This is followed by grouping of similar peaks across different samples and is needed to match those peaks over different samples. This step can be followed by an optional retention time correction. As a last step, peak filling is used to account for peak groups with missing data.^[101]

3.5.3 DYNAMIC METABOLOMICS

For more complex experiments, such as dynamic metabolomics, standardized workflows are lacking. No common default strategy is available yet for the analysis of large-scale, untargeted, longitudinal, multiclass metabolomic experiments in which simultaneously a large number of features and a variety of different time profiles needs to be considered.^[102] XCMS has the ability to discover features that are different between groups, but it is not able to take the longitudinal aspect into account.^[101] EDGE, a tool used in the field of genomics, provides the possibility for discriminating different time profiles and is thus used to find the features that exhibit differential transformation over time. However, EDGE is tailored to two-class problems, not multiclass experiments. EDGE fits two models to every feature. The null model assumes there is no difference between the groups and fits a single cubic spline to all the data of a feature. The alternative model fits a cubic spline to each group and calculates the goodness of fit. The difference between these groups, expressed as p-values, reflects the improvement in goodness of fit. This approach thus generates two p-values for every feature, one for sample vs. blank and one for sample vs. negative control, which is non-trivial to interpret or combine.^[103,104] However, our biotransformation

experiment resulted in three groups (samples, negative controls and method blanks) which needed to be compared against each other. Resolving this issue for multiclass data would take a considerable amount of time and expertise, since these results would need to be checked manually and compared to the raw data. An in-house workflow was therefore developed which incorporates this expert knowledge into the analysis pipeline in an easy and more efficient way. A Shiny web application was developed for this purpose in R, called *tinderesting*. Experts are shown a small subset of features, i.e. the training data, and can quickly rate whether that feature is interesting or not interesting. This labeled training data is then used to train a machine learning model, i.e. a random forest model, that can be used to analyze the complete data set, rating the features in a similar manner as the expert. Training the random forest model thus reduces false negative and false positive hits. The performance of the machine learning model is typically validated by 10-fold cross validation via ROC (receiver operator characteristic) curve and its corresponding AUC (area under the curve) value. The outcome of this workflow is a single score for each feature, referred to as *tinderesting* score, which is independent of the number of samples, classes or time points that are present in the features. The maximal score of 1 corresponds to the model labelling this feature as interesting, and the minimal score of 0 defines an uninteresting feature. This differs from the case versus control statistical tools that produce a score, usually a p-value, per feature for every two-class comparison. This new approach using *tinderesting*, mimics the human revision process and thus saves a tremendous amount of time in differentiating between relevant and irrelevant features. The complete workflow has been validated on data of a biotransformation experiment of the compound hederacoside C, as well as an extract of *Herniaria hirsuta*.^[98,105,106] Figure 3.8 shows an example of a biotransformation experiment with interesting and uninteresting features. When looking at the time profiles on the left, the curves of the samples clearly differ from the negative control and method blank. The abundance of an interesting compound in the sample can for example increase, decrease or a

combination of both. In the negative control, the same compound can be absent from the start, and thus be (almost) equal to the time profile of the method blank, or can be present but follows a different stable pattern compared to the time profile of the fermented sample. Uninteresting features are shown on the right, where the negative control and sample follow a similar time profile. Another example of an uninteresting feature happens when the time profiles of the method blank, negative control and sample mimic each other.

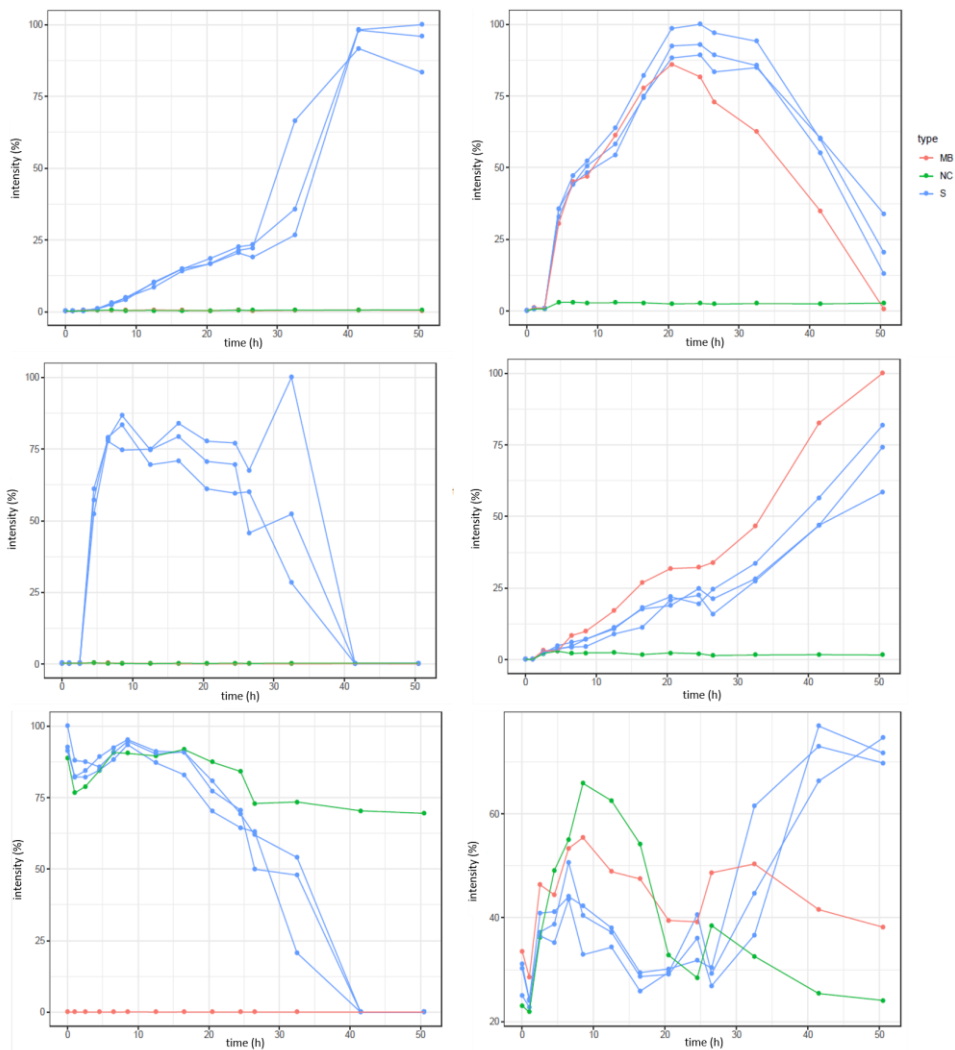


FIGURE 3.8: FEATURE EXAMPLES OF THREE INTERESTING (LEFT) AND THREE UNINTERESTING (RIGHT) DATA FEATURES FROM NEGATIVE POLARITY UHPLC-HRMS DATA. THE INTERESTING FEATURES SHOW A DIFFERENT TIME PROFILE FOR THE SAMPLES (BLUE), COMPARED TO THE METHOD BLANKS (RED) AND THE NEGATIVE CONTROLS (GREEN).

MATERIALS AND METHODS

3.6 SAMPLE PREPARATION

Filipendulae Ulmariae Herba (batch number 19969) was bought from Tilman SA (Baillonville, Belgium). The dried plant material was ground prior to extraction with a PF 10 basic Microfine grinder drive (IKA-Werke GmbH & Co. KG, Staufen, Germany) using a sieve mesh size 0.5 mm. To cover the full range of constituents in the plant material, a comprehensive extraction protocol was applied, previously described by Bijttebier et al. with minor adaptations and discussed in chapter 2.^[107] A combination of extraction with H₂O:EtOAc and CHCl₃:MeOH:H₂O yields both polar and apolar compounds. Approximately 18 g of sample was subsequently hydrated with 54 mL of water and 225 mL of EtOAc. The mixture was stirred for 2 h followed by 1 h of ultrasound-assisted extraction. Next, the solvent was removed, followed by washing the residue 3 times with 20 mL EtOAc and evaporating the extract to dryness. CHCl₃:MeOH:H₂O extraction was performed by adding 180 mL CHCl₃:MeOH:H₂O (4:4:2) to 18 g of sample. The mixture was stirred for 5 min, followed by 5 min of ultrasound-assisted extraction and stirred for an additional 15 min. The solvent was removed and the residue was washed 3 times with 20 mL CHCl₃:MeOH:H₂O (4:4:2). Finally, the dried H₂O:EtOAc extract was redissolved with the extract from the CHCl₃:MeOH:H₂O extraction method, leading to an apolar and a polar phase. Both phases were separated, dried and stored in the dark at -20 °C.

3.7 GASTROINTESTINAL MODEL

Many natural products are pro-drugs that are biotransformed and activated after oral ingestion. An *in vitro* Gastrointestinal Biotransformation Model, previously developed and validated in-house, was used to mimic human biotransformation processes in the

stomach, small intestine and colon including fermentation by pooled human feces.^[92] For this experiment, dialysis was not implemented as this change drastically increases the amount of handled samples. Moreover, the dialysis system simulates passive diffusion and thus acts as a filter, which can cause loss of compounds. The digestive juices and fecal suspension were formulated to simulate the human conditions, which were previously described by Breynaert et al. and Peeters et al.^[98,105,106]

3.7.1 PREPARATION OF FECAL SLURRY

Human fecal donors (n=3) were selected, meeting the following inclusion criteria: 25 to 58 years, non-smoking, non-vegetarian or vegan, normal defecation with no history of gastrointestinal disease or acute (gastrointestinal) disease at the moment of donation and no intake of anti/pre/probiotics 3 months prior to donation. A fecal suspension of 10% (w/v) feces was prepared by homogenizing each stool sample with a sterile phosphate-buffer solution (0.1 M, pH 7.0) in sterile filter bags (Bagpage® R/25 400 mL, VWR International, Haasrode, Belgium) in a stomacher during 3 min in order to remove particulate food material. The phosphate buffer solution consists of NaH₂PO₄·2H₂O (0.75% (w/v)), Na₂HPO₄·2H₂O (1.03% (w/v)), sodium thioglycolate solution (3.45% (v/v)) and glycerol (17% (v/v)). The buffer solution was sonicated and autoclaved (1 bar, 121 °C). The mixed fecal pool was stored in aliquots at -80 °C. Prior to use, an aliquot of the 10% (w/v) fecal suspension was cultivated by adding 90% (v/v) phosphate buffer. After continuously stirring for 1 h at 37 °C the suspension is ready to use. In every step, fecal samples are processed in an anaerobic glove box (5% H₂, 5% CO₂ and 90% N₂, Jacomex Glove Box T3, TCPS, Belgium) in order to ensure an anaerobic environment.

3.7.2 PREPARATION OF DIGESTIVE JUICES

The digestive juices were formulated corresponding to the human digestive conditions. The pepsin solution was prepared by dissolving 16% (w/v) of pepsin powder in 0.1 M HCl (622 000 FIP-U/100 mL). To obtain the pancreatin-bile mixture, 0.4% (w/v)

pancreatin and 2.5% (w/v) bile were dissolved in 0.1 M NaHCO₃ (32 000 FIP-U lipase, 143 600 FIP-U amylase, 16 400 FIP-U protease and 58.4 mmol bile/L).

3.7.3 SIMULATION OF THE STOMACH, SMALL INTESTINE AND COLON

This biotransformation experiment included three groups: samples containing the polar *Filipendula ulmaria* extract (treated with digestive enzymes and fecal microflora (FEX)), negative control samples (also containing the extract with addition of digestive enzymes but not of fecal slurry (NCFEX)) and method blanks (containing no extract but comprising of an equal volume of solvent and undergoing treatment with digestive enzymes and fecal bacteria (MB)). For preparation of the FEX samples, an amount of approximately 300 mg of the polar *Filipendula ulmaria* extract was weighed accurately in triplicate and mixed with 47 mL of ultrapure water. In the same manner, NCFEX samples were prepared *in duplo* (containing the same amount of *Filipendula ulmaria* extract) and 3 MB samples comprising an equal volume of water. Additionally, a positive control sample containing 75 mg chlorogenic acid and 240 mg salicin was included as confirmation of *in vitro* biotransformation in all gastrointestinal biotransformation experiments.

During simulation of the gastric phase, the pH of all the samples was adjusted to 2.0 using 6 M HCl and 3 mL of the pepsin solution was added. Afterwards, samples were incubated for 60 min in a shaking warm water bath at 37 °C (120 strokes/min). The small intestine phase is initiated by adding 50 mL of ultrapure water to the gastric digest and by increasing the pH of the samples to 7.5. This was done by adding an amount of 1 M NaHCO₃ to the negative control sample to obtain pH 7.5. The same amount was then added to the other corresponding samples using a small dialysis bag in order to obtain a gradual pH change. After 30 min, 15 mL of the pancreatin-bile mixture was added to the samples and stirring was continued for 1 h. In total, the samples were continuously stirred at 37 °C for 1.5 h. The colon phase was continued by transferring

all the samples to an anaerobic glove box (5% CO₂, 5% H₂ and 90% N₂, Jacomex Glove Box T3) set at 37 °C. Before starting, 10% (v/v) fecal suspension was cultivated in the anaerobic box during 1 h in 90% (v/v) sterile phosphate buffer (0.1 M, pH 7.0, without glycerine) in order to obtain a bacteria suspension of 10⁸ CFU/mL. Afterwards, 50 mL of phosphate buffer, without bacteria, was added to the negative control samples in order to adjust the pH of the samples to 5.8 using 1 M HCl. The same volume of 1 M HCl was then added to the 3 samples and the method blanks. In the anaerobic glove box, a volume of 50 mL of the cultivated fecal suspension was added to the pH-adjusted test samples and the blank. All samples were continuously stirred for 72 h.

3.7.4 VIABILITY AND BACTERIAL COMPOSITION

Viable cell concentrations were determined by means of decimal dilution series of the bacteria samples plated onto WCA (Wilkins Chalgren agar; Oxoid, Hampshire, UK). The agar was prepared by mixing 48 g of powder with 1 L H₂O and plates with a thickness of 0.5 cm were poured. Decimal dilution series of the bacteria suspension were prepared, ranging from 10⁻¹ to 10⁻⁸ CFU. A volume of 100 µL of every dilution was plated out in triplicate under anaerobic conditions and incubated for 24 h at 37 °C. To elucidate the microbial composition of the fecal suspension, 16S rDNA-targeting PCR was performed. The 16S region of a bacterial gene is small (size: 1.5 kb) and highly conserved, with nine hypervariable sites that provide species-specific signature sequences sufficient to distinguish various bacterial species. Amplification of the V3 and V4 regions of the 16S rDNA was executed in triplicate with 2x KAPA HiFi HotStart Ready Mix (Kapa Biosystems, Amsterdam, The Netherlands) with the following cycling profile: 95 °C for 3 min, [95 °C for 30 s, 62 °C for 30 s, and 72 °C for 50 s] x 25 and 72 °C for 10 min. An index PCR was performed with the Nextera XT Index Kit with dual indices, generating libraries. The concentration of each individual library was measured, mixed with a denatured PhiX control library and diluted to a final concentration of 4 pM. This library was loaded onto a MiSeq V2 500 cycle cartridge and sequenced (2 x 250 bp) with

the MiSeq (Illumina, Inc., San Diego, CA, USA). Raw sequence reads were quality assessed using fastQC and data analysis was done using the microbial genomics module, inbuilt in CLC Genomics workbench v9.5.3 (CLCbio, Qiagen). Briefly, contigs were created by heuristically merging paired-end reads based on the Phred quality score of both reads. Contigs were aligned to the SILVA 16S database v.132 and binned based on the sequence similarity.^[108] Taxonomic classification was performed on binned contigs with the SILVA v.132 database.^[94]

3.7.5 SAMPLING TIME POINTS AND SAMPLE PREPARATION

Sample aliquots were taken at several time points during the experiment: before biotransformation (t_0), after the gastric phase (S), after the small intestinal phase (SI) and during different time points of the colon phase (C2, C4, C6, C10, C14, C18, C22, C24, C32, C40, C48, C72; in which the number indicates the hours of fermentation in the colon phase). Samples were diluted with methanol (1:2) and centrifuged at 10 000 rpm for 10 min. The supernatant was diluted 10 times with MeOH:H₂O (60:40) before analysis.

3.8 INSTRUMENTAL ANALYSIS

For the qualitative UHPLC-UV-QTOF analysis of the obtained biotransformation samples, an aliquot of 5 μ L was injected on a Waters Acquity UHPLC BEH SHIELD RP18 column (3.0 mm \times 150 mm, 1.7 μ m; Waters). The temperature of the column was kept at 40 °C. The mobile phase solvents consisted of water + 0.1% formic acid (A) and acetonitrile + 0.1% formic acid (B), and the gradient was set as follows: 0/2, 1/2, 14/26, 24/65, 26/100, 29/100, 31/2, 41/2 (min/B%). The flow rate was set at 0.4 mL/min. Accurate mass measurements were done using a Xevo G2-XS QTOF spectrometer (Waters, Milford, MA, USA) coupled with an ACQUITY LC system equipped with MassLynx 4.1 software. During the first analysis, full scan data were recorded in ESI (+) and ESI (-) mode from m/z 50 to 2000, and the analyzer was used in sensitivity mode

(approximate resolution of 22 000 FWHM). The spray voltage was set at either +1.5 kV and -1.0 kV; cone gas flow and desolvation gas flow at 50.0 L/h and 1000.0 L/h respectively; source temperature and desolvation temperature at 120 °C and 500 °C respectively. Data were also recorded using MS^E in positive and negative ionization modes, providing separate MS and MS^E data. A ramp collision energy from 20 V to 30 V was applied to obtain additional structural information. Leucine-enkephalin was used as lock mass. To monitor analytical drift and assess precision, quality control samples were injected after every time point. A standard mix was prepared using stock solutions of the following analytes: apigenin, benzoic acid, caffeic acid, (+)-catechin, chlorogenic acid, cinnamic acid, *p*-coumaric acid, coumarin, emodin, epicatechin, ferulic acid, gallic acid, *p*-hydroxybenzoic acid, isorhamnetin, kaempferol, luteolin, naringenin, phloretin, protocatechuic acid, quercetin, quercitrin, isoquercitrin, rutin, spiraeoside, salicin, saligenin, salicylic acid, β -sitosterol, stigmasterol, syringic acid and vanillic acid. Standard stock solutions of the analytical standards were prepared at a concentration of 1 mg/mL in UHPLC-grade methanol for each analyte separately and stored in the dark at -80 °C. Dilutions of these solutions were prepared in 60:40 (v/v) methanol:40 mM ammonium formate buffer (aqueous). Standard stock and working solutions were stored at -80 °C in the dark. QC samples were prepared using a dilution of the standard solution mix (39 ng/mL).

3.9 DATA ANALYSIS

In order to process the complex and dynamic data of the biotransformation experiment, a novel workflow was implemented to render as much information as possible from the longitudinal LC-MS data and to select the most interesting time profiles. Data were converted to open source .mzXML format to allow further processing. The XCMS CentWave algorithm was used to convert the raw data into features via peak-picking, followed by grouping, using following parameters: ppm = 10, peakwidth = c(5, 25), snthresh = 10, noise = 1000, mzdiff = 0.01, prefilter = c(3, 5000),

integrate = 1. EDGE was used for the extraction of significant differential profiles since XCMS has the ability to discover features that are different between groups, but lacks the power to take longitudinal data into account. An interactive Shiny app developed in R, called tinderesting, was used to rate the quality of a subset of the resulting features. These labeled features were used to train a random forest model for predicting experts response. The machine learning model provided a single score for each feature, which is referred to as the tinderesting score. This score allowed ranking of all features based on the difference over time between the three groups (sample, blank and negative control). The maximal score of 1 corresponds to the model labeling this feature as interesting, whereas the minimal score of 0 defines an uninteresting feature. Biotransformer (v 3.0) was used as an additional software tool to predict human gut metabolites. The tool combines a knowledge-based approach with a machine-learning-based approach to predict biotransformation.^[109] The SMILES string of rutin was uploaded and “Human and Human Gut Microbial Transformation (allHuman)” was selected.

RESULTS AND DISCUSSION

3.10 BIOTRANSFORMATION OF THE POSITIVE CONTROL

As mentioned in paragraph 3.7.3 of the materials and methods section, the positive control sample contained salicin, which will be further discussed in detail in paragraph 3.11.2.5.1, and chlorogenic acid. An amount of 75 mg chlorogenic acid was selected for use in the positive control samples as this is approximately the daily ingestion of a non-coffee drinker.^[110] The gastrointestinal model was previously validated using chlorogenic acid and showed a good recovery and precision (coefficient of variation < 16%). Availability of chlorogenic acid in the small intestinal phase ($37 \pm 3\%$) of the gastrointestinal model is comparable with *in vivo* studies on ileostomy patients. In the colon phase, the human fecal microbiota deconjugated and further degraded chlorogenic acid to caffeic acid, 3,4-dihydroxyphenylpropionic acid, 4-hydroxybenzoic acid, 3- or 4-hydroxyphenyl acetic acid, 2-methoxy-4-methylphenol and 3-phenylpropionic acid.^[92] As expected, a decrease in intensity of the signal of chlorogenic acid over time was observed (see also Figure 3.22A, paragraph 3.11.2.5.2) and suspect screening for metabolites previously reported in literature resulted in detection of five metabolites.^[61,92,111-116] Hydrochlorogenic acid (m/z 355.1029 [M-H]⁻) (M1), quinic acid (m/z 191.0561 [M-H]⁻) (M2), caffeic acid (m/z 179.0350 [M-H]⁻) (M3), 3,4-dihydroxyphenylpropionic acid (m/z 181.0506 [M-H]⁻) (M4) and 3-(4-hydroxyphenyl)-propionic acid (m/z 165.0557 [M-H]⁻) (M5) were found during *in vitro* gastrointestinal biotransformation in the positive control sample. An overview of their structures, pathway and biotransformation profile is shown in Figure 3.9 and Figure 3.10. Formation of these metabolites was thus used as confirmation of adequate *in vitro* biotransformation in the gastrointestinal biotransformation experiment.

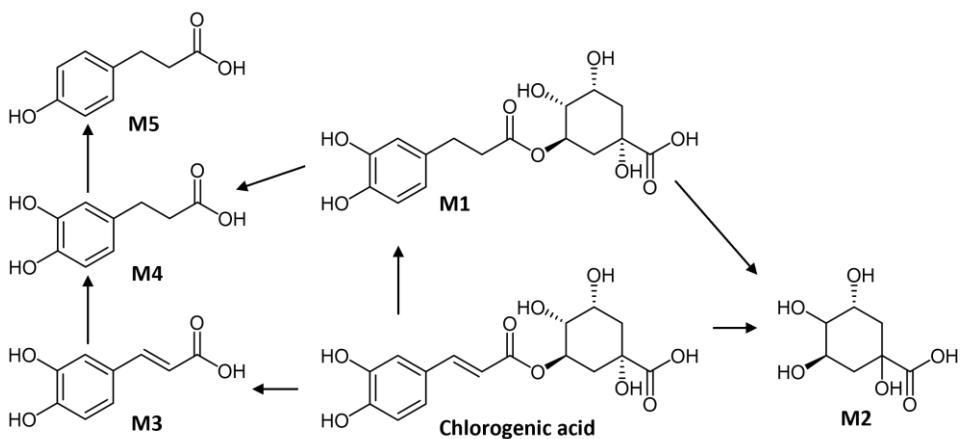


FIGURE 3.9: BIOTRANSFORMATION PRODUCTS OF CHLOROGENIC ACID OBSERVED IN THE POSITIVE CONTROL SAMPLE, WITH M1 = HYDROCHLOROGENIC ACID, M2 = QUINIC ACID, M3 = CAFFEIC ACID, M4 = 3,4-DIHYDROXYPHENYLPROPIONIC ACID AND M5 = 3-(4-HYDROXYPHENYL)-PROPIONIC ACID.

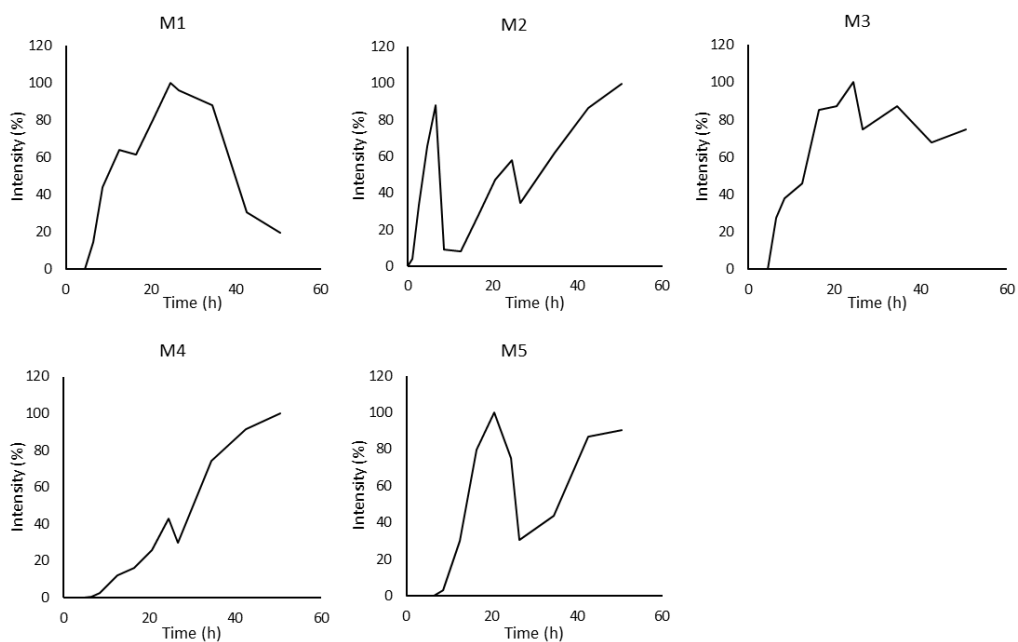


FIGURE 3.10: INTENSITY (MAX = 100%) OF METABOLITES OF CHLOROGENIC ACID OVER TIME IN NEGATIVE IONIZATION MODE.

3.11 BIOTRANSFORMATION OF A *FILIPENDULA ULMARIA* EXTRACT

Herbal extracts consist of a mixture of compounds, covering a wide range of bioactive constituents. As mentioned in depth in chapter 2, it has been shown that meadowsweet contains many phenolic constituents such as flavonoid aglycons (e.g. quercetin, kaempferol), glycosylated flavonoids (e.g. rutin, hyperoside, quercitrin, avicularin and astragalins) and hydrolysable tannins (tellimagrandin I and II, rugosin A, B, D, and E), as well as salicylates (salicylic acid, methyl salicylate, salicylaldehyde, salicylalcohol and their glycosides).^[107,117-123] Therefore, extensive biotransformation after oral intake can be expected. Consequently, gastrointestinal biotransformation of the lyophilized *Filipendula ulmaria* extract was simulated *in vitro* to monitor the levels of the identified compounds using amMS and UV data. Figure 3.11 shows the chromatogram of the *Filipendula ulmaria* extract before and after *in vitro* biotransformation. Before biotransformation (t_0), peaks of the chromatogram are mostly attributed to the tentatively identified compounds. After the colonic phase of gastrointestinal biotransformation, the chromatogram contains peaks of compounds, metabolites as well as matrix interferences, originating from enzymes, bile salts and fecal microflora, which are absent at t_0 .

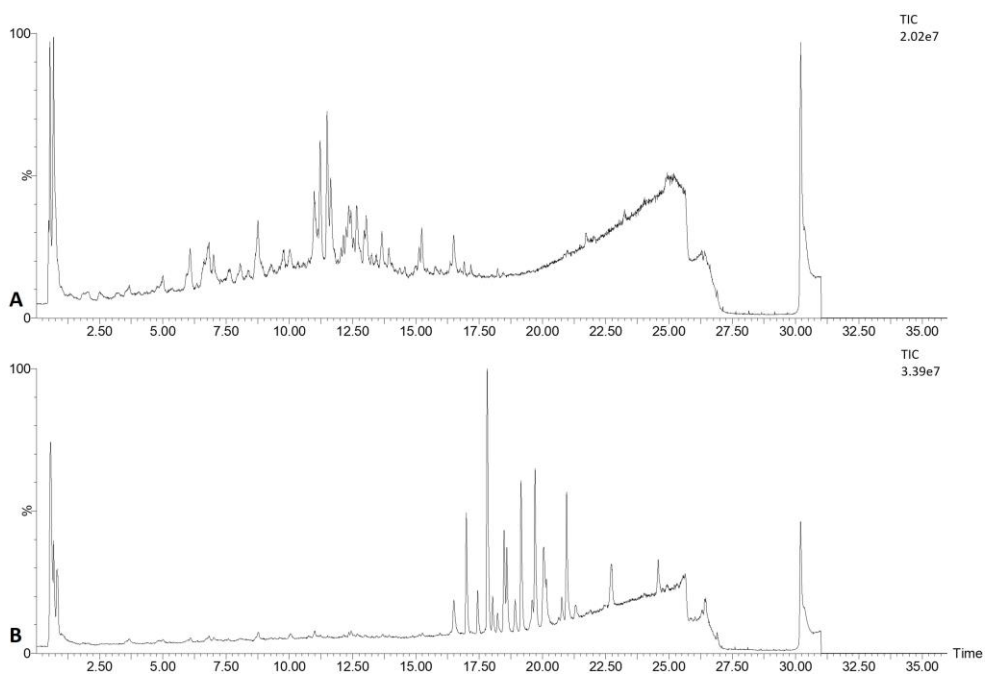


FIGURE 3.11: TOTAL ION CHROMATOGRAM OF THE *FILIPENDULA ULMARIA* EXTRACT BEFORE (A) AND AFTER (B) *IN VITRO* GASTROINTESTINAL BIOTRANSFORMATION.

The complexity of the data is thus increased immensely because of the presence of these gastrointestinal enzymes and fecal microflora in the samples, causing a lot of matrix derived information. Moreover, the multiclass samples are measured as a function of time, adding a longitudinal aspect to the complex data and impeding the interpretation of the data. Manual processing of the chromatograms of every time point for every compound allows monitoring of the intensity over time. The concentration of precursor compounds and metabolites can increase, decrease or show any combination of these patterns during biotransformation. However, this manual approach is very time-consuming and will only provide information about the abundance of previously identified compounds. Manual screening for metabolites is comparable to looking for a needle in a haystack because of the complexity of the chromatograms and matrix interferences. The automated data analysis workflow, previously described by Peeters et al. and Beirnaert et al., was thus used to screen

rapidly and unbiased for metabolites.^[98,105] The workflow resulted in 10 179 features in negative ion mode.

3.11.1 MATRIX COMPONENTS: BIOTRANSFORMATION OF BILE ACIDS

All samples (i.e. FEX samples, negative controls and method blanks) from the *in vitro* gastrointestinal model contain enzymes and bile salts, which were added during the stomach phase and the small intestinal phase. When looking at the total ion chromatogram in Figure 3.11, after biotransformation, large peaks appeared with retention times ranging from 17 to 23 min which can be allocated to changes in the bile acid profile by fecal bacteria (based on the tentatively identified masses shown in Table 3.1). The porcine bile extract used in the gastrointestinal model contains glycine and taurine conjugates of hyodeoxycholic acid (HDCA) and other bile salts, with similar ratios of glycine to taurine compared to human bile.^[124] Since 95% of bile acids are reabsorbed in the ileum and recycled back to the liver via the enterohepatic circulation, only 5% of bile acids will enter the colon. The impact of different concentrations of bile acids on the viability of bacteria was tested and described in previous research from Breynaert et al.^[92] Therefore, a concentration of 0.1% (w/v, 2.3 mmol/L) bile acids was selected in accordance with the *in vivo* situation.^[93] During the colon phase, these bile acids are thus also subjected to microbial biotransformation. The fecal bile acid profile mostly consists of unconjugated bile acids, due to the activity of bile salt hydrolases (BSH) and dehydroxylation. BSH activity is widespread in commensal bacteria of the small intestine and colon. Gram-positive gut bacteria have the most diverse distribution of BSH, including *Clostridium*, *Enterococcus*, *Bifidobacterium* and *Lactobacillus*. The distribution of BSH in Gram-negatives is detected in members of the genus *Bacteroides*.^[125] A 16S rDNA phylogenetic analysis of the fecal suspension has demonstrated the presence of bacteria complying to these genera (see Paragraph 3.11.4). As the method blanks contain no added extract, signals present in the chromatogram originate purely from the sample matrix (Figure 3.12). The bile acid

profile was tentatively identified at the small intestinal stage, summarized in Table 3.1. Besides HDCA and dehydro-HDCA, taurine and glycine conjugates were observed, respectively referred to as T-HDCA and G-HDCA, together with dehydrated and oxidated derivatives. Biotransformation reactions of bile salts present in the porcine bile extract were studied by monitoring the intensity of the signals over time. Over time, a decrease in intensity of the conjugates was observed (Table 3.2). After 18 h of colonic phase, all taurine and glycine conjugates and their derivatives were hydrolyzed into HDCA and dehydro-HDCA or isomers thereof (Figure 3.12). Further biotransformation reactions as reported by Owen et al. were not observed.^[126]



TABLE 3.1: BILE ACID PROFILE AT THE SMALL INTESTINAL STAGE.

Name	<i>m/z</i> (observed)	RT (min)	Formula	Mass error (ppm)	MS/MS product ions
HDCA	391.2829	19.70	C ₂₄ H ₄₀ O ₄	-4.9	373.2815 [C ₂₄ H ₃₇ O ₃] ⁻
HDCA	391.2834	20.97	C ₂₄ H ₄₀ O ₄	-3.6	373.2724 [C ₂₄ H ₃₇ O ₃] ⁻
dehydro-HDCA	389.2680	20.15	C ₂₄ H ₃₈ O ₄	-3.1	345.2794 [C ₂₃ H ₃₇ O ₂] ⁻
dehydro-HDCA	389.2683	20.77	C ₂₄ H ₃₈ O ₄	-2.3	343.2647 [C ₂₃ H ₃₅ O ₂] ⁻
T-HDCA	498.2879	19.99	C ₂₆ H ₄₅ NO ₆ S	-2.0	391.2824 [C ₂₄ H ₃₉ O ₄] ⁻ ; 389.2637 [C ₂₄ H ₃₇ O ₄] ⁻
T-HDCA	498.2889	22.64	C ₂₆ H ₄₅ NO ₆ S	0.0	391.2830 [C ₂₄ H ₃₉ O ₄] ⁻
oxo-T-HDCA	514.2850	18.89	C ₂₆ H ₄₅ NO ₇ S	2.3	391.2879 [C ₂₄ H ₃₉ O ₄] ⁻
dehydro-T-HDCA	496.2725	21.27	C ₂₆ H ₄₃ NO ₆ S	-1.6	391.2830 [C ₂₄ H ₃₉ O ₄] ⁻ ; 389.2611 [C ₂₄ H ₃₇ O ₄] ⁻
G-HDCA	448.3065	17.47	C ₂₆ H ₄₃ NO ₅	0.4	404.3150 [C ₂₅ H ₄₂ NO ₃] ⁻ ; 386.3035 [C ₂₅ H ₄₀ NO ₂] ⁻
G-HDCA	448.3064	17.83	C ₂₆ H ₄₃ NO ₅	0.2	404.3156 [C ₂₅ H ₄₂ NO ₃] ⁻ ; 386.3050 [C ₂₅ H ₄₀ NO ₂] ⁻
G-HDCA	448.3045	19.16	C ₂₆ H ₄₃ NO ₅	-4.0	404.3145 [C ₂₅ H ₄₂ NO ₃] ⁻ ; 386.3042 [C ₂₅ H ₄₀ NO ₂] ⁻
dehydro-G-HDCA	446.2891	18.49	C ₂₆ H ₄₁ NO ₅	-3.4	402.2991 [C ₂₅ H ₄₀ NO ₃] ⁻ ; 384.2888 [C ₂₅ H ₄₀ NO ₂] ⁻
oxo-G-HDCA	464.3012	17.00	C ₂₆ H ₄₃ NO ₆	0.0	420.3120 [C ₂₅ H ₄₂ NO ₄] ⁻ ; 389.2697 [C ₂₄ H ₃₇ O ₄] ⁻

TABLE 3.2: RELATIVE ABUNDANCE OF BILE COMPOUNDS DURING IN VITRO GASTROINTESTINAL BIOTRANSFORMATION OVER TIME.

Name	RT (min)	Formula	SI	C2	C6	C10	C18	C24	C32	C40	C48	C72
HDCA	19.70	C ₂₄ H ₄₀ O ₄	48.8 ± 2.8	73.6 ± 8.2	96.1 ± 7.5	99.8 ± 7.4	100.0 ± 11.2	88.4 ± 3.1	81.9 ± 14.9	83.6 ± 30.8	78.7 ± 20.8	74.1 ± 22.8
HDCA	20.97	C ₂₄ H ₄₀ O ₄	42.7 ± 9.8	76.4 ± 15.1	97.7 ± 17.8	80.8 ± 20.5	92.6 ± 12.1	81.6 ± 0.9	61.3 ± 17.7	73.6 ± 20.7	59.8 ± 8.5	65.4 ± 14.8
dehydro-HDCA	20.15	C ₂₄ H ₃₈ O ₄	50.9 ± 2.6	51.9 ± 2.5	58.3 ± 8.6	76.0 ± 3.5	87.0 ± 8.5	82.2 ± 1.3	83.7 ± 11.0	100.0 ± 20.7	96.5 ± 13.3	68.2 ± 19.6
dehydro-HDCA	20.77	C ₂₄ H ₃₈ O ₄	65.2 ± 11.1	60.4 ± 3.1	73.6 ± 5.5	84.3 ± 7.8	100.0 ± 15.6	90.6 ± 6.5	78.2 ± 13.7	82.5 ± 31.1	66.0 ± 21.2	62.9 ± 20.8
T-HDCA	19.99	C ₂₆ H ₄₅ NO ₆ S	100.0 ± 10.5	65.3 ± 4.6	26.0 ± 1.7	1.6 ± 1.3	0.0 ± 0.0	0.0 ± 0.0	0.0 ± 0.0	0.0 ± 0.0	0.0 ± 0.0	0.0 ± 0.0
T-HDCA	22.64	C ₂₆ H ₄₅ NO ₆ S	100.0 ± 10.1	53.3 ± 3.5	8.9 ± 0.6	1.9 ± 1.6	0.0 ± 0.0	0.0 ± 0.0	0.0 ± 0.0	0.0 ± 0.0	0.0 ± 0.0	0.0 ± 0.0
oxo-T-HDCA	18.89	C ₂₆ H ₄₅ NO ₇ S	100.0 ± 11.6	72.8 ± 4.7	44.8 ± 3.3	21.2 ± 1.3	1.9 ± 0.5	0.0 ± 0.0	0.0 ± 0.0	0.0 ± 0.0	0.0 ± 0.0	0.0 ± 0.0
dehydro-T-HDCA	21.27	C ₂₆ H ₄₃ NO ₆ S	100.0 ± 13.1	60.1 ± 3.4	24.2 ± 1.5	5.8 ± 0.6	0.0 ± 0.0	0.0 ± 0.0	0.0 ± 0.0	0.0 ± 0.0	0.0 ± 0.0	0.0 ± 0.0
G-HDCA	17.47	C ₂₆ H ₄₃ NO ₅	100.0 ± 11.0	81.4 ± 5.6	59.1 ± 3.3	27.0 ± 1.0	1.7 ± 0.5	0.0 ± 0.0	0.0 ± 0.0	0.0 ± 0.0	0.0 ± 0.0	0.0 ± 0.0
G-HDCA	17.83	C ₂₆ H ₄₃ NO ₅	100.0 ± 6.9	65.7 ± 3.4	8.4 ± 0.5	0.1 ± 0.0	0.0 ± 0.0	0.0 ± 0.0	0.0 ± 0.0	0.0 ± 0.0	0.0 ± 0.0	0.0 ± 0.0
G-HDCA	19.16	C ₂₆ H ₄₃ NO ₅	100.0 ± 6.8	35.8 ± 4.9	0.9 ± 0.1	0.1 ± 0.0	0.0 ± 0.0	0.0 ± 0.0	0.0 ± 0.0	0.0 ± 0.0	0.0 ± 0.0	0.0 ± 0.0
dehydro-G-HDCA	18.49	C ₂₆ H ₄₁ NO ₅	100.0 ± 14.1	90.5 ± 4.6	68.7 ± 3.4	37.4 ± 4.0	5.0 ± 1.2	0.6 ± 0.2	0.0 ± 0.0	0.0 ± 0.0	0.0 ± 0.0	0.0 ± 0.0
oxo-G-HDCA	17.00	C ₂₆ H ₄₃ NO ₆	100.0 ± 9.6	71.5 ± 2.9	41.2 ± 2.3	10.3 ± 0.8	0.3 ± 0.0	0.0 ± 0.0	0.0 ± 0.0	0.0 ± 0.0	0.0 ± 0.0	0.0 ± 0.0

SI: small intestinal phase ; C2 - C72: Colon phase after 2 h - Colon phase after 72 h

 100% relative abundance
 0% relative abundance

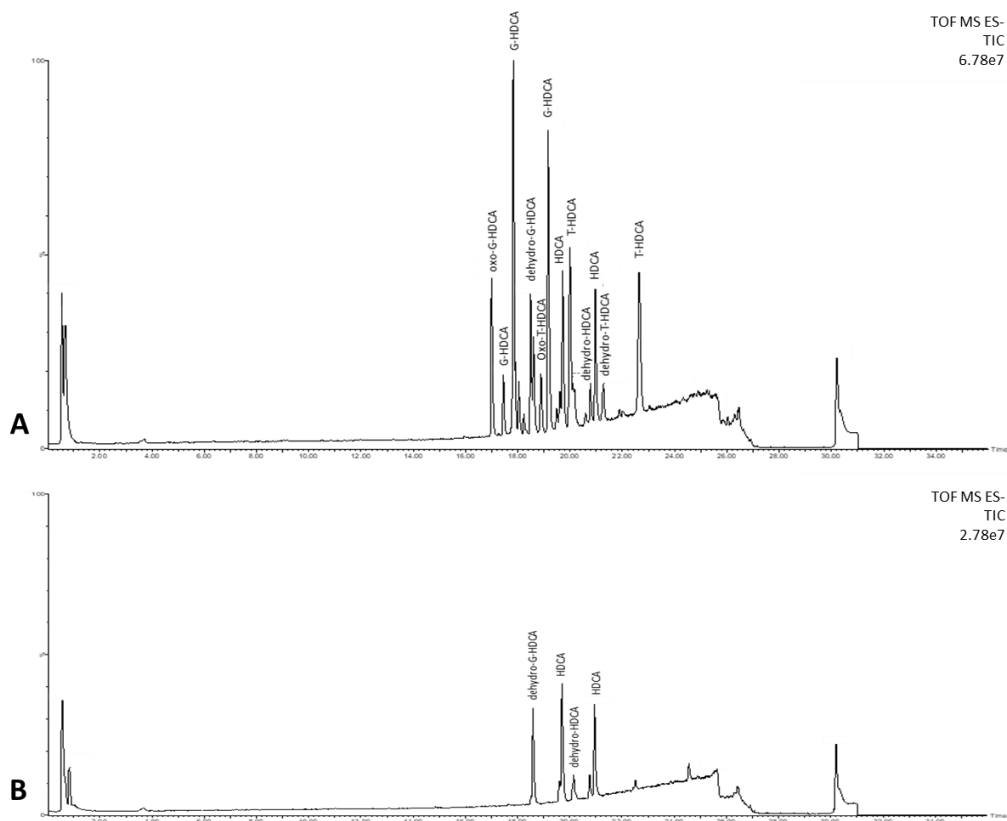


FIGURE 3.12: BILE ACID COMPOSITION BEFORE (A, SMALL INTESTINAL PHASE) AND AFTER (B, COLONIC PHASE) *IN VITRO* GASTROINTESTINAL BIOTRANSFORMATION IN A BLANK SAMPLE. OVER TIME, ALL TAURINE AND GLYCINE CONJUGATES AND THEIR DERIVATIVES WERE HYDROLYZED TO HDCA AND DEHYDRO-HDCA OR ISOMERS THEREOF.

3.11.2 BIOTRANSFORMATION OF GLYCOSYLATED COMPOUNDS

3.11.2.1 DEGLYCOSYLATION OF FLAVONOIDS: RUTIN AS CASE STUDY

The gut microbiota play a key role in the conversion of dietary flavonoids. In nature, the majority of flavonoids are present as *O*- or *C*-glycosides. These glycosides usually undergo deglycosylation by gastrointestinal biotransformation prior to their absorption and/or further conversion. In general, it appears that *C*-glycosides are more resistant towards acid, alkaline and enzymatic treatment than *O*-glycosides. The *O*-coupled flavonoid glucosides can be hydrolyzed by LPH and cytosolic β -glucosidase, while cleavage of *C*-glucosides appears to be restricted to gut bacteria. Moreover, the

majority of the identified C-glucoside-cleaving bacteria also act on the corresponding O-coupled glucosides. In addition, gut microflora are required to cleave off sugar moieties other than glucose, e.g. rhamnose and glucuronic acid.^[127,128] Quercetin glycosides, such as rutin, are abundantly present in *Filipendula ulmaria*. Rutin is a flavonol O-glycoside composed of quercetin and rutinose, a disaccharide of rhamnose and glucose.^[107] The proposed biotransformation pathway of rutin in this experiment is summarized in Figure 3.16. Table 3.3 lists additional details about the types of reactions, mass spectrometry data and tinderesting scores. When looking at the biotransformation pattern of rutin (identified with standard, m/z 609.1458; rt 11.26 min) in the gastrointestinal experiment, which is scored by tinderesting at 0.972, a decrease in intensity can be observed over time. As seen in Figure 3.13A, this decrease is already detected in the stomach phase and continues in the small intestinal phase and colonic phase until the signal is completely absent between 10 and 14 h of fermentation. In the negative control samples, due to the absence of fecal bacteria, the signal remains stable during the simulation of the colon phase. Lastly, the signal is not present in the method blank. The same pattern can be noticed for isoquercitrin (identified with standard, m/z 463.0872; rt 11.54 min; Figure 3.13B), which is rated by tinderesting with a score of 0.994. For quercetin (identified with standard, m/z 301.0345; rt 16.54 min; Figure 3.13C), although already present at t_0 , a clear increase in the samples can be noted over time. When looking at the negative controls and method blanks, no increase in intensity can be observed. This profile is also rated by tinderesting as interesting with a score of 1.000. These results suggest the deglycosylation of rutin and/or isoquercitrin, leading to the formation of quercetin (see Figure 3.13). In the colon, the gut microbiota hydrolyze rutin, removing the sugar moiety and permitting absorption of the aglycone and/or extensive breakdown into low-molecular-weight phenolic metabolites.^[41,129]

TABLE 3.3: LIST OF POTENTIAL BIOTRANSFORMATION PRODUCTS OF RUTIN BASED ON IN SILICO PREDICTIONS GENERATED BY BIOTRANSFORMER COMBINED WITH OBSERVED METABOLITES ENCOUNTERED BY FOLLOWING THE DATA ANALYSIS WORKFLOW USING TINDERESTING.

Compound	Molecular formula	Theoretical [m/z] [M-H] ⁻	Experimental [m/z] [M-H] ⁻	Δ ppm	rt (min)	Reaction	Precursor	Tinderesting score	Tinderesting ranking
Rutin	C ₂₇ H ₃₀ O ₁₆	609.1456	609.1458	0.3	11.26	/	/	0.972	1059
Isoquercitrin	C ₂₁ H ₂₀ O ₁₂	463.0877	463.0872	-1.1	11.54	Glycoside hydrolysis or Rhamnohydrolysis of alpha-L-rhamnoside	Rutin	0.994	511
Quercetin	C ₁₅ H ₁₀ O ₇	301.0348	301.0345	-1.0	16.54	Glycoside hydrolysis, 3'-O-Demethylation	Rutin and/or Isoquercitrin, isorhamnetin	1.000	20
Kaempferol	C ₁₅ H ₁₀ O ₆	285.0399	285.0396	-1.1	18.48	3'-Dehydroxylation of substituted benzene	Quercetin	1.000	13
Isorhamnetin	C ₁₆ H ₁₂ O ₇	315.0505	315.0497	-2.5	18.27	Catechol O-methylation	Quercetin	1.000	26
Chrysoeriol	C ₁₆ H ₁₂ O ₆	299.0556	299.0546	-3.3	17.91	3-Dehydroxylation, catechol O-methylation	Isorhamnetin, Luteolin	1.000	17
Luteolin	C ₁₅ H ₁₀ O ₆	285.0399	285.0393	-2.1	16.43	3-Dehydroxylation, 3'-O-Demethylation	Quercetin, Chrysoeriol	1.000	12
Apigenin	C ₁₅ H ₁₀ O ₅	269.0450	269.0444	-2.2	18.10	3'-Dehydroxylation of substituted benzene, 3-Dehydroxylation	Luteolin, Kaempferol	1.000	2
3'-methoxy-5,7-dihydroxyflavone	C ₁₆ H ₁₂ O ₅	283.0606	283.0600	-2.1	20.14	4'-Dehydroxylation of substituted benzene	Chrysoeriol	1.000	10
Naringenin	C ₁₅ H ₁₂ O ₅	271.0606	271.0600	-2.2	16.82	3'-Dehydroxylation of substituted benzene, reduction	(+/-)-Eriodictyol, Apigenin	1.000	4
Phloretin	C ₁₅ H ₁₄ O ₅	273.0763	273.0758	-1.8	17.01	Isomerization of the C-ring followed by reduction	Naringenin (naringenin chalcone)	0.998	142

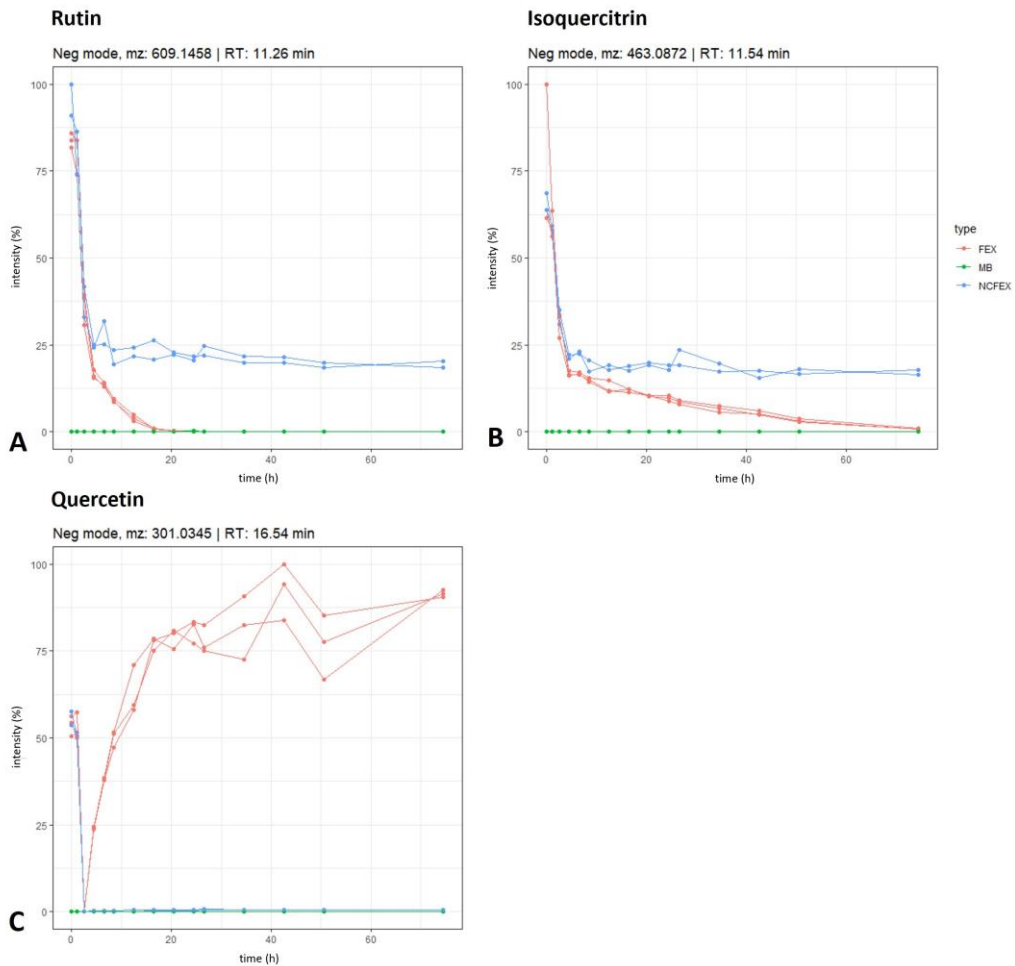


FIGURE 3.13: TIME PROFILES (TIME IN HOURS) OF RUTIN (A), ISOQUERCITRIN (B) AND QUERCETIN (C) DURING GASTROINTESTINAL BIOTRANSFORMATION.

Bacteria with the ability to biotransform rutin possess α -L-rhamnosidases which convert rutin into quercetin-3-glucoside (isoquercitrin). Bacteria can also express β -D-glucosidases that either convert quercetin-3-glucosides to quercetin or convert rutin directly to quercetin.^[115,128] *Lactobacillus acidophilus*, *Lactobacillus plantarum* and *Bifidobacterium dentium* have been shown to have these α -rhamnosidases involved in deglycosylation of flavonoids.^[130,131] *Bacteroides uniformis*, *Bacteroides ovatus* and *Enterococcus avium*, on the other hand, have the capability of degrading rutin to quercetin.^[132,133] *Parabacteroides distasonis* was shown to produce both

quercetin-3-glucosides and quercetin via α -rhamnosidase and β -glucosidase activity.^[132] *Eubacterium ramulus* and *Enterococcus casseliflavus* are able to biotransform quercetin-3-glucosides into quercetin.^[134,135] Moreover, in a study from Riva et al. who performed anaerobic incubations of human fecal microbiota amended with rutin, results showed different patterns of rutin product formation between participants. They divided them in groups of high quercetin-3-glucoside producers, high quercetin producers and low producers. Enrichment of *Enterobacteriaceae* (*Escherichia/Shigella*) was seen in high quercetin-3-glucoside producers. High quercetin producers had an enrichment of *Lachnospiraceae* (*Lachnoclostridium* and *Eisenbergiella*). Low producers, on the other hand, had a trend toward enrichment in *Tannerellaceae* (*Parabacteroides*) and *Erysipelotricaceae* (*Erysipelatoclostridium*). Their results suggest inter-individual variability in preference or capability for rutin metabolism.^[129] According to our 16S sequencing analysis, the fecal slurry did indeed contain *Lachnoclostridium* and the *Filipendula ulmaria* extract even appeared to cause enrichment in the total number of *Lachnospiraceae* (see also paragraph 3.11.4 results and discussion section and Figure 3.24).

3.11.2.2 DEGLYCOSYLATION OF FLAVONOIDS PRESENT IN *FILIPENDULA ULMARIA*

A rich diversity of glycosylated flavonoids can be found in *Filipendula ulmaria*. Rutin and isoquercitrin are thus not the only precursors of the quercetin aglycon: spiraeoside, quercitrin, avicularin and miquelianin can all act as possible precursors for quercetin. Multiple of these glycosylated compounds follow similar gastrointestinal biotransformation time profiles as seen in paragraph 3.11.2.1, where a decrease in intensity in the FEX samples can be observed over time, while the negative control remains relatively stable (data not shown). Interestingly, when comparing isoquercitrin (quercetin 3-O- β -D-glucoside) to spiraeoside (quercetin 4'-O- β -D-glucoside), a difference is seen in biotransformation speed. In Figure 3.14, a steady decrease in intensity can be observed for isoquercitrin, while a steep decline is observed for

spiraeoside (identified with standard, m/z 463.0868; rt 13.10 min; tinteresting score of 0.884) at 2 h of colonic phase. This might be explained by the activity of the β -glucosidase enzyme towards different substrates. Glycosylation at the C-4' and C-7 position on the flavonoid skeleton are apparently well tolerated whereas, substitution at the C-3 position leads to loss of catalytic activity. This decrease in affinity of the C-3 position by local steric hindrance was also rationalized by modelling studies.^[136] Spiraeoside might thus be a more favorable substrate compared to isoquercitrin, resulting in a faster biotransformation by the gut microbiota.^[137] However, another explanation might also be the fact that rutin is consequently converted to isoquercitrin. Hence, suggesting an equilibrium between formation and degradation of isoquercitrin at the first hours of colon phase, resulting in a slower observed decline in intensity.

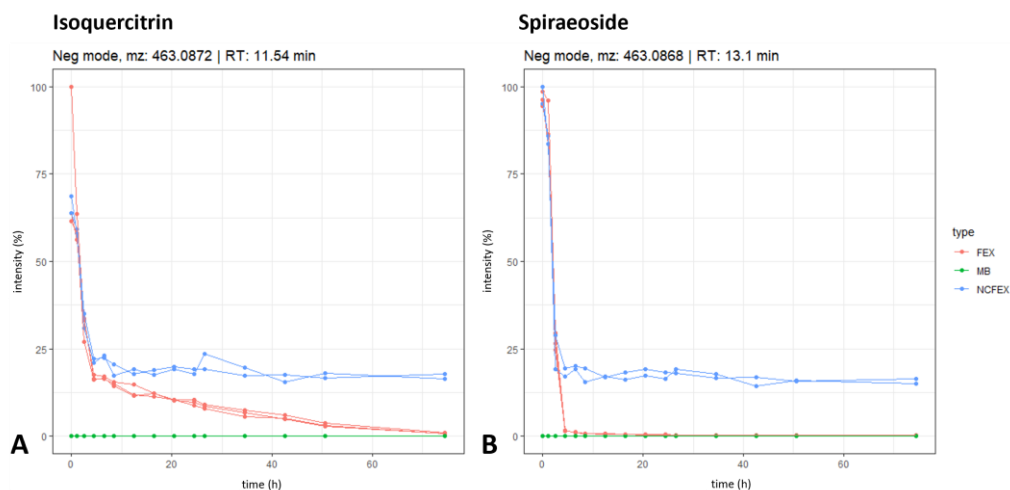


FIGURE 3.14: TIME PROFILES (TIME IN HOURS) OF ISOQUERCITRIN (A) AND SPIRAEOSIDE (B) DURING GASTROINTESTINAL BIOTRANSFORMATION.

Paragraph 3.11.2.3 will further discuss the gastrointestinal conversion of quercetin to other aglycons, such as kaempferol, luteolin and isorhamnetin. However, it is also possible that these compounds are preceded by their corresponding precursor. As an example, the time profile for astragalin (a kaempferol-*O*-glucoside) and isorhamnetin-*O*-hexoside is shown in Figure 3.15A and B, respectively. Astragalin was

tentatively identified (m/z 447.0921; rt 12.77 min; tinderesting score of 0.952) and can act as a precursor for the aglycon kaempferol. Furthermore, isorhamnetin can be released from isorhamnetin-O-hexoside (tentatively identified, m/z 477.1024; rt 12.86 min; tinderesting score of 0.966). Both glycosylated compounds follow a similar biotransformation time profile as rutin, isoquercitrin or spiraeoside: the negative control stays stable, the intensity in the FEX samples decreases and the compounds are absent in the method blanks.

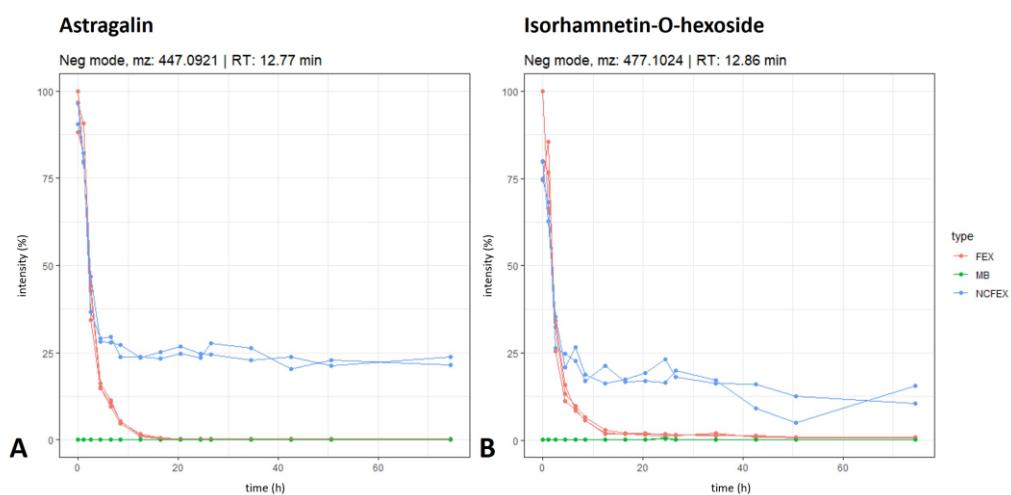


FIGURE 3.15: TIME PROFILES (TIME IN HOURS) OF ASTRAGALIN (A) AND ISORHAMNETIN-O-HEXOSIDE (B) DURING GASTROINTESTINAL BIOTRANSFORMATION.

3.11.2.3 CONVERSIONS OF FLAVONOID AGLYCONS

The released quercetin aglycon can be further metabolized by the intestinal microbiota. In literature, it is described that only a small part of released quercetin aglycon is absorbed by colonocytes in its intact form. A large percentage of the released quercetin is absorbed after a series of biotransformation reactions into phenolic catabolites by the action of colonic microbiota.^[138,139] As discussed in the introduction of this chapter, biochemical transformations by the gut microbiota include three major catabolic processes: hydrolysis (deglycosylations and ester hydrolysis), cleavage (C-ring cleavage, delactonization, demethylation) and reductions (dehydroxylation and double bond

reduction).^[42] Quercetin can thus be dehydroxylated to kaempferol or luteolin, or can be biotransformed to its metabolite isorhamnetin via catechol *O*-methylation, which is shown in Figure 3.16. An increase in kaempferol (identified with standard, m/z 285.0396; *rt* 18.48 min), luteolin (identified with standard, m/z 285.0393; *rt* 16.43 min) and isorhamnetin (identified with standard, m/z 315.497; *rt* 18.27 min) is seen during colonic biotransformation, which differs from the negative control and method blank, and these aglycones are once more clearly marked as interesting features by tinderesting with a score of 1.000 (see Figure 3.17A,B,C and Table 3.3). When looking at Figure 3.16, it is possible for kaempferol and/or luteolin to be further dehydroxylated to apigenin (m/z 269.0444; *rt* 18.10 min; tinderesting score of 1.000), which is indicated by the increasing intensity of apigenin in the fermented extract (Figure 3.17D). Furthermore, it is possible for apigenin to undergo reduction at the double bond between C-2 and C-3 resulting in the conversion to naringenin. On the other hand, reduction of luteolin at this double bond might lead to the formation of eriodictyol as an intermediate metabolite, eventually leading to the formation of naringenin via dehydroxylation. Although the metabolite eriodictyol could not be detected in this *in vitro* experiment, an increasing intensity for the time profile of naringenin (identified with standard, m/z 271.0600; *rt* 16.82 min; tinderesting score of 1.000) could be detected compared to the negative control and method blank (Figure 3.17E). Naringenin, in turn, is known as a precursor of phloretin (identified with standard, m/z 273.0758; *rt* 17.01 min). In this part of the pathway, the conversion of naringenin into naringenin chalcone is mediated by bacterial chalcone isomerase and the conversion of naringenin chalcone to phloretin by enoate reductase.^[48] The increase of intensity of phloretin in the samples, while no change is observed in negative control and method blank, can be seen in Figure 3.17F. The aglycon is again marked as interesting by tinderesting with a score of 0.998. When looking at isorhamnetin, it is possible that the *O*-methylated flavonol acts as a precursor for chrysoeriol (tentatively identified, m/z 299.0546; *rt* 17.91 min). Moreover, luteolin can

also be methylated at the 3'-position in order to convert to chrysoeriol. Chrysoeriol in turn can be further dehydroxylated to a tentatively identified metabolite 3'-methoxy-5,7-dihydroxyflavone (m/z 283.0600; rt 20.14 min). These biotransformation profiles are shown in Figure 3.17, where an increase of chrysoeriol (Figure 3.17G) and 3'-methoxy-5,7-dihydroxyflavone (Figure 3.17H) can be observed in the FEX samples over time. Lastly, both metabolites were marked as interesting with an interesting score of 1.000.

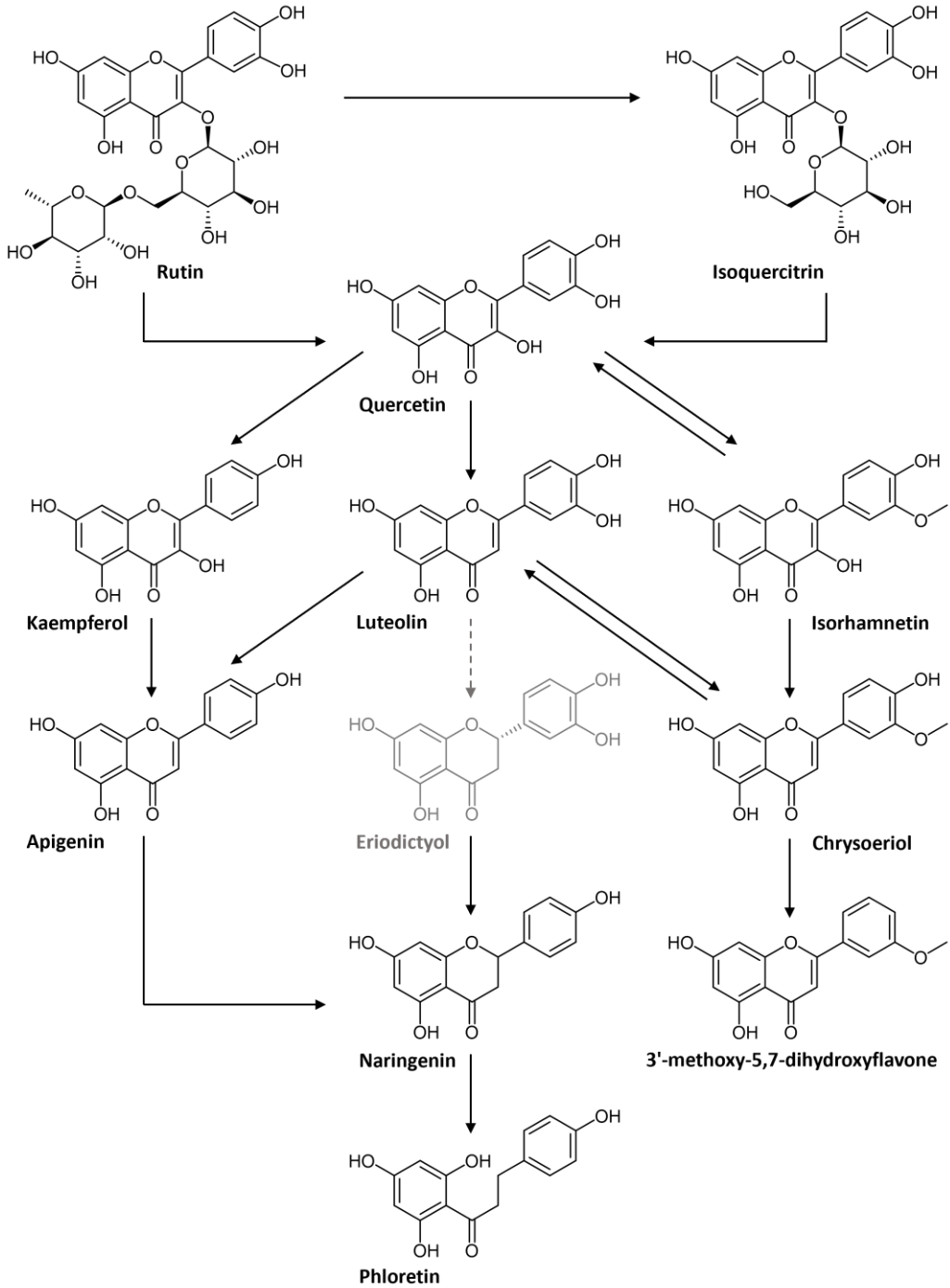


FIGURE 3.16: METABOLIC PATHWAY OF RUTIN BY IN VITRO GASTROINTESTINAL BIOTRANSFORMATION . DETECTED METABOLITES ARE IN BLACK, NON-DETECTED METABOLITES ARE IN GREY.

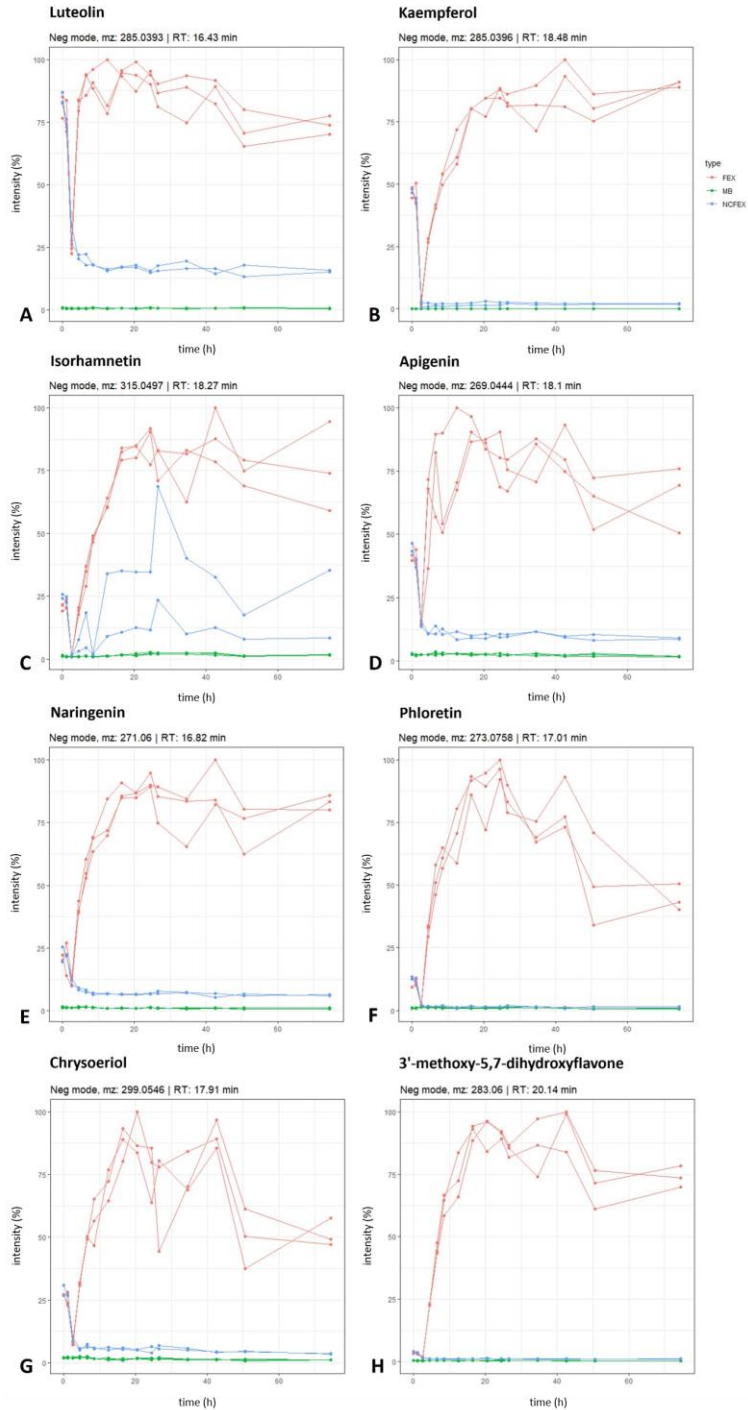


FIGURE 3.17: TIME PROFILE (TIME IN HOURS) OF LUTEOLIN (A), KAEMPFEROL (B), ISORHAMNETIN (C), APIGENIN (D), NARINGENIN (E), PHLORETIN (F), CHRYSOERIOL (G) AND 3'-METHOXY-5,7-DIHYDROXYFLAVONE (H) DURING GASTROINTESTINAL BIOTRANSFORMATION.

3.11.2.4 DEGRADATION TO LOW-MOLECULAR-WEIGHT AROMATIC COMPOUNDS

Despite the initially high degree of structural difference in polyphenolic structures, overlapping metabolic pathways result in the formation of only a relatively small number of intermediate metabolites in the colon. These intermediates subsequently enter a general degradation pathway, leading to the formation of typical, non-specific end products, such as phenylpropionic acid, phenylacetic acid and benzoic acid derivatives. Although bacteria can gain some energy from this degradation, the main rationale would be detoxification, since many flavonoids exert antibacterial activity.^[48] In general, the formed aglycons in the gastrointestinal experiment (which do seem to remain quite stable across the colonic phase, Figure 3.17) resulted only in a small number of low-molecular-weight metabolites, in contrast to reports in literature.^[48,139] With naringenin as example, as described above in paragraph 3.11.2.3 and shown in Figure 3.18, the degradation starts with isomerization of the C-ring at the hetero atom to the corresponding chalcone phloretin. After reduction to the dihydrochalcone, further splicing takes place at the carbonyl moiety, yielding phloroglucinol and phloretic acid (3-(4-hydroxyphenyl)propionic acid).^[48] Phloroglucinol, however is hardly ever recovered as final metabolite, as it can be degraded to acetate, butyrate and CO₂.^[140] Phloroglucinol was indeed not found in this gastrointestinal biotransformation experiment. Phloretic acid (*m/z* 165.0547; *rt* 6.46 min), however, was tentatively identified as a metabolite in the *Filipendula ulmaria* extract samples. When looking at the tinderesting score, the time profile of phloretic acid is scored at 0.762. This lower score can be explained by looking at the graph in Figure 3.19: an increase in intensity is observed in the FEX samples starting at 6 h of colon phase, while the abiotic negative control stays stable, but a rise in intensity is also clearly seen in the method blank at 4 h of fermentation. The profile is thus rated as less interesting, which confirms the setup of the data analysis workflow. Research from Di Pede et al., might give a possible explanation for this phenomenon. The *in vitro* experiment looked at the human microbial metabolism of quercetin, using a 10% (w/w) fecal slurry of 3 pooled donors

on a 48 h polyphenol free diet and comparing the fermentation of quercetin against method blanks. Not only their samples, but also the blank samples with growth medium and fecal slurry, contained phenylacetic acid and phloretic acid at quantifiable levels during fermentation.^[141] Firstly, a short polyphenol free diet does not fully guarantee blank feces.^[142] Secondly, these phenolic acids may also arise from the microbial fermentation of aromatic amino acids such as tryptophan, phenylalanine and tyrosine upon consumption of dietary proteins.^[143,144]

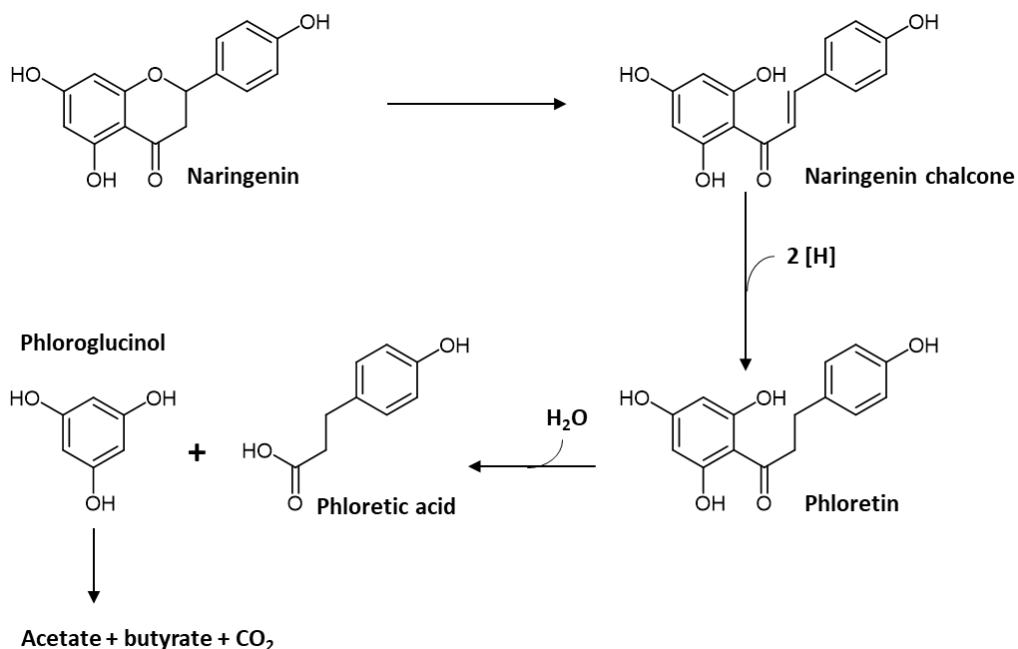


FIGURE 3.18: DEGRADATION OF NARINGENIN BY INTESTINAL BACTERIA. NARINGENIN DEGRADATION YIELDS PHLORETIC ACID AND PHLOROGLUCINOL.

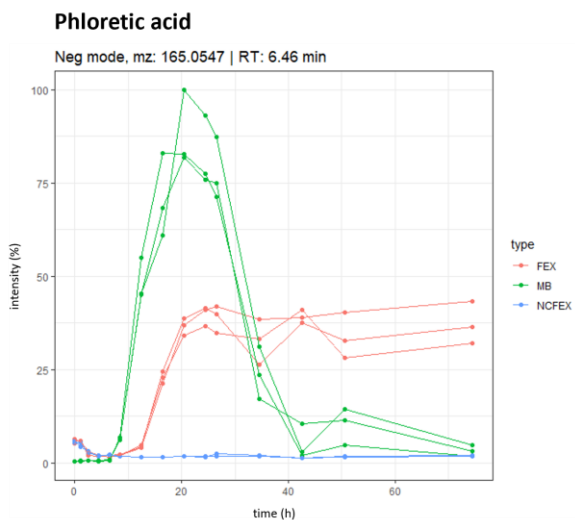


FIGURE 3.19: TIME PROFILE (TIME IN HOURS) OF PHLORETIC ACID DURING GASTROINTESTINAL BIOTRANSFORMATION.

3.11.2.5 BIOTRANSFORMATION OF COMPOUNDS: PURE CONSTITUENTS VERSUS EXTRACTS

In paragraph 3.11.2.5.1 and 3.11.2.5.2, the biotransformation of salicin and chlorogenic acid will be discussed, respectively. Mainly the difference between biotransformation patterns of these compounds as pure salicin or chlorogenic acid (positive control) and in the extract was explored in depth. Generally, a slower and/or incomplete biotransformation of the compounds in the extract was seen, while they were fully metabolized during biotransformation in the positive control where they were present as pure compounds. Slower and incomplete biotransformation of a compound in an extract compared to the same constituent as a pure compound, has been described and published in our research group before. For example, when comparing pure chlorogenic acid and chlorogenic acid in *Cecropia obtusifolia* leaf extract or strictosamide as a pure compound and strictosamide in *Nauclea pobeguinii*.^[116,145,146] This slower biotransformation rate can be caused by other compounds present in the extract, forming salicin or chlorogenic acid during biotransformation. Another possible explanation for these results may be that the presence of diverse chemicals in the crude extract, could negatively interfere with the biotransformation rate of chlorogenic acid

and salicin.^[116] A different hypothesis is that biotransformation reactions are hampered by a possible antibacterial effect of the extract, resulting in an insufficient amount of viable bacteria or an altered bacterial composition, inhibiting or changing biotransformation.^[147,148]

3.11.2.5.1 BIOTRANSFORMATION OF GLYCOSYLATED PRECURSORS OF SALICYLIC ACID

Glycosylated salicyl derivatives, such as the diglycoside monotropitin and the monoglycoside salicin, were detected in the *Filipendula ulmaria* extract (see also chapter 2). These compounds are often described as the active constituents of the extract, responsible for their anti-inflammatory effect.^[107] In literature, it is described that after oral ingestion, salicin is hydrolyzed to its aglycon saligenin by the gut microbiota and saligenin is then further oxidized in the liver to salicylic acid.^[149] Early *in vitro* studies from Fötsch and Pfeifer, using intestinal sections of normal and antibiotic-treated rats, found that the intestinal bacteria were able to biotransform salicin to saligenin.^[150] However, when comparing these results to *in vivo* pharmacokinetic studies in humans, the metabolite salicylic acid could already be detected in serum 1 h after oral administration of salicin or willow bark extract, which is rich in salicylates. This suggests that salicin might already be absorbed in the stomach or upper intestinal tract and hydrolyzed before or during absorption, thus even before reaching the colon.^[151] *In vivo* research in rats by Knuth et al., showed similar results when salicortin was orally administered.^[152] In the study of Pferschy-Wenzig et al., where willow bark extract was incubated with human fecal suspension under anoxic conditions (without being preceded by a gastric and small intestinal phase), the formation of saligenin and salicylic acid was observed. Nevertheless, their publication also mentioned that this observed hydrolysis by intestinal bacteria might not be relevant under physiological conditions.^[153] Moreover, bioavailability studies of pure salicin in humans resulted in salicylic acid metabolites, indicated a good oral bioavailability of the pure compound.^[154] In contrast, oral administration of willow bark

extract, which is rich in salicylates, showed lower bioavailability of salicin.^[151,155] Figure 3.20 shows the time profile for the glycosylated compound, monotropitin (tentatively identified, m/z 445.1338; rt 6.85 min), and the aglycon salicylic acid (identified with standard, m/z 137.0237; rt 10.09 min) in our study. The expected (intermediate) metabolite saligenin could not be detected. This, however, might be attributed to the applied ESI-MS conditions, which might not allow the satisfactory detection of some analytes present in the samples. Small aromatic compounds like saligenin, might ionize only weakly: saligenin could also not be detected in the standard mix, thereby hampering the detection of this microbial metabolites. Application of a second analytical technique, such as GC-MS, might be a solution for future studies. The biotransformation profile of both monotropitin and salicylic acid, shows a drop in intensity, observed during the stomach and small intestinal phase. In the colon phase however, no further breakdown of monotropitin or increase in intensity for salicylic acid could be observed. Additionally, no difference can be noted between the samples and the negative controls in the colon phase.

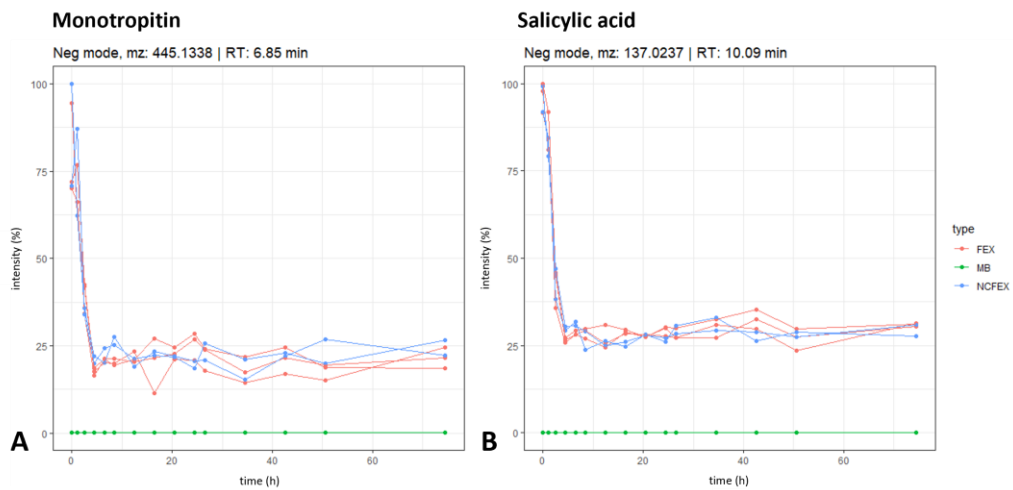


FIGURE 3.20: TIME PROFILES (TIME IN HOURS) OF MONOTROPITIN (A) AND SALICYLIC ACID (B) DURING GASTROINTESTINAL BIOTRANSFORMATION.

A similar pattern was noticed for salicin (identified with standard, m/z 285.0968; rt 4.07 min). Interestingly, when comparing the degradation of salicin in the positive control (Figure 3.21A) to salicin in the extract (Figure 3.21B), a clear difference in degradation speed can be noted. Pure salicin is detected up to 32 h of colon phase, while salicin in the extract decreases more steadily and remains quite stable from 22 to 72 h of colon phase.

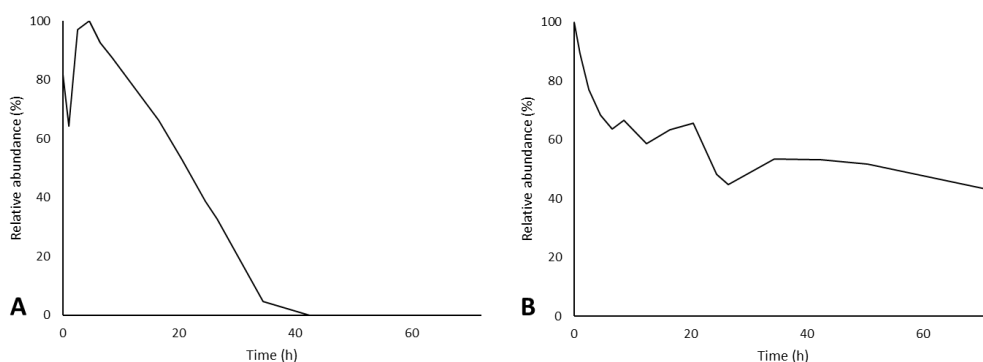


FIGURE 3.21: TIME PROFILES OF SALICIN DURING GASTROINTESTINAL BIOTRANSFORMATION IN THE POSITIVE CONTROL (A) AND IN THE *FILIPENDULA ULMARIA* EXTRACT (B).

3.11.2.5.2 BIOTRANSFORMATION OF CHLOROGENIC ACID

Interestingly, similar to the pattern of salicin described in 3.11.2.5.1, when comparing the degradation of chlorogenic acid in the positive control (Figure 3.22A) to chlorogenic acid in the extract (Figure 3.22B), a clear difference in degradation speed could once more be noted. Pure chlorogenic acid was detected up to 22 h of colon phase, while chlorogenic acid in the extract decreased much slower up until 40 h of colon phase. This phenomenon was also observed in another publication from our research group with similar methodological set-up: Rivera-Mondragón et al. showed that chlorogenic acid present in test samples was completely transformed during the colonic phase, but that the metabolism rate of chlorogenic acid in *Cecropia obtusifolia* leaf extract happened a lot slower compared to the single-compound incubation experiment in the positive control.^[116]

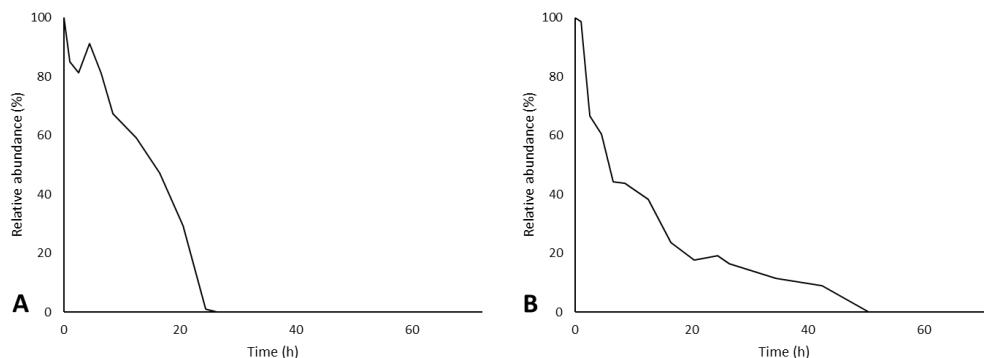


FIGURE 3.22: TIME PROFILES OF CHLOROGENIC ACID DURING GASTROINTESTINAL BIOTRANSFORMATION IN THE POSITIVE CONTROL (A) AND IN THE *FILIPENDULA ULMARIA* EXTRACT (B).

3.11.3 BIOTRANSFORMATION OF ELLAGITANNINS

In vivo and *ex vivo* studies have shown that food products rich in ellagitannins such as pomegranates, walnuts, raspberries, oak-aged red wine, tea and also medicinal plants like *Filipendula ulmaria*, *Geranium pratense*, *Lythrum salicaria* and *Rubus fruticosus* are able to be metabolized by gut microbiota to dibenzopyran-6-one derivatives with different hydroxyl substitutions, i.e. urolithins. In contrast to the ellagitannins present in ingested foods and extracts, urolithins possess good bioavailability and can be found in plasma at low micromolar concentrations.^[54,156] Contrary to the results obtained by Piwowarski and Popowski, in which the researchers fermented an aqueous *Filipendula ulmaria* extract, the formation of urolithins was not seen in our biotransformation experiment.^[156,157] After the stomach and small intestinal phase, no further breakdown is seen for monomeric ellagitannins such as tellimagrandin I, tellimagrandin II, rugosin A, rugosin B, casuarinin, casuarictin and pedunculagin. A similar pattern was seen for dimeric ellagitannins rugosin D and E. Figure 3.23A shows the biotransformation time profile for tellimagrandin II (tentatively identified, m/z 937.0944; rt 11.03 min, tindex score of 0.990) as an example for ellagitannins. A decrease can be noted in the intensity of ellagic acid (tentatively identified, m/z 300.9980; rt 10.82 min, tindex score of 1.000), shown in Figure

3.23B, when comparing the extract samples to the negative controls. However, this is in conflict with the hypothesis, where an increase in intensity after the small intestinal phase is expected, since ellagic acid is known to be released in the stomach and jejunum from ellagitannins possessing the hexahydroxydiphenoyl group. A decrease in ellagic acid in the colon phase in the FEX samples was presumed, where the gut flora metabolism leads to decarboxylation of one of the lactone rings of ellagic acid and the sequential removal of hydroxyl groups from different positions by different catechol dehydroxylases.^[156] Nevertheless, it should be noted that free ellagic acid was already present in the initial extract (see chapter 2 Table 2.2 and Table 2.3). The noted decrease of ellagic acid in the samples, however, does not lead to the expected formation of any of the known urolithins (i.e. precursor luteic acid, urolithin M5, M6, M7, A, B, C and isourolithin A or B), even after 72 h of fermentation. The production of urolithins *in vivo* can be quite slow, and it is possible to detect urolithin metabolites in urine after the intake of ellagitannins for three or even more days, hence the 72 h of fermentation in our experiment.^[158] A large interindividual variability in the production of urolithins has been associated with gut microbiota composition, which could explain these results. Metabotype A is characterized by the production of urolithin A, whereas metabotype B produces urolithin A, isourolithin A and urolithin B. However, metabotype 0 does not produce any of these final urolithins.^[55,56] The prevalence of metabotype 0 is estimated to have an average distribution of around 10% in a healthy population, while metabotype A is most abundant (around 50% and critically affected by aging).^[159-161] The genus *Gordonibacter* from the Eggerthellaceae family accommodates bacterial species, namely *G. pamelaiae* and *G. urolithinifaciens* that can biotransform ellagic acid into urolithin M5, M6 and C.^[158] *Ellagibacter isourolithinifaciens*, another genus from the Eggerthellaceae family, can also convert ellagic acid into urolithin M5, M6, C and isourolithin A. Strains of the closest neighbors of *Gordonibacter*, i.e. *Paraeggerthella* and *Eggerthella*, and *Ellagibacter*, i.e. *Senegalimassilia* and *Adlercreutzia*, were tested for their ability to catabolize ellagic acid, but were unable to produce urolithins.^[162]

When looking at the 16S sequencing results from our study, which are also discussed in paragraph 3.11.4 of the results and discussion section and Figure 3.24, *Gordonibacter* was not present in the fecal slurry incubated with the *Filipendula ulmaria* extract, while *Senegalimassilia* and *Adlercreutzia* were indeed detected.

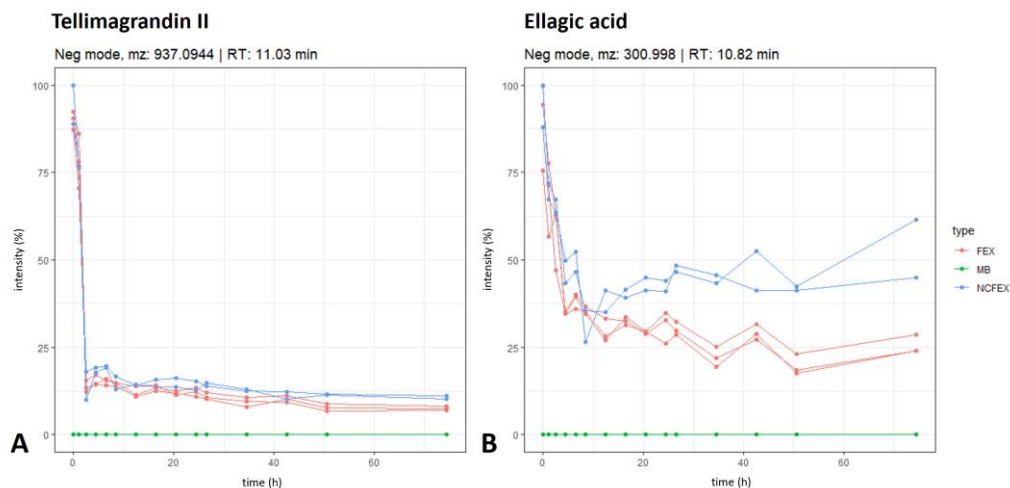


FIGURE 3.23: TIME PROFILES (TIME IN HOURS) OF TELLIMAGRANDIN II (A) AND ELLAGIC ACID (B) DURING GASTROINTESTINAL BIOTRANSFORMATION.

3.11.4 THE EFFECT OF PHYTOCHEMICALS ON MICROBIAL COMPOSITION

When looking at the number of viable bacteria for blank and sample, no significant differences were observed over time during *in vitro* gastrointestinal biotransformation, suggesting that the extract is not toxic to fecal bacteria in this concentration (data not shown). To elucidate the microbial composition of the fecal suspension, 16S rDNA-targeting PCR was performed. A possible effect of the *Filipendula ulmaria* extract on the bacterial composition of the fecal slurry during *in vitro* biotransformation in the GIM was assessed by comparing method blank and samples containing the extract over time using 16S rDNA-targeting PCR as described in paragraph 3.7.4 of the materials and methods section. In line with literature, the main intestinal microbiota belonged to the phylum Firmicutes, Bacteroidetes, Actinobacteria, Proteobacteria and Verrucomicrobia.^[11,12] Difference in relative ratios of the numbers of bacteria to the

total number was observed during the gastrointestinal biotransformation experiment, see also Figure 3.24, suggesting an antibacterial or prebiotic effect of *Filipendula ulmaria* on certain bacteria in the fecal slurry. The largest increase in relative ratio can be noted in the phylum Firmicutes, more specifically in the family *Lachnospiraceae*, when comparing the extract to the method blank. It is, however, not clear if modifications in intestinal bacteria were influenced by increases in microbial derived metabolites or by the parent compound alone. The reciprocal interrelation between gut microbiota and polyphenols is an interesting and complex topic in literature. The effects of polyphenols are often achieved by influencing the growth and metabolism of bacteria and by interfering with the cell function of the cell membrane. Most polyphenols also hinder biofilm formation or have the ability to act on bacterial quorum sensing (i.e. the regulation of gene expression in response to fluctuations in cell-population density). For example: studies have proven the antimicrobial activity of flavonols and flavones present in the extract, such as apigenin, naringin, luteolin, quercetin and kaempferol on bacteria like *Escherichia coli* or *Staphylococcus aureus*.^[163,164] Moreover, in a study performed by Duda-Chodak, the inhibition of intestinal bacteria growth by some polyphenols was observed: generally, aglycones were harmful to the bacteria while their glycosides did not have any effect. This implies that polyphenols can indirectly influence their uptake from the diet and this impact is dependent on the form of polyphenol.^[165] On the other hand, polyphenols exert their beneficial effects as prebiotic substrate by increasing the growth and settlement of bacterial families such as *Bifidobacteriaceae* and *Lactobacillaceae*. Polyphenols were also able to be used as a carbon source by these beneficial bacteria. Additionally, they can influence the Firmicutes to Bacteroidetes ratio through growth inhibition of specific bacterial species as well.^[166] Microbiome analyses revealed that incubation with willow bark extract, high in salicylic alcohol derivatives, flavonoids and catechin, had a marked effect on microbial community composition and functions. The extract's constituents were readily biotransformed by fecal bacteria and the proportion of *Bacteroides* in the

fecal sample was clearly enhanced when incubated with the willow bark extract. However, *Ruminococcaceae*, and in particular *Faecalibacterium prausnitzii*, was negatively affected by the willow bark extract. The researchers concluded that *F. prausnitzii* might either be out-competed by *Bacteroides*, is incapable of metabolizing the compounds in the extract, or is even inhibited by certain constituents found in willow bark.^[153] Studies on pomegranate extracts, composed mainly of phenolic acids, flavonoids, ellagitannins and proanthocyanidins, also observed alterations in gut microbiota after fermentation. An experiment with fecal batch-culture fermentations, showed that the pomegranate extracts had stimulatory effects on the beneficial bacteria groups of *bifidobacteria* and *lactobacilli*. Urolithin A, C and D were detected as metabolites.^[167] However, contradictory results were reported in another study where the proportion of *Bifidobacterium* decreased when pomegranate extract was tested against the human fecal bacteria using Twin-SHIME for 21 days and the population of *Lactobacillus* increased. They also reported elevated populations of *Akkermansia*, *Gordonibacter* and *Bacteroides* after treatment. Moreover, a positive correlation was found between *Gordonibacter* and urolithin A production.^[90] The altered bacterial composition in the *Filipendula ulmaria* extract can be a possible explanation for the different biotransformation pattern of salicin and chlorogenic acid in the extract versus pure compounds, which was discussed in paragraph 3.11.2.5 of the result and discussion section. The intestinal milieu is a continuously changing mixture of small and large molecules, along with an abundance of different bacteria, viral particles and eukaryotic cells. This complicates hypotheses regarding host-microbiome interactions immensely. Further studies on the impact of the *Filipendula ulmaria* extract on the gut microbiota could provide interesting insights into potential synergistic roles between its compounds and their metabolites in the regulation of the intestinal microbiota.

CONCLUSION

An innovative strategy was used to disclose metabolic pathways, namely *in vitro* biotransformation via a gastrointestinal simulation model followed by metabolomics profiling. The gastrointestinal biotransformation pathway of several compounds present in *Filipendula ulmaria* extract was revealed using this innovative workflow. The applied non-target screening analysis was capable of picking up features also discovered by the suspect screening approach, confirming its applicability to discover biotransformation products. Quercetin glycosides, such as rutin, are abundantly present in *Filipendula ulmaria*. When looking at the *in vitro* gastrointestinal biotransformation of rutin and/or isoquercitrin, deglycosylation is suggested as most likely biotransformation reaction, leading to the formation of quercetin. In the colon, the gut microbiota hydrolyze rutin, removing the sugar moiety and permitting absorption of the aglycon and/or extensive breakdown into low-molecular-weight phenolic metabolites. Other glycosylated precursors of the quercetin aglycon, such as spiraeoside, quercitrin, avicularin and miquelianin, were also present in the *Filipendula ulmaria* extract samples and showed to follow similar gastrointestinal biotransformation time profiles, where a decrease in intensity was observed during gastrointestinal biotransformation. Furthermore, a rise in intensity during the colon phase was also seen for a whole array of other aglycons such as kaempferol, luteolin, isorhamnetin, apigenin, naringenin, phloretin, chrysoeriol and a methoxyflavone. In this chapter the possible gastrointestinal conversion of quercetin into other aglycons was discussed. However, it is also possible that these compounds were preceded by their corresponding glycosylated precursor, e.g. kaempferol-*O*-glucoside and isorhamnetin-*O*-hexoside followed a similar biotransformation time profile as rutin, resulting in kaempferol and isorhamnetin respectively. Generally, these aglycons subsequently enter a general degradation pathway, leading to the formation of typical,

non-specific end products, such as phenylpropionic acid, phenylacetic acid and benzoic acid derivatives. The formed aglycons in the gastrointestinal experiment, however, appeared to remain quite stable across the colonic phase and resulted only in a small number of low-molecular-weight metabolites. Additionally, a slower and/or incomplete biotransformation of the compounds in the extract was seen for salicin and chlorogenic acid, while they were fully biotransformed in the *in vitro* model in the positive control where they were present as pure compounds. Moreover, although *Filipendula ulmaria* is rich in ellagitannins, the expected urolithin metabolites were not detected in the biotransformation experiment. No further breakdown was seen in monomeric ellagitannins (tellimagrandin I, tellimagrandin II, rugosin A, rugosin B, casuarinin, casuarictin and pedunculagin) and in dimeric ellagitannins (rugosin D and E) after the initial decline observed in the stomach and small intestinal phase. These slower or incomplete biotransformation rates could be caused by the presence of diverse compounds in the crude extract, which could negatively interfere with the biotransformation rate of some compounds. A different hypothesis is that biotransformation reactions are hampered by a possible antibacterial effect of the extract, resulting in an insufficient amount of viable bacteria or an altered bacterial composition, inhibiting or changing biotransformation. A possible effect of the *Filipendula ulmaria* extract on the bacterial composition of the fecal slurry during *in vitro* biotransformation was assessed using 16S rDNA-targeting PCR. A difference in relative ratios of the numbers of bacteria to the total number was observed during the gastrointestinal biotransformation experiment, suggesting an antibacterial or prebiotic effect of *Filipendula ulmaria* on certain bacteria in the fecal slurry. The largest increase in relative ratio was noted in the phylum *Firmicutes*, more specifically in the family *Lachnospiraceae*. Furthermore, a large inter- and intraindividual variability in gut microbiota exists and is an important confounding factor in studies on the formation of effect of nutrients, drugs and phytochemicals. Interindividual variability is clearly associated with the formation of urolithins, where metabolite 0 is unable to produce

them. Bacteria important for the production of urolithins, *Gordonibacter pamelaee* and *urolithinifaciens*, as well as *Ellagibacter isourolithinifaciens*, were not present in the fecal slurry incubated with the *Filipendula ulmaria* extract according to the 16S sequencing.

REFERENCES

- [1] **Van der Auwera A**, Peeters L, Foubert K, Piazza S, Vanden Berghe W, Hermans N, Pieters L. *In vitro* biotransformation and anti-inflammatory activity of constituents and metabolites of *Filipendula ulmaria*. *Pharmaceutics*. 2023;15:1291
- [2] Backhed F, Ley RE, Sonnenburg JL, Peterson DA, Gordon JI. Host-bacterial mutualism in the human intestine. *Science*. 2005;307(5717):1915-20.
- [3] Gill SR, Pop M, Deboy RT, Eckburg PB, Turnbaugh PJ, Samuel BS, et al. Metagenomic analysis of the human distal gut microbiome. *Science*. 2006;312(5778):1355-9.
- [4] Luckey TD. Introduction to intestinal microecology. *Am J Clin Nutr*. 1972;25(12):1292-4.
- [5] Collado MC, Rautava S, Aakko J, Isolauri E, Salminen S. Human gut colonisation may be initiated *in utero* by distinct microbial communities in the placenta and amniotic fluid. *Sci Rep*. 2016;6:23129.
- [6] Aagaard K, Ma J, Antony KM, Ganu R, Petrosino J, Versalovic J. The placenta harbors a unique microbiome. *Sci Transl Med*. 2014;6(237):237ra65.
- [7] Jimenez E, Fernandez L, Marin ML, Martin R, Odriozola JM, Nueno-Palop C, et al. Isolation of commensal bacteria from umbilical cord blood of healthy neonates born by cesarean section. *Curr Microbiol*. 2005;51(4):270-4.
- [8] Nuriel-Ohayon M, Neuman H, Koren O. Microbial Changes during Pregnancy, Birth, and Infancy. *Front Microbiol*. 2016;7:1031.
- [9] Thursby E, Juge N. Introduction to the human gut microbiota. *Biochem J*. 2017;474(11):1823-36.
- [10] Rodriguez JM, Murphy K, Stanton C, Ross RP, Kober OI, Juge N, et al. The composition of the gut microbiota throughout life, with an emphasis on early life. *Microb Ecol Health Dis*. 2015;26:26050.
- [11] Lloyd-Price J, Abu-Ali G, Huttenhower C. The healthy human microbiome. *Genome Med*. 2016;8(1):51.
- [12] Tremaroli V, Backhed F. Functional interactions between the gut microbiota and host metabolism. *Nature*. 2012;489(7415):242-9.
- [13] Nagpal R, Mainali R, Ahmadi S, Wang S, Singh R, Kavanagh K, et al. Gut microbiome and aging: Physiological and mechanistic insights. *Nutr Healthy Aging*. 2018;4(4):267-85.
- [14] Shimizu Y. Gut microbiota in common elderly diseases affecting activities of daily living. *World J Gastroenterol*. 2018;24(42):4750-8.
- [15] Tomova A, Bukovsky I, Rembert E, Yonas W, Alwarith J, Barnard ND, et al. The effects of vegetarian and vegan diets on gut microbiota. *Front Nutr*. 2019;6:47.

- [16] Gaulke CA, Sharpton TJ. The influence of ethnicity and geography on human gut microbiome composition. *Nat Med*. 2018;24(10):1495-6.
- [17] Azad MB, Konya T, Maughan H, Guttman DS, Field CJ, Sears MR, et al. Infant gut microbiota and the hygiene hypothesis of allergic disease: impact of household pets and siblings on microbiota composition and diversity. *Allergy Asthma Clin Immunol*. 2013;9(1):15.
- [18] Maier L, Pruteanu M, Kuhn M, Zeller G, Telzerow A, Anderson EE, et al. Extensive impact of non-antibiotic drugs on human gut bacteria. *Nature*. 2018;555(7698):623-8.
- [19] Willing BP, Russell SL, Finlay BB. Shifting the balance: antibiotic effects on host-microbiota mutualism. *Nat Rev Microbiol*. 2011;9(4):233-43.
- [20] Mathew S, Smatti MK, Al Ansari K, Nasrallah GK, Al Thani AA, Yassine HM. Mixed viral-bacterial infections and their effects on gut microbiota and clinical illnesses in children. *Sci Rep*. 2019;9(1):865.
- [21] Goodrich JK, Waters JL, Poole AC, Sutter JL, Koren O, Blekhman R, et al. Human genetics shape the gut microbiome. *Cell*. 2014;159(4):789-99.
- [22] Passamonti S, Vrhovsek U, Vanzo A, Mattivi F. The stomach as a site for anthocyanins absorption from food. *FEBS Lett*. 2003;544(1-3):210-3.
- [23] Crespy V, Morand C, Besson C, Manach C, Demigne C, Remesy C. Quercetin, but not its glycosides, is absorbed from the rat stomach. *J Agric Food Chem*. 2002;50(3):618-21.
- [24] Aulton ME, Taylor KM. *Aulton's Pharmaceutics: the design and manufacture of medicines*. 5 ed. London, UK: Elsevier Health Sciences; 2018.
- [25] Sekirov I, Russell SL, Antunes LC, Finlay BB. Gut microbiota in health and disease. *Physiol Rev*. 2010;90(3):859-904.
- [26] Sartor RB. Microbial influences in inflammatory bowel diseases. *Gastroenterology*. 2008;134(2):577-94.
- [27] Earle KA, Billings G, Sigal M, Lichtman JS, Hansson GC, Elias JE, et al. Quantitative Imaging of Gut Microbiota Spatial Organization. *Cell Host Microbe*. 2015;18(4):478-88.
- [28] De Weirdt R, Van de Wiele T. Micromanagement in the gut: microenvironmental factors govern colon mucosal biofilm structure and functionality. *NPJ Biofilms Microbiomes*. 2015;1:15026.
- [29] Schroeder BO. Fight them or feed them: how the intestinal mucus layer manages the gut microbiota. *Gastroenterol Rep*. 2019;7(1):3-12.
- [30] Rowland I, Gibson G, Heinken A, Scott K, Swann J, Thiele I, et al. Gut microbiota functions: metabolism of nutrients and other food components. *Eur J Nutr*. 2018;57(1):1-24.
- [31] Neish AS. Microbes in gastrointestinal health and disease. *Gastroenterology*. 2009;136(1):65-80.

- [32] Egert M, de Graaf AA, Smidt H, de Vos WM, Venema K. Beyond diversity: functional microbiomics of the human colon. *Trends Microbiol.* 2006;14(2):86-91.
- [33] Matsuoka K, Kanai T. The gut microbiota and inflammatory bowel disease. *Semin Immunopathol.* 2015;37(1):47-55.
- [34] Patterson E, Ryan PM, Cryan JF, Dinan TG, Ross RP, Fitzgerald GF, et al. Gut microbiota, obesity and diabetes. *Postgrad Med J.* 2016;92(1087):286-300.
- [35] Fujimura KE, Lynch SV. Microbiota in allergy and asthma and the emerging relationship with the gut microbiome. *Cell Host Microbe.* 2015;17(5):592-602.
- [36] Valles-Colomer M, Falony G, Darzi Y, Tigchelaar EF, Wang J, Tito RY, et al. The neuroactive potential of the human gut microbiota in quality of life and depression. *Nat Microbiol.* 2019;4(4):623-32.
- [37] Pathak S, Kesavan P, Banerjee A, Banerjee A, Celep GS, Bissi L, et al. Metabolism of dietary polyphenols by human gut microbiota and their health benefits. Watson RR, Preedy VR, Zibadi S, editors. *Polyphenols: mechanisms of action in human health and disease.* 2 ed. Massachusetts, USA: Academic Press; 2018. p. 347-59.
- [38] Marin L, Miguelez EM, Villar CJ, Lombo F. Bioavailability of dietary polyphenols and gut microbiota metabolism: antimicrobial properties. *Biomed Res Int.* 2015;2015:905215.
- [39] Kawabata K, Yoshioka Y, Terao J. Role of intestinal microbiota in the bioavailability and physiological functions of dietary polyphenols. *Molecules.* 2019;24(2).
- [40] Cardona F, Andres-Lacueva C, Tulipani S, Tinahones FJ, Queipo-Ortuno MI. Benefits of polyphenols on gut microbiota and implications in human health. *J Nutr Biochem.* 2013;24(8):1415-22.
- [41] Sun C, Chen L, Shen Z. Mechanisms of gastrointestinal microflora on drug metabolism in clinical practice. *Saudi Pharm J.* 2019;27(8):1146-56.
- [42] Espin JC, Gonzalez-Sarrias A, Tomás-Barberán FA. The gut microbiota: A key factor in the therapeutic effects of (poly)phenols. *Biochem Pharmacol.* 2017;139:82-93.
- [43] Duda-Chodak A, Tarko T, Satora P, Sroka P. Interaction of dietary compounds, especially polyphenols, with the intestinal microbiota: a review. *Eur J Nutr.* 2015;54(3):325-41.
- [44] Wilkinson AP, Gee JM, Dupont MS, Needs PW, Mellon FA, Williamson G, et al. Hydrolysis by lactase phlorizin hydrolase is the first step in the uptake of daidzein glucosides by rat small intestine in vitro. *Xenobiotica.* 2003;33(3):255-64.
- [45] Murota K, Nakamura Y, Uehara M. Flavonoid metabolism: the interaction of metabolites and gut microbiota. *Biosci Biotechnol Biochem.* 2018;82(4):600-10.

- [46] Wu B, Basu S, Meng S, Wang X, Hu M. Regioselective sulfation and glucuronidation of phenolics: insights into the structural basis. *Curr Drug Metab.* 2011;12(9):900-16.
- [47] Pollet RM, D'Agostino EH, Walton WG, Xu Y, Little MS, Biernat KA, et al. An atlas of beta-glucuronidases in the human intestinal microbiome. *Structure.* 2017;25(7):967-77 e5.
- [48] Stevens JF, Maier CS. The chemistry of gut microbial metabolism of polyphenols. *Phytochem Rev.* 2016;15(3):425-44.
- [49] Stevens Y, Rymenant EV, Grootaert C, Camp JV, Possemiers S, Masclee A, et al. The intestinal fate of citrus flavanones and their effects on gastrointestinal health. *Nutrients.* 2019;11(7).
- [50] Monagas M, Urpi-Sarda M, Sánchez-Patán F, Llorach R, Garrido I, Gómez-Cordovés C, et al. Insights into the metabolism and microbial biotransformation of dietary flavan-3-ols and the bioactivity of their metabolites. *Food Funct.* 2010;1(3):233-53.
- [51] Marquez Campos E, Stehle P, Simon MC. Microbial metabolites of flavan-3-ols and their biological activity. *Nutrients.* 2019;11(10).
- [52] Tian L, Tan Y, Chen G, Wang G, Sun J, Ou S, et al. Metabolism of anthocyanins and consequent effects on the gut microbiota. *Crit Rev Food Sci Nutr.* 2019;59(6):982-91.
- [53] Gaya P, Medina M, Sanchez-Jimenez A, Landete JM. Phytoestrogen metabolism by adult human gut microbiota. *Molecules.* 2016;21(8).
- [54] Espin JC, Larrosa M, Garcia-Conesa MT, Tomás-Barberán FA. Biological significance of urolithins, the gut microbial ellagic acid-derived metabolites: the evidence so far. *Evid Based Complement Alternat Med.* 2013;2013:270418.
- [55] Selma MV, Beltran D, Luna MC, Romo-Vaquero M, Garcia-Villalba R, Mira A, et al. Isolation of human intestinal bacteria capable of producing the bioactive metabolite isourolithin A from ellagic acid. *Front Microbiol.* 2017;8:1521.
- [56] Beltran D, Romo-Vaquero M, Espin JC, Tomás-Barberán FA, Selma MV. *Ellagibacter isourolithinifaciens* gen. nov., sp. nov., a new member of the family *Eggerthellaceae*, isolated from human gut. *Int J Syst Evol Microbiol.* 2018;68(5):1707-12.
- [57] Bode LM, Bunzel D, Huch M, Cho GS, Ruhland D, Bunzel M, et al. *In vivo* and *in vitro* metabolism of trans-resveratrol by human gut microbiota. *Am J Clin Nutr.* 2013;97(2):295-309.
- [58] Chaplin A, Carpenne C, Mercader J. Resveratrol, metabolic syndrome, and gut microbiota. *Nutrients.* 2018;10(11).
- [59] Henry-Vitrac C, Desmoulière A, Girard D, Mérillon J, Krisa S. Transport, deglycosylation, and metabolism of trans-piceid by small intestinal epithelial cells. *Eur J Nutr.* 2006;45(7):376-82.
- [60] Springer M, Moco S. Resveratrol and its human metabolites-effects on metabolic health and obesity. *Nutrients.* 2019;11(1).

- [61] Tomás-Barberán FA, Garcia-Villalba R, Quartieri A, Raimondi S, Amaretti A, Leonardi A, et al. *In vitro* transformation of chlorogenic acid by human gut microbiota. *Mol Nutr Food Res*. 2014;58(5):1122-31.
- [62] Macfarlane GT, Macfarlane S. Models for intestinal fermentation: association between food components, delivery systems, bioavailability and functional interactions in the gut. *Curr Opin Biotechnol*. 2007;18(2):156-62.
- [63] Becker N, Kunath J, Loh G, Blaut M. Human intestinal microbiota: characterization of a simplified and stable gnotobiotic rat model. *Gut Microbes*. 2011;2(1):25-33.
- [64] Hirayama K, Itoh K, Takahashi E, Mitsuoka T. Comparison of composition of faecal microbiota and metabolism of faecal bacteria among 'Human-Flora-Associated' mice inoculated with faeces from six different human donors. *Microb Ecol Health Dis*. 1995;8(5):199-211.
- [65] Shen J, Zhang B, Wei H, Che C, Ding D, Hua X, et al. Assessment of the modulating effects of fructo-oligosaccharides on fecal microbiota using human flora-associated piglets. *Arch Microbiol*. 2010;192(11):959-68.
- [66] Rawls JF, Samuel BS, Gordon JI. Gnotobiotic zebrafish reveal evolutionarily conserved responses to the gut microbiota. *Proc Natl Acad Sci USA*. 2004;101(13):4596-601.
- [67] Hold GL, Pryde SE, Russell VJ, Furrie E, Flint HJ. Assessment of microbial diversity in human colonic samples by 16S rDNA sequence analysis. *FEMS Microbiol Ecol*. 2002;39(1):33-9.
- [68] Hillman ET, Lu H, Yao T, Nakatsu CH. Microbial ecology along the gastrointestinal tract. *Microbes Environ*. 2017;32(4):300-13.
- [69] Wahlgren M, Axenstrand M, Hakansson A, Marefati A, Lomstein Pedersen B. *In vitro* methods to study colon release: state of the art and an outlook on new strategies for better *in vitro* biorelevant release media. *Pharmaceutics*. 2019;11(2).
- [70] Dupont D, Alric M, Blanquet-Diot S, Bornhorst G, Cueva C, Deglaire A, et al. Can dynamic *in vitro* digestion systems mimic the physiological reality? *Crit Rev Food Sci Nutr*. 2019;59(10):1546-62.
- [71] Estevez-Santiago R, Olmedilla-Alonso B, Fernandez-Jalao I. Bioaccessibility of provitamin A carotenoids from fruits: application of a standardised static *in vitro* digestion method. *Food Funct*. 2016;7(3):1354-66.
- [72] Alemany L, Cilla A, Garcia-Llatas G, Rodriguez-Estrada MT, Cardenia V, Alegría A. Effect of simulated gastrointestinal digestion on plant sterols and their oxides in enriched beverages. *Food Res Int*. 2013;52(1):1-7.
- [73] Peixoto RA, Mazon AM, Cadore S. Estimation of the bioaccessibility of metallic elements in chocolate drink powder using an *in vitro* digestion method and spectrometric techniques. *J Braz Chem Soc*. 2013;24(5):884-90.

- [74] Minekus M, Alminger M, Alvito P, Ballance S, Bohn T, Bourlieu C, et al. A standardised static *in vitro* digestion method suitable for food - an international consensus. *Food Funct.* 2014;5(6):1113-24.
- [75] Guerra A, Etienne-Mesmin L, Livrelli V, Denis S, Blanquet-Diot S, Alric M. Relevance and challenges in modeling human gastric and small intestinal digestion. *Trends Biotechnol.* 2012;30(11):591-600.
- [76] Minekus M, Marteau P, Havenaar R, Veld J. A multicompartmental dynamic computer-controlled model simulating the stomach and small intestine. *ATLA.* 1995;23:197-209.
- [77] Ribnicky DM, Roopchand DE, Oren A, Grace M, Poulev A, Lila MA, et al. Effects of a high fat meal matrix and protein complexation on the bioaccessibility of blueberry anthocyanins using the TNO gastrointestinal model (TIM-1). *Food Chem.* 2014;142:349-57.
- [78] Havenaar R, Anneveld B, Hanff LM, de Wildt SN, de Koning BA, Mooij MG, et al. In vitro gastrointestinal model (TIM) with predictive power, even for infants and children? *Int J Pharm.* 2013;457(1):327-32.
- [79] Wickham MJS, Faulks RM, Mann J, Mandalari G. The design, operation, and application of a dynamic gastric model. *Dissolution Technol.* 2012;19:15+.
- [80] Thuenemann EC, Mandalari G, Rich GT, Faulks RM. Dynamic Gastric Model (DGM). Verhoeckx K, Cotter P, López-Expósito I, Kleiveland C, Lea T, Mackie A, et al., editors. *The impact of food bioactives on health: in vitro and ex vivo models.* Cham, Switzerland: Springer International Publishing; 2015. p. 47-59.
- [81] Venema K, van den Abbeele P. Experimental models of the gut microbiome. *Best Pract Res Clin Gastroenterol.* 2013;27(1):115-26.
- [82] Duenas M, Munoz-Gonzalez I, Cueva C, Jimenez-Giron A, Sanchez-Patan F, Santos-Buelga C, et al. A survey of modulation of gut microbiota by dietary polyphenols. *Biomed Res Int.* 2015;2015:850902.
- [83] Martínez-Cuesta MC, Peláez C, Requena T. Laboratory simulators of the colon microbiome. Faintuch J, Faintuch S, editors. *Microbiome and metabolome in diagnosis, therapy, and other strategic applications.* Massachusetts, USA: Academic Press; 2019. p. 61-7.
- [84] Cinquin C, Le Blay G, Fliss I, Lacroix C. Immobilization of infant fecal microbiota and utilization in an *in vitro* colonic fermentation model. *Microb Ecol.* 2004;48(1):128-38.
- [85] Venema K. The TNO *in vitro* model of the colon (TIM-2). Verhoeckx K, Cotter P, Lopez-Exposito I, Kleiveland C, Lea T, Mackie A, et al., editors. *The impact of food bioactives on health: in vitro and ex vivo models.* Cham, Switzerland: Springer International Publishing; 2015. p. 293-304.
- [86] Feria-Gervasio D, Denis S, Alric M, Brugere JF. *In vitro* maintenance of a human proximal colon microbiota using the continuous fermentation system P-ECSIM. *Appl Microbiol Biotechnol.* 2011;91(5):1425-33.

- [87] Fehlbaum S, Chassard C, Haug MC, Fourmestraux C, Derrien M, Lacroix C. Design and investigation of PolyFermS *In vitro* continuous fermentation models inoculated with immobilized fecal microbiota mimicking the elderly colon. *PLoS One*. 2015;10(11):e0142793.
- [88] Salli K, Anglenius H, Hirvonen J, Hibberd AA, Ahonen I, Saarinen MT, et al. The effect of 2'-fucosyllactose on simulated infant gut microbiome and metabolites; a pilot study in comparison to GOS and lactose. *Sci Rep*. 2019;9(1):13232.
- [89] Van de Wiele T, Van den Abbeele P, Ossieur W, Possemiers S, Marzorati M. The Simulator of the Human Intestinal Microbial Ecosystem (SHIME). Verhoeckx K, Cotter P, Lopez-Exposito I, Kleiveland C, Lea T, Mackie A, et al., editors. *The impact of food bioactives on health: in vitro and ex vivo models*. Cham, Switzerland: Springer International Publishing; 2015. p. 305-17.
- [90] Garcia-Villalba R, Vissenaekens H, Pitart J, Romo-Vaquero M, Espin JC, Grootaert C, et al. Gastrointestinal Simulation Model TWIN-SHIME shows differences between human urolithin-metabotypes in gut microbiota composition, pomegranate polyphenol metabolism, and transport along the intestinal tract. *J Agric Food Chem*. 2017;65(27):5480-93.
- [91] Barroso E, Cueva C, Pelaez C, Martinez-Cuesta MC, Requena T. The computer-controlled multicompartmental dynamic model of the gastrointestinal system SIMGI. Verhoeckx K, Cotter P, Lopez-Exposito I, Kleiveland C, Lea T, Mackie A, et al., editors. *The impact of food bioactives on health: in vitro and ex vivo models*. Cham, Switzerland: Springer International Publishing; 2015. p. 319-27.
- [92] Breynaert A, Bosscher D, Kahnt A, Claeys M, Cos P, Pieters L, et al. Development and validation of an *in vitro* experimental gastrointestinal dialysis model with colon phase to study the availability and colonic metabolism of polyphenolic compounds. *Planta Med*. 2015;81(12-13):1075-83.
- [93] Blanquet S, Meunier JP, Minekus M, Marol-Bonnin S, Alric M. Recombinant *Saccharomyces cerevisiae* expressing P450 in artificial digestive systems: a model for biotransformation in the human digestive environment. *Appl Environ Microbiol*. 2003;69(5):2884-92.
- [94] Mortelet O, Iturrospe E, Breynaert A, Verdickt E, Xavier BB, Lammens C, et al. Optimization of an *in vitro* gut microbiome biotransformation platform with chlorogenic acid as model compound: From fecal sample to biotransformation product identification. *J Pharm Biomed Anal*. 2019;175:112768.
- [95] Kumar SV, Saravanan D, Kumar B, Jayakumar A. An update on prodrugs from natural products. *Asian Pac J Trop Med*. 2014;7S1:S54-9.
- [96] Wishart DS. Emerging applications of metabolomics in drug discovery and precision medicine. *Nat Rev Drug Discov*. 2016;15(7):473-84.
- [97] Zierer J, Jackson MA, Kastenmuller G, Mangino M, Long T, Telenti A, et al. The fecal metabolome as a functional readout of the gut microbiome. *Nat Genet*. 2018;50(6):790-5.

- [98] Beirnaert C, Peeters L, Meysman P, Bittremieux W, Foubert K, Custers D, et al. Using expert driven machine learning to enhance dynamic metabolomics data analysis. *Metabolites*. 2019;9(3).
- [99] Martens L, Chambers M, Sturm M, Kessner D, Levander F, Shofstahl J, et al. mzML-a community standard for mass spectrometry data. *Mol Cell Proteomics*. 2011;10(1):R110 000133.
- [100] Kessner D, Chambers M, Burke R, Agus D, Mallick P. ProteoWizard: open source software for rapid proteomics tools development. *Bioinformatics*. 2008;24(21):2534-6.
- [101] Smith CA, Want EJ, O'Maille G, Abagyan R, Siuzdak G. XCMS: processing mass spectrometry data for metabolite profiling using nonlinear peak alignment, matching, and identification. *Anal Chem*. 2006;78(3):779-87.
- [102] Smilde AK, Westerhuis JA, Hoefsloot HC, Bijlsma S, Rubingh CM, Vis DJ, et al. Dynamic metabolomic data analysis: a tutorial review. *Metabolomics*. 2010;6(1):3-17.
- [103] Leek JT, Mosen E, Dabney AR, Storey JD. EDGE: extraction and analysis of differential gene expression. *Bioinformatics*. 2006;22(4):507-8.
- [104] Storey JD, Xiao W, Leek JT, Tompkins RG, Davis RW. Significance analysis of time course microarray experiments. *Proc Natl Acad Sci USA*. 2005;102(36):12837-42.
- [105] Peeters L, Beirnaert C, **Van der Auwera A**, Bijttebier S, De Bruyne T, Laukens K, et al. Revelation of the metabolic pathway of hederacoside C using an innovative data analysis strategy for dynamic multiclass biotransformation experiments. *J Chromatogr A*. 2019;1595:240-7.
- [106] Peeters L, **Van der Auwera A**, Beirnaert C, Bijttebier S, Laukens K, Pieters L, et al. Compound characterization and metabolic profile elucidation after *in vitro* gastrointestinal and hepatic biotransformation of an *Herniaria hirsuta* extract using unbiased dynamic metabolomic data analysis. *Metabolites*. 2020;10(3).
- [107] Bijttebier S, **Van der Auwera A**, Voorspoels S, Noten B, Hermans N, Pieters L, et al. A first step in the quest for the active constituents in *Filipendula ulmaria* (meadowsweet): comprehensive phytochemical identification by liquid chromatography coupled to Quadrupole-Orbitrap Mass Spectrometry. *Planta Med*. 2016;82(6):559-72.
- [108] Pruesse E, Quast C, Knittel K, Fuchs BM, Ludwig W, Peplies J, et al. SILVA: a comprehensive online resource for quality checked and aligned ribosomal RNA sequence data compatible with ARB. *Nucleic Acids Res*. 2007;35(21):7188-96.
- [109] Djoumbou-Feunang Y, Fiamoncini J, Gil-de-la-Fuente A, Greiner R, Manach C, Wishart DS. BioTransformer: a comprehensive computational tool for small molecule metabolism prediction and metabolite identification. *J Cheminformatics*. 2019;11(1):2.

- [110] Olthof MR, Hollman PCH, Katan MB. Chlorogenic acid and caffeic acid are absorbed in humans. *J Nutr.* 2001;131(1):66-71.
- [111] Del Rio D, Stalmach A, Calani L, Crozier A. Bioavailability of coffee chlorogenic acids and green tea flavan-3-ols. *Nutrients.* 2010;2(8):820-33.
- [112] Gonthier MP, Remesy C, Scalbert A, Cheynier V, Souquet JM, Poutanen K, et al. Microbial metabolism of caffeic acid and its esters chlorogenic and caftaric acids by human faecal microbiota *in vitro*. *Biomed Pharmacother.* 2006;60(9):536-40.
- [113] Konishi Y, Kobayashi S. Transepithelial transport of chlorogenic acid, caffeic acid, and their colonic metabolites in intestinal caco-2 cell monolayers. *J Agric Food Chem.* 2004;52(9):2518-26.
- [114] Naranjo Pinta M, Montoliu I, Aura AM, Seppänen-Laakso T, Barron D, Moco S. *In Vitro* gut metabolism of [U-(13) C]-quinic acid, the other hydrolysis product of chlorogenic acid. *Mol Nutr Food Res.* 2018;62(22):e1800396.
- [115] Olthof MR, Hollman PC, Buijsman MN, van Amelsvoort JM, Katan MB. Chlorogenic acid, quercetin-3-rutinoside and black tea phenols are extensively metabolized in humans. *J Nutr.* 2003;133(6):1806-14.
- [116] Rivera-Mondragón A, Peeters L, **Van der Auwera A**, Breynaert A, Caballero-George C, Pieters L, et al. Simulated gastrointestinal biotransformation of chlorogenic acid, flavonoids, flavonolignans and triterpenoid saponins in *Cecropia obtusifolia* leaf extract. *Planta Med.* 2020;87(05):404-16.
- [117] Okuda T, Yoshida T, Hatano T, Iwasaki M, Kubo M, Orime T, et al. Hydrolysable tannins as chemotaxonomic markers in the Rosaceae. *Phytochemistry.* 1992;31(9):3091-6.
- [118] Pemp E, Reznicek G, Krenn L. Fast quantification of flavonoids in *Filipendula ulmariae* flos by HPLC/ESI-MS using a nonporous stationary phase. *J Anal Chem.* 2007;62(7):669-73.
- [119] Papp I, Simándi B, Blazics B, Alberti Á, Héthelyi É, Szőke É, Kéry Á. Monitoring volatile and non-volatile salicylates in *Filipendula ulmaria* by different chromatographic techniques. *Chromatographia.* 2008;68(1):125-9.
- [120] Fecka I. Qualitative and quantitative determination of hydrolysable tannins and other polyphenols in herbal products from meadowsweet and dog rose. *Phytochem Anal.* 2009;20(3):177-90.
- [121] Shilova IV, Semenov AA, Suslov NI, Korotkova EI, Vtorushina AN, Belyakova VV. Chemical composition and biological activity of a fraction of meadowsweet extract. *Pharm Chem J.* 2009;43(4):185-90.
- [122] Barros L, Alves CT, Dueñas M, Silva S, Oliveira R, Carvalho AM, Henriques, M, et al. Characterization of phenolic compounds in wild medicinal flowers from Portugal by HPLC–DAD–ESI/MS and evaluation of antifungal properties. *Ind Crops Prod.* 2013;44:104-10.
- [123] Olennikov DN, Kruglova MY. A new quercetin glycoside and other phenolic compounds from the genus *Filipendula*. *Chem Nat Compd.* 2013;49(4):610-6.

- [124] Begley M, Gahan CGM, Hill C. The interaction between bacteria and bile. *FEMS Microbiology Reviews*. 2005;29(4):625-51.
- [125] Bourgin M, Kriaa A, Mkaouar H, Mariaule V, Jablaoui A, Maguin E, et al. Bile Salt hydrolases: At the crossroads of microbiota and human health. *Microorganisms*. 2021;9(6).
- [126] Owen RW, Mason AN, Bilton RF. The degradation of cholesterol by *Pseudomonas* sp. NCIB 10590 under aerobic conditions. *J Lipid Res*. 1983;24(11):1500-11.
- [127] Németh K, Plumb GW, Berrin J, Juge N, Jacob R, Naim HY, et al. Deglycosylation by small intestinal epithelial cell β -glucosidases is a critical step in the absorption and metabolism of dietary flavonoid glycosides in humans. *Eur J Nutr*. 2003;42(1):29-42.
- [128] Braune A, Blaut M. Bacterial species involved in the conversion of dietary flavonoids in the human gut. *Gut Microbes*. 2016;7(3):216-34.
- [129] Riva A, Kolimár D, Spittler A, Wisgrill L, Herbold CW, Abrankó L, et al. Conversion of rutin, a prevalent dietary flavonol, by the human gut microbiota. *Front Microbiol*. 2020;11.
- [130] Beekwilder J, Marcozzi D, Vecchi S, de Vos R, Janssen P, Francke C, et al. Characterization of Rhamnosidases from *Lactobacillus plantarum* and *Lactobacillus acidophilus*. *Appl Environ Microbiol*. 2009;75(11):3447-54.
- [131] Bang SH, Hyun YJ, Shim J, Hong SW, Kim DH. Metabolism of rutin and poncirin by human intestinal microbiota and cloning of their metabolizing α -L-rhamnosidase from *Bifidobacterium dentium*. *J Microbiol Biotechnol*. 2015;25(1):18-25.
- [132] Bokkenheuser VD, Shackleton CH, Winter J. Hydrolysis of dietary flavonoid glycosides by strains of intestinal *Bacteroides* from humans. *Biochem J*. 1987;248(3):953-6.
- [133] Shin NR, Moon JS, Shin SY, Li L, Lee YB, Kim TJ, et al. Isolation and characterization of human intestinal *Enterococcus avium* EFEL009 converting rutin to quercetin. *Lett Appl Microbiol*. 2016;62(1):68-74.
- [134] Schneider H, Schwiertz A, Collins MD, Blaut M. Anaerobic transformation of quercetin-3-glucoside by bacteria from the human intestinal tract. *Arch Microbiol*. 1999;171(2):81-91.
- [135] Schneider H, Simmering R, Hartmann L, Pforte H, Blaut M. Degradation of quercetin-3-glucoside in gnotobiotic rats associated with human intestinal bacteria. *J Appl Microbiol*. 2000;89(6):1027-37.
- [136] Elferink H, Bruekers JPJ, Veeneman GH, Boltje TJ. A comprehensive overview of substrate specificity of glycoside hydrolases and transporters in the small intestine. *Cell Mol Life Sci*. 2020;77(23):4799-826.
- [137] Fraga CG. *Plant phenolics and human health: biochemistry, nutrition and pharmacology*. Chichester, UK: Wiley; 2009.

- [138] Williamson G, Kay CD, Crozier A. The bioavailability, transport, and bioactivity of dietary flavonoids: a review from a historical perspective. *Compr Rev Food Sci Food Saf.* 2018;17(5):1054-112.
- [139] Jaganath IB, Mullen W, Edwards CA, Crozier A. The relative contribution of the small and large intestine to the absorption and metabolism of rutin in man. *Free Radic Res.* 2006;40(10):1035-46.
- [140] Possemiers S, Bolca S, Verstraete W, Heyerick A. The intestinal microbiome: A separate organ inside the body with the metabolic potential to influence the bioactivity of botanicals. *Fitoterapia.* 2011;82(1):53-66.
- [141] Di Pede G, Bresciani L, Calani L, Petrangolini G, Riva A, Allegrini P, et al. The human microbial metabolism of quercetin in different formulations: an *in vitro* evaluation. *Foods.* 2020;9(8).
- [142] Jenner AM, Rafter J, Halliwell B. Human fecal water content of phenolics: The extent of colonic exposure to aromatic compounds. *Free Radic Biol Med.* 2005;38(6):763-72.
- [143] Dodd D, Spitzer MH, Van Treuren W, Merrill BD, Hryckowian AJ, Higginbottom SK, et al. A gut bacterial pathway metabolizes aromatic amino acids into nine circulating metabolites. *Nature.* 2017;551(7682):648-52.
- [144] Russell WR, Duncan SH, Scobbie L, Duncan G, Cantlay L, Calder AG, et al. Major phenylpropanoid-derived metabolites in the human gut can arise from microbial fermentation of protein. *Mol Nutr Food Res.* 2013;57(3):523-35.
- [145] Peeters L, Foubert K, Baldé MA, Tuenter E, Matheeußen A, Van Pelt N, et al. Antiplasmodial activity of constituents and their metabolites after *in vitro* gastrointestinal biotransformation of a *Nauclea pobeguinii* extract. *Phytochemistry.* 2022;194:113029.
- [146] Peeters L. An integrated strategy to characterize active constituents and their metabolites in *Herniaria hirsuta* and *Nauclea pobeguinii* (dissertation). Antwerp, Belgium: University of Antwerp; 2022.
- [147] Rauha JP, Remes S, Heinonen M, Hopia A, Kahkonen M, Kujala T, et al. Antimicrobial effects of Finnish plant extracts containing flavonoids and other phenolic compounds. *Int J Food Microbiol.* 2000;56(1):3-12.
- [148] Denev P, Kratchanova M, Ciz M, Lojek A, Vasicek O, Blazheva D, et al. Antioxidant, antimicrobial and neutrophil-modulating activities of herb extracts. *Acta Biochim Pol.* 2014;61(2):359-67.
- [149] Mills S, Bone K. Principles and practice of phytotherapy: modern herbal medicine. 2 ed. Edinburgh, Scotland: Churchill Livingstone; 2013.
- [150] Fötsch G, Pfeifer S. Die biotransformation der phenolglycoside leiocarposid und salicin — beispiele für besonderheiten von absorption und metabolismus glycosidischer verbindungen. *Pharmazie.* 1989;44(10):710-2.
- [151] Schmid B, Kötter I, Heide L. Pharmacokinetics of salicin after oral administration of a standardised willow bark extract. *Eur J Clin Pharmacol.* 2001;57(5):387-91.

- [152] Knuth S, Abdelsalam RM, Khayyal MT, Schweda F, Heilmann J, Kees MG, et al. Catechol conjugates are *in vivo* metabolites of Salicis cortex. *Planta Med.* 2013;79(16):1489-94.
- [153] Pferschy-Wenzig EM, Koskinen K, Moissl-Eichinger C, Bauer R. A Combined LC-MS Metabolomics- and 16S rRNA sequencing platform to assess interactions between herbal medicinal products and human gut bacteria *in vitro*: a pilot study on willow bark extract. *Front Pharmacol.* 2017;8:893.
- [154] Steinegger VE, Hovel H. Analytische und biologische untersuchungen an salicaceen-wirkstoffen, insbesondere an salicin. *Pharmaceutica Acta Helvetiae.* 1972;47:222-34.
- [155] Pentz R, Busse H, König R, Siegers C. Bioverfügbarkeit von salicylsäure und coffein aus einem phytoanalgetischen kombinationspräparat. *Z Phytother.* 1989;10:92-6.
- [156] Piwowski JP, Granica S, Zwierzyńska M, Stefańska J, Schopohl P, Melzig MF, et al. Role of human gut microbiota metabolism in the anti-inflammatory effect of traditionally used ellagitannin-rich plant materials. *J Ethnopharmacol.* 2014;155(1):801-9.
- [157] Popowski D, Pawłowska KA, Piwowski JP, Granica S. Gut microbiota-assisted isolation of flavonoids with a galloyl moiety from flowers of meadowsweet, *Filipendula ulmaria* (L.) Maxim. *Phytochem Lett.* 2019;30:220-3.
- [158] Selma MV, Beltrán D, García-Villalba R, Espín JC, Tomás-Barberán FA. Description of urolithin production capacity from ellagic acid of two human intestinal Gordonibacter species. *Food & Function.* 2014;5(8):1779-84.
- [159] Cortés-Martín A, García-Villalba R, González-Sarrías A, Romo-Vaquero M, Loria-Kohen V, Ramírez-de-Molina A, et al. The gut microbiota urolithin metabolites revisited: the human metabolism of ellagic acid is mainly determined by aging. *Food & Function.* 2018;9(8):4100-6.
- [160] Inada KOP, Tomás-Barberán FA, Perrone D, Monteiro M. Metabolism of ellagitannins from jaboticaba (*Myrciaria jaboticaba*) in normoweight, overweight and obese Brazilians: Unexpected laxative effects influence urolithins urinary excretion and metabolite distribution. *JFF.* 2019;57:299-308.
- [161] Xian W, Yang S, Deng Y, Yang Y, Chen C, Li W, et al. Distribution of urolithins metabolites in healthy Chinese youth: difference in gut microbiota and predicted metabolic pathways. *J Agric Food Chem.* 2021;69(44):13055-65.
- [162] García-Villalba R, Giménez-Bastida JA, Cortés-Martín A, Ávila-Gálvez M, Tomás-Barberán FA, Selma MV, et al. Urolithins: a comprehensive update on their metabolism, bioactivity, and associated gut microbiota. *Mol Nutr Food Res.* 2022:e2101019.
- [163] Cushnie TP, Lamb AJ. Antimicrobial activity of flavonoids. *Int J Antimicrob Agents.* 2005;26(5):343-56.

- [164] Plamada D, Vodnar DC. Polyphenols-Gut Microbiota interrelationship: a transition to a new generation of prebiotics. *Nutrients*. 2021;14(1).
- [165] Duda-Chodak A. The inhibitory effect of polyphenols on human gut microbiota. *J Physiol Pharmacol*. 2012;63(5):497-503.
- [166] Gowd V, Karim N, Shishir MRI, Xie L, Chen W. Dietary polyphenols to combat the metabolic diseases via altering gut microbiota. *Trends Food Sci Technol*. 2019;93:81-93.
- [167] Bialonska D, Ramnani P, Kasimsetty SG, Muntha KR, Gibson GR, Ferreira D. The influence of pomegranate by-product and punicalagins on selected groups of human intestinal microbiota. *Int J Food Microbiol*. 2010;140(2):175-82.



CHAPTER 4

*PHARMACOLOGICAL ACTIVITY
STUDIES ON FILIPENDULA ULMARIA*

*This chapter is part of an article published in Pharmaceutics: **Van der Auwera A, Peeters L, Foubert K, Piazza S, Vanden Berghe W, Hermans N, Pieters L. In vitro biotransformation and anti-inflammatory activity of constituents and metabolites of Filipendula ulmaria. Pharmaceutics. 2023;15(4):1291.***^[1]

INTRODUCTION

4.1 AIM

The anti-inflammatory properties of *Filipendula ulmaria* have been frequently claimed in ethnomedicine. It is well known that inflammation plays a key role in many chronic diseases such as cancer, diabetes, neurodegenerative and autoimmune disorders. In this chapter the effect of *Filipendula ulmaria* on several key mediators in the inflammatory process was examined, including: enzyme activity of cyclooxygenase-1 and -2, changes in cyclooxygenase-2 gene expression and the effect on nuclear factor κ B. The large diversity of identified phytochemicals are likely to contribute to the activity, since many of them have been reported to be beneficial for human health. However, biotransformation and pharmacological studies should be combined in order to investigate which of these constituents or metabolites contribute to the activity of *Filipendula ulmaria* after oral intake.

4.2 WHAT IS INFLAMMATION?

More than 2000 years ago, the Roman physician Cornelius Celsus described inflammation as a biological phenomenon. This process is characterized by 5 cardinal physiological signs: dolor (pain), rubor (redness), calor (local heat and fever), tumor (swelling), and functio laesa (loss of function), which was added later to the list in 1871 by Rudolf Virchow.^[2] Functionally, inflammation is the protective biological response of the immune system against invading pathogens, toxic compounds or endogenous signals such as damaged cells, resulting in the elimination of the stimulus, clearance of necrotic cells and tissue repair.^[3] Summarized, the steps can be remembered as the 5 R's: Recognition of the agent, Recruitment of leukocytes, Removal of the agent, Regulation of the response and Resolution.^[4] The host defense mechanism is also

divided into two separate, yet interconnected, pathways: the innate and adaptive immune response (illustrated in Figure 4.1). The innate immune response initiates a rapid, first line response to injury and detects a broad range of molecular patterns found on pathogens, while the slower adaptive immune response is able to recognize specific molecular structures and target threats with high specificity. Basophils, eosinophils, neutrophils, mast cells, natural killer cells, macrophages and dendritic cells mediate the innate immunity.^[5] Adaptive immunity occurs after exposure to an antigen and can fight back faster than the innate response if it has seen the pathogen before. Briefly, the cell-mediated immune response is controlled by activated T cells and the humoral response is controlled by B cells and antibodies. Macrophages and dendritic cells are unique as they have both innate and adaptive traits. These cells are professional antigen-presenting cells, which are critical in the induction of adaptive immunity by presenting the foreign antigens to antigen-specific T and B lymphocytes. Adaptive immunity also creates immunological memory, which gives the host long-term protection from reinfection by the same (or closely related) pathogen.^[5-8] The inflammatory response itself can be classified in two categories: acute and chronic inflammation. Acute is defined as a local, protective response. Chronic inflammation, on the other hand, is a prolonged and persistent type of inflammation which can render the host vulnerable.^[3] Both the innate and adaptive immunity participate in the process of acute and chronic inflammation.^[5,6]

4.2.1 ACUTE INFLAMMATION

Acute inflammation is an important physiologic process that starts immediately after the damaging stimulus and quickly resolves over a couple of hours to days in order to remove the insult and eventually repair the damaged tissue. Typically, acute inflammation is characterized by three main events: vasodilatation, increased permeability of blood vessels and leukocyte recruitment and activation.^[4,9] Cells of the innate immune system, which are able to recognize a broad spectrum of foreign

particles, pathogens and other danger related stimuli, are the first to encounter these injurious agents. The process is thus initiated by specialized sentinel cells in the tissue, i.e. mast cells, macrophages and certain non-immune cells like epithelial cells and fibroblast, which detect injury or the presence of pathogens via cellular receptors.^[4,10] PAMPs (Pathogen-Associated Molecular Patterns), which are motifs common to many microbes, and endogenous stress signals, called DAMPs (Damage-Associated Molecular Patterns), can be sensed by these cells through specific surface receptors called pattern recognition receptors or PRRs.^[6] Among the PRRs, the Toll-like receptors (TLR) have been studied most extensively, e.g. bacterial lipopolysaccharides (LPS) are typically recognized by TLR4.^[11] The sentinel cells react to the trigger by releasing mediators that attract additional immune cells (such as neutrophils, natural killer cells and monocytes). Examples of these mediators are cytokines (i.e. proteins important for cell signaling), but also small molecules like nitric oxide and eicosanoids. These recruited inflammatory cells release more proinflammatory cytokines, including tumor necrosis factor (TNF), IL-6, IL-12 and interferons (IFNs).^[5,7,8] Blood vessels react to acute inflammation in order to increase the movement of circulatory leukocytes and plasma proteins into the infected or injured site. One of the earliest signs of acute inflammation is vasodilatation (e.g. mediated by histamine), which results in increased blood flow and thus redness and increased warmth. This is followed by increased microvascular permeability (initiated by histamine, bradykinin, leukotrienes and other mediators), which creates exudate into the extravascular tissue (i.e. swelling). These changes create a stasis of blood flow, and together with an increased level of adhesion molecules along the vascular endothelium (i.e. selectins and integrins), facilitates the accumulation of leukocytes. This is a multistep process which starts with loose attachment to and rolling on the endothelium, followed by firm attachment to the endothelium and transmigration. Bacterial products, cytokines, components of the complement system (i.e. distinct plasma proteins that react with one another to help enhance antibodies and phagocytic cells to clear pathogens and damaged cells, promote inflammation and

attack the pathogen's cell membrane) and products of the lipoxygenase pathway then act as chemoattractants. These chemoattractants move the leukocytes toward the site of injury by a process called chemotaxis. These recruited leukocytes, mainly neutrophils and macrophages, are key in eliminating the agent via phagocytosis. The fast responding neutrophils predominate in the early phase and are replaced by more slow responding, but more long-lived, monocyte-derived macrophages.^[4,9]

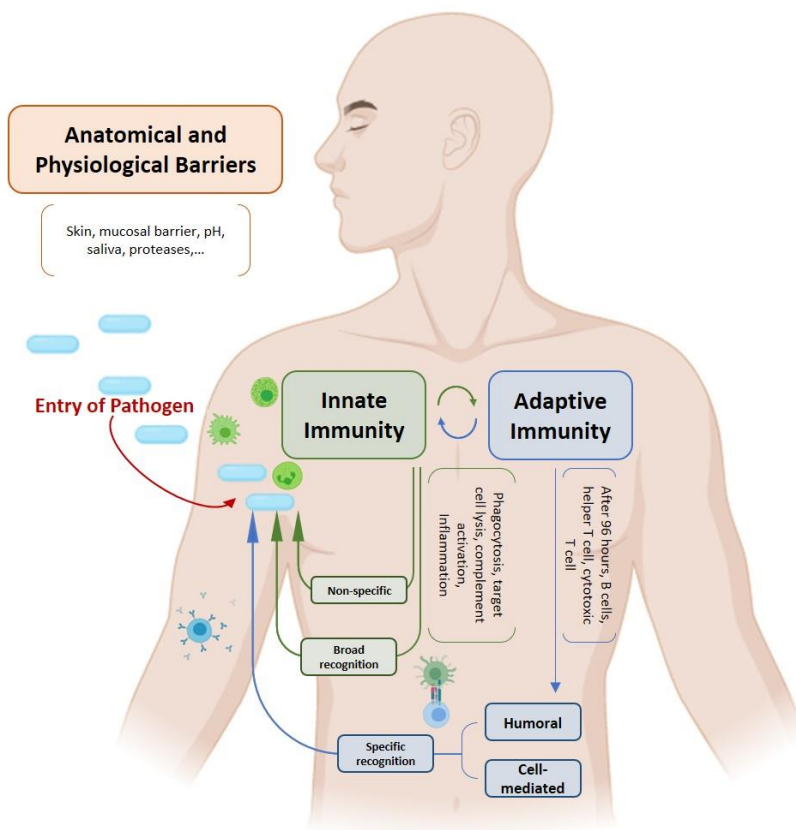


FIGURE 4.1: A PATHOGEN ATTEMPTING TO ENTER THE BODY FIRST ENCOUNTERS ANATOMICAL AND PHYSIOLOGICAL BARRIERS IN ORDER TO BLOCK THEIR ACCESS INTO THE BODY. HOWEVER, IF THE PATHOGEN MANAGES TO ENTER, MECHANISMS MEDIATED BY INNATE LEUKOCYTES ARE INDUCED DUE TO THEIR RELATIVELY BROAD RECOGNITION OF PAMPs. IF A MORE TARGETED, PATHOGEN-SPECIFIC RESPONSE BECOMES NECESSARY, ELEMENTS OF INNATE IMMUNITY THEN FACILITATE INDUCTION OF HIGHLY SPECIFIC ADAPTIVE RESPONSES INITIATED BY ENGAGEMENT OF THE ANTIGEN RECEPTORS OF B, HELPER T OR CYTOTOXIC T LYMPHOCYTES. ONCE ACTIVATED, LYMPHOCYTES MOUNT HUMORAL AND CELL-MEDIATED ANTI-PATHOGEN RESPONSES THAT ARE HIGHLY SPECIFIC. INNATE AND ADAPTIVE IMMUNE MECHANISMS THUS COLLABORATE TO ALLOW A FULL RANGE OF RESPONSES OF APPROPRIATE STRENGTH AND SPECIFICITY TO PROTECT THE HOST FROM ALL THREATS. FIGURE ADAPTED FROM BACON, F.^[6]

Pain, the fourth cardinal sign of inflammation, is due to activation of pain receptors, transmission and modulation of pain signals, neuro plasticity and central sensitization.^[9] The cells from the innate response attempt to control the pathogen until the highly specific and activated cells of the adaptive immune response are recruited by the innate immune cells in case of a relatively serious infection. In most cases, the situation is controlled by the innate defense before the adaptive immunity response is triggered. Nevertheless, the adaptive immunity is initiated when the foreign antigen is presented to B and T lymphocytes. The antigen receptors on the surface of a B cell are called B cell receptors (BCRs), whereas those on the T cell surface are known as T cell receptors (TCRs). The three major subgroups of lymphocytes are T helper cells (Th), cytotoxic T cells (Tc) and B cells, which are clonally selected and activated, followed by proliferation and differentiation into memory cells and effector cells that eliminate the pathogen via humoral and/or cell-mediated mechanisms. Since this comprises a time-consuming process, adaptive responses are usually not observed until at least 96 h after the start of infection. The interplay between the innate and adaptive immune response provides an optimal defense against pathogens: lymphocytes of the adaptive response require the involvement of cells and produced cytokines of the innate response to become activated and start differentiation, while activated lymphocytes stimulate and improve the effectiveness of innate leukocytes.^[6] When the inflammatory insult is finally resolved, the levels of pro-inflammatory mediators drops together with the number of acute inflammatory cells present in the tissue (e.g. neutrophils have a short lifespan). Moreover, a variety of stop signals are also triggered to terminate the pro-inflammatory process and switch to anti-inflammatory lipoxins or cytokines produced by macrophages and other cells. These specialized cells also clear microbial particles and damaged tissue by means of phagocytosis and initiate tissue repair. The ultimate objective is to clear the inciting insult and re-establish homeostasis.^[4,12]

4.2.2 CHRONIC INFLAMMATION

As described above, during acute inflammation, innate immune cells form the first line of immune defense. Moreover, they also regulate activation of the adaptive immune response. However, during chronic inflammation, adaptive immune responses can cause uninterrupted and excessive activation of the innate immune cells. Macrophages and T lymphocytes, which produce cytokines and enzymes that cause persistent and ongoing damage to cells if left unchecked, are the dominant cell types in chronic inflammation. In contrast to acute inflammation, chronic inflammation is characterized by infiltration with mononuclear cells, tissue destruction and attempts at healing, accomplished by angiogenesis and tissue fibrosis. Chronic inflammation is thus referred to as an inflammatory response lasting for prolonged periods of several weeks, months or even years, in which inflammation, tissue injury and attempts at repair coexist. It can follow a preceding acute inflammatory reaction, but can also begin insidiously. Chronic inflammation arises because of persistent infections that are difficult to eradicate (e.g. bacterial or parasitic infections), prolonged exposure to toxic agents (e.g. silica), but it also plays an important role in hypersensitivity diseases such as rheumatoid arthritis and allergies.^[4,13] In chronic inflammation, the normal regulation of the inflammatory response and thus homeostasis, is lost for an extended period. If inflammation fails to resolve, it may become pathological. Chronic inflammation is associated with non-communicable diseases such as cardiovascular diseases, cancer, diabetes, autoimmune disorders and neurodegenerative diseases.^[3,13,14]

4.3 NF- κ B SIGNALING IN INFLAMMATION

Activation of nuclear factor κ B (NF- κ B) is one of the main regulatory mechanisms of inflammation. It is a small family of inducible transcription factors that is ubiquitously present in almost all mammalian cells. The transcription factor modulates DNA transcription and is involved in a broad range of biological processes, including

immune responses (regulating the transcription of inflammatory proteins such as chemokines, cytokines, interleukins, interferons and cyclooxygenase-2), cell survival, differentiation, and proliferation. A tight regulation of NF- κ B maintains the balance of essential cell functions since deregulated activity is often observed in chronic inflammation and pathologies such as cancer.^[15-17]

4.3.1 THE NF- κ B FAMILY

The NF- κ B family consists of five structurally related members of the Rel family in mammals: NF- κ B1 (or p50/p105), NF- κ B2 (also called p52/p100), RelA (also named p65), RelB and c-Rel. These five proteins are able to mediate the transcription of target genes by binding to DNA via the κ B enhancer as homo/heterodimeric complexes.^[16,18] They all share a Rel homology domain at the N-terminal region, consisting of approximately 300 residues in their protein structure. This domain is responsible for dimerization, interaction with inhibitory kappa Bs (I κ Bs) proteins (more on this later), DNA binding and nuclear translocation.^[19,20] The NF- κ B family can theoretically form 15 potential NF- κ B dimers. The classic and most abundant NF- κ B dimer is represented by the p50/p65 heterodimer. However, not every combination of NF- κ B dimers is transcriptionally active. This is highly dependent on the transcription activation domain (TAD) on the C-terminal region, which only p65, RelB and c-Rel possess. NF- κ B1 and NF- κ B2, on the other hand, have a glycine-rich region instead of TAD. Their functional transcription factors, respectively p50 and p52, are products of partial proteolysis.^[17,20,21]

4.3.2 THE NF- κ B FAMILY SIGNALING PATHWAY

NF- κ B dimers need to translocate to the nucleus and bind to the specific DNA binding site in order to modulate transcription. In most resting cells, NF- κ B is retained in the cytosol and inactive through binding to I κ Bs proteins. This family of inhibitors consists of eight members: I κ B α , I κ B β , I κ B ϵ , I κ B ζ , Bcl-3, I κ BNS and the precursor proteins NF- κ B1

and NF- κ B2. Structurally, they all have 5 - 7 Ankyrin repeat domains in common, which mediates binding to the Rel homology domain of NF- κ B. Thus, masking the nuclear localization signal and therefore preventing nuclear translocation.^[17,22] To activate the NF- κ B transcription factor, the NF- κ B protein needs to be separated from the inhibitor. This step is performed by Inhibitory kappa B kinase (IKK) which phosphorylates the inhibitory I κ B protein, freeing the NF- κ B dimer. The IKK is a 500 to 900 kDa complex consisting of three subunits: IKK α (IKK1), IKK β (IKK2) and IKK γ (NF- κ B essential modulator, NEMO).^[16] The IKK α and IKK β subunits share 52% structure homology and are catalytically active, with 64% of similarity in their N-terminal kinase domain. The IKK γ subunit, however, is not structurally related and has an essential regulatory function. Activation of IKK α and IKK β regulates two different NF- κ B signaling pathways, called the canonical and non-canonical pathway, leading to the dissociation, and allows the translocation NF- κ B dimers from cytoplasm to the nucleus.^[23] A schematic overview of both pathways is summarized in Figure 4.2. The rapid and reversible inflammatory response mainly occurs through the canonical pathway, while the slower and irreversible immune cell differentiation and maturation processes takes place through the non-canonical pathway.^[24] The translocated NF- κ B complex binds to κ B sites, which is defined by sequence specific target DNA: 5'-GGGRNYYYCC-3', where R: purine, Y: pyrimidine and N: any nucleotide. These κ B sites are present in promoters of the target genes.^[25]

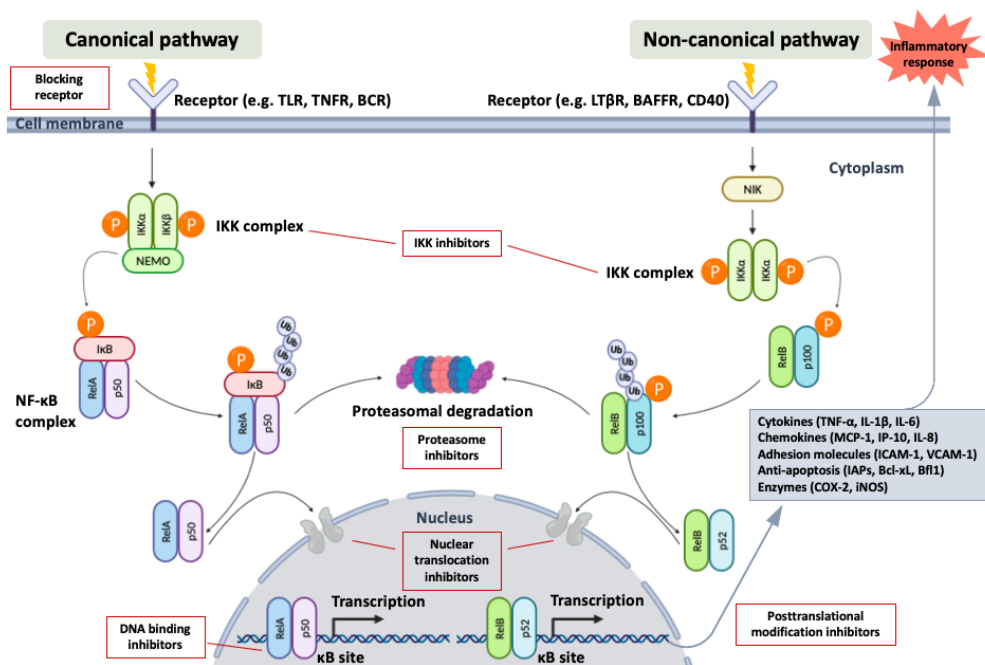


FIGURE 4.2: SCHEMATIC OF NF-κB PATHWAYS OF ACTIVATION, INDICATING TARGETS FOR INHIBITION. VARIOUS STIMULI RESULT IN THE ACTIVATION OF NF-κB THROUGH EITHER THE CANONICAL OR NONCANONICAL SIGNALING PATHWAYS. NUMEROUS INHIBITORS OF THE NF-κB PATHWAY HAVE BEEN IDENTIFIED, WITH THESE ABLE TO TARGET BOTH THE CANONICAL (CLASSICAL) AND NONCANONICAL SIGNALING PATHWAYS.

4.3.2.1 THE CANONICAL OR CLASSICAL PATHWAY

The canonical pathway responds to diverse pro-inflammatory stimuli, such as LPS, growth factors and cytokines like TNF- α . These ligands are recognized by extracellular and intracellular receptors including TLR, TNFR (tumor necrosis factor receptor), TCR and BCR. Once exposed to the stimulus, the receptors trigger signaling cascades that activate the IKK complex. Activated IKK phosphorylates two serine residues of the I κ B regulatory domain (e.g. serine 32 and 36 in I κ B α), resulting in polyubiquitination and subsequent degradation of I κ B by the proteasome.^[23] Ubiquitination requires the sequential actions of three enzymes: an activating enzyme (E1), a conjugating enzyme (E2) that carries the activated ubiquitin molecule as a thiol ester and eventually a ubiquitin-protein ligase (E3) which attaches ubiquitin to the target protein through an isopeptide bond between the C-terminus of ubiquitin and the ϵ -amino group of a lysine

residue in the target protein, tagging them for destruction by the proteasome.^[26,27] The liberated NF- κ B dimers, predominantly the p50/p65 and p50/c-Rel dimer, thus translocate into the nucleus and start gene transcription.^[16]

4.3.2.2 THE NON-CANONICAL OR ALTERNATIVE PATHWAY

The non-canonical pathway is activated by a select set of developmental signals or cell-differentiating stimuli, triggering the activation of receptors such as LT β R (lymphotoxin β receptor), RANK (receptor activator of NF- κ B), BAFFR (B cell activating factor receptor), CD40 (cluster of differentiation 40) and CD27. In this alternative pathway, NF- κ B activation does not involve I κ B α degradation, but focusses on processing the p100 NF- κ B2 precursor protein. This p100 protein not only serves as the precursor of p52, it also functions as an I κ B-like molecule which inhibits nuclear translocation of RelB. This pathway thus predominantly targets activation of the p52/RelB heterodimer complex. Upon receptor-ligand activation, the non-canonical NF- κ B pathway is activated by intracellular assembling of the adapter molecule complex (TRAF2, cIAPs, TRAF3), which further leads to the activation the enzyme NF- κ B-inducing kinase (NIK). Once activated, NIK functionally cooperates with IKK α to mediate p100 phosphorylation, which induces p100 ubiquitination and proteasomal processing. NIK partially phosphorylates the C-terminal region of p100 at serine 866 and 870 and also activates IKK α . IKK α phosphorylates p100 at multiple serine residues (Serine 99, 108, 115, 123, 872). The proteasomal processing of p100 results in generation of mature NF- κ B2 p52 and nuclear translocation of the non-canonical p52/RelB complex.^[16,28]

4.3.3 NF- κ B IN HUMAN PATHOLOGIES

NF- κ B is considered to be the “master switch” of the inflammatory response, regulating the transcription of an exceptionally large number of genes (more than 500 genes) involved in inflammation, cell proliferation and apoptosis.^[15] The constitutive activation

of NF- κ B contributes to the pathogenesis of a large number of diseases. This enormous list includes several types of cancer (such as esophageal cancer, colon cancer, acute myelogenous leukemia, melanoma, breast cancer and ovarian cancer)^[20,29], autoimmune diseases (e.g. rheumatoid arthritis, lupus, type I diabetes, multiple sclerosis, inflammatory bowel disease)^[30], cardiovascular diseases (including atherosclerosis, myocardial ischemia, cardiac hypertrophy and heart failure)^[31], but NF- κ B also plays a role in neuropathology (Alzheimer's disease, Huntington's disease and Parkinson's disease).^[32,33] Constitutive NF- κ B activity is seen in a significant number of human cancers, both in solid and hematopoietic malignancies, due to the inflammatory microenvironment (a process driven by inflammatory cells and pro-inflammatory mediators) and various oncogenic mutations. NF- κ B activation may also energize the immune system to favor tumor growth and to disable the immune system from attacking tumor cells, resulting in a subset of cells that escapes the surveillance and outperforms the immune system. In short, constitutive NF- κ B activity promotes upregulation of antiapoptotic and cell proliferation-associated genes (e.g. via upregulated expression of Cyclin D1, c-Myc, EGFR, Bcl-2, IAP proteins and TRAF), regulates angiogenesis (e.g. via VEGF), facilitating distant metastasis through epithelial mesenchymal transition and also increasing chemo- and radioresistance in diverse cancer types.^[20,29] Although NF- κ B is required for normal mammary gland morphogenesis (for example: NF- κ B activity is high during pregnancy, decreases during lactation, and increases again during involution), abnormal and constitutive NF- κ B activation has been demonstrated to drive tumor development and progression in breast cancer.^[34] It is considered to be a major marker for poor prognosis, associated specifically with a particularly aggressive estrogen receptor (ER)-negative and human epidermal growth factor receptor 2 (HER2)-positive breast cancer subtype known as inflammatory breast cancer (IBC).^[35,36] In acute myeloid leukemia, constitutive NF- κ B activation has been detected in 40% of the cases, enabling leukemia cells to escape apoptosis and stimulate proliferation.^[37] Rheumatoid arthritis (RA) is an autoimmune

disease, characterized by progressive joint destruction caused by chronic inflammation of the synovial lining. Activated NF- κ B and high levels of TNF- α , IL-1 and IL-6 have been detected in human synovial tissue in the early stage of inflammation, but also in specimens obtained at the later stages of the disease. This suggests that NF- κ B activation plays an essential role in both the initiation stage and perpetuation of inflammation in RA. Aggressive synovial tissue proliferation, called pannus, has been considered a late, inactive and irreversible manifestation of RA. Experimental evidence indicates that NF- κ B possibly facilitates this hyperplasia by promoting proliferation and inhibiting apoptosis of fibroblast-like synovial cells.^[38] Atherosclerosis is a disease which is also associated with chronic inflammation and is recognized by recruitment of circulating leukocytes into the vascular wall. Because of its involvement in angiogenic, apoptotic and neoplastic processes, constitutively activated NF- κ B is involved in the different stages of the disease: from the beginning of plaque formation to its destabilization and eventually its rupture. For example, NF- κ B activation is responsible for controlling the various chemokines and adhesion molecules that are necessary for chemotaxis and the migration of leukocytes across the endothelium, as well as migration of smooth muscle cells, thus remodeling the extracellular matrix. Moreover, the canonical pathway plays an essential role in regulating the thrombotic mediators, including tissue factor (TF), matrix metalloproteinases (MMPs) and inflammatory cytokines.^[39,40] Alzheimer's disease is the most common form of dementia, in which excessive build-up of amyloid protein leads to cell death, brain atrophy, and cognitive and functional decline. However, this hypothesis has not led to successful treatment of the disease. Chronic inflammation is a shared mechanism in the initiation and progression of multiple neurodegenerative diseases. NF- κ B in the nervous system can be activated by growth factors and synaptic transmission such as glutamate. Impairment of the NF- κ B pathway has been shown to cause homeostatic abnormalities in the brain because of neuroinflammation, activation of microglia, oxidative stress related complications and apoptotic cell death. IL-1 β and TNF- α have been detected at

an increased level in the brains of these patients. This increased cytokine level in the brains could be a result of NF- κ B action due to microglial amyloid beta stimulation. Therefore, the alternate hypothesis to the amyloid hypothesis suggests that NF- κ B activation and neuroinflammation could be the point of convergence of multiple pathways associated with the development of Alzheimer's disease.^[32,33,41-43]

4.3.4 THE NF- κ B PATHWAY AS POTENTIAL TARGET FOR DRUG DISCOVERY

As described above, NF- κ B controls multiple genes involved in chronic inflammation and different human diseases. The NF- κ B signaling pathway thus makes an interesting target for therapy at various levels of regulation. More than 700 inhibitors of the NF- κ B activation pathway have been described, including: antioxidants, peptides, small RNA/DNA, microbial and viral proteins, small molecules, and engineered dominant-negative or constitutively active polypeptides (see Figure 4.3 for structures of various examples). Some of these are more general inhibitors, while other molecules target specific or multiple steps in the cascade.^[44] Inhibitors can potentially target one of the essential key points in the NF- κ B pathway: kinases, phosphatases, ubiquitination, nuclear translocation, DNA binding, protein acetyl transferases and methyl transferases.^[45] Initial NF- κ B activation requires the ligand docking to its receptors. One strategy for inhibiting activation of NF- κ B is thus to block the signal before it activates IKK. This can be achieved, for example, by blocking TNF receptor or by using anti-TNF antibodies (infliximab, etanercept, adalimumab, golimumab and certolizumab).^[46] Since the phosphorylation reaction is a common step of many NF- κ B activating pathways, inhibiting the kinase activity of IKK is considered an interesting approach. This inhibition can be achieved by binding to the subunits of IKK. Adenosine triphosphate analogs, such as β -carboline and the synthetic quinazoline analogue SPC-839, show some specificity for interacting with IKK. Compounds, like BMS-345541, have allosteric effects on the IKK structure. Another group of compounds, including parthenolide, arsenite and some epoxyquinoids, interact with a specific cysteine

residue (Cys-179) in the activation loop of IKK β .^[45] Other interesting options are proteasome inhibitors and I κ B ubiquitination blockers, resulting in stabilizing I κ B proteins and thereby preventing nuclear NF- κ B translocation.^[47] An interesting proteasome inhibitor is bortezomib, which has been approved by the FDA in 2003 to treat multiple myeloma.^[37] Among I κ B ubiquitination blockers, Yersinia virulence factor YopJ acts as a deubiquitinase to inhibit NF- κ B activation.^[48] Preventing nuclear translocation is yet another therapeutic approach. Small peptides, such as the synthetic SN50, cross the cell membrane and block the nuclear translocation of the NF- κ B dimer through competition for the machinery responsible for the nuclear translocation of NF- κ B.^[49] Dehydroxymethylepoxyquinomicin has also been reported to effectively block NF- κ B nuclear translocation, with shown therapeutic effectivity in preclinical models of multiple autoimmune diseases, including RA.^[50-52] The most direct strategy, however, is blocking NF- κ B binding to specific κ B sites on DNA. This can be achieved by some sesquiterpene lactones as well as synthetic double-stranded DNA oligodeoxynucleotides (ODNs).^[53] ODNs are short synthetic nucleotide sequences acting as decoy cis elements, mimicking the NF- κ B consensus and thus entrapping NF- κ B subunits, resulting in inhibition of target gene transcription. NF- κ B ODNs are being investigated in several chronic inflammatory-based diseases and also appear to be successful in the clinic to suppress restenosis after nonsurgical interventions for the treatment of coronary diseases.^[54] NF- κ B activity is also altered by extensive posttranslational modifications of the subunits, altering both the strength and duration of NF- κ B activity. Acetylation, for example, results in either enhanced activation or reduced DNA binding specificity and nuclear export, depending on the specific lysine residues targeted.^[55] Vorinostat and romidepsin are two examples of histone deacetylase inhibitory chemotherapeutic drugs against T cell lymphomas.^[56]

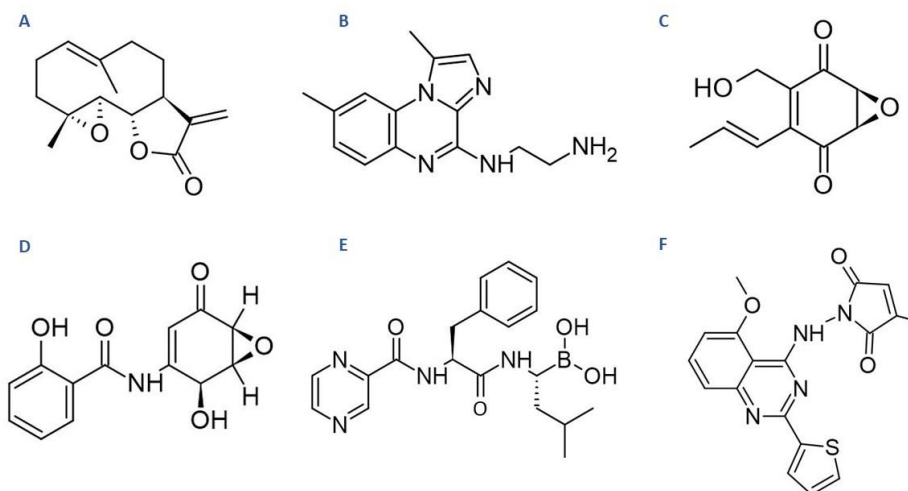


FIGURE 4.3: STRUCTURES OF SEVERAL SMALL MOLECULES, WHICH ARE KNOWN NF-κB PATHWAY INHIBITORS. (A) PARTHENOLIDE (A SESQUITERPENE LACTONE), WHICH INTERACTS WITH CYS-179 IN THE ACTIVATION LOOP OF IKKβ; (B) BMS-345541, WHICH HAS AN ALLOSTERIC EFFECTS ON THE IKK STRUCTURE; (C) EPOXYQUINONE A MONOMER (AN EPOXYQUINOID), WHICH ALSO INTERACTS WITH THE CYSTEINE RESIDUE IN THE ACTIVATION LOOP OF IKKβ; (D) DEHYDROXYMETHYLEPOXYQUINOMICIN, WHICH EFFECTIVELY BLOCKS NF-κB NUCLEAR TRANSLOCATION; (E) BORTEZOMIB, ACTING AS A PROTEASOME INHIBITOR; (F) SPC-839 (A SYNTHETIC QUINAZOLINE ANALOGUE), KNOWN TO INTERACTS WITH IKK.

To conclude, NF-κB has attracted widespread interest because of the variety of stimuli that activate it, the diverse genes and biological responses that it controls, and because NF-κB inhibition could be beneficial in treating inflammatory diseases. NF-κB inhibition is already successfully used for the treatment of a variety of malignancies. There are, however, questions regarding safety as well as long-term use, since NF-κB plays a central role in homeostasis and is also required for maintaining normal immune responses and cell survival. For example, IKK inhibitors have shown promise in preclinical studies, but relatively few IKK inhibitors have made it to clinical trials. A more promising use of NF-κB inhibitors are cases where the inhibitor is applied topically, locally or in a highly directed fashion (e.g. to a specific tumor type).^[38] A future goal will be to discover molecules that can inhibit distinct NF-κB complexes induced by selected stimuli in specific cell types. Nevertheless, it is certainly possible that the long-term systemic ingestion of low-dose NF-κB inhibitors may have general beneficial effects in

reducing inflammation and possibly cancer.^[20,57] This is an interesting hypothesis, which fits well with the basic idea that a “healthy and balanced diet”, abundant in numerous types of phytochemicals, exerts a protective action on human health. Epidemiological studies correlate flavonoid intake with a reduced incidence of chronic diseases. These bioactive compounds have the ability to act on several molecular targets and to act as cellular signals, e.g. altering signal transduction events or gene expression, even at very low concentrations.^[58-62]

4.4 THE CYCLOOXYGENASE PATHWAY IN INFLAMMATION

4.4.1 THE CYCLOOXYGENASE ISOENZYMES

Cyclooxygenase, also called prostaglandin endoperoxide synthase (PTGS), is the rate-limiting enzyme that plays a pivotal role in the conversion of arachidonic acid (AA) to the prostaglandin (PG) precursor PGH₂. COX enzymes have elaborate roles in human physiology as well as pathology, because of their involvement in cardiovascular, neuronal, renal, immune, gastrointestinal and reproductive systems.^[63,64] Three isoforms of COX have been identified: COX-1, COX-2 and COX-3.^[65] Each isoform possesses similar activities, but they mainly differ in expression characteristics and inhibition profiles by NSAIDs. COX-1 is expressed constitutively in many cells and tissues and is thus often called the housekeeping enzyme (the COX-1 gene possesses a typical GC-rich housekeeping promoter), synthesizing prostanoids involved in homeostasis and normal physiological functioning. COX-2, on the other hand, has negligible basal expression, although basal expression does occur in the stomach, kidney, central nervous system and the female reproduction system. COX-2 expression can be induced strongly and rapidly by a variety of growth factors (e.g. PDGF or EGF), pro-inflammatory cytokines (e.g. TNF- α and IL-1), LPS, hormones (such as luteinizing hormone), mitogens and oncogenes. Moreover, NF- κ B is a key regulator of COX-2 expression.^[66-68] COX-3, which was discovered more recently, is a splice variant of COX-1. COX-3 protein and

mRNA have been identified in human tissues, most abundantly in the cerebral cortex and the heart. This isoenzyme is inhibited by paracetamol and is considered to play a role in biosynthesis of prostanoids that mediate fever and pain. However, controversy about this COX-3 inhibition and its mechanism in humans still exists. The mechanism for conversion of COX-3 mRNA to the active enzyme has also not completely been elucidated yet.^[69,70] The main focus of this subchapter will thus be on COX-1 and COX-2. The COX enzymes function as homodimers and are covalently membrane-bound to the endoplasmic reticulum. The COX-1 and -2 isoenzymes are quite structurally homologous and share about 60% sequence identity and are characterized by three major folding domains: an N-terminal epidermal growth factor-like domain, a membrane-binding domain (an adjoining region) and a catalytic domain with two distinct active sites. These two interconnected enzymatic sites, known as the peroxidase active site (which contains heme) and the cyclooxygenase active site, are the core structures of the catalytic domain. The cyclooxygenase active site comprises about 80% of the protein and forms a long, narrow, largely hydrophobic channel from the C-terminal to the membrane-binding domain. The structural difference between both isoforms can be found in this active site: A valine at position 523 in COX-2 instead of a bulkier isoleucine residue at the same position in COX-1, creates an extra hydrophobic side pocket in COX-2. Additionally, COX-2 also contains a valine at position 434 instead of isoleucine, which improves accessibility to this side pocket. These differences thus result in a 20% larger and more accessible channel in COX-2. A third difference can be found at the 513 position, where arginine is located instead of histidine. This does not alter the shape, but instead changes its chemical environment. This substitution allows COX-2 to interact with more polar moieties.^[63,71] An overview of these structural differences between the substrate-binding channels of COX-1 and -2 can be found in Figure 4.4.

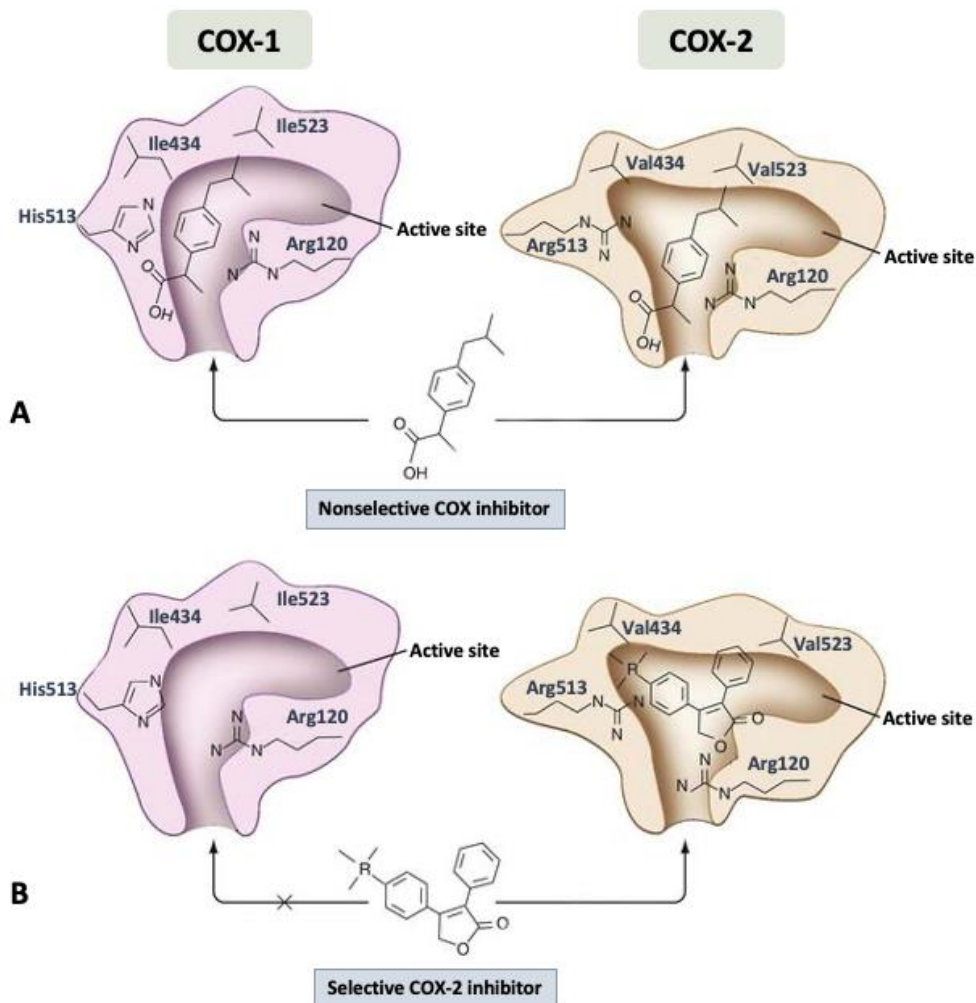


FIGURE 4.4: SCHEMATIC VIEW OF THE STRUCTURAL DIFFERENCES BETWEEN THE SUBSTRATE-BINDING CHANNELS OF COX-1 AND COX-2, ILLUSTRATING THE BINDING OF SELECTIVE COX-2 INHIBITORS. THE AMINO ACID RESIDUES VAL-434, ARG-513 AND VAL-523 FORM A SIDE POCKET IN COX-2 THAT IS ABSENT IN COX-1. (A) NONSELECTIVE INHIBITORS HAVE ACCESS TO THE BINDING CHANNELS OF BOTH ISOFORMS. (B) THE MORE VOLUMINOUS RESIDUES IN COX-1, ILE-434, HIS-513 AND ILE-523, OBSTRUCT ACCESS OF THE BULKY SIDE CHAINS OF COX-2 INHIBITORS. FIGURE MODIFIED FROM GROSSER ET AL.^[72]

4.4.2 BIOCHEMISTRY AND FUNCTIONS OF PROSTANOIDS

As mentioned before, prostanoids are a subclass of eicosanoids and include prostaglandins (PGE₂, PGD₂, PGF_{2α}), thromboxanes (TXA₂) and prostacyclins (PGI₂). Prostaglandins act as hormone-like bioactive substances, are released rapidly in response to extracellular hormonal stimuli and mediate autocrine and paracrine

signaling over short distances. They are involved in many different physiological and pathological processes. The COX enzymes synthesize prostanoids, starting from AA, in three steps: (1) mobilization of AA from membrane phospholipids via the enzymatic activity of phospholipase A₂; (2) biotransformation of AA in a bifunctional manner. COX generates an unstable PGG₂ by the cyclooxygenase reaction, which immediately converts into PGH₂ through the peroxidase reaction. These two activities occur at distinct, but interactive sites within the COX protein; (3) PGH₂ is converted into specific prostanoids through the action of downstream synthases and isomerases.^[63] These prostanoids then act via specific G-protein-coupled receptors (GPCRs), designated EP for PGE₂ receptors, and FP, DP, IP and TP for PGF_{2α}, PGD₂, PGI₂, and TXA₂ receptors, respectively.^[73] PGD₂ and PGE₂, as well as PGI₂, are potent vasodilators in the cardiovascular system. TXA₂, on the other hand, acts as a vasoconstrictor and also plays an important role in the induction of platelet aggregation. Contrarily, PGI₂ shows anticoagulant properties. In the gastrointestinal tract PGE₂, PGF_{2α} and PGI₂ have protective effects on the gastric mucosa. These PGs lower the acid secretions, enhance the mucosal blood flow and stimulate the mucus formation and bicarbonate secretion. PGs also present effects in the lungs: PGF_{2α} and TXA₂ act as bronchoconstrictors, whereas PGI₂ and PGE₂ are bronchodilators. In the kidney, PGE₂ assist in the regulation of vascular tone, blood flow, salt and water excretion. PGs are also involved in many aspects of reproduction in females. The synthesis of PGE₂ and PGF_{2α} is significantly increased during labor; PGE₂ and PGF_{2α} strongly contract the uterine smooth muscle. Prostanoids are also extremely important in mediating the inflammatory response. Furthermore, PGE₂ is also the most important pro-inflammatory PG involved in the typical cardinal symptoms of inflammation. As mentioned above, PGE₂ mediates vasodilatation and increases microvascular permeability resulting in redness and swelling in the inflamed area.^[74,75] Hyperalgesia results from the action of PGE₂ on peripheral sensory neurons and on central sites within the spinal cord and the brain, where it lowers the threshold for pain.^[76] An overview is summarized in Figure 4.5.

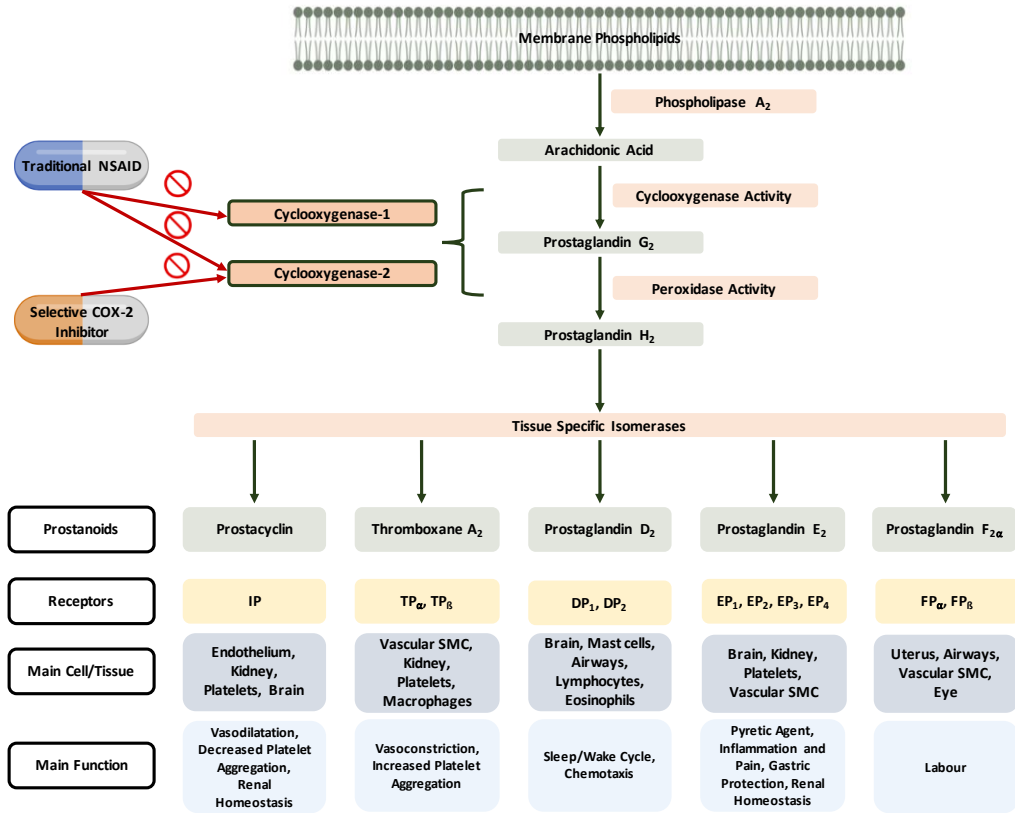


FIGURE 4.5: BIOSYNTHESIS AND ACTIVITIES OF PROSTAGLANDINS AND SITE OF NSAIDS AND SELECTIVE COX-2 INHIBITOR ACTIONS. CYCLOOXYGENASE METABOLISM OF ARACHIDONIC ACID LEADS TO THE FORMATION OF PROSTAGLANDINS THAT EXERT A VARIETY OF BIOLOGICAL ACTIVITIES THROUGH THEIR RESPECTIVE RECEPTORS.

4.4.3 CYCLOOXYGENASE-2 IN HUMAN PATHOLOGIES

COX-2 is an interesting target of pharmaceutical intervention to treat inflammation, pain and fever. Furthermore, COX-2 also appears to play a major role in numerous degenerative conditions, including several kinds of cancers, but also autoimmune, cardiovascular and neurological diseases.^[63] COX-2 exerts a pleiotropic and multifaceted role in the genesis of cancer, and is also required throughout the entire evolutionary process of cancer development and progression.^[77] In many types of cancer, COX-2 is frequently expressed and high levels have been found in breast, lung, prostate, bladder, pancreatic, skin, esophageal, gastric and colorectal tumors. In affected patients, COX-2 overexpression is a marker indicating worse prognosis since it

is related to a reduction in survival, a higher cancer recurrence, as well as resistance to chemo- and radiotherapy.^[78-86] As mentioned before, COX-2 expression can dramatically increase by various pro-inflammatory stimuli.^[87] Important cancer-causing factors are also known to be COX-2 inducers, including: nicotine and its metabolites, a variety of other compounds in tobacco smoke (such as benzo(a)pyrene), radiation, ultraviolet B, free radicals, hypoxia, hormones, oncogenes, growth factors, endotoxins and infectious agents (e.g. *Helicobacter pylori* and Human papilloma virus).^[88] The COX-2 gene possesses an enhancer-box (E-box) and a TATA box and contains several potential transcriptional regulatory elements to which specific transcription factors can bind, including two NF- κ B binding sites, but also two cyclic AMP response elements (CRE), a CAAT enhancer binding protein (C/EBP) or nuclear factor for IL-6 expression (NF-IL6)) motif, a peroxisome proliferator response element (PPRE), a sterol response element (SRE), a specificity protein 1 (SP1) site and two activator protein-2 (AP-2) sites.^[68,89] In a large number of solid tumors increased levels of PGs (mainly PGE₂), as well as other pro-inflammatory products, are secreted by cancer cells, stromal cells and immune cells to the tumor microenvironment, with NF- κ B as a central upstream mediator. COX-2 is not only able to induce inflammation, but also displays multitasking roles that promote cancer: apoptotic resistance (delay in G1 phase, induction of survivin, Mcl-2 and Bcl-2, plus repression of caspase-3), angiogenesis (e.g. upregulation of VEGF), tumor growth (including the upregulation of EGFR), cancer stem cell-like activity (such as activation of WNT/ β -catenin/TCF pathway), cancer cell survival (through interaction with PI3K/AKT), immunosuppression in the tumor milieu (blocking the activity of cytotoxic T lymphocytes and increasing the activity of regulatory T cells), invasion (e.g. upregulation of ERK), metastasis (upregulation of MMPs type 2 and 9), multidrug resistance, chemoresistance and tumor recurrence.^[67] Upregulated COX-2 activity and elevated levels of PGs have been diagnosed in the synovial fluid and membrane of RA patients. Specifically, PGE₂ has been associated with the contribution to the pathogenesis of RA, playing a role in edema and the progressive erosion of

cartilage and juxta-articular bone.^[90-92] In atherosclerosis, evidence seems to suggest that increased COX-2 expression is also critical in the evolution of atherosclerotic plaques towards instability. COX-2 modulates angiogenesis within the lesion and thus contributes to the formation of new blood vessels, allowing the plaque to expand. Moreover, PGE₂ induces the expression and production of 2 metalloproteinases in macrophages, MMP-2 and MMP-9, which are considered crucial in the degradation of carotid plaque stability. In patients with atherosclerosis, the endothelium increases the release of PGI₂, which is an inhibitor of platelet activation and is responsible for cholesterol accumulation. Furthermore, the antiproliferative and antimigratory actions of COX-2 on smooth muscle cells could contribute towards a smooth muscle cell-depleted and macrophage-enriched plaque, rendering the plaque more vulnerable.^[93] Increased COX-2 expression and elevated PGE₂ levels in the brain have also been associated with pro-inflammatory activities, linking it to neurodegenerative diseases. Evidence of a direct role of COX-2 on neurological diseases, such as multiple sclerosis, amyotrophic lateral sclerosis, Parkinson disease and Alzheimer disease, remains controversial.^[94-96] COX-2 is expressed under normal conditions in the central nervous system, contributing to fundamental brain functions (e.g. synaptic activity), and neuroinflammation appears to be more controlled (and mainly sustained by the local microglia cells) than inflammation in peripheral tissues. However, findings demonstrate that COX-2 is activated during the course of Alzheimer disease development and progression.^[94,97] Moreover, the dysregulated production of PGs can upregulate the production of amyloid- β and seems to be associated with the hyperphosphorylation of tau, affecting its aggregation and deposition.^[98]

4.4.4 CYCLOOXYGENASE INHIBITORS

Nonsteroidal anti-inflammatory drugs block the biosynthesis of PGs through inhibition of COX enzymes. NSAIDs are amongst the most commonly used medications in the world, either by prescription or over-the-counter, with more than 30 million people

worldwide using these drugs daily for their efficient anti-inflammatory, analgesic and antipyretic properties.^[99] NSAIDs are used as first-line therapeutics in the symptomatic treatment of osteoarthritis, rheumatoid arthritis and systemic lupus erythematosus.^[100] To further illustrate, more than 111 million prescriptions for NSAIDs in the USA are written annually, accounting for almost 60% of the over-the-counter analgesic market in the USA.^[99] NSAIDs share similarities in their mechanism of action, but they differ slightly in the manner they each interact with the COX enzyme (see Figure 4.6). Most NSAIDs reversibly bind to the active site in the COX enzymes. Acetyl salicylic acid or aspirin, for instance, irreversibly inhibits the COX enzyme by acetylating it, while other NSAIDs (such as ibuprofen and naproxen) bind reversibly. All currently marketed NSAIDs are inhibitors of both COX-1 and COX-2, with differences in their degree of selectivity. NSAIDs can thus also be differentiated by their specificity for inhibition of the two COX isoenzymes: nonselective COX-1 and COX-2 inhibitors (e.g. acetyl salicylic acid, ibuprofen, diclofenac, ketoprofen, indomethacin and naproxen), preferential COX-2 inhibitors (e.g. meloxicam, nimesulide and etodolac) and selective COX-2 inhibitors (e.g. celecoxib and rofecoxib). To illustrate: aspirin diffuses quickly into the active pocket of COX, undergoes weak binding with Arg-120 and is thus perfectly positioned for optimal acetylation of Ser-530. Because of the larger active pocket in COX-2, the orientation differs slightly and acetylation of Ser-530 is much weaker than in COX-1. This increases the selectivity of aspirin for COX-1. Indomethacin, for example, causes a slow and time-dependent competitive inhibition by penetrating very deeply into the channel of COXs. Due to tight complex forming, acting by ionic interactions between the carboxylic function and the arginine residue of the enzyme, the effect is extended and requires a longer wash-out time. Ibuprofen is an example of a time-independent competitive inhibitor, binding rapidly to the active site as well as leaving the site quickly.^[101-103] With regard to the most common serious adverse events, it is important to take a closer look at the role of the isoenzymes. Drugs with a higher selectivity towards COX-1 cause more detrimental gastrointestinal side effects. As

described before, COX-1 derived PGE₂ and PGI₂ play a protective role in the gastric mucosa: reduction of gastric acid secretion, enhanced thickness of the mucus layer, bicarbonate secretion and increased mucosal blood flow. Blocking COX-1 thus increases the risk of upper and lower gastrointestinal side effects, ranging from mild irritation to more severe adverse events such as bleeding and perforation. To reduce the associated gastrointestinal side effects, selective COX-2 inhibitors were introduced. The chemical structures of COX-2 inhibitors are heterogenic, belong to two major structural classes: tricyclics (also known as ortho-diaryl heterocycles or carbocycles) and non-tricyclics (possessing acyclic central systems such as olefinic, iminic, azo, acetylenic and α,β -unsaturated ketone structures).^[104] In spite of the initial success after the launch of selective COX-2 inhibitors, such as celecoxib and rofecoxib, concerns were raised regarding their potential adverse cardiovascular events. A well-known downfall of a blockbuster drug happened to rofecoxib, known under the trade name Vioxx. Rofecoxib was withdrawn voluntarily by Merck from the market in 2004 because of increased cardiovascular risks, which were observed in the Adenomatous Polyp Prevention on Vioxx (APPROVe) study. Compared to naproxen, this selective COX-2 inhibitor caused fatal heart attacks and strokes during this study.^[105] The FDA estimated that, during its 5 years sales on the market, Vioxx was responsible for at least 140 000 heart attacks or strokes and 55 000 deaths in the United States.^[106] A similar withdrawal happened to valdecoxib, known as Bextra, which was suspended by Pfizer in 2005 after seeing a higher prevalence of serious cardiovascular adverse events.^[107] Selective COX-2 inhibition is believed to tip the balance between the levels of COX-2 generated vasodilatory and atheroprotective PGI₂ and COX-1 synthesized prothrombotic and vasoconstrictor TXA₂. This imbalance could increase the possibility of a thrombotic cardiovascular event. However, studies that were prospectively designed to assess the relative cardiovascular safety of selective COX-2 inhibitors and traditional NSAIDs (both in populations with mixed baseline cardiovascular risk and in patients with elevated baseline risk), show a similar degree of harmful cardiovascular effects with traditional

NSAIDs. Observational studies and meta-analyses of observational studies suggest that the use of these traditional NSAIDs is thus not free of cardiovascular risk. Diclofenac, for example, often appears at the higher end of the spectrum of cardiovascular risk.^[108-114] Aspirin, however, is a special case since it prevents, rather than triggers, cardiovascular events. This mechanism involves the unique pharmacology of aspirin, which acts as an irreversible inhibitor of COX. In platelets, blocking COX-1 selectively targets TXA₂, causing an antiplatelet effect that lasts for the lifetime of the platelet since platelets are anucleate and lack the machinery to synthesize new enzyme.^[115] The risk of cardiovascular adverse events during treatment with NSAIDs could depend on a complex interplay of factors including COX-2 selectivity and drug exposure, as determined by dose, duration of action as well as duration of treatment, which act synergistically to determine the level of risk with a particular medicine.^[116]

It should also be mentioned that inhibition of COX-2 could also aid in prevention and therapeutic outcomes in different kinds of cancer. In 2007, Harris et al. comprehensively reviewed the published scientific literature on NSAIDs and cancer. They found that the daily use of selective COX-2 inhibitors (standard dosage, taken for two or more years) resulted in a significant risk reduction of 71% for breast cancer, 55% for prostate cancer, 70% for colon cancer and 79% for lung cancer, thus showing potential for the chemoprevention of these types of cancer. Nonselective NSAIDs, such as aspirin, ibuprofen and naproxen, also produced significant risk reductions, although less strong than selective COX-2 inhibitors. Paracetamol, on the other hand, did not produce a significant change.^[77,117] These results suggest that strongly upregulated COX-2, and as a consequence the prostaglandin cascade, plays a significant role in human carcinogenesis and inhibiting this step has potential for cancer intervention. COX-2 inhibitors are also able to sensitize cancer cells to treatments like radiotherapy and chemotherapy, which are known to induce COX-2 expression in cancer cells. Compared to standard cancer therapies, COX-2 inhibitors are relatively inexpensive and

have more tolerable side effects. It could thus be advisable to use COX-2 inhibitors as an adjuvant with chemo- or radiotherapy.^[67,118]

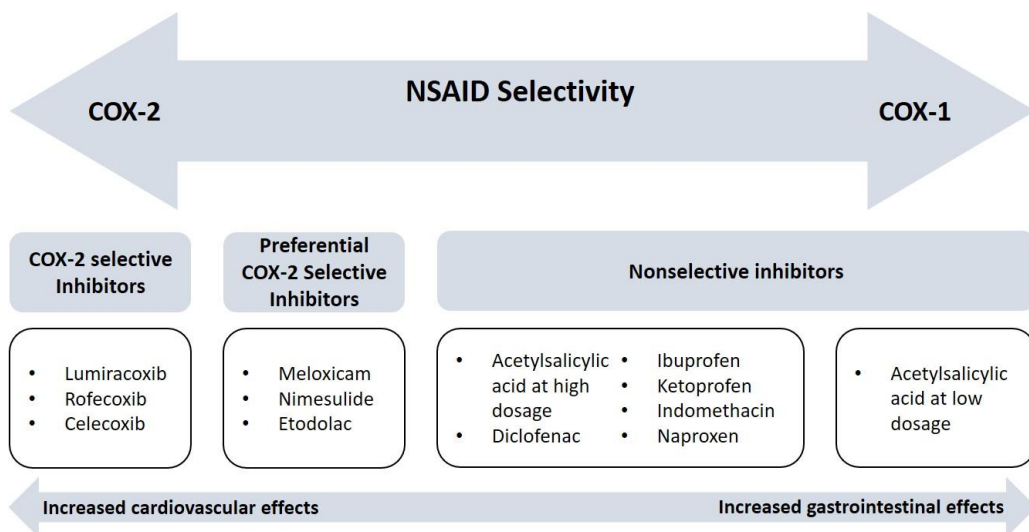


FIGURE 4.6: SCHEMATIC OVERVIEW OF THE SELECTIVITY OF NSAIDS FOR COX-1 AND COX-2 ENZYMES. ALL CURRENTLY MARKETED NSAIDS ARE INHIBITORS OF BOTH COX-1 AND -2, WITH DIFFERENCES IN THEIR DEGREE OF SELECTIVITY: NONSELECTIVE INHIBITORS, PREFERENTIAL COX-2 INHIBITORS AND SELECTIVE COX-2 INHIBITORS. AN NSAID THAT IS MORE SELECTIVE TO COX-2 MAY BE A SAFER OPTION FOR PATIENTS AT HIGH RISK FOR GASTROINTESTINAL ADVERSE EFFECTS. HOWEVER, NSAIDS THAT ARE MORE SELECTIVE FOR THE COX-2 ISOFORM HAVE BEEN ASSOCIATED WITH AN INCREASED RISK IN CARDIOVASCULAR ADVERSE EFFECTS.

To conclude, NSAIDs have been used to treat inflammation, pain and fever. They show promising results as chemopreventive agents and may allow future use as adjunctive treatments in cancer. Even though some NSAIDs are readily available over-the-counter and have a wide use in the general population, especially among the elderly who frequently use them on a long-term basis, the risk-benefit balance should not be underestimated. NSAIDs can have serious gastrointestinal and cardiovascular side effects and are among the ten top groups of medication associated with serious medication errors.^[119]

MATERIALS AND METHODS

4.5 NF- κ B LUCIFERASE REPORTER GENE ASSAY

4.5.1 REAGENTS

Murine fibrosarcoma L929 cells were purchased from ATCC (VA, USA) and transfected with a TNF-induced NF- κ B driven luciferase reporter gene construct by the lab of Protein Chemistry, Proteomics and Epigenetic Signaling (PPES) at the University of Antwerp. Dulbecco's modified eagle medium (DMEM), fetal bovine serum (FBS), phosphate buffered saline (PBS), penicillin, streptomycin and TNF- α (specific activity: 5.0×10^7 - 2.0×10^8 units/mg) were purchased from Gibco (NY, USA). DMSO (Uvasol), isopropanol, thiazolyl blue tetrazolium bromide (MTT) and dexamethasone were provided by Sigma-Aldrich (MO, USA). The luciferase assay system with reporter lysis buffer was purchased from Promega (WI, USA).

4.5.2 L929 CELL CULTURE

Murine fibrosarcoma L929 cells transfected with a TNF-induced NF- κ B driven luciferase reporter gene construct were cultured in DMEM supplemented with 10% heat-inactivated FBS, penicillin (100 units/mL) and streptomycin (100 μ g/mL) in a humidified incubator under a 5% CO₂ atmosphere at 37 °C. The L929 cells were seeded in 24-well plates at a cell density of 100 000 cells/well and incubated for 24 h before testing.

4.5.3 SAMPLE PREPARATION

All samples were dissolved in DMSO and aliquots of the stock solution were stored at -20 °C. Stock solutions of the samples were diluted in DMEM supplemented with penicillin and streptomycin, in order to obtain a maximal concentration of 0.1% DMSO.

After aspirating the old medium from the cells, the diluted samples were added to the wells and the plates were incubated for 1 h. Test samples included a non-biotransformed *Filipendula ulmaria* extract (20, 50 and 100 µg/mL) and a mixed sample (i.e., mix) composed of aglycons present after 72 h of fermentation (end concentrations in the assay were 20 µM of gallic acid and salicylic acid, 6 µM of quercetin and 4 µM of syringic acid). Dexamethasone at a concentration of 1 µM was used as a positive control. Solvent vehicle (DMSO) did not exceed 0.1% in the final test solutions.

4.5.4 NF-κB LUCIFERASE REPORTER GENE ASSAY

The seeded L929 cells were pre-incubated with test samples for 1 h (37 °C), subsequently followed by a stimulation of 10 ng/mL recombinant mouse TNF-α for an additional 3 h (37 °C). The reporter quantitation was done following the manufacturer's protocol from Promega. To summarize: after aspirating cell medium, the L929 cells were lysed with reporter lysis buffer, which requires one single freeze-thaw cycle to achieve complete lysis. Lysates were vortexed, centrifuged at 12 000 g for 15 sec and stored at -80 °C until analysis. Reading was done using the GloMax 96 Microplate Luminometer from Promega (WI, USA). In a black 96-well plate (Greiner Bio-One, Vilvoorde, Belgium), 20 µL of cell lysate was pipetted manually per well, followed by the automatic addition of 100 µL Luciferase Assay Reagent per well in the GloMax 96 Microplate Luminometer. The produced light was measured for a period of 10 sec after a delay time of 2 sec.

4.5.5 CELL VIABILITY ASSAY

An MTT assay was carried out to evaluate the cytotoxicity of the test samples. The seeded L929 cells were pre-incubated with samples for 1 h, subsequently followed by a stimulation of 10 ng/mL recombinant mouse TNF-α for 3 h. The medium was removed and the cells were treated with 200 µL of an MTT solution during 30 min at 37 °C. The

MTT assay involves the conversion of the water-soluble yellow dye MTT, 3-(4,5-dimethylthiazol-2-yl)-2,5-diphenyltetrazolium bromide, to an insoluble purple formazan by the action of mitochondrial reductase. Subsequently, the formazan was then solubilized with 150 μ L per well of an isopropanol:DMSO (9:1; v/v) solution. The concentration of formazan was determined by measuring the optical density at 550 nm using a Biotek Eon plate reader (Agilent Technologies, CA, USA).

4.6 COX-1 AND COX-2 ENZYME INHIBITION

4.6.1 REAGENTS

Ultrapure water with a resistivity of 18.2 M Ω -cm at 25 °C was generated with a Millipore purification system (Merck, Darmstadt, Germany). Reagents for the *in vitro* COX-1 and -2 enzyme inhibition assays were purchased as follows: DMSO (Uvasol), formic acid, TRIS/HCl, epinephrine hydrogen tartrate, porcine hematin and celecoxib from Sigma-Aldrich (MO, USA). Indomethacin was purchased from MP Biomedicals (Huissen, The Netherlands). Na₂EDTA (Titriplex III) was from purchased from VWR International (Leuven, Belgium). Arachidonic acid, purified COX-1 from ram seminal vesicles and human recombinant COX-2 are from Cayman Chemical (MI, USA). The competitive PGE₂ EIA kit was purchased from Enzo Life Science (NY, USA).

4.6.2 SAMPLE PREPARATION

A stock solution of extracts and compounds in DMSO (Uvasol) was stored as aliquots at -20 °C. For the pharmacological assay, a non-biotransformed extract of *Filipendula ulmaria* was tested at final concentrations of 5, 10, 25, 50 and 100 μ g/mL. For single compounds, a test concentration of 20 μ M was used. The mix, as mentioned before, was prepared in the same manner as described in 4.5.3. Lastly, a preliminary experiment was performed to purify a 72 h fermentation sample of the *Filipendula ulmaria* extract (i.e. FEX 72 h), as well as a blank fermentation sample (i.e. containing

no extract, but including fecal suspension) via a methanol, ethyl acetate and acetone extraction protocol. In short: a liquid-liquid extraction of sample:solvent 50:50 (v/v) was performed, collecting the supernatant, repeating the extraction procedure twice, followed by drying of the collected sample. These extracts were processed in the same manner as the other samples and were tested at a concentration of 10, 25 and 50 µg/mL. Indomethacin (1.25 µM) and celecoxib (2.5 µM) were used as positive controls for COX-1 and COX-2, respectively. Solvent vehicle (DMSO) did not exceed 2.5% in the final test solutions.

4.6.3 COX-1 AND COX-2 ENZYME INHIBITION ASSAY

4.6.3.1 STEP 1: THE FORMATION OF PGE₂

COX-1 and COX-2 inhibition assays were performed in 96-well plates with purified COX-1 from ram seminal vesicles and human recombinant COX-2. From each test sample, 10 µL stock solution was added to 180 µL of the incubation mixture containing 0.1 M TRIS/HCl buffer (pH 8.0), 5 µM hematin, 18 mM epinephrine hydrogen tartrate, 1 unit/mL of enzyme preparation and 50 µM Na₂EDTA (only added in the COX-2 assay). This was followed by a preincubation step for 5 min at room temperature. Initiation of the reaction was started by adding 5 µM arachidonic acid and incubating at 37 °C for 20 min. The reaction was terminated by addition of 10 µl formic acid 10%.

4.6.3.2 STEP 2: MEASURING THE CONCENTRATION OF PGE₂

The concentration of PGE₂, the main arachidonic acid metabolite in this reaction, was determined immediately after the assay by a competitive PGE₂ EIA kit from Enzo Life Sciences according to the manufacturer's protocol. In short, the kit uses a monoclonal antibody to PGE₂ to bind, in a competitive manner, the PGE₂ in the sample, standard or an alkaline phosphatase molecule which has PGE₂ covalently attached to it. After a simultaneous incubation of 2 h at room temperature the excess reagents was washed away and substrate was added. After 1 h incubation time the enzyme reaction was

stopped and the absorbance was measured at 405 nm using a Biotek Eon plate reader (Agilent Technologies, CA, USA). Inhibition of COX refers to the reduction of PGE₂ formation in comparison to a blank vehicle control run without inhibitor.

4.7 COX-2 GENE EXPRESSION

4.7.1 REAGENTS

Reagents for the COX-2 gene expression assay were purchased as follows: human leukemic monocytic cell line THP-1 from ATCC (VA, USA), RPMI (Roswell Park Memorial Institute Medium) 1640-GlutaMAX medium, FBS, 4-(2-hydroxyethyl)-1-piperazineethanesulfonic acid (HEPES), PBS, penicillin and streptomycin from Gibco (NY, USA); dexamethasone, phorbol 12-myristate 13-acetate (PMA), lipopolysaccharide (LPS), dexamethasone and a GenElute Mammalian Total RNA Miniprep Kit from Sigma-Aldrich (MO, USA). The isolated RNA was reverse transcribed by using the SensiFast cDNA Synthesis kit from Bioline (TN, USA). The amplification of target cDNA was conducted with 2x SensiFast Probe Hi-ROX Mix from Bioline and Taqman primers (FAM-MGB) against the human COX-2 (assay ID: Hs00153133_m1) and human GAPDH (glyceraldehyde 3-phosphatase dehydrogenase, assay ID: Hs99999905_m1) were purchased from Applied Biosystems (NY, USA).

4.7.2 THP-1 CELL CULTURE

Human THP-1 monocytes were maintained in RPMI 1640-GlutaMAX medium supplemented with 10% (v/v) heat-inactivated fetal calf serum, 10mM HEPES, penicillin (100 U/mL) and streptomycin (100 µg/mL) in a humidified atmosphere of 95% air and 5% CO₂. Passage number was kept below 25. Moreover, the cell concentration was not allowed to exceed 8×10^5 cells/mL. In order to initiate the differentiation from monocyte to macrophage, THP-1 cells were seeded 1×10^6 cells/mL in a 24-well plate and incubated with fresh complete medium containing 12 nM PMA for 48 h.

4.7.3 SAMPLE PREPARATION

A stock solution of non-biotransformed *Filipendula ulmaria* extract in DMSO was stored as aliquots at -20 °C. For the pharmacological assay, the extract was freshly diluted in PBS and a final concentration of 20 and 50 µg/mL in cell culture medium was obtained. Dexamethasone (2.5 nM) was used as a positive control. Solvent vehicle (DMSO) did not exceed 0.1% in the final test solutions.

4.7.4 COX-2 GENE EXPRESSION ASSAY

PMA-differentiated THP-1 cells were pre-incubated with test compounds or extract for 1 h (37 °C), followed by stimulation with 7.5 ng/mL final concentration of LPS for an additional 3 h (37 °C). At the end of the experiment, medium was aspirated and cells were washed three times with ice cold PBS to remove non-attached cells. RNA was isolated with the GenElute™ Mammalian Total RNA Miniprep Kit according to the instruction manual. Pure total RNA was stored at -80 °C. The RNA was then reverse transcribed with the SensiFast cDNA Synthesis kit from Bioline according to manufacturer's instructions. The conditions of the PCR cycler were set to 25 °C for 10 min, 42 °C for 15 min, 48 °C for an additional 15 min and 85 °C for 5 min. The RNA concentration used for reverse transcription was 1 µg to gain a total volume of 20 µL cDNA, which is approximately 40 ng/µL cDNA. COX-2 gene expression analysis was performed in duplicate (25 µL reaction volumes containing SensiFast Probe Hi-ROX Mix from Bioline) on an ABIPrism 7300 sequence detector system (Applied Biosystems, NY, USA). The parameters for PCR amplification were 50 °C for 2 min, 95 °C for 10 min, followed by 40 cycles of 95 °C for 15 sec and 60 °C for 1 min. The COX-2 target gene was normalized to the endogenous reference gene GAPDH and relative quantification was performed using the using the $2^{-\Delta\Delta CT}$ method.

4.7.5 CELL VIABILITY ASSAY

An MTT assay was carried out to evaluate the cytotoxicity of the test samples. The PMA-differentiated THP-1 cells were pre-incubated with samples for 1 h, subsequently followed by a LPS stimulation of 7.5 ng/mL for 3 h. The medium was removed and the cells were treated with 200 μ L of an MTT solution (2.2 μ g/mL) during 30 min at 37 °C. Subsequently, the cells were lysed with 150 μ L per well of an isopropanol:DMSO (9:1; v/v) solution. The absorbance of 100 μ L lysate was measured at 550 nm using a Biotek Eon plate reader (Agilent Technologies).

4.8 STATISTICAL ANALYSIS

The data were expressed as mean \pm standard deviation (SD). Statistical evaluation of the data was performed by one-way analysis of variance (ANOVA), followed by the Tukey test, using GraphPad Prism, version 8.4.3. The results were considered as statistically significant at $p \leq 0.05$.

RESULTS AND DISCUSSION

As discussed in chapter 2, the anti-inflammatory properties of *Filipendula ulmaria* have been frequently claimed in ethnomedicine.^[120] Inflammation is a complex process in which the causative factors at the site of the inflammatory response are similar. Chemical mediators, such as prostaglandins for example, are present in excess at the site of the inflammation. Inhibition of prostaglandins synthesis from arachidonic acid, by inhibiting the prostaglandin generating enzymes or by controlling the induced expression of its gene, can thus be considered a very important anti-inflammatory mechanism.^[64] Therefore, the effect on enzyme activity of COX-1 and -2, as well as the inducible gene expression of COX-2, is reported in the present study. Moreover, NF- κ B was also tested as an interesting target. NF- κ B has been identified as a major driving force of the inflammatory reaction and activation of this important transcription factor leads to the production of mediators such as COX-2, contributing to a variety of chronic diseases with an inflammatory background.^[15-17] It has been shown that meadowsweet is rich in phenolic constituents such as flavonoid aglycons (e.g. quercetin, kaempferol), glycosylated flavonoids (e.g. rutin, hyperoside, quercitrin, avicularin and astragalin) and hydrolysable tannins (tellimagrandin I and II, rugosin A, B, D and E), as well as salicylates (salicylic acid, methyl salicylate, salicylaldehyde, salicylalcohol and their glycosides).^[121-127] Only a limited number of non-phenolic constituents such as phytosterols, carotenoids, triterpenes and chlorophyll derivatives have been reported.^[125,128] The large diversity of identified phytochemicals are likely to contribute to the activity, since many of them have been reported to be beneficial for human health.^[129,130] However, biotransformation and pharmacological studies should be combined in order to investigate which of these constituents or metabolites contribute to the activity of *Filipendula ulmaria* after oral intake.

4.9 NF-κB LUCIFERASE REPORTER GENE ASSAY

As described above, NF-κB is considered to be the “master switch” of the inflammatory response, regulating multiple genes involved in chronic inflammation via managing the transcription of inflammatory proteins such as chemokines, cytokines, interleukins, interferons and COX-2. Proinflammatory cytokines, e.g. TNF-α, have been shown to activate NF-κB. The NF-κB signaling pathway plays a critical role in the normal and pathophysiological immune responses, and therefore it is an interesting therapeutic target at various levels of regulation.^[15] In order to determine the anti-inflammatory activity of *Filipendula ulmaria*, murine fibrosarcoma L929 cells, transfected with a TNF-induced NF-κB driven luciferase reporter gene construct, were pretreated with the extract for 1 h and subsequently stimulated with the proinflammatory cytokine TNF-α for an additional 3 h. According to the results, the comprehensive extract of *Filipendula ulmaria* showed a clear inhibition on the NF-κB reporter gene induction by TNF-α compared to the stimulated control, and also showed a clear dose-response behavior. The non-biotransformed extract of *Filipendula ulmaria* reached an IC₅₀ of 40.53 μg/mL (with a 95% C.I. of 33.51 to 49.03, see Figure 4.7). When looking at the literature, Vogl et al. examined the anti-inflammatory efficacy of herbal drugs reported in Austrian folk medicine, among which *Filipendula ulmaria*. The extract of the herb, at a concentration of 10 μg/mL, showed a moderate (50 - 75%, dichloromethane extract) to strong (75 - 100%, detannified methanol extract) inhibition of NF-κB in a transactivation assay with a luciferase transporter gene in HEK293 cells. An extract of the flowers of *Filipendula ulmaria* showed moderate activation of nuclear factors PPARα (peroxisome proliferator-activated receptor) and PPARγ, which was also performed in a transactivation assay with a luciferase transporter gene in HEK293 cells.^[131] These nuclear factors are important molecular players inhibiting NF-κB responses. Possible mechanisms of this inactivation include direct binding of p65 or ubiquitination leading to proteolytic degradation of p65. PPAR also exerts indirect

effects on NF-κB: it promotes the expression of antioxidant enzymes (e.g. catalase, superoxide dismutase, heme oxygenase-1), which results in a reduction in the concentration of reactive oxygen species (i.e. secondary transmitters in inflammatory reactions). PPAR also causes an increase in the expression of IκBα, which interferes with the activation and function of NF-κB.^[132]

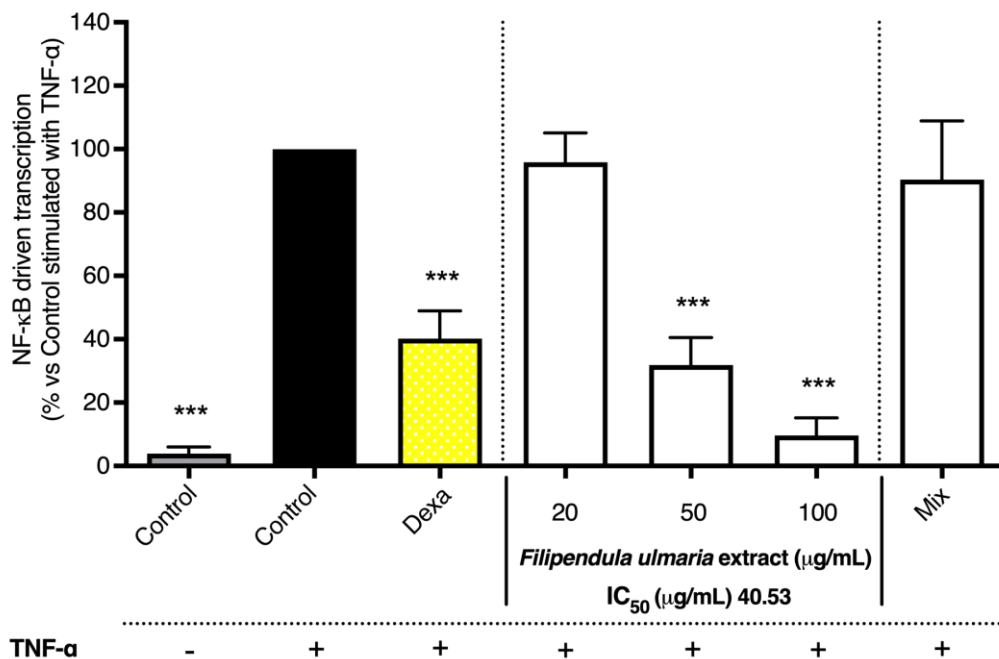


FIGURE 4.7: THE EFFECT OF THE *FILIPENDULA ULMARIA* EXTRACT AND THE MIX (20 μM OF GALLIC ACID AND SALICYLIC ACID, 6 μM OF QUERCETIN AND 4 μM OF SYRINGIC ACID) ON NF-κB DRIVEN TRANSCRIPTION. DEXAMETHASONE (DEXA, 1 μM), IN YELLOW, SERVED AS POSITIVE CONTROL. THE GRAPH DEPICTS COMPILED DATA OF 3 INDEPENDENT EXPERIMENTS (MEAN + SD). P-VALUES ARE EXPRESSED AS ***p<0.0001 COMPARED TO CONTROL STIMULATED WITH TNF-α.

To further link the presence of compounds and/or metabolites present after gastrointestinal biotransformation to the pharmacological activity, a mix containing constituents of different groups present in the extract after biotransformation was prepared, since testing samples containing fecal suspension proved to be difficult and challenging in cell-based assays such as the NF-κB luciferase reporter gene assay. This mix contained a combination of 20 μM of gallic acid and salicylic acid, 6 μM of quercetin and 4 μM of syringic acid. However, for the mix, no significant activity was observed. It

has been shown that polyphenols target multiple inflammatory mechanisms, one of them being the inactivation of NF- κ B.^[133] The results of the mix are thus not completely in line with literature, which might also be because of differences in test concentrations and assay conditions.

For example, the suppression of TNF- α induced NF- κ B activation by gallic acid (IC₅₀ of 76 μ M) has been determined with stably transfected 293/NF κ B-Luc human embryonic kidney cells.^[134] In a more recent paper from Lu et al., the NF- κ B inhibitory effect of gallic acid (ranging from 1 to 100 μ M) was also shown in transfected HEK293 cells.^[135] The study of Choi et al. provided evidence to support the idea that gallic acid suppresses hyperacetylation of p65 *in vitro* and *in vivo* by inhibiting the histone acetyltransferase p300, and subsequent, NF- κ B activation.^[136]

Research has shown that salicylic acid inhibits the activation of NF- κ B. The general accepted mechanism of action of aspirin is the irreversible inhibition of cyclooxygenase activity by acetylation of an essential serine at the active site of the enzyme, with an inhibitory potency that is independent of arachidonic acid concentration. Aspirin is, however, rapidly deacetylated to salicylic acid. It has thus been assumed that the anti-inflammatory effect is largely mediated by salicylic acid. Nevertheless, only weak inhibition of cyclooxygenase by salicylic acid has been reported. Other possible sites of action that are not directly related to cyclooxygenase inhibition, such as the effect on NF- κ B activity, have been suggested based on observations made *in vitro* using high concentrations of aspirin and sodium salicylate.^[137] Kopp and Ghosh, for example, showed that relatively high concentrations of sodium salicylate (and aspirin), ranging between 2 and 20 mM, were able to prevent the degradation of I κ B in a dose-dependent manner.^[138] Similar results were obtained in subsequent studies by Bayón et al.^[139], Grilli et al.^[140], Pierce et al.^[141] and Yin et al.^[142], testing salicylic acid in millimolar concentrations. Therapy with high-dose aspirin results in plasma salicylate concentrations of 0.95 - 1.9 mM. The concentration of free salicylic acid can be

expected to be in the range of 250 μM , when taking into account a plasma protein binding of 80 to 90%. Data obtained with millimolar concentration should therefore be discussed and their relevance should be questioned in an *in vivo* situation.^[137]

Quercetin has also been reported to inhibit NF- κB activation to a great extent and to reduce inflammation. In an article from Cho et al., quercetin (1 - 20 μM) significantly inhibited NF- κB reporter gene activity in a dose-dependent manner in a luciferase reporter assay in HUVEC cells. Quercetin did not show any effect on I $\kappa\text{B}\alpha$ degradation.^[143] This is in contrast with research from Comalada et al., where quercetin inhibited the phosphorylation of I $\kappa\text{B}\alpha$ in LPS-induced bone marrow-derived macrophages, hence inhibiting the NF- κB pathway.^[144] In PMA-stimulated human mast cells (HMC-1), quercetin (30 μM) appeared to prevent the degradation of I $\kappa\text{B}\alpha$, as well as the nuclear translocation of p65 resulting in reduction of TNF- α , IL-1 β , IL-6 and IL-8. Moreover, quercetin significantly reduced the induced luciferase activity of NF- κB .^[145] Another study in RAW264.7 macrophages found that 10 μM of quercetin blocks the nuclear translocation of p50 and p65 subunits and thus also represses pro-inflammatory genes such as iNOS and COX-2.^[146] Furthermore, quercetin (100 μM) can modulate chromatin remodeling: the compound appears to inhibit the recruitment of the NF- κB cofactor histone acetyl transferase called CBP/p300 to the promoters of interferon-inducible protein 10 (IP-10) and macrophage inflammatory protein-2 (MIP-2) genes in primary murine small intestinal epithelial cells. This effect results in the inhibition of the expression of these pro-inflammatory cytokines.^[147] Additionally, in a study from Chen et al., quercetin attenuated IKK activity and lowered I $\kappa\text{B}\alpha$ phosphorylation in a dose-dependent manner (10 - 30 μM) in LPS- and IFN- γ -induced mouse BV-2 microglia cells, as well as inhibiting the DNA binding activity of NF- κB . Moreover, 10 μM of quercetin also showed an inhibitory effect of NF- κB activation confirmed by a luciferase reporter assay.^[148]

Syringic acid has been reported to down-regulate the expression of NF- κ B in a diet-induced hepatic dysfunction mice model.^[149] A recent article from Fang et al., showed an inhibiting effect of syringic acid on the expression of p65 and phosphorylated I κ B α in an ulcerative colitis model mice induced with dextran sulfate sodium (orally treated with 25 mg/kg bodyweight syringic acid), as well as in LPS-induced RAW 264.7 macrophages (10 - 20 μ M).^[150] Similar results were seen in the study of Manjunatha et al., where syringic acid (50 mg/kg bodyweight) was administered to isoproterenol-induced cardio-toxicity in rats, reducing the expression of NF- κ B and TNF- α .^[151]

4.10 COX-1 AND COX-2 ENZYME INHIBITION

As shown in Figure 4.8 and Figure 4.9, the non-biotransformed *Filipendula ulmaria* extract inhibited COX-1 and -2 enzyme activities in a dose-dependent manner. *Filipendula ulmaria* showed to be a more potent inhibitor of the COX-1 enzyme, with an IC₅₀ of 7.45 μ g/mL, compared to the results obtained in the COX-2 enzyme inhibition assay. For COX-2 enzyme inhibition, an IC₅₀ of 90.26 μ g/mL was obtained. Table 4.1 shows the summary of the IC₅₀ on both COX enzymes, with respective 95% C. I. values. The positive control indomethacin inhibited the COX-1 enzyme by 63.01%. Celecoxib, the positive control for COX-2 enzyme inhibition, decreased the enzyme activity by 42.90%. Elevated eicosanoids production, derived by enzymatically catalyzed transformation of arachidonic acid via COX enzymes, often accompanies inflammatory processes and suppression of their biosynthesis represents a clinically useful therapeutic approach.^[152] In literature, Tunón et al. reported that a water extract of *Filipendula ulmaria* leaves showed inhibition of prostaglandin biosynthesis in bovine seminal vesicle microsomes, which was hypothesized to be related to the presence of salicylic acid derivatives (e.g. methyl salicylate).^[153] In an article from Katanić et al., methanolic meadowsweet extracts of both the aerial part and the roots were assessed at a concentration of 50 μ g/mL in a COX-1 and -2 enzyme inhibition assay. Both extracts

inhibited the enzyme activity of COX-1 (62.84% for the aerial parts and 32.11% for the roots) and COX-2 (46.43% for the aerial parts and 20.20% for the roots). The aerial part extract was twice as effective as the roots. The extract of the aerial part contained rutoside, spiraeoside, isoquercitrin, gallic acid, catechin, epicatechin, as well as derivatives of gallic acid, ellagic acid and quercetin. In the root extract, catechin, epicatechin and high amounts of total condensed tannins and gallotannins were identified.^[154] In literature, an *ex vivo* experiment in human platelets monitored the effect of *Filipendula ulmaria* and *Filipendula vulgaris* (aqueous extract of the flowers) on eicosanoid biosynthesis. These extracts, in a concentration range of 0.25 - 10 mg/mL, decreased the production of these proinflammatory eicosanoids. Several isolated flavonoids, such as astragalin 2''-O-gallate, a mixture of hyperoside 2''-O-gallate and isoquercitrin 2''-O-gallate (1:2), as well as spiraeoside, were also found to attenuate the synthesis of PGE₂. This is an interesting finding, since it indicates the contribution of different active constituent other than salicylic acid contributing to the anti-inflammatory effect.^[152] Cholet et al. also studied the anti-inflammatory effects of a methanolic extract of the aerial parts of *Filipendula ulmaria* (50 µg/mL) on COX-2 and PGE₂ in LPS-stimulated human peripheral blood mononuclear cells. PGE₂ secretion in the cell medium was significantly decreased after treatment with the extract.^[155]

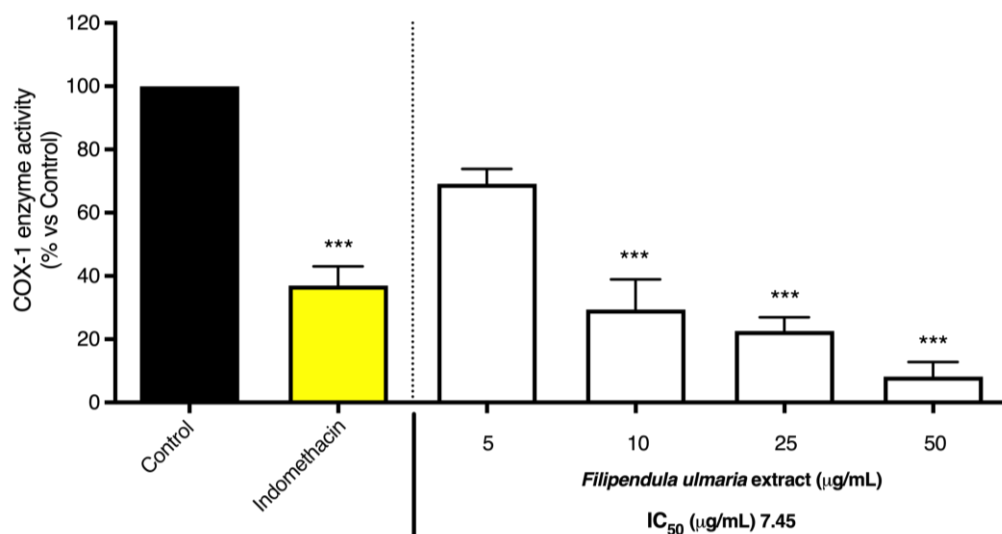


FIGURE 4.8: THE EFFECT OF THE *FILIPENDULA ULMARIA* EXTRACT ON COX-1 ENZYME INHIBITION. INDOMETHACIN (1.25 μ M), IN YELLOW, SERVED AS POSITIVE CONTROL. THE GRAPH DEPICTS COMPILED DATA OF 3 INDEPENDENT EXPERIMENTS (MEAN \pm SD). P-VALUES ARE EXPRESSED AS *** $p > 0.0001$ COMPARED TO CONTROL.

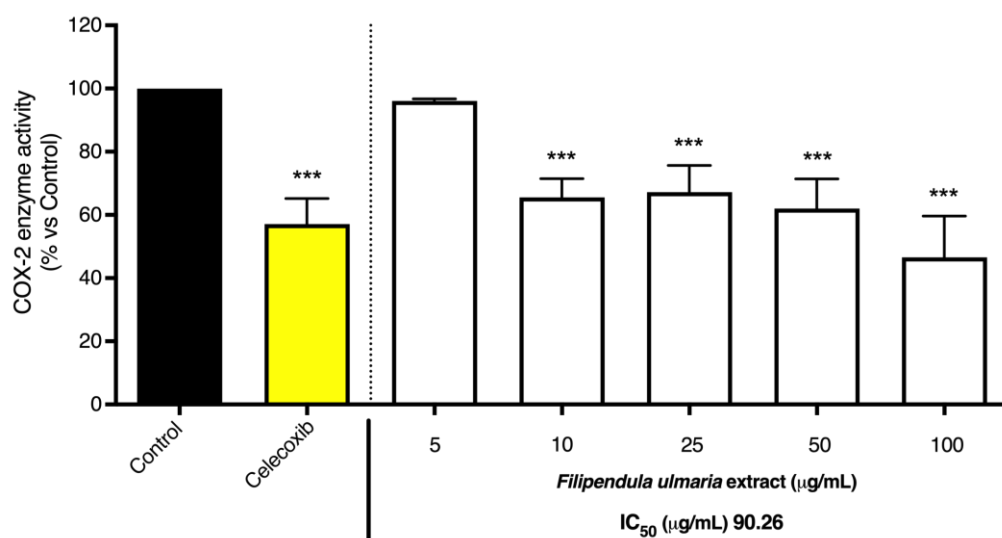


FIGURE 4.9: THE EFFECT OF THE *FILIPENDULA ULMARIA* EXTRACT ON COX-2 ENZYME INHIBITION. CELECOXIB (2.5 μ M), IN YELLOW, SERVED AS POSITIVE CONTROL. THE GRAPH DEPICTS COMPILED DATA OF 3 INDEPENDENT EXPERIMENTS (MEAN \pm SD). P-VALUES ARE EXPRESSED AS *** $p > 0.0001$ COMPARED TO CONTROL.

TABLE 4.1: IC₅₀ OF *FILIPENDULA ULMARIA* EXTRACT ON COX ACTIVITY. 95% C.I.; 95% INTERVAL OF CONFIDENCE.

COX Isoform	IC ₅₀ (μ g/mL)	95% C.I.
COX-1	7.45	5.46 to 9.83
COX-2	90.26	60.95 to 135.70

Filipendula ulmaria is rich in polyphenols which were reported in literature to exhibit anti-inflammatory properties, among which inhibiting the COX enzymes.^[156] Quercetin, for example, inhibited the enzyme activity in purified COX-1 and -2 preparations, reaching an IC₅₀ near 5 μM. Moreover, quercetin (5 - 40 μM) also decreased PGE₂ levels in the supernatant of HCA-7 and HCEC cells after 6 h of incubation. Interestingly, incubation with 20 or 40 μM of quercetin for 24 h elevated PGE₂ levels in HCEC cells up to approximately 5-fold compared to the control.^[157] El-Seedi et al. also found an inhibitory effect of quercetin on the COX-1 enzyme: an inhibition of 44% was achieved when testing at a relatively high concentration of 200 μM. For caffeic acid (100 μM), the research group noted a 32% inhibition of the COX-2 enzyme.^[158] In an article from Kutil et al., phenolic compounds from wine were investigated for COX-1 and COX-2 inhibitory activity. Weak activity was found for quercetin, having an IC₅₀ of 44 μM and kaempferol, with an IC₅₀ near 60 μM in case of COX-1.^[159] Landofri et al. have reported that kaempferol, but also flavonoids such as phloretin and apigenin were COX inhibitors when evaluating the arachidonic acid metabolism in platelets at a test concentration of 50 μM.^[160] Furthermore, phloretin was also able to suppress PGE₂ production in a dose-dependent manner (20 - 100 μM) in *Propionibacterium acnes*-induced HaCaT cells.^[161] The anti-inflammatory health effects of nuts, seeds and fruits like pomegranate have been associated with their high content of ellagitannins and ellagic acid.^[162-166] The relevance of their efficacy is, however, questioned by their low oral bioavailability. Ellagitannins are rarely detected in plasma or tissues after consumption and ellagic acid, although being a smaller molecule, has much lower water solubility compared to the ellagitannins.^[167-169] As seen in the previous chapter, ellagitannins and ellagic acid pass unmodified to the colon, resulting in extensive biotransformation by the gut microbiota providing urolithins. These urolithins are 25- to 80-fold more bioavailable and are much better absorbed than ellagic acid. The hypothesis that urolithins are the actual bioactive compounds, rather than the ellagitannins or ellagic acid, is thus considered the most plausible one.^[168,170] Masamune et al. found no inhibition by

ellagic acid (1, 5, 10, 25 $\mu\text{g}/\text{mL}$) on NF- κB activation in IL-1 β and TNF- α induced pancreatic stellate cells. Likewise, González-Sarrías et al. demonstrated no inhibitory effect of 10 μM ellagic acid on NF- κB activation in colon fibroblasts after IL-1 β treatment. Several other *in vivo* animal studies did observe results where ellagic acid acted as an anti-inflammatory agent, modulating the NF- κB pathway. However, it must be taken into account that ellagic acid was administered *per os*, which means the activity is probably related to its active metabolites.^[171-173] In the study of El-Shitany et al., ellagic acid (100 mg/kg bodyweight, intraplantar injection) attenuated COX-2 mRNA expression in carrageenan-induced acute inflammation in rats. Moreover, their docking study revealed a high affinity of ellagic acid towards the active site of COX-2, forming four hydrogen bonds with Arg120, Ser530, Tyr355 and Tyr385.^[174] Ellagic acid (10 - 30 μM) was also found to suppress PGE₂ release in LPS-induced human monocytes, which was mediated by the inhibitory effect on COX-2 protein expression. No apparent inhibitory effect on the COX enzymes was observed in cell-free assays.^[175] Zhang et al. did find ellagic acid to inhibit COX-1 enzyme activity, but the compound had no effect on COX-2. However, it should be mentioned that the test concentration of 100 $\mu\text{g}/\text{mL}$ is less relevant *in vivo*.^[176] Urolithins A and B are considered to be the major metabolites formed from ellagitannins and ellagic acid, and they can reach a high concentration at micromolar level as glucuronide derivatives in the bloodstream. Similar to our results, research from Noshadi et al., indicated that these urolithins were not potent inhibitors of both COX enzymes in a cell-free assay.^[177] This is in concordance with research from González-Sarrías, who also found no inhibition of COX-1 or COX-2 activity at any concentration tested of urolithin A, B and ellagic acid (1 - 40 μM) in purified COX-1 (ovine) and COX-2 (human recombinant) enzymes. Their study also showed that treatment with urolithin A and B, but not ellagic acid, attenuated PGE₂ levels in IL-1 β -induced colonic fibroblasts. Furthermore, urolithin A reduced COX-2 expression at both the mRNA and protein level in the human colonic fibroblasts stimulated with IL-1 β , while urolithin B and ellagic acid had no effect. Interestingly, both

uroolithins also inhibited NF- κ B translocation to the nucleus.^[178] More detailed mechanistic studies in LPS-stimulated BV2 microglial cells showed that urolithin B inhibited NF- κ B activity by reducing the phosphorylation and degradation of I κ B α .^[179] In an *in vivo* colitis rat model, induced by dextran sodium sulfate, urolithin A supplementation led to a decrease in PGE₂ levels in colon mucosa by down-regulating the over-expressed COX-2 levels.^[163] As mentioned before, only weak inhibition of COX by salicylic acid has been found in several studies. In purified enzyme preparations, sodium salicylate was inactive up to 6.25 mM.^[180] Experiments in intact cells also found salicylic acid to be a weak inhibitor of COX-1, with an IC₅₀ that is usually more than 1.5 mM.^[181-183] For COX-2 enzyme inhibition, it seems to depend on the experimental conditions (IC₅₀ values ranging between 30 μ M and 1.5 mM).^[181,184] The potency of salicylic acid to inhibit COX-2 could also be dependent on the concentration of exogenously added arachidonic acid. To illustrate this: in COX-2-induced human pulmonary epithelial cells, salicylic acid effectively inhibited prostaglandin biosynthesis in the presence of arachidonic acid ≤ 10 μ M with an IC₅₀ of 31 μ M, which was increased to more than 625 μ M in the presence of a higher concentration of 30 μ M arachidonic acid.^[184] Moreover, the impact of large amounts of endogenous arachidonic acid liberated in cells by inflammatory stimuli, such as endotoxins, also appeared to lower the potency of salicylic acid to inhibit COX-2.^[181,182,185] It can thus be assumed that weak competitive COX-2 inhibition by salicylic acid cannot fully explain its anti-inflammatory effects *in vivo*. Gallic acid, in contrast to our results, is known in literature to inhibit both COX isoenzymes. Madlener et al. determined IC₅₀ values of 3.5 and 4.4 nM for COX-1 and COX-2, respectively.^[186] Reddy et al. also found a strong inhibitory effect of gallic acid, with an IC₅₀ of 1.5 μ M for COX-1 and 74 nM for COX-2, thus showing a much stronger preference towards COX-2. The docking results of their research show that the carboxylate moiety of gallic acid interacts with the amino acids at the entrance of the hydrophobic active site channel of COX-2, mainly with Arg120 and Glu524.^[187] Docking studies from Amaravani et al. also found interactive binding in the active site of

COX-2.^[188] In LPS-induced RAW264.7 cells the expression of the COX-2 protein was not affected by gallic acid (0.1 to 1 μ M). However, this study did find that gallic acid inhibited the production of PGE₂ in a dose-dependent manner. On the contrary, other studies did observe a reduced expression of COX-2.^[189] Pandurangan et al., for example, demonstrated that gallic acid treatment (10 mg/kg bodyweight orally) in mice with dextran sodium sulfate-induced colitis lowered the mRNA expression of COX-2 and iNOS. Moreover, expression levels of inflammatory cytokines (TNF- α , IL-1 β , IFN- γ , IL-6 and IL-17) were significantly attenuated as well.^[190] A study done in rheumatoid arthritis fibroblast-like synoviocytes also showed suppression by gallic acid (0.1 and 1 μ M) of expression level cytokines (IL-1 β and IL-6) and COX-2.^[191] Furthermore, syringic acid is also known in literature for its anti-inflammatory properties.^[192] In a cell-based experiment from the research group of Stanikunaite, a strong inhibition of the COX-2 enzyme (IC₅₀ of 2 μ M) in LPS-stimulated RAW 264.7 cells was observed. These results were determined by the conversion of exogenous arachidonic acid to PGE₂.^[193] In animal studies, oral administration of syringic acid was able to reduce the expression of COX-2 and other markers such as iNOS and TNF- α .^[194,195]

In our study, several of the compounds mentioned above, present in *Filipendula ulmaria*, were tested in the COX enzyme inhibition assay at a concentration of 20 μ M. These results are shown in Figure 4.10 and Figure 4.11.

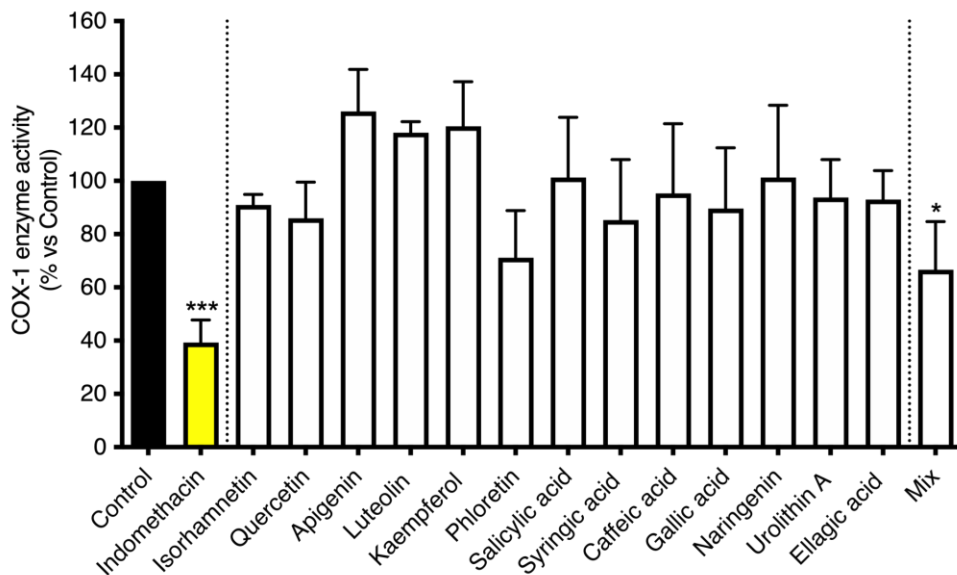


FIGURE 4.10: COX-1 ENZYME INHIBITION BY SEVERAL COMPOUNDS PRESENT IN *FILIPENDULA ULMARIA*. ALL COMPOUNDS WERE SUBJECTED TO AN *IN VITRO* COX-1 ENZYME INHIBITION ASSAY AT A CONCENTRATION OF 20 μ M, EXCEPT FOR THE MIX (20 μ M OF GALLIC ACID AND SALICYLIC ACID, 6 μ M OF QUERCETIN AND 4 μ M OF SYRINGIC ACID). INDOMETHACINE (1.25 μ M), IN YELLOW, SERVED AS POSITIVE CONTROL. THE GRAPH DEPICTS COMPILED DATA OF 3 INDEPENDENT EXPERIMENTS (MEAN \pm SD). P-VALUES ARE EXPRESSED AS * $p < 0.05$ AND *** $p > 0.0001$ COMPARED TO CONTROL.

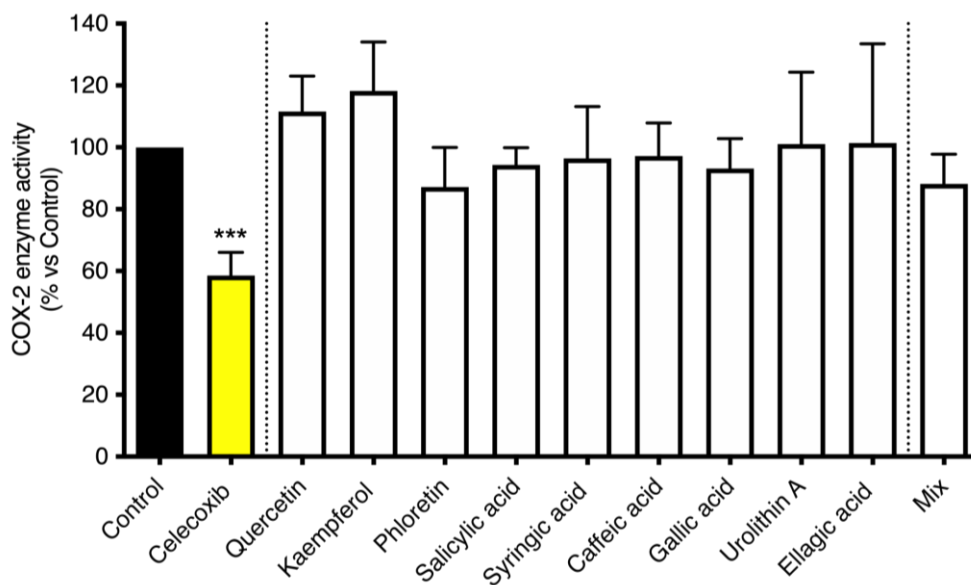


FIGURE 4.11: COX-2 ENZYME INHIBITION BY SEVERAL COMPOUNDS PRESENT IN *FILIPENDULA ULMARIA*. ALL COMPOUNDS WERE SUBJECTED TO AN *IN VITRO* COX-2 ENZYME INHIBITION ASSAY AT A CONCENTRATION OF 20 μ M, EXCEPT FOR THE MIX (20 μ M OF GALLIC ACID AND SALICYLIC ACID, 6 μ M OF QUERCETIN AND 4 μ M OF SYRINGIC ACID). CELECOXIB (2.5 μ M), IN YELLOW, SERVED AS POSITIVE CONTROL. THE GRAPH DEPICTS COMPILED DATA OF 3 INDEPENDENT EXPERIMENTS (MEAN \pm SD). P-VALUES ARE EXPRESSED AS *** $p > 0.0001$ COMPARED TO CONTROL.

None of these isolated compounds appeared to significantly inhibit the COX-1 or -2 enzyme at the test concentration. When comparing to literature, some of these results are contradictory. Gallic acid, for example, is known to achieve IC₅₀ values in the nM range for both COX isoenzymes.^[186] On the contrary, similar to our results, salicylic acid is known to be a weak inhibitor of COX (mM range).^[180,181,184] In concordance to other studies, urolithin A did not appear to be a potent inhibitor of both COX enzymes.^[177,178] Interestingly, the mix, which was described in the previous NF-κB experiment (containing 20 μM of gallic acid and salicylic acid, 6 μM of quercetin and 4 μM of syringic acid), did show a significant inhibition of 33.33% of the COX-1 enzyme. This might be explained by a synergistic or additive effect, since the single compounds (all tested at a concentration of 20 μM) showed no clear activity on the enzyme. For the COX-2 enzyme, however, no significant activity was observed for the mix. The positive control indomethacin inhibited the COX-1 enzyme by 60.69%. Celecoxib, the positive control for COX-2 enzyme inhibition, decreased the enzyme activity by 41.48%.

Finally, a preliminary experiment was performed in order to clean up the colon samples from the gastrointestinal model. Different extraction methods were applied to a 72 h fermentation sample of a *Filipendula ulmaria* extract, named FEX 72 h, as well as a blank sample (including fermentation without addition of the extract). These results were summarized in Figure 4.12 and Figure 4.13. Firstly, the pure FEX 72 h sample was tested at a concentration of 10, 25 and 50 μg/mL (in green). Secondly, 3 different extraction methods were compared in the same concentration range: a methanol extraction (in orange), an ethyl acetate extraction (in blue) and an acetone extraction (in pink). Across all different extraction methods and the pure FEX 72 h sample, a preference in selectivity for the COX-1 over the COX-2 enzyme can still be seen (see also Table 4.2), which is similar to the results obtained for the non-biotransformed *Filipendula ulmaria* extract. Moreover, the acetone extraction showed the lowest IC₅₀ values. Polarity also does not seem to explain the trend observed in the different IC₅₀ values.

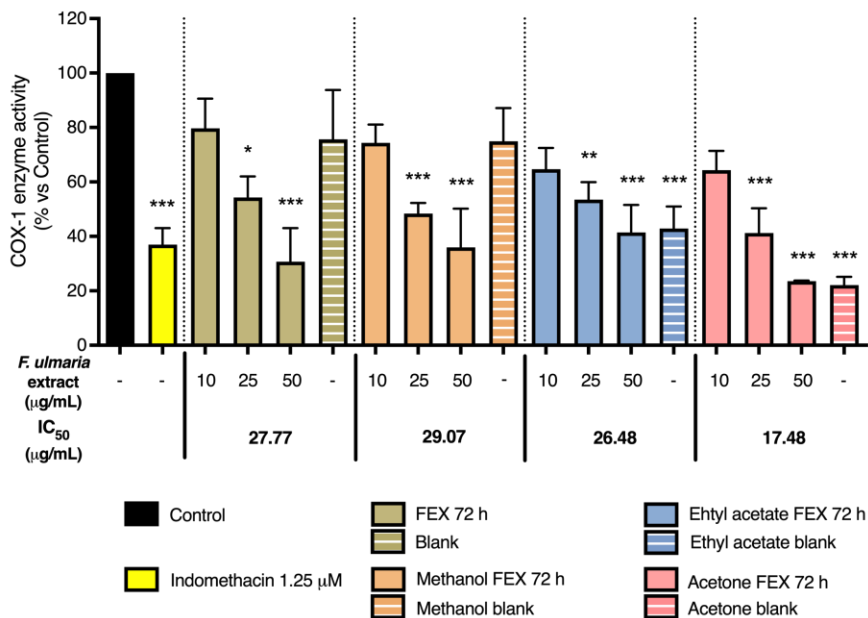


FIGURE 4.12: THE EFFECT OF THE DIGESTED *FILIPENDULA ULMARIA* EXTRACT (FEX 72 h) AND DIFFERENT EXTRACTION PROCEDURES OF FEX 72 h ON COX-1 ENZYME INHIBITION. INDOMETHACIN (1.25 µM), IN YELLOW, SERVED AS POSITIVE CONTROL. THE GRAPH DEPICTS COMPILED DATA OF 3 INDEPENDENT EXPERIMENTS (MEAN + SD). P-VALUES ARE EXPRESSED AS * $p < 0.05$, ** $p < 0.01$ AND *** $p > 0.0001$ COMPARED TO CONTROL.

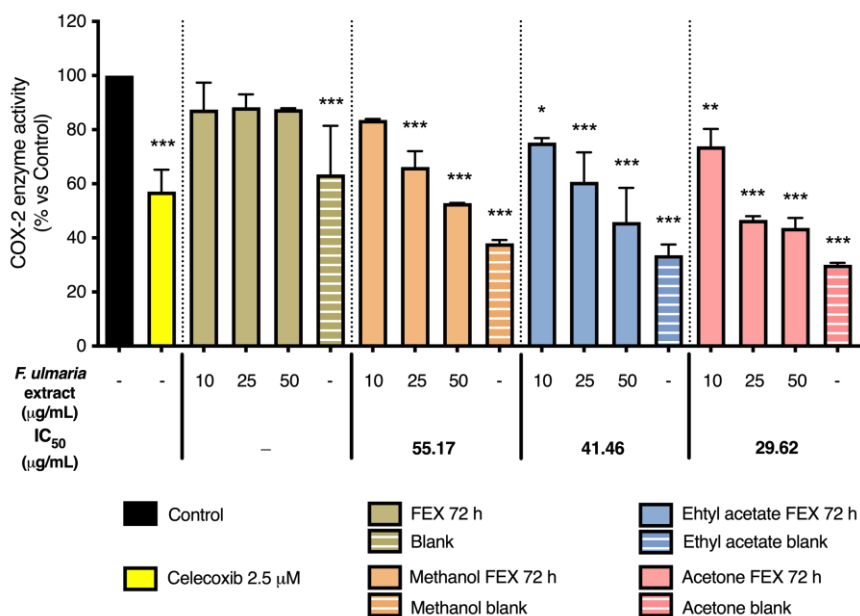


FIGURE 4.13: THE EFFECT OF THE DIGESTED *FILIPENDULA ULMARIA* EXTRACT (FEX 72 h) AND DIFFERENT EXTRACTION PROCEDURES OF FEX 72 h ON COX-2 ENZYME INHIBITION. CELECOXIB (2.5 µM), IN YELLOW, SERVED AS POSITIVE CONTROL. THE GRAPH DEPICTS COMPILED DATA OF 3 INDEPENDENT EXPERIMENTS (MEAN + SD). P-VALUES ARE EXPRESSED AS * $p < 0.05$, ** $p < 0.01$ AND *** $p > 0.0001$ COMPARED TO CONTROL.

TABLE 4.2: IC₅₀ OF DIGESTED *FILIPENDULA ULMARIA* EXTRACT ON COX ACTIVITY. 95% C.I.; 95% INTERVAL OF CONFIDENCE.

Digested <i>Filipendula ulmaria</i> Extract	COX Isoform	IC ₅₀ (µg/mL)	95% C.I.
FEX (72 h)	COX-1	27.77	18.39 to 38.51
Methanol FEX		29.07	19.14 to 44.14
Ethyl acetate FEX		26.48	19.33 to 36.30
Acetone FEX		17.48	13.09 to 23.34
FEX (72 h)	COX-2	/	/
Methanol FEX		55.17	42.04 to 72.38
Ethyl acetate FEX		41.46	21.75 to 79.02
Acetone FEX		29.62	18.85 to 46.53

Thin-layer chromatography (TLC, data not shown) confirmed the absence of flavonoids in the different blank samples. Surprisingly, a very clear effect can also be observed for the blank samples extracted with ethyl acetate or acetone. Therefore, the observed inhibition could be due to other compounds present in these blank samples. Hence, the contribution of short-chain fatty acids (SCFAs) would be an interesting lead to follow. SCFAs, primarily butyric, acetic or propionic acid, are the bacterial end-products of fiber fermentation processes. García-Villalba et al., for example, found that liquid-liquid extraction with ethyl acetate showed good extraction efficiencies of SCFAs in aqueous fecal suspensions. Moreover, the SCFAs were stable in ethyl acetate at room temperature for up to 36 h and at -20 °C for long-term storage.^[196] There is a growing interest in these compounds due to the increasing evidence of their positive physiological effects, especially in relation to colonic function as they contribute to normal bowel function, colonic vasculature and musculature. Moreover, their absence has been associated to inflammatory bowel diseases and they seem to play an important role in the protection against colon cancer.^[196,197] SCFAs might play an essential role in regulation of inflammation, for example by regulating cytokine and chemokine production. They might regulate the immune system through G-protein-coupled receptors (e.g. GPR41, GPR43 and GPR109A) signaling. In addition, SCFAs also seem to regulate the histone deacetylase activity which affects inhibition of

NF- κ B.^[197,198] Interestingly, propionic acid has moderate inhibitory activity on the COX enzymes.^[199] And indeed, several NSAIDs, such as flurbiprofen, ibuprofen and naproxen are propionic acid derivatives.^[198] Docking studies found that the carboxylate of flurbiprofen and ibuprofen is necessary for inhibition of the COX enzymes, interacting with Arg-120, Tyr-355 and Glu-524 at the active site.^[200-202]

4.11 COX-2 GENE EXPRESSION

The results of the inhibition of COX-2 gene expression in THP-1 macrophages by the non-biotransformed *Filipendula ulmaria* extract are presented in Figure 4.14. The results were compared with the positive control, i.e. dexamethasone. The tested *Filipendula ulmaria* extract exhibited no inhibitory effect on COX-2 gene expression in THP-1 cells at a concentration of 20 and 50 µg/mL. The positive control dexamethasone at a concentration 2.5 nM, showed 42.27% inhibition of COX-2 gene expression.

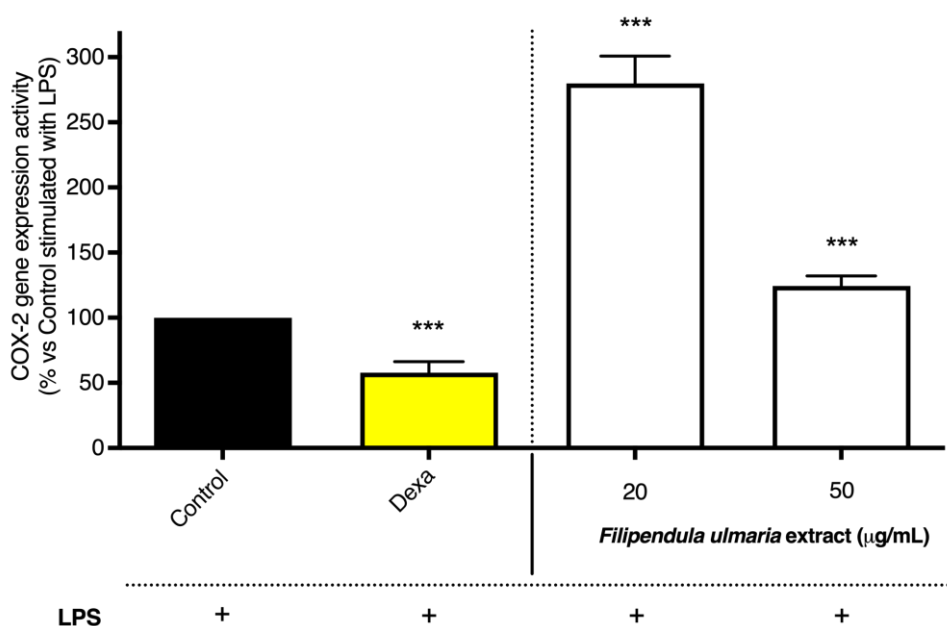


FIGURE 4.14: THE EFFECT OF THE *FILIPENDULA ULMARIA* EXTRACT ON COX-2 GENE EXPRESSION IN THP-1 MACROPHAGES. DEXAMETHASONE (2.5 nM), IN YELLOW, SERVED AS POSITIVE CONTROL. THE GRAPH DEPICTS COMPILED DATA OF 3 INDEPENDENT EXPERIMENTS (MEAN \pm SD). P-VALUES ARE EXPRESSED AS *** $p < 0.0001$ COMPARED TO CONTROL.

As mentioned before, Katanić et al. obtained similar results for COX enzyme inhibition, where the methanolic meadowsweet extracts of both the aerial part and the roots inhibited the enzyme activity of COX-1 and -2. However, the extracts had a negligible effect on COX-2 gene expression in THP-1 cells at a concentration of 25 µg/mL. The extracts hardly inhibited the level of COX-2 gene expression, with 10.19% inhibition for

the aerial extract and 8.54% for the roots extract. Moreover, their study also demonstrated that both extracts were able to suppress the edema formation until 6 h after carrageenan injection in rats. Immunohistochemical analysis showed that COX-2 gene expression was not directly correlated with the reduction of edema, which suggests that *Filipendula ulmaria* possibly has other mechanisms influencing edema, rather than through inhibition of COX-2 gene expression.^[154] Katanić et al. also tested the effect of *Filipendula vulgaris* in the same setting, a plant which is comparable to and sometimes used as a substitute of *Filipendula ulmaria*. This extract showed similar anti-inflammatory properties on COX-1 and -2 isoenzymes *in vitro*, but again no significant activity towards COX-2 gene expression.^[203] Cholet et al. discussed another interesting finding in their paper, studying a methanol extract of the aerial parts of *Filipendula ulmaria* and its effect on COX-2 expression in PBMCs incubated with or without LPS. In the basal state, the extract (50 µg/mL for 4 h) increased the relative gene expression of COX-2, showing a slight pro-inflammatory effect in a physiological situation. In LPS-stimulated PBMCs, the extract showed a tendency to decrease the COX-2 expression, although the effect was not significant. Moreover, this effect was also seen on the release of extracellular PGE₂ levels (measured after 24 h). Depending on the condition of incubation, the extract had a totally opposite effect: the basal state showed an increase in the secretion of PGE₂, while its secretion was decreased in stimulated cells. It was postulated that this increase in the COX-2 relative expression and the release of extracellular PGE₂, could be significant and necessary for the resolution of the first stages of acute inflammation.^[155] An induction of the COX-2 gene by a COX-2 enzyme inhibitor, which is observed in this experiment, is quite a contradictory finding which has been reported in literature before (e.g. experiments with celecoxib). The lack of an additive or synergistic effect between gene expression and enzyme inhibition might be related to the observation that, if the COX-2 enzyme is inhibited, the cell may paradoxically counterbalance with more protein expression.^[204]

Filipendula ulmaria, as discussed before, contains a rich diversity of polyphenols which are known in literature to have an effect on inflammation and specifically on COX-2 gene expression. *In vitro* and *in vivo* studies on pomegranate juice, which is rich in ellagitannins, have shown to lower COX-2 gene and protein expression.^[163,205-207] Keeping the aspect of biotransformation in mind, urolithin A also appeared to reduce both gene and protein levels of COX-2. In a study by González-Sarrías et al., no effect was seen for urolithin B and ellagic acid on COX-2 expression.^[178] Cocoa, containing large amounts of epicatechin, catechin and procyanidin B1 and B2, also lowered COX-2 gene expression.^[208,209] Another example can be found when looking at the inhibiting effect on COX-2 expression in *in vitro* studies of extracts of sultanas (golden-colored dried grapes), which are high in vanillic acid, caffeic acid, gallic acid, syringic acid, *p*-coumaric acid, ferulic acid and quercetin, as well as the positive effects of Willow bark extracts, rich in catechin, catechol and salicin.^[210-212] It is however important to remember that the numerous plant polyphenols in extracts may exert their activity by having synergetic effects. Several authors showed that pure compounds such as quercetin and other flavonoids, as aglycons, downregulate COX-2 expression in a variety of cell lines where expression was induced by various agents. Moreover, flavonoids with an *ortho*-dihydroxy substitution pattern on the B-ring, such as quercetin, luteolin and rhamnetin, showed a more potent effect on COX-2 gene expression. The number of hydroxyl-groups on the B-ring seems to be related to conformational interactions on enzymes such as tyrosine kinase and protein kinase C, which are involved in the transcriptional COX-2 activity.^[213-218] Regarding salicylate's possible interference on the COX-2 gene, conflicting results appear in literature. Several reports have shown inhibitory effects; however, other articles describe no such inhibitory effects or even stimulatory effects on the expression of the COX-2 gene.^{[219-}

223]

4.12 CELL VIABILITY ASSAYS IN L929 AND THP-1 CELLS

An MTT assay was carried out to evaluate the cytotoxicity of the test samples in the NF- κ B luciferase reporter gene assay in L929 cells. The L929 cells were pre-incubated with samples for 1 h and stimulated with TNF- α for 3 h.

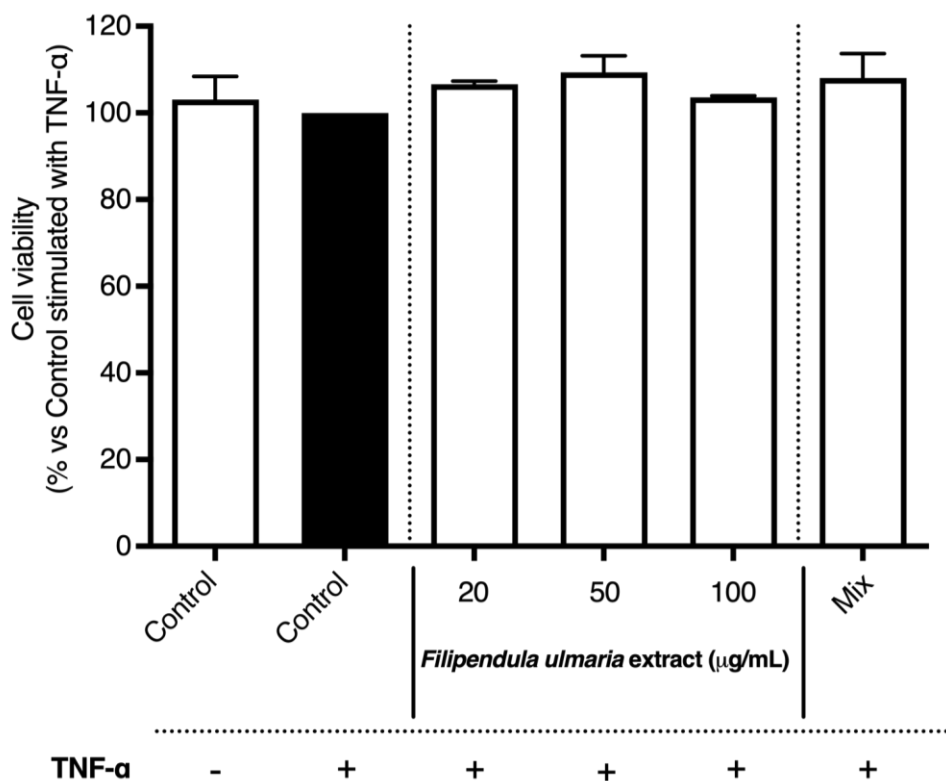


FIGURE 4.15: EFFECT OF *FILIPENDULA ULMARIA* EXTRACT AND MIX ON CELL VIABILITY. L929 CELLS WERE TREATED WITH 20, 50 AND 100 $\mu\text{g/mL}$. THE MIX CONTAINED 20 μM OF GALLIC ACID AND SALICYLIC ACID, 6 μM OF QUERCETIN AND 4 μM OF SYRINGIC ACID. AFTER 4 H OF INCUBATION, METABOLIC ACTIVITY WAS ASSESSED USING AN MTT ASSAY. NO SIGNIFICANT TOXICITY OR NO SIGNIFICANT DIFFERENCE IN CELL VIABILITY IS SEEN WITH RESPECT TO THE UNTREATED CONTROL. THE GRAPH DEPICTS COMPILED DATA OF 3 INDEPENDENT EXPERIMENTS (MEAN \pm SD).

As shown in Figure 4.15, the test concentrations of the extract and the mix did not appear to be toxic to the L929 cells in this experimental setting. Treatment with the *Filipendula ulmaria* extract at 100 $\mu\text{g/mL}$ resulted in 103.57% viability, as well as 108.09% viability for the mix, compared to the control stimulated with TNF- α . The inhibitory actions of the *Filipendula ulmaria* extract thus did not appear to result from

non-specific cellular toxicity, but rather were specific for NFκB-dependent gene transcription.

The same MTT assay was also performed for the COX-2 gene expression experiment in PMA-differentiated THP-1 cells, pre-incubated with test samples for 1 h and subsequently stimulated with LPS for an additional 3 h (Figure 4.16). The test concentrations of the *Filipendula ulmaria* extract, up to a concentration of 50 µg/mL with a total incubation time of 4 h (i.e. 102.21% of viable cells compared to LPS-stimulated control), also showed no significant toxicity on PMA-differentiated THP-1 cells.

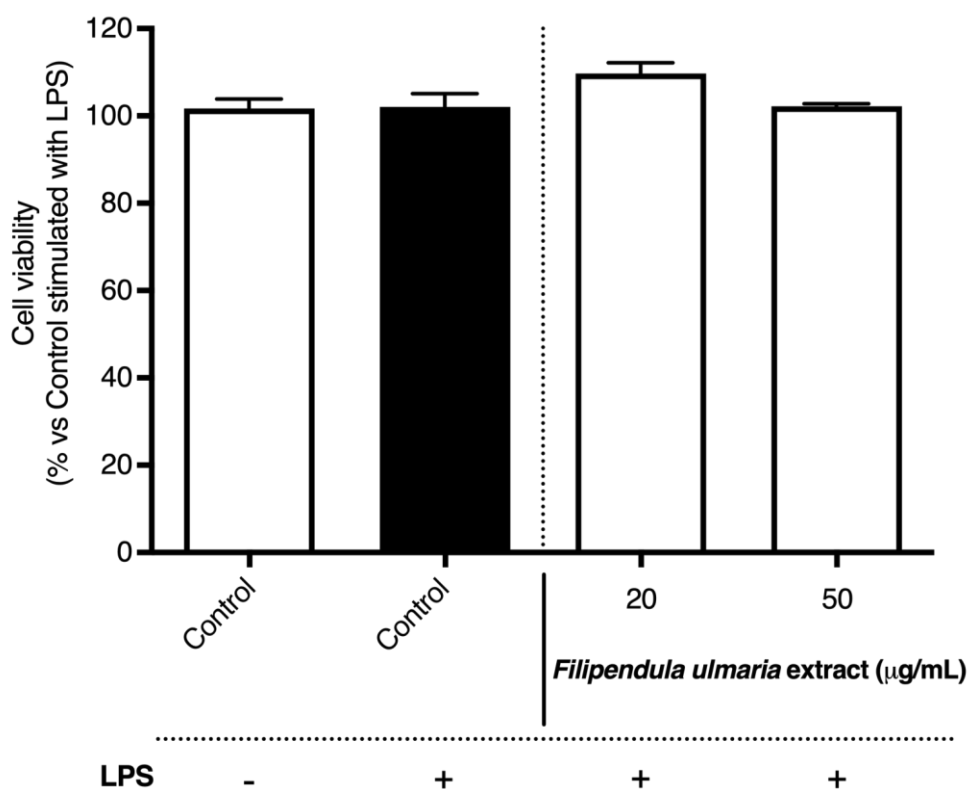


FIGURE 4.16: EFFECT OF *FILIPENDULA ULMARIA* EXTRACT ON CELL VIABILITY. THP-1 CELLS WERE TREATED WITH 20 AND 50 µg/mL. AFTER 4 H OF INCUBATION, METABOLIC ACTIVITY WAS ASSESSED USING AN MTT ASSAY. NO SIGNIFICANT TOXICITY OR NO SIGNIFICANT DIFFERENCE IN CELL VIABILITY IS SEEN WITH RESPECT TO THE UNTREATED CONTROL. THE GRAPH DEPICTS COMPILED DATA OF 3 INDEPENDENT EXPERIMENTS (MEAN ± SD).

CONCLUSION

It is well known that inflammation plays a key role in many chronic diseases such as cancer, diabetes, neurodegenerative and autoimmune disorders. Inflammation is a complex process and the causative factors present in excess at the site of the inflammatory response are mainly chemical mediators, including prostaglandins. An important anti-inflammatory mechanism is thus suppressing the generation of prostaglandins from arachidonic acid by inhibiting the COX-1 and -2 enzymes.^[64] The presented research in this thesis, demonstrated that the comprehensive, non-biotransformed *Filipendula ulmaria* extract significantly inhibited the activity of both COX isoenzymes in a dose-dependent manner. *Filipendula ulmaria* showed to be a more potent inhibitor of the COX-1 enzyme, with an IC₅₀ of 7.45 µg/mL, compared to the COX-2 enzyme, with an IC₅₀ of 90.26 µg/mL. However, the extract showed no effect on COX-2 gene expression at the test concentrations of 20 and 50 µg/mL in PMA-stimulated THP-1 cells. The absence of an additive or synergistic effect between inhibition of COX-2 gene expression and enzyme inhibition, might occur because of a paradoxical counterbalance by the cells with more protein expression if the COX-2 enzyme is inhibited.

Activation of NF-κB is one of the main mechanisms of inflammation, regulating the transcription of inflammatory proteins such as chemokines, cytokines, interleukins, interferons and COX-2. A tight regulation of NF-κB maintains the balance of essential cell functions since deregulated activity is often observed in chronic inflammation. Therefore, NF-κB also is an interesting target at various levels of regulation.^[15] Our research showed a clear dose-dependent inhibition on the TNF-α-induced NF-κB luciferase reporter gene induction in L929 cells compared to the stimulated control: the non-biotransformed extract of *Filipendula ulmaria* reached an IC₅₀ of 40.53 µg/mL.

While evidence from such *in vitro* experiments does not necessarily prove its *in vivo* activity, these studies do support and provide a rationale for the use of *Filipendula ulmaria* to suppress inflammation *in vivo*. Moreover, *in vivo* experiments are time-consuming and expensive, while *in vitro* (enzyme or cell-based) studies are predominantly used because of their lower costs and because they are easier to perform. These tests are also convenient for better evaluation of the complex interaction between polyphenols and the intracellular environment to study specific mechanisms of action, e.g. by studying interesting signaling pathways. Interpreting data obtained in this way, however, requires caution. First of all, the bioactive compounds might be formed *in vivo* due to biotransformation reactions carried out by the intestinal microflora or by the hepatic metabolism, which means they were not present in the original extract. Secondly, another important aspect is whether the concentration of the extract's constituents are realistic or achievable *in vivo*: typically, many plant constituents are not completely bioavailable since they are not easily absorbed. Therefore, a preliminary experiment was performed in order to clean up the colon samples from the gastrointestinal model, after 72 h of fermentation of the *Filipendula ulmaria* extract. Across all different extraction methods (methanol, ethyl acetate and acetone extraction) and the genuine 72 h fermentation sample, a preference in selectivity for the COX-1 over the COX-2 enzyme can still be observed in the enzyme inhibition assay, which is similar to the results obtained for the non-biotransformed *Filipendula ulmaria* extract. Moreover, the acetone extract showed the lowest IC₅₀ values. However, an effect of the blank samples, which contain no flavonoids, was also observed. It could be speculated that SCFAs might contribute to the inhibitory activity of the blanks on the COX enzymes. Testing samples containing fecal material proved to be difficult and challenging in cell-based assays, therefore, to further link the presence of compounds and/or metabolites present after gastrointestinal biotransformation to the pharmacological activity, a mix containing constituents of different groups present in the extract after biotransformation was

prepared. This mix composed of 20 μM of gallic acid and salicylic acid, 6 μM of quercetin and 4 μM of syringic acid, was used to test the effect on TNF- α -induced NF- κB luciferase reporter gene induction in L929 cells. However, no significant activities were observed. Interestingly, the mix did show a significant inhibition of 33.33% on the COX-1 enzyme. This might be explained by a synergistic or additive effect, since the single compounds tested in the assay showed no clear activity on the enzyme. For the COX-2 enzyme, no significant activity was observed for the mix, as well as for the single compounds.

REFERENCES

- [1] **Van der Auwera A**, Peeters L, Foubert K, Piazza S, Vanden Berghe W, Hermans N, Pieters L. *In vitro* biotransformation and anti-inflammatory activity of constituents and metabolites of *Filipendula ulmaria*. *Pharmaceutics*. 2023;15:1291
- [2] Medzhitov R. Inflammation 2010: new adventures of an old flame. *Cell*. 2010;140(6):771-6.
- [3] Chen L, Deng H, Cui H, Fang J, Zuo Z, Deng J, et al. Inflammatory responses and inflammation-associated diseases in organs. *Oncotarget*. 2018;9(6):7204-18.
- [4] Kumar V, Abbas AK, Aster JC. *Robbins Basic Pathology (E-Book)*. 10 ed: Elsevier Health Sciences; 2017.
- [5] Vaknin I, Baniyash M. Inflammatory Response and Immunity. Schwab M, editor. *Encyclopedia of Cancer*. Berlin, Germany: Springer Berlin Heidelberg; 2011. p. 1859-64.
- [6] Bacon F. Introduction to the immune response. Mak TW, Saunders ME, Jett BD, editors. *Primer to the immune response*. 2 ed. Boston, USA: Academic Cell; 2014. p. 3-20.
- [7] Horiguchi H, Loftus TJ, Hawkins RB, Raymond SL, Stortz JA, Hollen MK, et al. Innate immunity in the persistent inflammation, immunosuppression, and Catabolism Syndrome and its implications for therapy. *Front Immunol*. 2018;9:595.
- [8] Cronkite DA, Strutt TM. The regulation of inflammation by innate and adaptive lymphocytes. *J Immunol Res*. 2018;2018:1467538.
- [9] Furie MB. An Overview of inflammation. McManus LM, Mitchell RN, editors. *Pathobiology of human disease*. San Diego, USA: Academic Press; 2014. p. 226-30.
- [10] Ferrero-Miliani L, Nielsen OH, Andersen PS, Girardin SE. Chronic inflammation: importance of NOD2 and NALP3 in interleukin-1beta generation. *Clin Exp Immunol*. 2007;147(2):227-35.
- [11] Akira S, Uematsu S, Takeuchi O. Pathogen recognition and innate immunity. *Cell*. 2006;124(4):783-801.
- [12] Serhan CN, Savill J. Resolution of inflammation: the beginning programs the end. *Nat Immunol*. 2005;6(12):1191-7.
- [13] Fleit HB. Chronic Inflammation. McManus LM, Mitchell RN, editors. *Pathobiology of Human Disease*. San Diego, USA: Academic Press; 2014. p. 300-14.
- [14] Hofseth LJ. Inflammation. Schwab M, editor. *Encyclopedia of Cancer*. Berlin, Germany: Springer Berlin Heidelberg; 2011. p. 1848-51.

- [15] Gupta SC, Sundaram C, Reuter S, Aggarwal BB. Inhibiting NF- κ B activation by small molecules as a therapeutic strategy. *Biochim Biophys Acta*. 2010;1799(10-12):775-87.
- [16] Hayden MS, Ghosh S. NF- κ B, the first quarter-century: remarkable progress and outstanding questions. *Genes Dev*. 2012;26(3):203-34.
- [17] Serasanambati M, Chilakapati SR. Function of Nuclear Factor Kappa B (NF- κ B) in human diseases - A Review. *SIJBS*. 2016;2:368-87.
- [18] Liu T, Zhang L, Joo D, Sun SC. NF- κ B signaling in inflammation. *Signal Transduct Target Ther*. 2017;2.
- [19] Ghosh G, Wang VY, Huang DB, Fusco A. NF- κ B regulation: lessons from structures. *Immunol Rev*. 2012;246(1):36-58.
- [20] Xia L, Tan S, Zhou Y, Lin J, Wang H, Oyang L, et al. Role of the NF κ B-signaling pathway in cancer. *Onco Targets Ther*. 2018;11:2063-73.
- [21] Hayden MS, Ghosh S. Shared principles in NF- κ B signaling. *Cell*. 2008;132(3):344-62.
- [22] Cervantes CF, Markwick PR, Sue SC, McCammon JA, Dyson HJ, Komives EA. Functional dynamics of the folded ankyrin repeats of I kappa B alpha revealed by nuclear magnetic resonance. *Biochemistry*. 2009;48(33):8023-31.
- [23] Gamble C, McIntosh K, Scott R, Ho KH, Plevin R, Paul A. Inhibitory kappa B Kinases as targets for pharmacological regulation. *Br J Pharmacol*. 2012;165(4):802-19.
- [24] Shih VF, Tsui R, Caldwell A, Hoffmann A. A single NF κ B system for both canonical and non-canonical signaling. *Cell Res*. 2011;21(1):86-102.
- [25] Srivastava SK, Ramana KV. Focus on molecules: nuclear factor-kappaB. *Exp Eye Res*. 2009;88(1):2-3.
- [26] Pickart CM. Mechanisms underlying ubiquitination. *Annu Rev Biochem*. 2001;70:503-33.
- [27] Chen ZJ. Ubiquitin signalling in the NF- κ B pathway. *Nature Cell Biology*. 2005;7(8):758-65.
- [28] Sun SC. Non-canonical NF- κ B signaling pathway. *Cell Res*. 2011;21(1):71-85.
- [29] Xia Y, Shen S, Verma IM. NF- κ B, an active player in human cancers. *Cancer Immunol Res*. 2014;2(9):823-30.
- [30] Sun SC, Chang JH, Jin J. Regulation of NF- κ B in autoimmunity. *Trends Immunol*. 2013;34(6):282-9.
- [31] Van der Heiden K, Cuhlmann S, Luong le A, Zakkar M, Evans PC. Role of nuclear factor kappaB in cardiovascular health and disease. *Clin Sci (Lond)*. 2010;118(10):593-605.
- [32] Srinivasan M, Lahiri DK. Significance of NF- κ B as a pivotal therapeutic target in the neurodegenerative pathologies of Alzheimer's disease and multiple sclerosis. *Expert Opin Ther Targets*. 2015;19(4):471-87.
- [33] Cechetto DF. Role of nuclear factor kappa B in neuropathological mechanisms. *Prog Brain Res*. 2001;132:391-404.

- [34] Sau A, Cabrita MA, Pratt MAC. NF- κ B at the crossroads of normal mammary gland biology and the pathogenesis and prevention of BRCA1-mutated breast cancer. *Cancer Prev Res (Phila)*. 2018;11(2):69-80.
- [35] Wang W, Nag SA, Zhang R. Targeting the NF κ B signaling pathways for breast cancer prevention and therapy. *Curr Med Chem*. 2015;22(2):264-89.
- [36] Khongthong P, Roseweir AK, Edwards J. The NF- κ B pathway and endocrine therapy resistance in breast cancer. *Endocr Relat Cancer*. 2019;26(6):R369-R80.
- [37] Zhou J, Ching YQ, Chng WJ. Aberrant nuclear factor-kappa B activity in acute myeloid leukemia: from molecular pathogenesis to therapeutic target. *Oncotarget*. 2015;6(8):5490-500.
- [38] Makarov SS. NF- κ B in rheumatoid arthritis: a pivotal regulator of inflammation, hyperplasia, and tissue destruction. *Arthritis Res*. 2001;3(4):200-6.
- [39] Monaco C, Andreakos E, Kiriakidis S, Mauri C, Bicknell C, Foxwell B, et al. Canonical pathway of nuclear factor kappa B activation selectively regulates proinflammatory and prothrombotic responses in human atherosclerosis. *Proc Natl Acad Sci U S A*. 2004;101(15):5634-9.
- [40] Pamukcu B, Lip GY, Shantsila E. The nuclear factor-kappa B pathway in atherosclerosis: a potential therapeutic target for atherothrombotic vascular disease. *Thromb Res*. 2011;128(2):117-23.
- [41] Jha NK, Jha SK, Kar R, Nand P, Swati K, Goswami VK. Nuclear factor-kappa B as a therapeutic target for Alzheimer's disease. *J Neurochem*. 2019;150(2):113-37.
- [42] Jones SV, Kounatidis I. Nuclear factor-kappa b and Alzheimer Disease, unifying genetic and environmental risk factors from cell to humans. *Front Immunol*. 2017;8:1805.
- [43] Snow WM, Albenis BC. Neuronal gene targets of NF- κ B and their dysregulation in Alzheimer's Disease. *Front Mol Neurosci*. 2016;9:118.
- [44] Gilmore TD, Herscovitch M. Inhibitors of NF- κ B signaling: 785 and counting. *Oncogene*. 2006;25(51):6887-99.
- [45] Herrington FD, Carmody RJ, Goodyear CS. Modulation of NF- κ B signaling as a therapeutic target in autoimmunity. *J Biomol Screen*. 2016;21(3):223-42.
- [46] Monaco C, Nanchahal J, Taylor P, Feldmann M. Anti-TNF therapy: past, present and future. *Int Immunol*. 2015;27(1):55-62.
- [47] Kanarek N, London N, Schueler-Furman O, Ben-Neriah Y. Ubiquitination and degradation of the inhibitors of NF- κ B. *Cold Spring Harb Perspect Biol*. 2010;2(2):a000166.
- [48] Cao Y, Guan K, He X, Wei C, Zheng Z, Zhang Y, et al. Yersinia YopJ negatively regulates IRF3-mediated antibacterial response through disruption of STING-mediated cytosolic DNA signaling. *Biochim Biophys Acta*. 2016;1863(12):3148-59.
- [49] Torgerson TR, Colosia AD, Donahue JP, Lin YZ, Hawiger J. Regulation of NF- κ B, AP-1, NFAT, and STAT1 nuclear import in T lymphocytes by noninvasive delivery

- of peptide carrying the nuclear localization sequence of NF- κ B p50. *J Immunol.* 1998;161(11):6084-92.
- [50] Matsumoto N, Ariga A, To-e S, Nakamura H, Agata N, Hirano S, et al. Synthesis of NF- κ B activation inhibitors derived from epoxyquinomicin C. *Bioorg Med Chem Lett.* 2000;10(9):865-9.
- [51] Kubota T, Hoshino M, Aoki K, Ohya K, Komano Y, Nanki T, et al. NF- κ B inhibitor dehydroxymethylepoxyquinomicin suppresses osteoclastogenesis and expression of NFATc1 in mouse arthritis without affecting expression of RANKL, osteoprotegerin or macrophage colony-stimulating factor. *Arthritis Res Ther.* 2007;9(5):R97.
- [52] Wakamatsu K, Nanki T, Miyasaka N, Umezawa K, Kubota T. Effect of a small molecule inhibitor of nuclear factor- κ B nuclear translocation in a murine model of arthritis and cultured human synovial cells. *Arthritis Res Ther.* 2005;7(6):R1348-59.
- [53] Rungeler P, Castro V, Mora G, Goren N, Vichnewski W, Pahl HL, et al. Inhibition of transcription factor NF- κ B by sesquiterpene lactones: a proposed molecular mechanism of action. *Bioorg Med Chem.* 1999;7(11):2343-52.
- [54] De Stefano D. Oligonucleotides decoy to NF- κ B: becoming a reality? *Discov Med.* 2011;12(63):97-105.
- [55] Chen LF, Mu Y, Greene WC. Acetylation of RelA at discrete sites regulates distinct nuclear functions of NF- κ B. *EMBO J.* 2002;21(23):6539-48.
- [56] Tiffon C, Adams J, van der Fits L, Wen S, Townsend P, Ganesan A, et al. The histone deacetylase inhibitors vorinostat and romidepsin downmodulate IL-10 expression in cutaneous T-cell lymphoma cells. *Br J Pharmacol.* 2011;162(7):1590-602.
- [57] Bennett J, Capece D, Begalli F, Verzella D, D'Andrea D, Tornatore L, et al. NF- κ B in the crosshairs: Rethinking an old riddle. *Int J Biochem Cell Biol.* 2018;95:108-12.
- [58] Lima GPP, Vianello F, Corrêa CR, Campos R, Borguini MG. Polyphenols in fruits and vegetables and its effect on human health. *Food Nutr Sci.* 2014;5(11):1065-82.
- [59] Rossi L, Mazzitelli S, Arciello M, Capo CR, Rotilio G. Benefits from dietary polyphenols for brain aging and Alzheimer's Disease. *Neurochem Res.* 2008;33(12):2390-400.
- [60] Joven J, Micol V, Segura-Carretero A, Alonso-Villaverde C, Menéndez JA. Polyphenols and the modulation of gene expression pathways: can we eat our way out of the danger of chronic disease? *Crit Rev Food Sci Nutr.* 2014;54(8):985-1001.
- [61] Choy KW, Murugan D, Leong X, Abas R, Alias A, Mustafa MR. Flavonoids as natural anti-inflammatory agents targeting Nuclear Factor-Kappa B (NF κ B) signaling in cardiovascular diseases: a mini review. *Front Pharmacol.* 2019;10:1295-.

- [62] Serreli G, Deiana M. *In vivo* formed metabolites of polyphenols and their biological efficacy. *Food Funct.* 2019;10(11):6999-7021.
- [63] Simmons DL, Botting RM, Hla T. Cyclooxygenase isozymes: the biology of prostaglandin synthesis and inhibition. *Pharmacol Rev.* 2004;56(3):387-437.
- [64] Vane JR, Bakhle YS, Botting RM. Cyclooxygenases 1 and 2. *Annu Rev Pharmacol.* 1998;38(1):97-120.
- [65] Botting R. COX-1 and COX-3 inhibitors. *Thromb Res.* 2003;110(5-6):269-72.
- [66] Rouzer CA, Marnett LJ. Cyclooxygenases: structural and functional insights. *J Lipid Res.* 2009;50 Suppl:S29-34.
- [67] Hashemi GN, Najafi M, Salehi E, Farhood B, Mortezaee K. Cyclooxygenase-2 in cancer: A review. *J Cell Physiol.* 2019;234(5):5683-99.
- [68] Kang YJ, Mbonye UR, DeLong CJ, Wada M, Smith WL. Regulation of intracellular cyclooxygenase levels by gene transcription and protein degradation. *Prog Lipid Res.* 2007;46(2):108-25.
- [69] Warner TD, Mitchell JA. Cyclooxygenase-3 (COX-3): filling in the gaps toward a COX continuum? *Proc Natl Acad Sci USA.* 2002;99(21):13371-3.
- [70] Schwab JM, Schluesener HJ, Meyermann R, Serhan CN. COX-3 the enzyme and the concept: steps towards highly specialized pathways and precision therapeutics? *Prostaglandins Leukot Essent Fatty Acids.* 2003;69(5):339-43.
- [71] Smith WL, Murphy RC. The eicosanoids: cyclooxygenase, lipoxygenase, and epoxygenase pathways. Vance DE, Vance JE, editors. *Biochemistry of lipids, lipoproteins and membranes.* 5 ed. San Diego, USA: Elsevier; 2008. p. 331-62.
- [72] Grosser T, Fries S, FitzGerald GA. Biological basis for the cardiovascular consequences of COX-2 inhibition: therapeutic challenges and opportunities. *J Clin Invest.* 2006;116(1):4-15.
- [73] Breyer RM, Bagdassarian CK, Myers SA, Breyer MD. Prostanoid receptors: subtypes and signaling. *Annu Rev Pharmacol Toxicol.* 2001;41:661-90.
- [74] Smyth EM, Grosser T, Wang M, Yu Y, FitzGerald GA. Prostanoids in health and disease. *J Lipid Res.* 2009;50 Suppl:S423-8.
- [75] Ricciotti E, FitzGerald GA. Prostaglandins and inflammation. *Arterioscler Thromb Vasc Biol.* 2011;31(5):986-1000.
- [76] Fujikawa M, Ibuki T, Matsumura K, Sawa T. Inflammatory hyperalgesia: The role of the prostaglandin system in the spinal cord. *Adv Neuroimmune Biol.* 2012;3:197-207.
- [77] Harris RE. Cyclooxygenase-2 (cox-2) blockade in the chemoprevention of cancers of the colon, breast, prostate, and lung. *Inflammopharmacology.* 2009;17(2):55-67.
- [78] Ristimaki A, Sivula A, Lundin J, Lundin M, Salminen T, Haglund C, et al. Prognostic significance of elevated cyclooxygenase-2 expression in breast cancer. *Cancer Res.* 2002;62(3):632-5.

- [79] Hosomi Y, Yokose T, Hirose Y, Nakajima R, Nagai K, Nishiwaki Y, et al. Increased cyclooxygenase 2 (COX-2) expression occurs frequently in precursor lesions of human adenocarcinoma of the lung. *Lung Cancer*. 2000;30(2):73-81.
- [80] Gupta S, Srivastava M, Ahmad N, Bostwick DG, Mukhtar H. Over-expression of cyclooxygenase-2 in human prostate adenocarcinoma. *Prostate*. 2000;42(1):73-8.
- [81] Komhoff M, Guan Y, Shappell HW, Davis L, Jack G, Shyr Y, et al. Enhanced expression of cyclooxygenase-2 in high grade human transitional cell bladder carcinomas. *Am J Pathol*. 2000;157(1):29-35.
- [82] Matsubayashi H, Infante JR, Winter J, Klein AP, Schulick R, Hruban R, et al. Tumor COX-2 expression and prognosis of patients with resectable pancreatic cancer. *Cancer Biol Ther*. 2007;6(10):1569-75.
- [83] Higashi Y, Kanekura T, Kanzaki T. Enhanced expression of cyclooxygenase (COX)-2 in human skin epidermal cancer cells: evidence for growth suppression by inhibiting COX-2 expression. *Int J Cancer*. 2000;86(5):667-71.
- [84] Zimmermann KC, Sarbia M, Weber AA, Borchard F, Gabbert HE, Schror K. Cyclooxygenase-2 expression in human esophageal carcinoma. *Cancer Res*. 1999;59(1):198-204.
- [85] Uefuji K, Ichikura T, Mochizuki H. Cyclooxygenase-2 expression is related to prostaglandin biosynthesis and angiogenesis in human gastric cancer. *Clin Cancer Res*. 2000;6(1):135-8.
- [86] Soumaoro LT, Uetake H, Higuchi T, Takagi Y, Enomoto M, Sugihara K. Cyclooxygenase-2 expression: a significant prognostic indicator for patients with colorectal cancer. *Clin Cancer Res*. 2004;10(24):8465-71.
- [87] Shi G, Li D, Fu J, Sun Y, Li Y, Qu R, et al. Upregulation of cyclooxygenase-2 is associated with activation of the alternative nuclear factor kappa B signaling pathway in colonic adenocarcinoma. *Am J Transl Res*. 2015;7(9):1612-20.
- [88] Harris RE. *Inflammation in the pathogenesis of chronic diseases: The COX-2 controversy*. New York, USA: Springer; 2007.
- [89] Stasinopoulos I, Shah T, Penet MF, Krishnamachary B, Bhujwalla ZM. COX-2 in cancer: Gordian knot or Achilles heel? *Front Pharmacol*. 2013;4:34.
- [90] McCoy JM, Wicks JR, Audoly LP. The role of prostaglandin E2 receptors in the pathogenesis of rheumatoid arthritis. *J Clin Invest*. 2002;110(5):651-8.
- [91] Fattahi MJ, Mirshafiey A. Prostaglandins and rheumatoid arthritis. *Arthritis*. 2012;2012:239310.
- [92] Akaogi J, Nozaki T, Satoh M, Yamada H. Role of PGE2 and EP receptors in the pathogenesis of rheumatoid arthritis and as a novel therapeutic strategy. *Endocr Metab Immune Disord Drug Targets*. 2006;6(4):383-94.
- [93] Cipollone F, Fazia ML. COX-2 and atherosclerosis. *J Cardiovasc Pharmacol*. 2006;47 Suppl 1:S26-36.
- [94] Minghetti L. Cyclooxygenase-2 (COX-2) in inflammatory and degenerative brain diseases. *J Neuropathol Exp Neurol*. 2004;63(9):901-10.

- [95] Bartels AL, Leenders KL. Cyclooxygenase and neuroinflammation in Parkinson's disease neurodegeneration. *Curr Neuropharmacol*. 2010;8(1):62-8.
- [96] Liu N, Zhuang Y, Zhou Z, Zhao J, Chen Q, Zheng J. NF- κ B dependent up-regulation of TRPC6 by Abeta in BV-2 microglia cells increases COX-2 expression and contributes to hippocampus neuron damage. *Neurosci Lett*. 2017;651:1-8.
- [97] Sil S, Ghosh T. Role of COX-2 mediated neuroinflammation on the neurodegeneration and cognitive impairments in colchicine induced rat model of Alzheimer's Disease. *J Neuroimmunol*. 2016;291:115-24.
- [98] Guan PP, Yu X, Zou YH, Wang P. Cyclooxygenase-2 is critical for the propagation of beta-amyloid protein and reducing the glycosylation of tau in Alzheimer's disease. *Cell Mol Immunol*. 2019;16(11):892-4.
- [99] Conaghan PG. A turbulent decade for NSAIDs: update on current concepts of classification, epidemiology, comparative efficacy, and toxicity. *Rheumatol Int*. 2012;32(6):1491-502.
- [100] Crofford LJ. Use of NSAIDs in treating patients with arthritis. *Arthritis Res Ther*. 2013;15 Suppl 3:S2.
- [101] Dannhardt G, Kiefer W. Cyclooxygenase inhibitors-current status and future prospects. *Eur J Med Chem*. 2001;36(2):109-26.
- [102] Rao P, Knaus EE. Evolution of nonsteroidal anti-inflammatory drugs (NSAIDs): cyclooxygenase (COX) inhibition and beyond. *J Pharm Pharm Sci*. 2008;11(2):81s-110s.
- [103] Varga Z, Sabzwari SRA, Vargova V. Cardiovascular risk of nonsteroidal anti-inflammatory drugs: an under-recognized public health issue. *Cureus*. 2017;9(4):e1144.
- [104] Zarghi A, Arfaei S. Selective COX-2 inhibitors: a review of their structure-activity relationships. *Iran J Pharm Res*. 2011;10(4):655-83.
- [105] Karha J, Topol EJ. The sad story of Vioxx, and what we should learn from it. *Cleve Clin J Med*. 2004;71(12):933-4, 6, 8-9.
- [106] Culp DR, Berry I. Merck and the vioxx debacle: Deadly Loyalty. *John's J Legal Comment*. 2007;22:1-34.
- [107] Atukorala I, Hunter DJ. Valdecoxib : the rise and fall of a COX-2 inhibitor. *Expert Opin Pharmacother*. 2013;14(8):1077-86.
- [108] Farkouh ME, Kirshner H, Harrington RA, Ruland S, Verheugt FW, Schnitzer TJ, et al. Comparison of lumiracoxib with naproxen and ibuprofen in the Therapeutic Arthritis Research and Gastrointestinal Event Trial (TARGET), cardiovascular outcomes: randomised controlled trial. *Lancet*. 2004;364(9435):675-84.
- [109] Cannon CP, Curtis SP, FitzGerald GA, Krum H, Kaur A, Bolognese JA, et al. Cardiovascular outcomes with etoricoxib and diclofenac in patients with osteoarthritis and rheumatoid arthritis in the Multinational Etoricoxib and Diclofenac Arthritis Long-term (MEDAL) programme: a randomised comparison. *Lancet*. 2006;368(9549):1771-81.

- [110] Nissen SE, Yeomans ND, Solomon DH, Luscher TF, Libby P, Husni ME, et al. Cardiovascular safety of celecoxib, naproxen, or ibuprofen for arthritis. *N Engl J Med*. 2016;375(26):2519-29.
- [111] McGettigan P, Henry D. Cardiovascular risk with non-steroidal anti-inflammatory drugs: systematic review of population-based controlled observational studies. *PLoS Med*. 2011;8(9):e1001098.
- [112] Salvo F, Antoniazzi S, Duong M, Molimard M, Bazin F, Fourrier-Reglat A, et al. Cardiovascular events associated with the long-term use of NSAIDs: a review of randomized controlled trials and observational studies. *Expert Opin Drug Saf*. 2014;13(5):573-85.
- [113] Varas-Lorenzo C, Riera-Guardia N, Calingaert B, Castellsague J, Pariente A, Scotti L, et al. Stroke risk and NSAIDs: a systematic review of observational studies. *Pharmacoepidemiol Drug Saf*. 2011;20(12):1225-36.
- [114] Bally M, Dendukuri N, Rich B, Nadeau L, Helin-Salmivaara A, Garbe E, et al. Risk of acute myocardial infarction with NSAIDs in real world use: bayesian meta-analysis of individual patient data. *BMJ*. 2017;357:j1909.
- [115] Mitchell JA, Kirkby NS. Eicosanoids, prostacyclin and cyclooxygenase in the cardiovascular system. *Br J Pharmacol*. 2019;176(8):1038-50.
- [116] Walker C, Biasucci LM. Cardiovascular safety of non-steroidal anti-inflammatory drugs revisited. *Postgrad Med*. 2018;130(1):55-71.
- [117] Harris RE, Beebe-Donk J, Alshafie GA. Cancer chemoprevention by cyclooxygenase 2 (COX-2) blockade: results of case control studies. *Subcell Biochem*. 2007;42:193-212.
- [118] Ghosh N, Chaki R, Mandal V, Mandal SC. COX-2 as a target for cancer chemotherapy. *Pharmacol Rep*. 2010;62(2):233-44.
- [119] Saedder EA, Brock B, Nielsen LP, Bonnerup DK, Lisby M. Identifying high-risk medication: a systematic literature review. *Eur J Clin Pharmacol*. 2014;70(6):637-45.
- [120] EMA. Assessment report on *Filipendula ulmaria* (L.) Maxim., herba and *Filipendula ulmaria* (L.) Maxim., flos. European Medicines Agency; 2011.
- [121] Okuda T, Yoshida T, Hatano T, Iwasaki M, Kubo M, Orime T, et al. Hydrolysable tannins as chemotaxonomic markers in the rosaceae. *Phytochemistry*. 1992;31(9):3091-6.
- [122] Pemp E, Reznicek G, Krenn L. Fast quantification of flavonoids in *Filipendulae ulmariae* flos by HPLC/ESI-MS using a nonporous stationary phase. *J Anal Chem*. 2007;62(7):669-73.
- [123] Papp I, Simandi B, Blazics B, Alberti Á, Héthelyi É, Szőke É, Kéry Á. Monitoring volatile and non-volatile salicylates in *Filipendula ulmaria* by different chromatographic techniques. *Chromatographia*. 2008;68(1):125-9.
- [124] Fecka I. Qualitative and quantitative determination of hydrolysable tannins and other polyphenols in herbal products from meadowsweet and dog rose. *Phytochem Anal*. 2009;20(3):177-90.

- [125] Shilova IV, Semenov AA, Suslov NI, Korotkova EI, Vtorushina AN, Belyakova VV. Chemical composition and biological activity of a fraction of meadowsweet extract. *Pharm Chem J*. 2009;43(4):185-90.
- [126] Barros L, Alves CT, Dueñas M, Silva S, Oliveira R, Carvalho AM, et al. Characterization of phenolic compounds in wild medicinal flowers from Portugal by HPLC–DAD–ESI/MS and evaluation of antifungal properties. *Ind Crops and Prod*. 2013;44:104-10.
- [127] Olennikov DN, Kruglova MY. A new quercetin glycoside and other phenolic compounds from the genus *Filipendula*. *Chem Nat Compd*. 2013;49(4):610-6.
- [128] Barros L, Cabrita L, Vilasboas M, Carvalho A, Ferreira I. Chemical, biochemical and electrochemical assays to evaluate phytochemicals and antioxidant activity of wild plants. *Food Chemistry*. 2011;127.
- [129] Del Rio D, Rodriguez-Mateos A, Spencer JP, Tognolini M, Borges G, Crozier A. Dietary (poly)phenolics in human health: structures, bioavailability, and evidence of protective effects against chronic diseases. *Antioxid Redox Signal*. 2013;18(14):1818-92.
- [130] Lu MF, Xiao ZT, Zhang HY. Where do health benefits of flavonoids come from? Insights from flavonoid targets and their evolutionary history. *Biochem Biophys Res Commun*. 2013;434(4):701-4.
- [131] Vogl S, Picker P, Mihaly-Bison J, Fakhrudin N, Atanasov AG, Heiss EH, et al. Ethnopharmacological *in vitro* studies on Austria's folk medicine-an unexplored lore in vitro anti-inflammatory activities of 71 Austrian traditional herbal drugs. *J Ethnopharmacol*. 2013;149(3):750-71.
- [132] Korbecki J, Bobiński R, Dutka M. Self-regulation of the inflammatory response by peroxisome proliferator-activated receptors. *Inflamm Res*. 2019;68(6):443-58.
- [133] Yahfoufi N, Alsadi N, Jambi M, Matar C. The immunomodulatory and anti-inflammatory role of polyphenols. *Nutrients*. 2018;10(11):1618.
- [134] Morais M, Luqman S, Kondratyuk TP, Petronio MS, Regasini LO, Silva DHS, et al. Suppression of TNF- α induced NF- κ B activity by gallic acid and its semi-synthetic esters: possible role in cancer chemoprevention. *Nat Prod Res*. 2010;24(18):1758-65.
- [135] Lu Y, Liu W, Zhang M, Deng Y, Jiang M, Bai G. The Screening Research of NF- κ B inhibitors from moutan cortex based on bioactivity-integrated UPLC-Q/TOF-MS. *eCAM*. 2019;2019:6150357.
- [136] Choi K, Lee Y, Jung MG, Kwon SH, Kim M, Jun WJ, et al. Gallic acid suppresses lipopolysaccharide-induced nuclear factor- κ B signaling by preventing RelA acetylation in A549 lung cancer cells. *Mol Cancer Res*. 2009;7(12):2011-21.
- [137] Amann R, Peskar BA. Anti-inflammatory effects of aspirin and sodium salicylate. *Eur J Pharmacol*. 2002;447(1):1-9.
- [138] Kopp E, Ghosh S. Inhibition of NF- κ B by sodium salicylate and Aspirin. *Science*. 1994;265(5174):956-9.

- [139] Bayón Y, Alonso A, Crespo MS. 4-trifluoromethyl derivatives of salicylate, triflusal and its main metabolite 2-hydroxy-4-trifluoromethylbenzoic acid, are potent inhibitors of nuclear factor κ B activation. *Br J Pharmacol*. 1999;126(6):1359-66.
- [140] Grilli M, Pizzi M, Memo M, Spano P. Neuroprotection by Aspirin and sodium salicylate through blockade of NF- κ B activation. *Science*. 1996;274(5291):1383-5.
- [141] Pierce JW, Read MA, Ding H, Luscinskas FW, Collins T. Salicylates inhibit I kappa B-alpha phosphorylation, endothelial-leukocyte adhesion molecule expression, and neutrophil transmigration. *J Immunol*. 1996;156(10):3961.
- [142] Yin M, Yamamoto Y, Gaynor RB. The anti-inflammatory agents aspirin and salicylate inhibit the activity of I κ B kinase- β . *Nature*. 1998;396(6706):77-80.
- [143] Cho Y, Kim C, Ha T, Ahn H. Inhibition of NF- κ B and STAT3 by quercetin with suppression of adhesion molecule expression in vascular endothelial cells. *Farmacia*. 2016;64:668-73.
- [144] Comalada M, Camuesco D, Sierra S, Ballester I, Xaus J, Gálvez J, et al. *In vivo* quercitrin anti-inflammatory effect involves release of quercetin, which inhibits inflammation through down-regulation of the NF- κ B pathway. *Eur J Immunol*. 2005;35(2):584-92.
- [145] Min YD, Choi CH, Bark H, Son HY, Park HH, Lee S, et al. Quercetin inhibits expression of inflammatory cytokines through attenuation of NF- κ B and p38 MAPK in HMC-1 human mast cell line. *Inflamm Res*. 2007;56(5):210-5.
- [146] De Stefano D, Maiuri MC, Simeon V, Grassia G, Soscia A, Cinelli MP, et al. Lycopene, quercetin and tyrosol prevent macrophage activation induced by gliadin and IFN- γ . *Eur J Pharmacol*. 2007;566(1):192-9.
- [147] Ruiz PA, Braune A, Hözlwimmer G, Quintanilla-Fend L, Haller D. Quercetin Inhibits TNF-Induced NF- κ B transcription factor recruitment to proinflammatory gene promoters in murine intestinal epithelial cells. *J Nutr*. 2007;137(5):1208-15.
- [148] Chen J, Ho F, Pei-Dawn Lee C, Chen C, Jeng KG, Hsu H, et al. Inhibition of iNOS gene expression by quercetin is mediated by the inhibition of I κ B kinase, nuclear factor-kappa B and STAT1, and depends on heme oxygenase-1 induction in mouse BV-2 microglia. *Eur J Pharmacol*. 2005;521(1):9-20.
- [149] Ham JR, Lee H, Choi R, Sim M, Seo K, Lee M. Anti-steatotic and anti-inflammatory roles of syringic acid in high-fat diet-induced obese mice. *Food & function*. 2016;7(2):689-97.
- [150] Fang W, Zhu S, Niu Z, Yin Y. The protective effect of syringic acid on dextran sulfate sodium-induced experimental colitis in BALB/c mice. *Drug Dev Res*. 2019;80(6):731-40.
- [151] Manjunatha S, Shaik AH, Maruthi Prasad E, Al Omar SY, Mohammad A, Kodihela LD. Combined cardio-protective ability of syringic acid and

- resveratrol against isoproterenol induced cardio-toxicity in rats via attenuating NF-kB and TNF- α pathways. *Scientific Reports*. 2020;10(1):3426.
- [152] Samardzic S, Arsenijevic J, Bozic D, Milenkovic M, Tesevic V, Maksimovic Z. Antioxidant, anti-inflammatory and gastroprotective activity of *Filipendula ulmaria* (L.) Maxim. and *Filipendula vulgaris* Moench. *J Ethnopharmacol*. 2018;213:132-7.
- [153] Tunón H, Olavsdotter C, Bohlin L. Evaluation of anti-inflammatory activity of some Swedish medicinal plants. Inhibition of prostaglandin biosynthesis and PAF-induced exocytosis. *J Ethnopharmacol*. 1995;48(2):61-76.
- [154] Katanić J, Boroja T, Mihailovic V, Nikles S, Pan SP, Rosic G, et al. *In vitro* and *in vivo* assessment of meadowsweet (*Filipendula ulmaria*) as anti-inflammatory agent. *J Ethnopharmacol*. 2016;193:627-36.
- [155] Cholet J, Decombat C, Varelle-Delarbre M, Gainche M, Berry A, Ogeron C, et al. Comparison of the anti-inflammatory and immunomodulatory mechanisms of two medicinal herbs: meadowsweet (*Filipendula ulmaria*) and harpagophytum (*Harpagophytum procumbens*). *IJPAES*. 2019;9:145-63.
- [156] Bijttebier S, Van der Auwera A, Voorspoels S, Noten B, Hermans N, Pieters L, et al. A first step in the quest for the active constituents in *Filipendula ulmaria* (meadowsweet): comprehensive phytochemical identification by liquid chromatography coupled to quadrupole-orbitrap mass spectrometry. *Planta Med*. 2016;82.
- [157] Al-Fayez M, Cai H, Tunstall R, Steward WP, Gescher AJ. Differential modulation of cyclooxygenase-mediated prostaglandin production by the putative cancer chemopreventive flavonoids tricrin, apigenin and quercetin. *Cancer Chemother. Pharmacol*. 2006;58(6):816-25.
- [158] El-Seedi HR, Ringbom T, Torszell K, Bohlin L. Constituents of *Hypericum laricifolium* and their cyclooxygenase (COX) enzyme activities. *Chem Pharm Bull (Tokyo)*. 2003;51(12):1439-40.
- [159] Kutil Z, Temml V, Maghradze D, Pribylova M, Dvorakova M, Schuster D, et al. Impact of wines and wine constituents on cyclooxygenase-1, cyclooxygenase-2, and 5-lipoxygenase catalytic activity. *Mediat Inflamm*. 2014;2014:178931.
- [160] Landolfi R, Mower RL, Steiner M. Modification of platelet function and arachidonic acid metabolism by bioflavonoids: Structure-activity relations. *Biochem Pharmacol*. 1984;33(9):1525-30.
- [161] Kum H, Roh KB, Shin S, Jung K, Park D, Jung E. Evaluation of anti-acne properties of phloretin *in vitro* and *in vivo*. *Int J Cosmet Sci*. 2016;38(1):85-92.
- [162] Larrosa M, Garcia-Conesa MT, Espin JC, Tomás-Barberan FA. Ellagitannins, ellagic acid and vascular health. *Mol Aspects Med*. 2010;31(6):513-39.
- [163] Larrosa M, Gonzalez-Sarrias A, Yanez-Gascon MJ, Selma MV, Azorin-Ortuno M, Toti S, et al. Anti-inflammatory properties of a pomegranate extract and its metabolite urolithin-A in a colitis rat model and the effect of colon inflammation on phenolic metabolism. *J Nutr Biochem*. 2010;21(8):717-25.

- [164] Tomás-Barberan FA, Espín JC, García-Conesa MT. Bioavailability and metabolism of ellagic acid and ellagitannins. Quideau S, editor. Chemistry and biology of ellagitannins: an underestimated class of bioactive plant polyphenols: World Scientific; 2009. p. 273-97.
- [165] Beretta G, Rossoni G, Santagati NA, Facino RM. Anti-ischemic activity and endothelium-dependent vasorelaxant effect of hydrolysable tannins from the leaves of *Rhus coriaria* (Sumac) in isolated rabbit heart and thoracic aorta. *Planta Med.* 2009;75(14):1482-8.
- [166] Ríos J, Giner R, Marín M, Recio MC. A pharmacological update of ellagic acid. *Planta Med.* 2018;84 15:1068-93.
- [167] Akhtar S, Ismail T, Fraternali D, Sestili P. Pomegranate peel and peel extracts: Chemistry and food features. *Food Chem.* 2015;174:417-25.
- [168] Alfei S, Turrini F, Catena S, Zunin P, Grilli M, Pittaluga AM, et al. Ellagic acid a multi-target bioactive compound for drug discovery in CNS? A narrative review. *Eur J Med Chem.* 2019;183:111724.
- [169] Muthukumaran S, Tranchant C, Shi J, Ye X, Xue SJ. Ellagic acid in strawberry (*Fragaria* spp.): Biological, technological, stability, and human health aspects. *Food Qual Saf.* 2017;1(4):227-52.
- [170] Andrade MA, Lima V, Silva AS, Vilarinho F, Castilho MC, Khwaldia K, et al. Pomegranate and grape by-products and their active compounds: Are they a valuable source for food applications? *Trends Food Sci Technol.* 2019;86:68-84.
- [171] Rosillo MA, Sánchez-Hidalgo M, Cárdeno A, Aparicio-Soto M, Sánchez-Fidalgo S, Villegas I, et al. Dietary supplementation of an ellagic acid-enriched pomegranate extract attenuates chronic colonic inflammation in rats. *Pharmacol Res.* 2012;66(3):235-42.
- [172] Zhou E, Fu Y, Wei Z, Yang Z. Inhibition of allergic airway inflammation through the blockage of NF- κ B activation by ellagic acid in an ovalbumin-induced mouse asthma model. *Food & function.* 2014;5(9):2106-12.
- [173] Ghasemi-Niri SF, Maqbool F, Baeri M, Gholami M, Abdollahi M. Phosalone-induced inflammation and oxidative stress in the colon: Evaluation and treatment. *World J Gastroenterol.* 2016;22(21):4999-5011.
- [174] El-Shitany NA, El-Bastawissy EA, El-desoky K. Ellagic acid protects against carrageenan-induced acute inflammation through inhibition of nuclear factor kappa B, inducible cyclooxygenase and proinflammatory cytokines and enhancement of interleukin-10 via an antioxidant mechanism. *Int Immunopharmacol.* 2014;19(2):290-9.
- [175] Karlsson S, Nånberg E, Fjaeraa C, Wijkander J. Ellagic acid inhibits lipopolysaccharide-induced expression of enzymes involved in the synthesis of prostaglandin E2 in human monocytes. *Br J Nutr.* 2010;103(8):1102-9.
- [176] Zhang Y, DeWitt DL, Murugesan S, Nair MG. Novel lipid-peroxidation- and cyclooxygenase-inhibitory tannins from *Picrorhiza kurroa* seeds. *Chem Biodivers.* 2004;1(3):426-41.

- [177] Noshadi B, Ercetin T, Luise C, Yuksel MY, Sippl W, Sahin MF, et al. Synthesis, characterization, molecular docking, and biological activities of some natural and synthetic urolithin analogs. *Chem Biodivers*. 2020;17(8):e2000197.
- [178] González-Sarrías A, Larrosa M, Tomás-Barberán FA, Dolara P, Espín JC. NF- κ B-dependent anti-inflammatory activity of urolithins, gut microbiota ellagic acid-derived metabolites, in human colonic fibroblasts. *Br J Nutr*. 2010;104(4):503-12.
- [179] Lee G, Park J, Lee E, Ahn J, Kim H. Anti-inflammatory and antioxidant mechanisms of urolithin B in activated microglia. *Phytomedicine*. 2019;55:50-7.
- [180] Mitchell JA, Akarasereenont P, Thiemermann C, Flower RJ, Vane JR. Selectivity of nonsteroidal antiinflammatory drugs as inhibitors of constitutive and inducible cyclooxygenase. *PNAS*. 1993;90(24):11693-7.
- [181] Patrignani P, Panara MR, Sciulli MG, Santini G, Renda G, Patrono C. Differential inhibition of human prostaglandin endoperoxide synthase-1 and -2 by nonsteroidal anti-inflammatory drugs. *J Physiol Pharmacol*. 1997;48(4):623-31.
- [182] Giuliano F, Warner TD. *Ex vivo* assay to determine the cyclooxygenase selectivity of non-steroidal anti-inflammatory drugs. *Br J Pharmacol*. 1999;126(8):1824-30.
- [183] Warner TD, Giuliano F, Vojnovic I, Bukasa A, Mitchell JA, Vane JR. Nonsteroid drug selectivities for cyclooxygenase-1 rather than cyclooxygenase-2 are associated with human gastrointestinal toxicity: A full *in vitro* analysis. *PNAS*. 1999;96(13):7563-8.
- [184] Mitchell JA, Saunders M, Barnes PJ, Newton R, Belvisi MG. Sodium salicylate inhibits cyclooxygenase-2 activity independently of transcription factor (Nuclear Factor κ B) activation: role of arachidonic acid. *Mol Pharmacol*. 1997;51(6):907-12.
- [185] Amann R, Egger T, Schuligoi R, Heinemann A, Peskar BA. Sodium salicylate enhances the expression of cyclooxygenase-2 in endotoxin-stimulated human mononuclear cells. *Eur J Pharmacol*. 2001;433(1):129-34.
- [186] Madlener S, Illmer C, Horvath Z, Saiko P, Losert A, Herbacek I, et al. Gallic acid inhibits ribonucleotide reductase and cyclooxygenases in human HL-60 promyelocytic leukemia cells. *Cancer Lett*. 2007;245(1):156-62.
- [187] Reddy TC, Aparoy P, Babu NK, Kumar KA, Kalangi SK, Reddanna P. Kinetics and docking studies of a COX-2 inhibitor isolated from *Terminalia bellerica* fruits. *Protein Pept Lett*. 2010;17(10):1251-7.
- [188] Amaravani M, Prasad NK, Ramakrishna V. COX-2 structural analysis and docking studies with gallic acid structural analogues. *Springerplus*. 2012;1(1):58.
- [189] BenSaad LA, Kim KH, Quah CC, Kim WR, Shahimi M. Anti-inflammatory potential of ellagic acid, gallic acid and punicalagin A&B isolated from *Punica granatum*. *BMC Complement Altern Med*. 2017;17(1):47-.

- [190] Pandurangan AK, Mohebbali N, Mohd. Esa N, Looi CY, Ismail S, Saadatdoust Z. Gallic acid suppresses inflammation in dextran sodium sulfate-induced colitis in mice: Possible mechanisms. In. *Immunopharmacol.* 2015;28(2):1034-43.
- [191] Yoon C, Chung S, Lee S, Park Y, Lee S, Park M. Gallic acid, a natural polyphenolic acid, induces apoptosis and inhibits proinflammatory gene expressions in rheumatoid arthritis fibroblast-like synoviocytes. *Joint Bone Spine.* 2013;80(3):274-9.
- [192] Srinivasulu C, Ramgopal M, Ramanjaneyulu G, Anuradha CM, Suresh Kumar C. Syringic acid (SA) – A review of its occurrence, biosynthesis, pharmacological and industrial importance. *Biomed Pharmacother.* 2018;108:547-57.
- [193] Stanikunaite R, Khan SI, Trappe JM, Ross SA. Cyclooxygenase-2 inhibitory and antioxidant compounds from the truffle *Elaphomyces granulatus*. *Phytother Res.* 2009;23(4):575-8.
- [194] Rekha KR, Selvakumar GP, Sivakamasundari RI. Effects of syringic acid on chronic MPTP/probenecid induced motor dysfunction, dopaminergic markers expression and neuroinflammation in C57BL/6 mice. *Biomed Aging Pathol.* 2014;4(2):95-104.
- [195] Periyannan V, Annamalai V, Veerasamy V. Syringic acid modulates molecular marker-involved cell proliferation, survival, apoptosis, inflammation, and angiogenesis in DMBA-induced oral squamous cell carcinoma in Syrian hamsters. *J Biochem Mol Toxicol.* 2020:e22574.
- [196] García-Villalba R, Giménez-Bastida JA, García-Conesa MT, Tomás-Barberán FA, Espín JC, Larrosa M. Alternative method for gas chromatography-mass spectrometry analysis of short-chain fatty acids in faecal samples. *J Sep Sci.* 2012;35(15):1906-13.
- [197] Markowiak-Kopeć P, Śliżewska K. The effect of probiotics on the production of short-chain fatty acids by human intestinal microbiome. *Nutrients.* 2020;12(4):1107.
- [198] Al-Lahham SH, Peppelenbosch MP, Roelofsen H, Vonk RJ, Venema K. Biological effects of propionic acid in humans; metabolism, potential applications and underlying mechanisms. *Biochim Biophys Acta Mol Cell Biol Lipids.* 2010;1801(11):1175-83.
- [199] Dannhardt G, Lehr M. Nonsteroidal antiinflammatory agents, XVII: Inhibition of bovine cyclooxygenase and 5-lipoxygenase by N-alkyldiphenyl-pyrrolyl acetic and propionic acid derivatives. *Archiv der Pharmazie.* 1993;326(3):157-62.
- [200] Gupta K, Kaub CJ, Carey KN, Casillas EG, Selinsky BS, Loll PJ. Manipulation of kinetic profiles in 2-aryl propionic acid cyclooxygenase inhibitors. *Bioorganic Med Chem Lett.* 2004;14(3):667-71.
- [201] Blobaum AL, Marnett LJ. Structural and functional basis of cyclooxygenase inhibition. *J Med Chem.* 2007;50(7):1425-41.
- [202] Bittencourt JAHM, Neto MFA, Lacerda PS, Bittencourt RCVS, Silva RC, Lobato CC, et al. *In Silico* evaluation of ibuprofen and two benzoylpropionic acid

- derivatives with potential anti-inflammatory activity. *Molecules*. 2019;24(8):1476.
- [203] Katanić J, Pferschy-Wenzig E, Mihailović V, Boroja T, Pan S, Nikles S, et al. Phytochemical analysis and anti-inflammatory effects of *Filipendula vulgaris* Moench extracts. *Food Chem Toxicol*. 2018;122:151-62.
- [204] Ramer R, Walther U, Borchert P, Laufer S, Linnebacher M, Hinz B. Induction but not inhibition of COX-2 confers human lung cancer cell apoptosis by celecoxib. *J Lipid Res*. 2013;54(11):3116-29.
- [205] Adams LS, Seeram NP, Aggarwal BB, Takada Y, Sand D, Heber D. Pomegranate juice, total pomegranate ellagitannins, and punicalagin suppress inflammatory cell signaling in colon cancer cells. *J Agric Food Chem*. 2006;54(3):980-5.
- [206] Mandal A, Bhatia D, Bishayee A. Anti-inflammatory mechanism involved in pomegranate-mediated prevention of breast cancer: the role of NF- κ B and Nrf2 signaling pathways. *Nutrients*. 2017;9(5):436.
- [207] Banerjee N, Kim H, Talcott S, Mertens-Talcott S. Pomegranate polyphenolics suppressed azoxymethane-induced colorectal aberrant crypt foci and inflammation: possible role of miR-126/VCAM-1 and miR-126/PI3K/AKT/mTOR. *Carcinogenesis*. 2013;34(12):2814-22.
- [208] Rodríguez-Ramiro I, Ramos S, López-Oliva E, Agis-Torres A, Bravo L, Goya L, et al. Cocoa polyphenols prevent inflammation in the colon of azoxymethane-treated rats and in TNF- α -stimulated Caco-2 cells. *Br J Nutr*. 2013;110(2):206-15.
- [209] Hong MY, Nulton E, Shelechi M, Hernández LM, Nemosock T. Effects of dark chocolate on azoxymethane-induced colonic aberrant crypt foci. *Nutr Cancer*. 2013;65(5):677-85.
- [210] Kountouri AM, Gioxari A, Karvela E, Kaliora AC, Karvelas M, Karathanos VT. Chemopreventive properties of raisins originating from Greece in colon cancer cells. *Food & Function*. 2013;4(3):366-72.
- [211] Bounaama A, Enayat S, Ceyhan MS, Moulahoum H, Djerdjouri B, Banerjee S. Ethanol extract of bark from *Salix aegyptiaca* ameliorates 1,2-dimethylhydrazine-induced colon carcinogenesis in mice by reducing oxidative stress. *Nutr Cancer*. 2016;68(3):495-506.
- [212] Bonaterra GA, Kelber O, Weiser D, Metz J, Kinscherf R. *In vitro* anti-proliferative effects of the willow bark extract STW 33-I. *Arzneimittelforschung*. 2010;60(6):330-5.
- [213] Mutoh M, Takahashi M, Fukuda K, Matsushima-Hibiya Y, Mutoh H, Sugimura T, et al. Suppression of cyclooxygenase-2 promoter-dependent transcriptional activity in colon cancer cells by chemopreventive agents with a resorcin-type structure. *Carcinogenesis*. 2000;21(5):959-63.
- [214] Mutoh M, Takahashi M, Fukuda K, Komatsu H, Enya T, Matsushima-Hibiya Y, et al. Suppression by flavonoids of cyclooxygenase-2 promoter-dependent

- transcriptional activity in colon cancer cells: structure-activity relationship. *Jpn J Cancer Res.* 2000;91(7):686-91.
- [215] Hou D, Yanagita T, Uto T, Masuzaki S, Fujii M. Anthocyanidins inhibit cyclooxygenase-2 expression in LPS-evoked macrophages: Structure-activity relationship and molecular mechanisms involved. *Biochem Pharmacol.* 2005;70(3):417-25.
- [216] Yi Lau GT, Leung LK. The dietary flavonoid apigenin blocks phorbol 12-myristate 13-acetate-induced COX-2 transcriptional activity in breast cell lines. *Food Chem Toxicol.* 2010;48(10):3022-7.
- [217] Liang Y, Huang Y, Tsai S, Lin-Shiau S, Chen C, Lin J. Suppression of inducible cyclooxygenase and inducible nitric oxide synthase by apigenin and related flavonoids in mouse macrophages. *Carcinogenesis.* 1999;20(10):1945-52.
- [218] Chen L, Teng H, Jia Z, Battino M, Miron A, Yu Z, et al. Intracellular signaling pathways of inflammation modulated by dietary flavonoids: The most recent evidence. *Crit Rev Food Sci Nutr.* 2018;58(17):2908-24.
- [219] Wu K, Sanduja R, Tsai A, Ferhanoglu B, Loose-Mitchell D. Aspirin inhibits interleukin 1-induced prostaglandin H synthase expression in cultured endothelial cells. *PNAS.* 1991;88(6):2384-7.
- [220] Xu X, Sansores-Garcia L, Chen X, Matijevic-Aleksic N, Du M, Wu K. Suppression of inducible cyclooxygenase 2 gene transcription by aspirin and sodium salicylate. *PNAS.* 1999;96(9):5292-7.
- [221] Barrios-Rodiles M, Keller K, Belley A, Chadee K. Nonsteroidal antiinflammatory drugs inhibit cyclooxygenase-2 enzyme activity but not mRNA Expression in human macrophages. *Biochem Biophys Res Commun.* 1996;225(3):896-900.
- [222] Osullivan M, Huggins E, McCall C. Lipopolysaccharide-induced expression of prostaglandin H synthase-2 in alveolar macrophages is inhibited by dexamethasone but not by aspirin. *Biochem Biophys Res Commun.* 1993;191(3):1294-300.
- [223] Hinz B, Kraus V, Pahl A, Brune K. Salicylate metabolites inhibit cyclooxygenase-2-dependent prostaglandin E2 synthesis in murine macrophages. *Biochem Biophys Res Commun.* 2000;274(1):197-202.

GENERAL CONCLUSIONS AND FUTURE PERSPECTIVES

The burden of communicable and non-communicable diseases, and the obstacles of finding new drug candidates that can treat these conditions with little or no side effects is a huge challenge for the pharmaceutical industry. Drug discovery and development did not guarantee a steady flow of new pharmaceuticals and remains a lengthy process with a low success rate as well as a huge capital investment. However, nature has been a vital source of active ingredients to treat diseases before the dawn of modern medicine and there has been a renewed interest in natural products to deliver new lead compounds in key therapeutic areas. This thesis focused on inflammation, since many of the currently used NSAIDs show severe gastrointestinal side effects. There is thus a high need for new and safer anti-inflammatory drugs. In addition, it is well known that inflammation plays a key role in many chronic diseases such as cancer, diabetes, neurodegenerative and autoimmune disorders. Preparations from the herb and/or flowers of *Filipendula ulmaria* have been used traditionally since the late 16th and 17th century for the treatment of inflammatory diseases. Moreover, its anti-inflammatory activity has been documented by *in vitro* and *in vivo* animal studies. Despite the fact that this supports the use of meadowsweet preparations against inflammatory diseases, the plant's active constituents, however, were not yet elucidated. Nevertheless, many natural products are prodrugs which must undergo *in vivo* metabolic conversion in order to become activated after oral administration. This aspect is usually overlooked when searching for new therapeutic agents using classical approaches. Therefore, identification of plant metabolites after biotransformation might give new insights into the quest to identify new therapeutic agents which might be activated after oral administration. Biotransformation experiments of natural

products or plant extracts produce large amounts of data, but there is no common strategy for data analysis of large-scale, untargeted, dynamic metabolomics experiments. Commercially available workflows are often not sufficiently sophisticated to analyze longitudinal multiclass data, necessary to monitor the biotransformation processes. Moreover, processing this amount of data manually is extremely time-consuming and bias is inherent to the human revision process. Therefore, the aim of this project was to develop an **integrated strategy to characterize new anti-inflammatory lead compounds derived from *Filipendula ulmaria***, based on biotransformation studies, followed by an automated data analysis workflow.

As a first step, the **phytochemical composition of *Filipendula ulmaria* was explored in a comprehensive manner** for the first time in the search for its active constituents. Two complementary generic UHPLC-PDA-amMS methods were combined to enable analysis of the full range of phytochemicals. Since method validation is often omitted in plant metabolome studies, the performance of different comprehensive sample preparation protocols was assessed based on extraction efficiency, repeatability and intermediate precision and on matrix effect. It was also concluded that a combination of two complementary extraction methods, namely chloroform:methanol:water and ethyl acetate:water, best fitted the goals and constraints of this untargeted metabolomics workflow. A rich diversity of phenolic constituents was (tentatively) identified. In total, 119 compounds were tentatively identified, of which 69 compounds were not reported before in *Filipendula ulmaria*. A rich diversity of phenolic constituents was detected and only a few non-phenolic phytochemicals were observed. Even though mass spectrometry does not provide enough information for complete structural characterization, it does allow rapid tentative identification of a wide range of constituents. In view of the integrated strategy, complete structural characterization is not the main goal. For example, the exact linkage position of the sugar moieties is

less important, as it is expected that they are removed during gastrointestinal biotransformation.

Secondly, a new strategy was used to disclose metabolic pathways, namely ***in vitro* biotransformation via a gastrointestinal simulation model followed by metabolomics profiling**. The gastrointestinal biotransformation pathway of several compounds present in the *Filipendula ulmaria* extract was revealed using this innovative workflow. In general, extensive biotransformation of glycosylated compounds in the gastrointestinal tract was observed, leading to the formation of a whole array of corresponding aglycons. The applied non-target screening analysis was capable of picking up features also discovered by the suspect screening approach, confirming its applicability to discover biotransformation products. The automated data analysis workflow can thus replace laborious human revision processing in an unbiased manner, allowing rapid scoring of large amounts of data. The *in vitro* gastrointestinal biotransformation model, including fecal fermentation using a culture of pooled human feces in an anaerobic environment, is a valuable tool and was optimized to resemble *in vivo* conditions as much as possible. Nonetheless, the digestive tract is highly complex and extrapolation from *in vitro* findings to *in vivo* conclusions requires caution. An *in vitro* model remains a simplified approach to predict biotransformation since active transport, passive diffusion and enterohepatic circulation are missing. Nonetheless, the GIM provides an insight in enzymatic and microbial biotransformation occurring in the gastrointestinal tract. It is therefore suitable for screening phases, omitting animal testing in early phases of natural product research. In future research, it would be very interesting and useful to combine the GIM with human intestinal epithelial Caco-2 cell absorption to mimic the intestinal barrier *in vitro*. The use of co-cultures of colonic mucin-producing HT-29 cells with Caco-2 cells may also be an interesting addition for the biological relevance of the simulated intestinal wall, as the mucin layer may have an impact on (poly)phenol bioavailability. Addition of hepatic

cells, microsomes or S9 fractions could also provide new insights in phase I and II metabolism in the liver and build on to more *in vivo*-like conditions. Lastly, large inter- and intraindividual variability in gut microbiota exists and this is an important confounding factor in studies on the formation of effect of nutrients, drugs and phytochemicals. Therefore, 16S rDNA-targeting PCR was used to observe a possible effect of the *Filipendula ulmaria* extract on the bacterial composition of the fecal slurry during *in vitro* biotransformation. However, it would be very interesting to pay more attention to this part in future research, for example by comparing the effect on the biotransformation of the extract when using different groups of pooled feces screened for different metabotypes.

As a last step, the **activity was evaluated with *in vitro* anti-inflammatory assays**, focusing on cyclooxygenase and NF- κ B. It can be concluded that *Filipendula ulmaria* clearly exerted anti-inflammatory potential, which confirms its use in European traditional medicine against inflammatory diseases. The non-biotransformed *Filipendula ulmaria* extract significantly inhibited the activity of both COX isoenzymes in a dose-dependent manner and showed to be a more potent inhibitor of the COX-1 enzyme compared to the COX-2 enzyme. However, the extract showed no effect on COX-2 gene expression in PMA-stimulated THP-1 cells. A clear dose-dependent inhibition on the TNF- α -induced NF- κ B luciferase reporter gene induction in L929 cells was also seen. While evidence from such *in vitro* experiments does not necessarily prove its *in vivo* activity, these studies do support and provide a rationale for the use of *Filipendula ulmaria* to suppress inflammation *in vivo*. Moreover, *in vivo* experiments are time-consuming and expensive, while *in vitro* (enzyme or cell-based) studies are predominantly used because of their lower costs and because they are easier to perform. These tests are also convenient for better evaluation of the complex interaction between polyphenols and the intracellular environment to study specific mechanisms of action, e.g. by studying interesting signaling pathways.

Interpreting data obtained in this way, however, requires caution. First of all, the bioactive compounds might be formed *in vivo* due to biotransformation reactions carried out by the intestinal microflora or by the hepatic metabolism, which means they were not present in the original extract. Secondly, another important aspect is whether the concentration of the extract's constituents are realistic or achievable *in vivo*: typically, many plant constituents are not completely bioavailable since they are not easily absorbed. Therefore, a preliminary experiment was performed in order to clean up the fermented *Filipendula ulmaria* extract of the GIM, using methanol, ethyl acetate and acetone extraction. A preference in selectivity for the COX-1 over the COX-2 enzyme could still be observed in the enzyme inhibition assay. Flavonoids have various mechanisms of action, depending on their chemical structures. Any single mechanism could not explain all of their *in vivo* activities, since they probably have multiple cellular mechanisms acting on multiple sites. For future research it would thus be interesting to test the extract's anti-inflammatory ability in much more detail to explain its true mechanisms of action on inflammation. First of all, since there is an inhibitory effect on the COX enzymes and not on the COX-2 gene expression, it would be a good idea to study the release of prostaglandins (e.g. PGE₂ levels in cell culture medium) in macrophages, as well as the changes in COX-2 protein expression measured via western blot analysis. Secondly, our research showed an inhibition on the TNF- α -induced NF- κ B luciferase reporter gene induction in L929 cells. However, it would be interesting to untangle this NF- κ B inhibition more in depth, for example by measuring the effects on I κ B α phosphorylation and p65 nuclear translocation through ELISA. Furthermore, other interesting results can be obtained by looking at the influence of *Filipendula ulmaria* on pro-inflammatory cytokines such as IL-1 β , IL-6, IL-8, and TNF- α or its possible anti-inflammatory activity on the lipoxygenase or the iNOS pathway.

It is important to point out that for a complete understanding of the mode of action of plant extracts, the biotransformation of plant constituents during digestion and metabolic reactions in biological systems has to be considered. Most polyphenols in medicinal plants are present in the form of esters, glycosides or polymers, which are hardly absorbed. They undergo metabolic conversion in the human body and may be hydrolyzed or oxidized; absorbed metabolites may undergo enzymatic methylation, glucuronidation and sulfation reactions. Hence, polyphenolic compounds may thus be prodrugs. Therefore, a first step was made to verify whether constituents of a *Filipendula ulmaria* extract were metabolized and whether these metabolites exhibit anti-inflammatory activity. Nevertheless, more research is necessary in the future to find a method to purify these samples containing fecal material, digestive enzymes and bile salts, without risking to lose metabolites and other compounds during purification.

To conclude, this integrated workflow was developed to be widely applicable for different classes of plants and to focus on various clinical conditions. This innovative approach offers added value in screening phases, allowing phytochemical identification of compounds and their metabolites after *in vitro* biotransformation, followed by preliminary *in vitro* activity testing, avoiding *in vivo* studies in early stages of research. Purification might need to be adapted for different compound classes, depending on the chemical properties of the compounds of interest and the matrix. To further attribute activity to one specific metabolite or compound, or to a synergistic effect of multiple compounds or metabolites, *in vitro* activity testing should be repeated with the compound(s) of interest. This, however, requires large amounts of relatively pure substances, which are not always readily available for purchase. The *in vitro* biotransformation models, however, hamper isolation of compounds or metabolites in sufficient amounts since these models provide low concentration levels of metabolites and contain large amounts of matrix. Compounds of interest should be fully characterized by NMR spectroscopy and consequent synthetic production might be

necessary in some cases to obtain a sufficient amount. Once activity is correlated to one or more compounds, their precursor should be identified and evaluated in *in vivo* studies, where metabolites in blood, urine or feces are monitored to confirm activity of a possible new lead compound.

SUMMARY

Worldwide, there is a high need for new lead compounds to meet the continuing demand of better drugs against all kinds of diseases. This is definitely also the case for anti-inflammatory drugs. A large number of non-steroidal anti-inflammatory drugs (NSAIDs) are on the market, many of which have severe gastrointestinal side effects like ulcerations, bleedings and perforations.

The scope of this PhD thesis was to develop an integrated strategy, based on natural pro-drugs and their metabolites, to characterize new anti-inflammatory lead compounds derived from *Filipendula ulmaria* (meadowsweet). Preparations from the herb and/or flowers of meadowsweet have been used traditionally since the late 16th and 17th century for the treatment of inflammatory diseases, as a diuretic and as an antirheumatic. *Filipendula ulmaria* is administered as herbal tea, as a powdered herbal substance in solid dosage form for oral use and as a tincture. In some countries of the European Union, tinctures or tincture-based products containing alcoholic extracts of Filipendulae Herba are on the market as food supplements used for complaints such as rheumatic and arthritic pain. Many natural products are pro-drugs, e.g. glycosides, which are biotransformed and activated after oral administration. Nevertheless, this aspect is usually overlooked when using traditional approaches when searching for new lead compounds for therapeutic agents. Therefore, an integrated strategy to characterize new active compounds was developed.

As a first step, the phytochemical composition of *Filipendula ulmaria* was explored in a comprehensive manner in the search for its active constituents. Two complementary generic UHPLC-PDA-amMS methods were combined to enable analysis of the full range of phytochemicals. Since method validation is often omitted in plant metabolome studies, the performance of different comprehensive sample preparation protocols

was assessed based on extraction efficiency, repeatability and intermediate precision and on matrix effect. It was also concluded that a combination of two complementary extraction methods, namely H₂O:EtOAc and CHCl₃:MeOH:H₂O, best fitted the goals and constraints of this untargeted metabolomics workflow. A rich diversity of phenolic constituents was (tentatively) identified. In total, 119 compounds were tentatively identified, of which 69 compounds were not reported before in *Filipendula ulmaria*.

After oral administration, a herbal extract is inevitably brought into contact with gastrointestinal enzymes and the intestinal microflora. In view of the phenolic nature of the main constituents, extensive biotransformation after oral intake before absorption can be expected. This urges the need for identification and activity profiling of the intestinal metabolites. Therefore, the *Filipendula ulmaria* extract was subjected to *in vitro* gastrointestinal biotransformation, which mimics the gastric, intestinal and colonic phase, including fecal fermentation using a culture of pooled human feces in an anaerobic environment. Three groups were included in this experiment: (1) samples containing the *Filipendula ulmaria* extract, which were treated with digestive enzymes and fecal microflora; (2) Negative control samples, which also contained the extract but without addition of the fecal bacteria; (3) Method blank samples, comprising an equal volume of solvent instead of extract and undergoing treatment with digestive enzymes and fecal bacteria. Samples before, during and after biotransformation (with the endpoint at 72 h of colon phase) were analyzed with UPLC-DAD-HRMS.

To tackle the dynamic and complex nature of this data, an in-house automated data analysis workflow for multiclass longitudinal data was used to screen interesting biotransformation profiles in an unbiased manner. In short, a limited number of biotransformation time profiles was rated by an expert scientist, which was then used to train a machine learning model in the background to analyze the large amount of data. This results in a ranking of features, according to one single score, taking the longitudinal aspect and the three sample classes into account, which facilitates

selection of features of interest. Mainly in the colon phase, a decrease in relative abundance in the samples was observed for a diversity of different glycosylated flavonoids such as rutin, spiraeoside, quercitrin and isoquercitrin. At the same time, the relative abundance of aglycons such as quercetin, apigenin, naringenin and kaempferol increased, indicating microbial deglycosylation. These changes were not observed in the negative control and method blanks. Although *Filipendula ulmaria* is rich in ellagitannins, the expected urolithin metabolites were not detected in the biotransformation experiment.

As a last step, the activity was evaluated with *in vitro* anti-inflammatory assays, focusing on cyclooxygenase (COX) and nuclear factor κ B (NF- κ B). The non-biotransformed *Filipendula ulmaria* extract showed significant inhibitory activity in a NF- κ B luciferase assay on L929 cells. Significant inhibition was also seen on both COX enzymes, with a preference for COX-1 compared to COX-2. However, no inhibitory effect was observed on the cell-based COX-2 gene expression assay in PMA-differentiated THP-1 macrophages. Nevertheless, metabolites often display different biological activities compared to their precursors. Therefore, a preliminary experiment was performed in order to clean up the colon samples from the gastrointestinal model, after 72 h of fermentation of the *Filipendula ulmaria* extract. Across all different extraction methods (MeOH, EtOAc and ACE) and the genuine 72 h fermentation sample, a preference in selectivity for the COX-1 over the COX-2 enzyme remained visible in the enzyme inhibition assay. Since testing samples containing fecal material proved to be difficult and challenging in cell-based assays, a mix of aglycons and metabolites present after 72 h of fermentation was tested. No inhibition was observed in the NF- κ B luciferase assay, but the mix did show a significant inhibition on the COX-1 enzyme; interestingly, this effect was not achieved when testing single compounds.

To conclude, this new integrated approach offers added value medicinal plant research, allowing phytochemical identification of compounds and their metabolites after *in vitro* biotransformation, followed by preliminary *in vitro* activity testing, omitting time-consuming and expensive *in vivo* studies in early stages of research.

SAMENVATTING

Wereldwijd is er grote behoefte aan nieuwe lead compounds om aan de aanhoudende vraag naar betere medicijnen tegen allerlei ziekten te voldoen. Dit geldt zeker ook voor ontstekingsremmers. Er is een groot aantal niet-steroïde anti-inflammatoire geneesmiddelen (NSAID's) op de markt, waarvan vele ernstige gastro-intestinale bijwerkingen hebben, waaronder ulceraties, bloedingen en perforaties.

Het doel van deze doctoraatstudie was om een geïntegreerde strategie te ontwikkelen, gebaseerd op natuurlijke pro-drugs en hun metabolieten, om nieuwe ontstekingsremmende lead compounds uit *Filipendula ulmaria* te karakteriseren. Preparaten van het kruid en/of de bloemen van moerasspirea (moerasspirea) worden sinds het einde van de 16^{de} en 17^{de} eeuw traditioneel gebruikt voor de behandeling van ontstekingsziekten, als diureticum en als antireumatisch middel. *Filipendula ulmaria* wordt toegediend als kruidenthee, als poedervormige kruidensubstantie in vaste doseringsvorm voor oraal gebruik en als tinctuur. In sommige landen van de Europese Unie zijn tincturen of op tincturen gebaseerde producten met alcoholische extracten van Filipendulae Herba op de markt als voedingssupplementen, gebruikt bij pijnklachten ten gevolge van reuma en artrose. Veel natuurlijke producten zijn pro-drugs, b.v. glycosiden, die na orale toediening worden gebiotransformeerd en geactiveerd. Desalniettemin wordt dit aspect meestal over het hoofd gezien in klassieke onderzoeksstrategieën bij het zoeken naar nieuwe lead compounds voor geneesmiddelen. Daarom werd in dit project een geïntegreerde strategie ontwikkeld om nieuwe actieve componenten te karakteriseren.

Als eerste stap werd de fytochemische samenstelling van *Filipendula ulmaria* op een comprehensieve manier ontleed in de zoektocht naar de actieve bestanddelen. Twee complementaire, generieke UHPLC-PDA-amMS methoden werden gecombineerd om

analyse van het volledige scala aan fytochemicaliën mogelijk te maken. Aangezien methodevalidatie vaak wordt weggelaten in plantenmetaboloomstudies, werd de performantie van verschillende uitgebreide staalvoorbereidingsprotocollen beoordeeld op basis van extractie-efficiëntie, herhaalbaarheid, intermediaire precisie en op matrixeffect. Er kon geconcludeerd worden dat een combinatie van twee complementaire extractiemethoden, namelijk H₂O:EtOAc en CHCl₃:MeOH:H₂O, het best paste bij de doelen en beperkingen van deze untargeted metabolomics workflow. Een rijke diversiteit aan fenolische componenten werd (tentatief) geïdentificeerd. In totaal werden 119 componenten tentatief geïdentificeerd, waarvan 69 inhoudsstoffen nog niet eerder werden gerapporteerd in *Filipendula ulmaria*.

Na orale toediening komt een plantenextract onvermijdelijk in contact met gastro-intestinale enzymen en de darmmicroflora. Gezien de fenolische aard van de hoofdbestanddelen, kan een uitgebreide biotransformatie na orale inname vóór absorptie worden verwacht. Daarom dringt de noodzaak zich op van identificatie en het in kaart brengen van de activiteit van de intestinale metabolieten. Om deze reden werd het *Filipendula ulmaria* extract onderworpen aan *in vitro* gastro-intestinale biotransformatie, waarbij de maag-, darm- en colonfase gesimuleerd wordt, inclusief fecale fermentatie met behulp van een cultuur van gepoolde humane feces in een anaërobe omgeving. Drie groepen werden in dit experiment opgenomen: (1) stalen die het *Filipendula ulmaria* extract bevatten, die werden behandeld met spijsverteringsenzymen en fecale microflora; (2) Negatieve controlestalen, die ook het extract bevatten maar zonder toevoeging van de fecale bacteriën; (3) Methode blanco stalen, bestaande uit een gelijk volume solvent in plaats van extract, die worden behandeld met spijsverteringsenzymen en fecale bacteriën. Stalen voor, tijdens en na biotransformatie (met als eindpunt 72 u colonfase) werden geanalyseerd met UPLC-DAD-HRMS.

Om de dynamische en complexe aard van deze gegevens aan te pakken, werd een in-house geautomatiseerde workflow voor data-analyse voor longitudinale gegevens van meerdere groepen gebruikt om interessante biotransformatieprofielen op een onafhankelijke manier te screenen. Samengevat, een beperkt aantal biotransformatie-tijdsprofielen werd beoordeeld door een expert, en deze werden vervolgens gebruikt om een machine learning model te trainen om de grote hoeveelheid data te analyseren. Dit resulteert in een rangschikking van features volgens één enkele score, rekening houdend met het longitudinale aspect en de drie groepen, wat de selectie van interessante features sterk vergemakkelijkt. Voornamelijk in de colonfase werd een afname in relatieve abundantie in de teststalen waargenomen voor een diversiteit aan geglycosyleerde flavonoïden zoals rutine, spiraeoside, quercitrine en isoquercitrine. Terzelfdertijd nam de relatieve abundantie aan aglyconen zoals quercetine, apigenine, naringenine en kaempferol toe, wat wijst op microbiële deglycosylering. Deze veranderingen werden niet waargenomen in de methode blanco's en de negatieve controles. Hoewel *Filipendula ulmaria* rijk is aan ellagitannines, werden de verwachte urolithine metabolieten niet gedetecteerd in het biotransformatie experiment.

Als laatste stap werd de activiteit geëvalueerd via *in vitro* anti-inflammatoire testen, gericht op cyclooxygenase (COX) en nuclear factor κ B (NF- κ B). Het niet-gebiotransformeerde *Filipendula ulmaria* extract vertoonde significante inhiberende activiteit in een NF- κ B luciferase assay op L929-cellen. Significante inhibitie werd ook gezien op beide COX-enzymen, met een voorkeur voor COX-1 in vergelijking met COX-2. Er werd echter geen remmend effect waargenomen op de COX-2 genexpressie assay in PMA-gedifferentieerde THP-1 macrofagen. Niettemin vertonen metabolieten vaak verschillende biologische activiteiten in vergelijking met hun precursoren. Daarom werd een eerste experiment uitgevoerd om de colonstalen van het gastro-intestinale model op te zuiveren, na 72 u fermentatie van het *Filipendula ulmaria* extract. Bij alle verschillende extractiemethoden (MeOH, EtOAc en

ACE) en het pure fermentatiestaal na 72 u colonfase, bleef een voorkeur in selectiviteit voor het COX-1 t.o.v. het COX-2 enzym zichtbaar in de enzym inhibitie test. Aangezien het testen van stalen met fecaal materiaal moeilijk en uitdagend bleek te zijn in celtesten, werd een mix getest bestaande uit aglyconen en metabolieten aanwezig na 72 u fermentatie. Er werd geen remming waargenomen in de NF- κ B luciferase assay. Interessant is dat de mix een significante remming van het COX-1 enzym vertoonde, terwijl dit effect niet werd bereikt bij het testen van de afzonderlijke componenten.

In het kort, biedt deze nieuwe geïntegreerde strategie een toegevoegde waarde in onderzoek van medicinale planten. De fytochemische samenstelling kan bepaald worden, gevolgd door identificatie van metabolieten na *in vitro* biotransformatie, en preliminaire *in vitro* activiteitstesten. Hierdoor kunnen tijdrovende en dure *in vivo* studies in vroege onderzoeksstadia worden vermeden.

ACKNOWLEDGEMENTS

Helen Keller zei ooit: “Alone we can do so little; together we can do so much”. Deze quote vat mijn doctoraatsthesis mooi samen. Het behalen van een doctoraat is een monumentale prestatie, en ik vind het nog steeds moeilijk te geloven dat ik deze mijlpaal heb bereikt. Daarom wil ik een toast uitbrengen op iedereen die samen met mij deel heeft uitgemaakt van deze ongelooflijke reis, want een doctoraatsonderzoek tot een goed einde brengen doe je niet alleen.

Eerst en vooral wil ik mijn promotor en co-promotor, Prof. Luc Pieters en Prof. Nina Hermans, bedanken. Jullie voortdurende steun, begeleiding en aanmoediging zijn gedurende het hele proces van onschatbare waarde geweest. Vanaf de eerste fasen van het verfijnen van mijn onderzoeksvorstel tot de uiteindelijke indiening van mijn thesis, jullie stonden steeds klaar om mij te helpen en om advies te geven. Ik apprecieer zeer hard dat jullie mij de tijd gegeven hebben die ik nodig had om mezelf opnieuw ‘voldoende Anastasia te voelen’ en me te ondersteunen waar nodig. Ook Prof. Sandra Apers verdient een speciale vermelding. Zij heeft me mee warm gemaakt voor dit project en haar ideeën hebben deze thesis vorm gegeven.

Naast mijn promotoren, wil ik ook al mijn ex-collega’s en labgenoten van NatuRA bedanken aangezien zij een constante bron van motivatie en steun geweest zijn. Laura, Maxime, Stefaniya, Emmy, de Annelies’en, Kenn, Tania, Mart, Tess, Baldé, Yunita, Hien, Sebastiaan, Deborah, Andrés, Maxim, Anne-Sophie, Stef, en de vele studenten die telkens geplaatst werden in mijn bureau: bedankt voor de hulp, de vele babbeltjes en leuke vriendschappen! Ook nog een extra bedankje voor Charlie die Laura en mij geweldig heeft ondersteund met het uitwerken van Tinderesting (zelfs ondanks de foto’s van jou in een jurkje die we tussendoor te zien kregen in de eerste versie van de app). Stefano, I also want to thank you for all your hard work and crazy ideas. Without

you, I wouldn't have the full story on *Filipendula ulmaria*. By the way, you should totally make *Stefanococcus* a thing!

Ook wil ik mijn dankbaarheid uiten aan de leden van mijn commissie en de externe jury: Prof. Wim Martinet, Prof. Wim Vanden Berghe, Prof. Peter de Witte en Prof. Rudi Bauer. In English for Prof. Rudi Bauer (my German is still not good enough, even after 1 month in Graz): I want to thank all of you for your time and effort, reading all the pages of my thesis and for providing valuable feedback and thought-provoking questions. Your insights have greatly enriched the quality of my work.

Laura, jij verdient nog een tweede bedankje. Ik zou eigenlijk gewoon perfect jouw dankwoord kunnen kopiëren aangezien we hetzelfde hebben meegemaakt. Wij hebben samen toch echt wel de gekste ideeën uitgewerkt... Kamperen op een leuke luchtmatras of veldbedje in ons bureau, om 10 uur 's avonds een familiepak frieten delen met 2 (gevolgd door nog een zak popcorn) of pipetteren in het midden van de nacht op lachend kakske pantoffels... En uiteraard Griekenland: laten we nooit meer een appartement boeken met een groene wc. En nog een derde bedankje: bedankt om mij het laatste jaar zo goed te ondersteunen. Ik ben zo ontzettend dankbaar voor onze vriendschap.

Ik had dit doctoraat niet kunnen voltooien zonder de ongelooflijke steun van mijn vrienden en familie. In het bijzonder ook bedankt aan Stephanie, Stefanie en Sofie. Jullie stonden altijd klaar om me terug moed in te praten, mij af te leiden door iets leuks te doen en om een luisterend oor te bieden (of een glas wijn in het geval van Sofie). Ook zeker een bedankje aan Ian, Ellen, Greta en Geert. Oma, opa en Hugo: jullie had ik er graag bij gehad. Bedankt voor jullie aanmoediging en levenslessen.

Mama en papa, bedankt om telkens alle twijfels over mezelf weg te toveren. Ik ben er zeker van, mama, dat jij eigenlijk ook een diploma in de Biomedische Wetenschappen hebt met hoe vaak ik mijn leerstof jaar na jaar tegen jou herhaald heb.

Papa, wat had ik jou vandaag graag in de zaal zien zitten... eerlijk, ik kon het me een hele tijd niet inbeelden dat ik zonder jou zou kunnen verdedigen. Maar ik ben er zeker van dat je trots bent dat ik goed omringd ben met mensen die me hebben gesteund en geholpen om vandaag toch hier te staan, en dat het me alsnog gelukt is om dit hoofdstuk af te sluiten. Dankjewel voor je eeuwige enthousiasme, schrijftalent en leergierige geest.

Devin, bedankt om al sinds 2007 mijn rots in de branding te zijn. Ik denk dat ik zonder jouw chemiekennis alvast mijn diploma nooit had behaald... Ik heb nog nachtmerries van Mastering Chemistry. Ik zal het grootste deel van de melige tekst die ik hier wou neerpennen houden voor onze trouwdag, maar weet alvast dat ik zeer hard apprecieer wat je allemaal voor mij hebt gedaan: van mijn humeur oppeppen tot autoritjes tot hulp bij concentratieberekeningen. Zonder jou, zou ik niet de persoon zijn die ik vandaag ben.

Les in optimisme

Altijd eindigend met hoop op een begin.
Neergang slechts tijdelijke knik. Verval

dat zo ontegensprekelijk in ieder van ons
vordert aangrijpend als loutering: stilaan

zit jij zo in elkaar. Het zwart als radicale
synthese van alle kleuren, amant van wit.

Als je rondom kijkt zie je alleen kansen,
te breken drempels te verleggen grenzen.

Geen demon die je enthousiasme kan of
durft ontgoochelen, want iedereen beseft:

je bent je eigen therapie. Een ruimdenker.

September 2013 – Frank Van der Auwera

SCIENTIFIC CURRICULUM VITAE

Personalia Name: Anastasia Van der Auwera
Date of birth: December 23, 1991
Place of birth: Antwerp, Belgium
E-mail: Anastasia.VanderAuwera@uantwerpen.be

Education

2015-2020 PhD candidate in Pharmaceutical Sciences (Flemish Fund for Scientific Research (FWO) supported this research (project number 1S19016N))
Natural Products & Food Research and Analysis (NatuRA)
University of Antwerp, Wilrijk, Belgium

2012-2014 Master of Science: Biomedical Sciences
Major: Health and Environmental Sciences
Minor: Clinical Research
University of Antwerp, Wilrijk, Belgium

2009-2012 Bachelor in Biomedical Sciences
University of Antwerp, Wilrijk, Belgium

2003-2009 Secondary school: Latin mathematics
Sint-Agnes Instituut, Antwerp, Belgium

Scientific experience

Jan 2023 – Current	Medical Writer CellCarta, Wilrijk, Belgium
May 2021 – Jan 2023	Clinical Research Associate ICON, Mechelen, Belgium
Nov 2020 – May 2021	In-house Clinical Research Associate ICON, Mechelen, Belgium
Jan 2015 – Mar 2020	PhD Researcher in Pharmacy “An integrated strategy to characterize anti-inflammatory lead compounds derived from <i>Filipendula ulmaria</i> (meadowsweet).” Natural Products & Food Research and Analysis (NatuRA) University of Antwerp, Wilrijk, Belgium
Nov 2013 – May 2014	Master thesis Clinical trial with 50 patients with Metabolic Syndrome to test a red yeast rice-olive extract supplement. Natural Products & Food Research and Analysis (NatuRA) University of Antwerp, Wilrijk, Belgium

Scientific research stays abroad

April – May 2019	Medihealth project: Marie Curie Actions – RISE 691158 Laboratory of Pharmacognosy and Natural Products Chemistry University of Athens, Athens, Greece
Oct 2015	Research stay at the University of Graz Institute of Pharmaceutical Sciences, Department of Pharmacognosy Karl-Franzens-Universität Graz, Graz, Austria

Scientific publications

Papers in peer-reviewed journals

2023 **Van der Auwera A**, Peeters L, Foubert K, Piazza S, Vanden Berghe W, Hermans N, Pieters L. (2023). *In vitro* biotransformation and anti-inflammatory activity of constituents and metabolites of *Filipendula ulmaria*. *Pharmaceutics*, 15(4), 1291.

DOI: 10.3390/pharmaceutics15041291

2021 Méndez-Rodríguez D, Escalona-Arranz JC, Foubert K, Matheussen A, **Van der Auwera A**, Piazza S, Cuypers A, Cos P, Pieters L. (2021). Chemical and Pharmacological Potential of *Coccoloba cowellii*, an Endemic Endangered Plant from Cuba. *Molecules*, 26(04), 935.

DOI: 10.3390/molecules26040935

Berenguer-Rivas CA, Escalona-Arranz JC, Llauradó-Maury G, **Van der Auwera A**, Piazza S, Méndez-Rodríguez D, Foubert K, Cos P, Pieters L. (2021). Anti-inflammatory effect of *Adelia ricinella* L. aerial parts. *Journal of Pharmacy and Pharmacology*, 73(04), 553-559.

DOI: 10.1093/jpp/rgaa057

Rivera-Mondragón A, Peeters L, **Van der Auwera A**, Breynaert A, Caballero-George C, Pieters L., Foubert K. (2021). Simulated gastrointestinal biotransformation of chlorogenic acid, flavonoids, flavonolignans and triterpenoid saponins in *Cecropia obtusifolia* leaf extract. *Planta Medica*, 87(05), 404-416.

DOI: 10.1055/a-1258-4383

- 2020 Peeters L, **Van der Auwera A**, Beirnaert C, Bijttebier S, Laukens K, Pieters L, Foubert K. (2020). Compound characterization and metabolic profile elucidation after in vitro gastrointestinal and hepatic biotransformation of an *Herniaria hirsuta* extract using unbiased dynamic metabolomic data analysis. *Metabolites*, 10(3), 111.
DOI: 10.3390/metabo10030111
- 2019 Beirnaert C, Peeters L, Meysman P, Bittremieux W, Foubert K, Custers D, **Van der Auwera A**, Cuykx M, Pieters L, Covaci A, Laukens K. (2019). Using expert driven machine learning to enhance dynamic metabolomics data analysis. *Metabolites*, 9(3), 54.
DOI: 10.1021/acs.jnatprod.6b00131
- Peeters L, Beirnaert C, **Van der Auwera A**, Bijttebier S, De Bruyne T, Laukens K, Foubert K. (2019). Revelation of the metabolic pathway of hederacoside C using an innovative data analysis strategy for dynamic multiclass biotransformation experiments. *Journal of Chromatography A*, 1595, 240-247.
DOI: 10.1016/j.chroma.2019.02.055
- 2017 Hermans N and **Van der Auwera A**, Breynaert A, Verlaet A, De Bruyne T, Van Gaal L, Pieters L, Verhoeven V. (2017). A red yeast rice-olive extract supplement reduces biomarkers of oxidative stress, OxLDL and Lp-PLA2, in subjects with metabolic syndrome: A randomised, double-blind, placebo-controlled trial. *BMC Trials*, 18, 302.
DOI: 10.1186/s13063-017-2058-5

- 2016 Bijttebier S, **Van der Auwera A**, Foubert K, Voorspoels S, Pieters L, Apers S. (2016). Bridging the gap between comprehensive extraction protocols in plant metabolomics studies and method validation. *Analytica Chimica Acta*, 935, 136-150.
DOI: 10.1016/j.aca.2016.06.047
- Bijttebier S, **Van der Auwera A**, Voorspoels S, Noten B, Hermans N, Pieters L, Apers S. (2016). A First Step in the Quest for the Active Constituents in *Filipendula ulmaria* (Meadowsweet): Comprehensive Phytochemical Identification by Liquid Chromatography Coupled to Quadrupole-Orbitrap Mass Spectrometry. *Planta Medica*, 82(06), 559-572.
DOI: 10.1055/s-0042-101943
- 2015 Verhoeven V, **Van der Auwera A**, Van Gaal L, Remmen R, Apers S, Stalpaert M, Wens J, Hermans N. (2015). Can red yeast rice and olive extract improve lipid profile and cardiovascular risk in metabolic syndrome?: A double blind, placebo controlled randomized trial. *BMC Complementary and Alternative Medicine*, 15, 52.
DOI: 10.1186/s12906-015-0576-9

Oral presentations

2019 The use of an *in vitro* biotransformation model and data analysis workflow to characterize anti-inflammatory lead compounds derived from *Filipendula ulmaria*.

Research day of the Faculty of Pharmaceutical, Biomedical and Veterinary Sciences, University of Antwerp, Antwerp, Belgium, 25th of October 2019

The use of an *in vitro* biotransformation model and data analysis workflow to characterize anti-inflammatory lead compounds derived from *Filipendula ulmaria*.

Congress: COST Action NutRedOx meeting, Lisbon, Portugal, 2nd of October until the 4th of October 2019

An integrated strategy to characterize new anti-inflammatory lead compounds derived from *Filipendula ulmaria* (meadowsweet).

Congress: 20th Forum of Pharmaceutical Sciences (Belgian Society of Pharmaceutical Sciences), Brussels, Belgium, 20th of May 2019.

Poster presentations

2019 Van der Auwera A, Peeters L, Bijttebier S, Foubert K, Hermans N, Pieters L. An integrated strategy to characterize new anti-inflammatory lead compounds derived from *Filipendula ulmaria* (meadowsweet).

67th International Congress and Annual Meeting of the Society for Medicinal Plant and Natural Product Research, 4th of September 2019, Innsbruck, Austria.

2018 Van der Auwera A, Bijttebier S, Peeters L, Foubert K, Hermans N, Pieters L.
An integrated strategy to characterize new anti-inflammatory lead
compounds derived from *Filipendula ulmaria* (meadowsweet).
11th International Symposium on Drug Analysis and 29th International
Symposium on Pharmaceutical and Biomedical Analysis, 10th of September
2018, Leuven, Belgium.